ENGINEER

international scientific journal

ISSUE 1, 2025 Vol. 3
E-ISSN
3030-3893
ISSN
3060-5172

SLIB.UZ
Scientific library of Uzbekistan

A bridge between science and innovation

TOSHKENT DAVLAT TRANSPORT UNIVERSITETI
Tashkent state transport university

ENGINEER

A bridge between science and innovation

E-ISSN: 3030-3893

ISSN: 3060-5172

VOLUME 3, ISSUE 1

MARCH, 2025

engineer.tstu.uz

TASHKENT STATE TRANSPORT UNIVERSITY

ENGINEER

INTERNATIONAL SCIENTIFIC JOURNAL
VOLUME 3, ISSUE 1 MARCH, 2025

Founder of the international scientific journal "Engineer" – Tashkent State Transport University, 100167, Republic of Uzbekistan, Tashkent, Temiryo'lchilar str., 1, office: 465, e-mail: publication@tstu.uz.

The "Engineer" publishes the most significant results of scientific and applied research carried out in universities of transport profile, as well as other higher educational institutions, research institutes, and centers of the Republic of Uzbekistan and foreign countries.

The journal is published 4 times a year and contains publications in the following main areas:

- Engineering;
- General Engineering;
- Aerospace Engineering;
- Automotive Engineering;
- Civil and Structural Engineering;
- Computational Mechanics;
- Control and Systems Engineering;
- Electrical and Electronic Engineering;
- Industrial and Manufacturing Engineering;
- Mechanical Engineering;
- Mechanics of Materials;
- Safety, Risk, Reliability and Quality;
- Media Technology;
- Building and Construction;
- Architecture.

Tashkent State Transport University had the opportunity to publish the international scientific journal "Engineer" based on the **Certificate No. 1183** of the Information and Mass Communications Agency under the Administration of the President of the Republic of Uzbekistan. **E-ISSN: 3030-3893, ISSN: 3060-5172.** Articles in the journal are published in English language.

ENGINEER
INTERNATIONAL SCIENTIFIC JOURNAL
VOLUME 3, ISSUE 1 MARCH, 2025

EDITORIAL BOARD

Improvement of pavement concrete by industrial waste microfillers

S.S. Shaumarov[1][a], S.I. Kandakhorov[1][b], Z.O. Okilov[1][c], A.A. Gulomova[1]
[1]Tashkent state transport university, Tashkent, Uzbekistan

Abstract: Determination of the composition of pavement concrete using industrial waste in the most optimal options, determination of its flow limit, surface activity, and other properties of the composition, such as water separation, are presented.

Keywords: Pedestrian road surface, concretes, paving slabs, microfillers, putty

1. Introduction

Pedestrian pavement has long been firmly established in the image of a modern city. ¬A distinctive feature of the pavement made of composite material with concrete coating is its diverse properties and various configurations. At the same time, the strength and frost resistance of concrete are of great importance for road pavements. However, the tendency to use vibrocompression concrete products in areas where heavy vehicles move, combined with the aggressive effect of freezing and thawing on the properties of the pavement concrete, leads to a decrease in these physical and mechanical properties. The use of composite binders is an effective tool in eliminating this problem. At the same time, the multi-component composition of the pavement concrete is a product based not on reducing the amount of clinker in the mixture, but on effectively controlling the processes of structure formation, ensuring high quality of the resulting concrete.

At the same time, current trends in building materials science today are reducing the energy intensity of building materials production and the use of man-made raw materials in their production. From this point of view, one of the effective materials in terms of saving cement is crushed high-calcium oxide slag. The advantages of binders made from this type of slag and cement compared to Portland cement binders are greater resistance to chemical influences, hydration at low temperatures, and cost-effectiveness. Adding slag to Portland cement is an effective means of combating the harmful effects of hydroxide oxides. Therefore, it is proposed to use a composite slag-cement binder for the production of vibropressed roadbed slabs.

Today, the amount of PM particles in the air around the world is increasing, polluting the air. The main reason for this is the large amount of industrial waste, its non-recycling, the expansion of waste areas and the dumping of large amounts of waste into water resources. These harmful substances are causing widespread diseases among humanity.

In this article, we propose a simple, inexpensive, and safe method for disposing of slag waste.

Although slag is a waste product resulting from the melting of various substances, it can be used as a binder in the building materials industry.

Literature analysis shows that, based on previous studies, binder granules are crushed fractions of slag, the specific surface tension of which should not exceed at least 2000 m2/kg and a maximum of 3000 m2/kg. Slags with this surface tension are optimal for use in road construction and pavements.

Figure 1. Various types of pavement slabs

Currently, in developed foreign countries, natural stone and cement-based paving slabs are used in the construction of pedestrian crossings, squares and other road structures, and they have become very widely used in our country. Decorative concrete paving elements are increasingly used on sidewalks in city centers, playgrounds, pedestrian recreation areas, and pedestrian walkways of civil buildings. The main reason for this is their variety of configurations and rich colors (Figure 1). Also, the resistance of the paving slabs to various climatic conditions, frost and various climate changes ensures a long service life even in urban conditions [1-6].

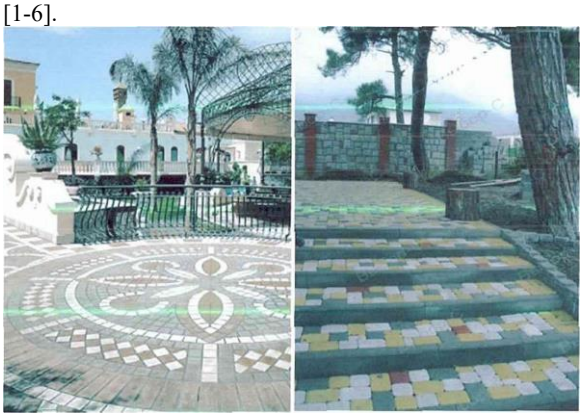

Figure 2. Types of paving slabs

[a] https://orcid.org/0000-0002-3689-8794
[b] https://orcid.org/0000-0002-3689-8794
[c] https://orcid.org/0009-0002-5946-2050

Pedestrian paving slabs add a cultural and aesthetic appeal to urban or suburban areas, and replacing cobblestone and gravel pavements with concrete pavements has many advantages (Figure 2). The advantages of this type of pavement are ease of installation with minimal labor, attractive appearance, absence of small water puddles, and durability of paving slabs compared to other coatings [7].

At the same time, this type of pedestrian pavement can be used in the construction of highways. In this case, replacing asphalt concrete with concrete pavement helps to eliminate one of the current pressing environmental problems. Thus, the effect of evaporation on asphalt concrete surfaces, which increases in our region, especially on hot summer days, is often not taken into account. It is known that during the preparation and laying of hot asphalt concrete mixtures, this concrete releases polycyclic hydrocarbons. To improve the adhesive properties of the binder, surface-active additives, such as toxic coal tar products, are added to them during surface treatment. During operation, they are partially washed out and evaporated, thereby polluting the environment [8-10].

2. Materials and method

Experimental studies Laboratory tests using waste materials from copper mining at the Almalyk Mining and Metallurgical Combine were carried out using non-standard methods developed by scientific research specialists according to generally accepted standards.

The average density and water absorption of cement stone were studied in cubic samples measuring 2x2x2 cm in accordance with GOST 12730.1-78 and 12730.3-78, and the above-mentioned properties of cement-sand mixture and heavy concrete were studied in prisms measuring 4x4x16 cm and cubic samples with sides of 10 cm after drying to constant mass at a temperature of 105ºC.

Determination of water release of the components was carried out in accordance with GOST310.6-2020 “Cement. Method for determining water release”. When conducting research, 350 g of cement and 350 g of water are weighed. Cement is weighed to an accuracy of 1 g, and water is weighed to an accuracy of 0.5 g or measured in a beaker with a volume of 0.5 cm3.

Water is poured into a beaker, then the measured cement is added for 1 minute, the contents are continuously stirred with a metal spatula for another 4 minutes, and carefully poured into a graduated glass cylinder.

The cylinder is placed on a horizontal surface and the volume of the cement paste is marked on the cylinder scales (cm3). During the study period, the cylinder should be placed in a stationary position in a place free from air currents, vibrations, and other external factors.

The grinding process of mineral raw materials was carried out in the impact-erosion mode of a ball mill. The dispersion of the obtained minerals was evaluated by the relative surface area on the PSX-11A device. The relative surface area on the PSX-11A device is determined based on the Kozeni-Karman method (via the air permeability and porosity of the compacted powder layer). The granulometric composition of microfillers was studied by laser particle diffraction on the MicroSizer 201 device. This method allows for a complete distribution of particle sizes and obtaining accurate results. The MicroSizer 201 device allows for the study of particles from 0.2 to 600 microns and dividing the specified range into 40 fractions.

3. Results and discussion

The transition to the construction of rigid road structures using cement as a binder reduces the total emissions of dust particles and toxic substances released during the asphalt concrete production process (Table 1) [11].

Table 1

The amount of harmful gases emitted from surfactants

The substance name	Concentration, g/m
Inorganic dust	12-40
Sulfur dioxide	0.016
Carbon oxide	0.0008
Nitrogen oxides	0.00007

A decisive factor in favor of expanding the construction of cement-concrete pavements in the future is the indispensability of bitumen in the repair of almost all types of pavements. Unlike bitumen, the raw material reserves for the production of cement are almost unlimited [12-13].

One of the important properties of concrete mixtures for monolithic structures is not only viscosity, but also flowability and its change over time. For this reason, the change in flowability of concrete mixtures over time for composites was studied (Figure 3).

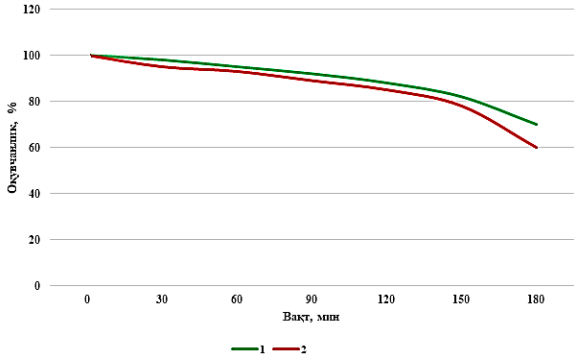

Figure 3. Change in flowability of concrete mix over time (1-Cement + OKMK microfiller; 2-cement)

Analysis of the obtained data shows that the control compositions of the concrete mix with a KCH of 4-6 cm lose their initial fluidity after 20-30 minutes. The addition of the SP modifier extends the period of formation of the coagulation structure and maintains the fluidity of the concrete mix for a long time. After 2 hours, the fluidity index of this composition is 85-88% of the initial value.

The finite element method uses a numerical approach to solve complex engineering problems. It allows you to approximate complex geometric structures and materials by dividing them into simpler elements. This method is widely used in various fields such as mechanics, heat transfer, electromagnetism, etc. We will consider the basic principles of the finite element method, its advantages and disadvantages, as well as examples of its application.

The finite element method (FEM) is a numerical method used to solve various mathematical modeling and analysis problems. It is based on dividing a complex geometric domain into simpler subdomains called finite elements. Each finite element represents a small part of the domain for which the mathematical model can be easily defined and solved analytically or numerically.

The finite element method is widely used in various fields such as mechanics, heat transfer, electromagnetism, fluid dynamics, etc. It allows modeling and analyzing the

behavior of complex systems such as mechanical structures, electrical circuits, thermal processes, etc.[1]

The basic idea of the finite element method is to approximate the solution of the problem over the entire domain by combining the solutions of individual finite elements. To do this, each finite element is described by a set of equations that relate the values of the desired function and its derivatives at the boundaries of the element under consideration.

4. Conclusion

It was found that using 12% micro aggregate is sufficient to obtain a self-compacting concrete mix with a low viscosity value. Using 8% slag increases the effect of reducing the viscosity of the concrete mix.

The use of microfiller admixture and binary microfiller allows maintaining the flowability of the concrete mix for 100-120 minutes, which helps to increase the efficiency of the self-compacting mix for monolithic pedestrian pavement.

Mathematical models were obtained that depended on the strength of concrete, microfiller additives, cement consumption, recipe, and technological factors, based on which the composition of the concrete mix was optimized.

References

[1] Samouplotnyayushchiysya beton – put v budushchee / D. Shutter // CPI. Mejdunar . concrete. pr-vo. – 2013. – No. 3. – S. 40–45.

[2] Classification razmernostey nanostruktur i svoystva kompozitssionnyx materialov / P. G. Komokhov [i dr.] // Academia . Architecture i strvo . – 2008. – No. 4. – S. 90– 93.

[3] Akchurin T. K. Teoreticheskie i metodologicheskie voprosy opredeleniya kharacteristic treshchinostoykosti betona pri staticheskom nagruzhenii / T. K. Akchurin, A. V. Ushakov. - Volgograd, 2005. - 407 p.

[4] Biopovrejdeniya v stroitelstve / pod ed. F. M. Ivanova, S. N. Gorshina. - M. : Stroyizdat , 1984. - 320 p.

[5] Lukutseva N.P. Osobennosti strukturobrazovaniya cementnogo kamnya s carbon-silica nanodispersnoy dobavkoy / N. P. Lukutseva , A. A. Pykin , E. G. Karpikov // Building materials. – 2011. – No. 9. – S. – 66–67.

[6] Sheikin A.E. Struktura i svoystva tsementnyx betonov / A.E. Sheykin , Yu.V. Chekhovsky, M. I. Brusser . - M. : Stroyizdat , 1979. -344 p.

[7] Belov V. V. Formation of optimal macrostructural building mixture / V. V. Belov, M. A. Smirnov // Stroit. material – 2009. – No. 9. – S. 88–90.

[8] Vybor kineticheskoy model destruction of composite material / E. V. Korolev, A. P. Proshin, S. A. Boltyshev , O. V. Koroleva . Chetenia RAASN. – Samara: SGASU, 2004. - S. 278–281.

[9] Glico A. O. Influence of the solid phase process on the formation of a hydrothermal solution and the formation of cracks and the evolution of the penetration system // Fizika zemli. – 2002. – No. 1– S. 53–59.

[10] Gorchakov G. I. Koeffitsienty temperature expansion and temperature deformation of building material / G. I. Gorchakov, I. N. Lifanov, L. N. Terexin. - M. : Izd-vo standartov, 1968. – 168 p.

[11] Gusev B. V. Vibrating technology for concrete / B. V. Gusev, V. G. Zazimko . - Kyiv, 1991. - 158 p.

[12] Dobshitz L. M. Physico-mathematical model of razrusheniya betona pri peremennom zamorajivanii i ottaivanii / L. M. Dobshits // Zhilishch. str -vo. – 2017. – No. 12. – S. 30–36.

[13] Pashchenko A.A. Armirovanie cementnogo kamnya mineralnym voloknom / A. A. Pashchenko, V. P. Serbian. – Kyiv: UkrNIINTI , 1970. - 45 p.Leonov A.A. Maintenance of automatic locomotive signaling. - M.: Transport, 1982. – 255.

Information about the author

Shaumarov Said Sanatovich	Tashkent State Transport University, “Building and industry facilities Construction Department professor (DSc), E-mail: shaumarovss@mail.ru Tel.: + 998712990026 https://orcid.org/0000-0001-8935-7513
Kandakhorov Sanjar Ishratovich	Tashkent State Transport University, “Building and industry facilities Construction Department associate professor (PhD), E-mail: sanjar.kandakharov@mail.ru Tel.: + 998500717191 https://orcid.org/0000-0002-3689-8794
Okilov Zafar Amon ugli	Tashkent State Transport University, doctoral student E-mail: zafar00700792@gmail.com Tel.: + 998903279009 https://orcid.org/0009-0002-5946-2050
Gulomova Aziza Abdumumin kizi	Tashkent State Transport University, doctoral student Tel.: + 998912078088

Modeling of curing under IR lamp of multilayer fiberglass parts based on epoxy binder and determination of heating effect on the process kinetics

U.D. Kosimov[1][a], A.D. Novikov[2], G.V. Malysheva[2][b]
[1]Tashkent state transport university, Tashkent, Uzbekistan
[2]Bauman Moscow State Technical University, Moscow, Russia

Abstract: The results of modeling the kinetics of the heating process of a 20 mm thick GFRP part are presented. Exothermic effects related to the peculiarities of epoxy binder curing were taken into account during modeling. Using Siemens NX software, the temperature distribution along the thickness of the fiberglass sample was determined. It was found that the curing process of composite structures of large thickness is significantly influenced by self-heating of oligomer, as well as the changing value of volumetric heat capacity in the process of polymerization.

Keywords: fiberglass, glass fiber-reinforced polymer (GFRP), epoxy binder, curing, infrared heating

1. Introduction

Nowadays, such polymer composite materials as glass plastics, organoplastics and basalt plastics are becoming more and more widespread and are used in aircraft construction, mechanical engineering, in the manufacture of rocket and space technology products and in many other industries [1, 2]. If the reinforcing filler in such PCMs is a fabric, in conditions of single and small-scale production, the main technology of parts manufacturing is vacuum infusion, and in conditions of mass production - pressure impregnation (a variation of which is RTM technology) [3].

As a rule, epoxy materials are used as a binder in the production of composite structures, the curing of which can occur at elevated temperatures ranging from 100°C to 200°C. The process of curing (or formation of mesh polymers) is an irreversible transition of the binder from liquid to solid state, which leads to polymers with a spatial structure. The choice of curing temperature is determined by the composition of the binder used, however, the kinetics of the heating process and the total duration of the curing process is influenced by the heat transfer mechanism, which is completely determined by the technological equipment used. In addition, the effect of self-heating has a significant influence, which is greater the greater the height of the liquid column of the polymerizing oligomer.

Most fiber reinforcing materials have low thermophysical characteristics (heat capacity and thermal conductivity), which leads to the occurrence of large temperature differences across the thickness of the composite structure during curing. Such reinforcing fillers include glass, basalt and organic fabrics (tapes, fibers). In the scientific literature, much attention has been paid to the study of the kinetics of the heating process during the curing of PCM parts, including glass-reinforced plastics [4-8], however, the vast majority of researchers considered only heating under convection conditions, in which drying cabinets (or ovens) are used as the technological equipment for heating. Nowadays, infrared heating units (IR units), which provide fast heating of thin-walled composite structures to temperatures of +150°C and even more due to radiation, are becoming more and more widespread.

The aim of the work is to study the kinetics of the curing process of fiberglass parts under the influence of infrared heaters of different radiation power.

2. Objects and methods of research

Theoretical evaluation of temperature distribution in the process of heating the part depending on the power of the used heater is carried out in this work. The calculation model is a square part made of fiberglass (Table 1) with geometric dimensions of 200x200x20mm. The tooling is made of the same material as the part. Stochastic glass mat was used as filler, which allowed to consider this PCM as isotropic. As a binder the epoxy composition of VSK-14-1 grade was used, which is widely used in aircraft construction.

Table 1

Properties of GFRP

Density, kg/m^2	1800
Specific heat capacity, J/(kg·°C)	900
Thermal conductivity, W/(m·°C):):	
λ_1	0,55
λ_2	0,55
λ_3	0,51
Coefficient of thermal expansion, °C^{-1}	$5 \cdot 10^6$

The simulation process was performed in the CAD/CAM/CAE program Siemens NX in the Pre/postprocessor application with tools for finite element modeling and visualization of results, which includes reference multidisciplinary simulation workflows.

The modeling process consisted of several steps:

- creation of an electronic geometric model of the part and tooling;
- creation of a finite element model that takes into account material properties and thermophysical properties of the structure;
- setting of boundary conditions and loads on the modeling object.

In addition, convection is modeled on all surfaces of the part, except for the bottom surface, to take into account the

[a] https://orcid.org/0009-0000-5681-524X
[b] https://orcid.org/0000-0003-1053-4906

characteristics of the environment - the air in the room. For this purpose, characteristics such as:

- convection coefficient, with a value of 15 $\frac{W}{m^2K}$;
- the initial ambient temperature is 25°C.

But at the same time, the settings were set to heat the ambient air at a rate of 0.5$\frac{°C}{min}$ max. to 36°C.

The next step was to set the radiation heating directed from the heaters from top to bottom on the part. The settings were:

- IR spectrum;
- value of heat loads at different lamp heating modes of 1600W and 2400W.

The thermo-optical properties of fiberglass with an emission coefficient equal to 0.8 were set for the parts.

The values of heat load, depending on the power of the used heating source, are given in Table 2.

Table 2

Heat load values as a function of time per grid element

Time, minutes	IR lamp power, W	Heat load
0-37	1600	0,05
37-40		0,14
40-…		0,27
0-20	2400	0,07
20-23		0,1
23-…		0,35

3. Results and discussion

Figure 1 shows the temperature distributions on the top, center and bottom of the part at 55 minutes of heating. Initially, heating was carried out to a temperature of +120°C. It was assumed that the heating duration would not exceed 30 min. Figs. 2 and 3 show how the temperature value changes along the thickness of the GFRP part depending on the power of the IR unit used for heating.

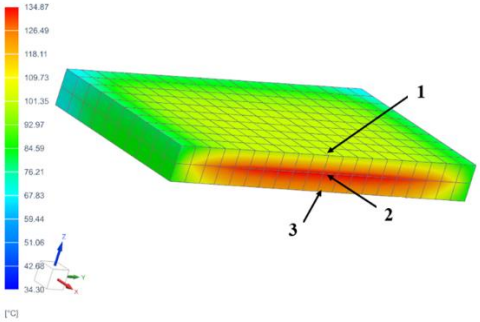

Figure 1. Example of temperature calculation on different parts of the part: 1 - top; 2 - middle; 3 - bottom

As a result of calculations, it was found that at the power of the heating unit of 1600 W (Fig. 2) it is not possible to provide heating to the required temperature for a given period of time (30 min) and therefore we limited heating to a temperature of +110°C. At 35 min, the heating was turned off, resulting in the top of the part cooling very quickly to a temperature of +80°C. However, at the same time, an exothermic reaction began, which actually provided an additional source of heat, allowing the temperature in the middle part of the part to reach +130°C at 55 minutes. The exothermic reaction provided heating of the middle and bottom parts of the part, e.g., the temperature on the bottom part of the part reached a temperature of +100°C only by 60 min. Thus, the use of an IR unit for heating, with a power of 1600 W not only does not provide uniform heating of the fiberglass part thickness, but also does not allow to reach the required heating temperature in a given period of time. At 60 minutes of heating, the difference between the top and bottom of the GFRP part was just over 20 °C.

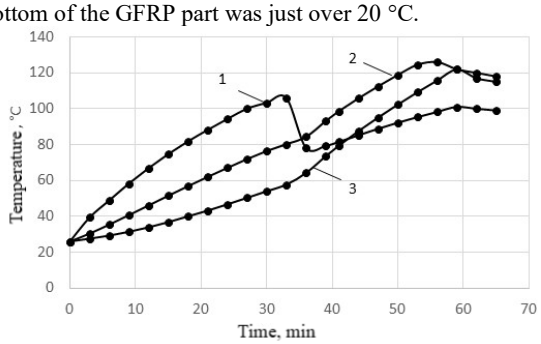

Figure 2. Temperature gradient along the thickness of the specimen at 1600W heater power for different parts of the part: 1 - top; 2 - middle; 3 - bottom.

Analysis of the results shown in fig. 3, allows us to draw the following conclusions: at a power of 2400 W the fiberglass part is heated significantly faster and reaches the temperature +160°C within 30 min. However, the character of temperature distribution in different parts of the part is completely similar to that presented in Fig. 2, i.e. immediately after switching off the heating source, there is a rapid cooling of the upper part of the part, while the middle and lower parts, on the contrary, are heated. Thus, at the peak of the exothermic reaction, a more uniform heating of all layers and reaching the required temperature values is observed over the entire time interval. At 50 minutes of heating, the difference between the upper and lower parts of the GFRP part was about 10°C.

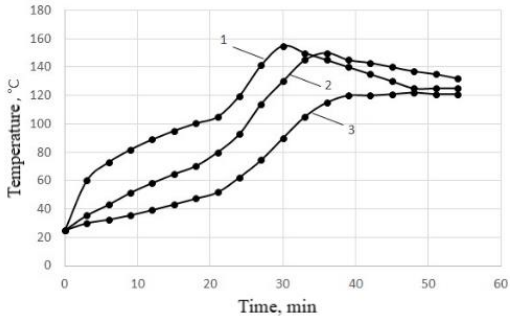

Figure 3. Temperature gradient along the specimen thickness at 2400W heater power for different parts of the part: 1 - top; 2 - middle; 3 - bottom

As the thickness of the part decreases, there is a proportional decrease in the values of the temperature gradient along the thickness, and for fiberglass parts, 5 mm thick, it is not more than 15°C, and for parts, 10 mm thick, it does not exceed 26°C.

4. Conclusion

A model of isotropic fiberglass plastic was developed and calculations were performed to determine the kinetics of temperature changes in different parts of the part (top, middle and bottom) when using infrared units for heating.

https://doi.org/10.56143/3030-3893-2025-1-8-10 A bridge between science and innovation

As a result of these calculations it was found that for an isotropic fiberglass part with a thickness of 20 mm, it is not possible to ensure its uniform heating along the thickness when using infrared heating units with a given power of 1600W and 2400W. The comparative analysis of two considered installations showed that only the installation with the power of 2400W allows to provide heating of the upper part of the fiberglass part up to the set temperature of +130°C for 22 min, but the values of temperature gradient along the thickness amounted to 45°C.

Thus, only the IR-heating unit with the power of 2400 W can be used for curing of GFRP parts with the thickness of 20 mm and more.

The structural properties are much better for composite parts with foam filler. While the Airex is about 1.5 times thicker, it is 4 times lighter than impregnated non-woven reinforcement material.

References

[1] Kablov E.N., CHursova L.V., Lukina N.F., Kutsevich K.E., Rubtsova E.V., Petrova A.P. Issledovanie epoksidno-polisul'fonovykh polimernykh sistem kak osnovy vysokoprochnykh kleev aviatsionnogo naznacheniia // Klei. Germetiki. Tekhnologii. 2017. №3. PP.7-12.

[2] Baurova N.I., Zorin V.A. Primenenie polimernykh kompozitsionnykh materialov pri proizvodstve i remonte mashin: ucheb. posobie. Moscow: MADI, 2016. 264 p.

[3] Maung P.P., Htet T.L., Malysheva G.V. Simulation and optimization of vacuum assisted resin infusion process for large0sized structures made of carbon fiber-reinforced plastic // IOP Conference Series: Materials Science and Engineeries. 2020. 709 (2). 022041.

[4] Kepman A V, Makarenko I V, Strakhov V L. Eksperimental'noe issledovanie kompleksa termokhimicheskikh, teplofizicheskikh svoistv i kinetiki protsessa otverzhdeniia polimernykh kompozitsionnykh materialov // Kompozity i nanostruktury, 2016. № 8(4): PP. 251-264.

[5] Borodulin, A. S. INFLUENCE OF CHEMICAL NATURE OF FILLER ON VALUE OF RESIDUAL STRESSES / A. S. Borodulin, U. D. Kosimov, G. V. Malysheva // Klei. Germetiki. Tekhnologii. 2024. no 3. pp. 17-20.

[6] KHaskov M A, Safronov E V. Modelirovanie protsessov otverzhdeniia termoreaktivnykh matrits na primere slozhnoprofil'nogo obraztsa // Trudy VIAM, 2019 №12 PP.46-54.

[7] Barinov D.IA., Maiorova I.A., Marakhovskii P.S., Zuev A.V., Kutsevich K.E., Lukina N.F. Matematicheskoe modelirovanie temperaturnykh polei pri otverzhdenii tolstostennoi plity stekloplastika // Perspektivnye materialy. 2015. №4. PP.5-14.

[8] Friedrich, K. Structure and properties of additive manufactured polymer components / K. Friedrich, R. Walter – M: Woodhead Publishing, 2020. – 431 p.

Information about the author

Kosimov Umidbek Dilshod ugli	Assistant of the “Aviation Engineering” Department of Tashkent state transport university E-mail: umidbek.k@yandex.ru Tel.: +99897 761 99 16 https://orcid.org/0009-0000-5681-524X
Novikov Andrey Dmitrievch	Ph.D. of Engineering Sciences, associate professor of the Department "Rocket and space composite structures" of Bauman Moscow State Technical University, Russia, Moscow E-mail: novikov.andrey.sm13@gmail.com
Malysheva Galina Vladlenovna	DSc. of Engineering Sciences, professor of the Department "Rocket and space composite structures" of Bauman Moscow State Technical University, Russia, Moscow E-mail: malyin@mail.ru https://orcid.org/0000-0003-1053-4906

Investigation of impregnation speed depending on fillers during the manufacturing of parts by the vacuum infusion method

U.D. Kosimov[1][a], I.A. Yudin[2], V.A. Eliseev[2], A.D. Novikov[2]
[1]Tashkent state transport university, Tashkent, Uzbekistan
[2]Bauman Moscow State Technical University, Moscow, Russia

Abstract: In the article examines the process of manufacturing three-layer carbon-fiber-reinforced plastic (CFRP) panels using the vacuum infusion method. A comparative analysis is conducted to assess the impact of various fillers on the manufacturability of the three-layer panel. Specifically, the study compares the impregnation speed of the part depending on the type of filler used.
For the research, the layers of carbon fabric and filler were laid simultaneously before sealing with vacuum film. A comparison was made between the manufacturability of using a non-woven reinforcing material (Soric) and polystyrene foam (Airex).

Keywords: polymer composite materials, carbon-fiber-reinforced polymer, vacuum infusion, filler, non-woven reinforcing material, polystyrene foam

1. Introduction

Polymer fiber composites have become indispensable in the aviation industry due to their unique combination of structural and special properties. Composite materials are an excellent alternative to traditional materials, as they offer significant advantages in terms of specific strength and stiffness. However, composite material products have significant anisotropy of properties. The three-layer design of the panels allows to adjust their stiffness anisotropy within wide limits, significantly increasing the stiffness of the structure with a slight increase in mass.[1]

The principles of operation of I-beam and three-layer structures are identical. In a three-layer structure, the role of the wall is played by the filler, due to which the load-bearing layers are separated, which gives the package of layers high characteristics of stiffness and strength at a relatively low weight. By combining materials of bearing layers and filler, it is possible to achieve the desired physical and mechanical properties of three-layer structures. The outer layers are called bearing layers and the inner layer is called filler. The outer layers are made of stronger materials (carbon fiber reinforced plastic). The inner layer (filler) is made of relatively low-strength materials with low density (nonwoven materials, plastic, polymer foam, lightweight methane.[2]

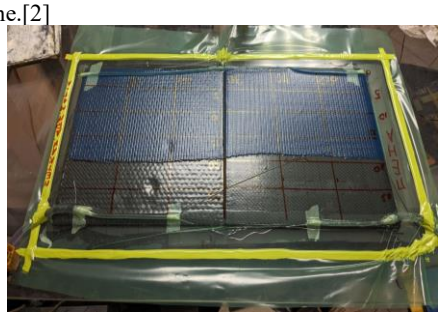

Figure 1. Test specimen

For products with small wall thicknesses, the most suitable is the technology of three-layer plate production, the carbon fiber cladding that is produced directly during panel forming by vacuum infusion. This production technology does not require expensive equipment and a large-sized production room, but makes it impossible to use honeycombs and corrugations as filler.

2. Research methodology

Degassed binder is fed into the prepared samples under pressure P=0.9 atm through the drainage system and distributed over the surface of the sample using a distribution grid. Then the binder is distributed on the package.

The package surface is marked in the Cartesian coordinate system to simplify the tracking of the binder front movement. During the experiment, time-synchronized photographic recording of the test was performed. During the test, the movement of the binder front was tracked from the top and bottom sides of the plates. Figure 2 is labeled: 1 - specimen with nonwoven reinforcing filler, 2 - specimen with foam, 3 - sacrificial fabric layer, 4 - conductive mesh, 5 - spiral tube, 6 - binder supply tube, 7 - tubes of connection to vacuumization unit.

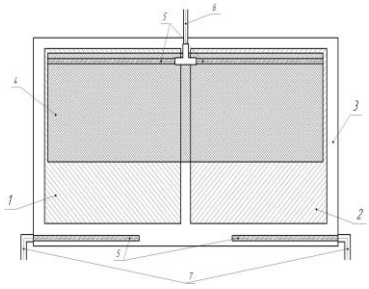

Figure 2. Schematic of the test specimen

3. Materials

2 laminates with dimensions of 300 x 300 mm were prepared as samples: 1st of 5 layers of carbon fabric, non-woven reinforcing material, 5 layers of carbon fabric; 2nd of 5 layers of carbon fabric, layer of perforated foam, 5 layers of carbon fabric. The detailed characteristics are summarized

[a] https://orcid.org/0009-0000-5681-524X

in Table 1 and Table 2. A glass plate was chosen as the tooling. On top of the carbon fabric, 1 layer of sacrificial fabric and a layer of conductive mesh were placed over the entire area.

Table 1

Characteristics of carbon fabric

Carbon fabric	
Weave type	Twill
Fiber	UMT45
Surface density, g/m²	240
Reinforcement directions, °	+45/-45

Table 2

Characteristics of fillers

Fillers	
Material type	Non-woven reinforcing material
Material grade	Lantor Soric XF
Density, g/m²	180
Impregnated density, kg/m³	600
Thickness, mm	3
Material type	Structural foam
Material grade	AIREX C70
Density, g/m²	200
Impregnated density, kg/m³	70
Thickness, mm	5

Table 3

Characteristics of consumables

Material type	Peel ply
Density, g/m²	80
Material type	Resin-conducting mesh
Surface density, g/m²	160

Table 4

Technological characteristics of epoxy resin

Wide processing window	2 hours
Initial viscosity, mPa*s	300
Binder temperature, °C	17-30

The first advantage of nonwoven reinforcing material - flexibility - is revealed at the stage of package molding; in order to bend the foam, it is necessary to heat it up to 70°C. It is also necessary to perforate the foam to improve the impregnation of the lower crust. However, the impregnated density of the foam is much lower.

4. Results and discussion

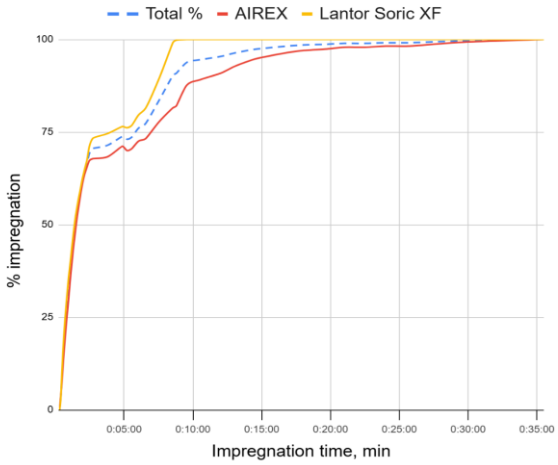

Figure 3. Graph of time dependence of percentage of binder impregnation on the top part of the plate

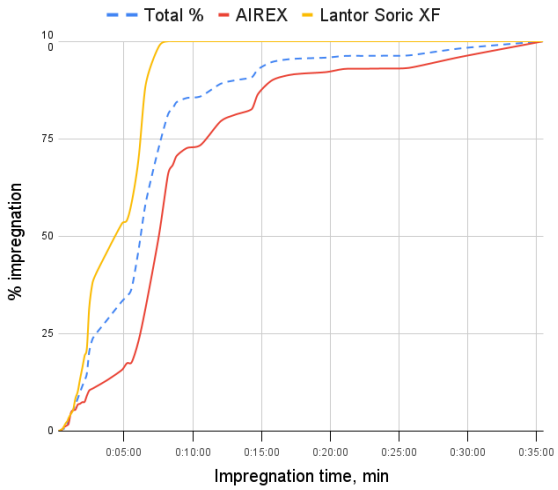

Figure 4. Graph of time dependence of the percentage of binder impregnation of the bottom part of the plate

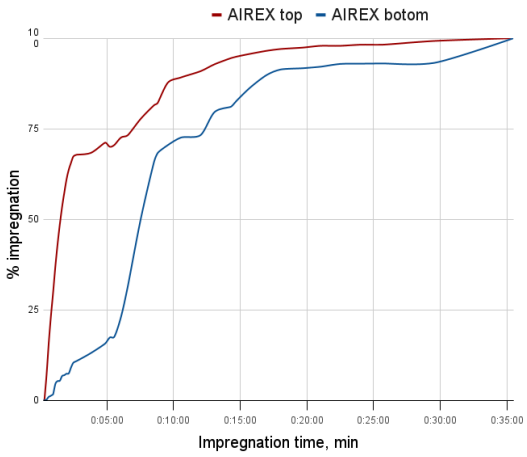

Figure 5. Graph of time dependence of the percentage of binder impregnation of the top and bottom part of the AIREX plate

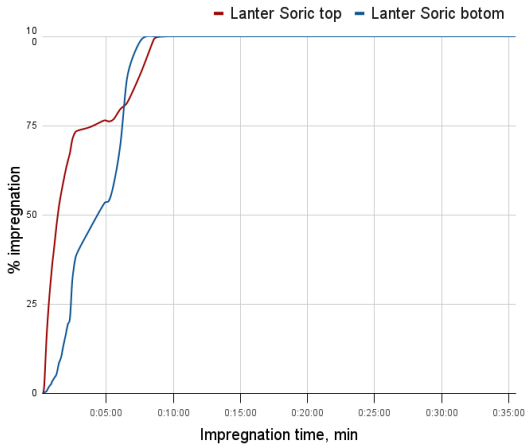

Figure 6. Graph of time dependence of the percentage of binder impregnation of the top and bottom part of the SORIC plate

Based on the processed results (fig. 3-6), the impregnation of the bag can be divided into 3 stages: 1 all inlets and outlets were open, until the binder passed through the entire distribution grid; 2 blocking the exit on the foam side; 3 Opening the exit on the foam side and blocking the exit on the SORIC side. The plate with SORIC soaked 3.7 times faster (9:20) than the similar plate with Airex(35:15). The lower crusts of both plates soaked much slower than the upper crusts, this is due to the presence of a distributing grid on the top. However, as soon as the binder front has reached the end of the distribution grid, the lower crust of the plate with SORIC starts to soak much faster than the upper crust due to the good conductivity of the non-woven filler. In the case of foam, this does not happen due to its lack of any conductivity.

5. Conclusion

Technological properties of non-woven reinforcing material are much better than similar properties of foam filler. Soric is easier to lay out, it is much better impregnated (3.7 times faster than foam).

When using non-woven reinforcing materials, it is necessary to leave a much larger retaining strip because of their good conductivity.

The structural properties are much better for composite parts with foam filler. While the Airex is about 1.5 times thicker, it is 4 times lighter than impregnated non-woven reinforcement material.

References

[1] Borodulin, A. S. INFLUENCE OF CHEMICAL NATURE OF FILLER ON VALUE OF RESIDUAL STRESSES / A. S. Borodulin, U. D. Kosimov, G. V. Malysheva // Klei. Germetiki. Tekhnologii. 2024. no 3. pp. 17-20.

[2] Borodulin, A. S. INFLUENCE OF CHEMICAL NATURE OF FILLER ON ADHESION STRENGTH VALUE / A. S. Borodulin, V. V. Mal'tsev, G. V. Malysheva // Klei. Germetiki. Tekhnologii. 2024. no 2. pp. 26-30.

[3] Tarasov D. D., Boiarchuk M. V., CHaplina E. S. INVESTIGATION OF EFFECT OF TECHNOLOGICAL SUPPORT ON MOLDING PROCESS QUALITY OF BASALTPLASTICS BY VACUUM INFUSION METHOD/ D. D. Tarasov, M. V. Boiarchuk, E. S. CHaplina // Klei. Germetiki. Tekhnologii. 2024. no 4. pp. 14-18.

[4] Konoplin A. Y., Baurova N. I. Hardness of the near-weld zone during contact spot welding of steels using an adhesive-weld technology // Russian Metallurgy (Metally). 2016. V. 2016. No 13. P. 1308-1311.

[5] Craddock, J.D. Method for direct measurement of on-axis carbon fiber thermal diffusivity using the laser flash technique / J.D. Craddock, J.J. Burgess, S.E. Edrington // Journal of Thermal Science and Engineering Applications. − 2017. − V. 9. − No. 1. − p. 014502.

[6] Das, T.K. Preparation, development, outcomes, and application versatility of carbon fiber-based polymer composites: a review / T.K. Das, P. Ghosh, N.C. Das // Advanced Composites and Hybrid Materials. − 2019. − No. 2. − pp. 214−233.

[7] Ding, J. Study on the curing reaction kinetics of a novel epoxy system / J. Ding, W. Peng, T. Luo // Rsc Advances. − 2017. − V. 7. − No. 12. − pp. 6981−6987. [8] Dmitriev, O.S. Thermo-chemical analysis of the cure process of thick polymer composite structures for industrial applications / O.S. Dmitriev, A.A. Zhyvenkova, A.O. Dmitriev // Advanced Materials & Technologies. − 2016. − No. 2. − pp. 53−60.

Information about the author

Kosimov Umidbek Dilshod ugli	Assistant of the “Aviation Engineering” Department of Tashkent state transport university E-mail: umidbek.k@yandex.ru Tel.: +99897 761 99 16 https://orcid.org/0009-0000-5681-524X
Yudin Ivan Alekseevich	Student of the " Rocket and space composite structures" Department of Bauman Moscow State Technical University, Russia, Moscow E-mail: ivan.a.yudin@gmail.com
Eliseev Vasiliy Andreevich	Student of the " Rocket and space composite structures" Department of Bauman Moscow State Technical University, Russia, Moscow E-mail: 13VasilyEliseev@gmail.com
Novikov Andrey Dmitrievch	Ph.D. of Engineering Sciences, associate professor of the Department "Rocket and space composite structures" of Bauman Moscow State Technical University, Russia, Moscow E-mail: novikov.andrey.sm13@gmail.com

Strength requirements for locomotive load-bearing structures: a literature review

Sh.Kh. Abdurasulov[1][a], N.S. Zayniddinov[1][b], Kh.R. Kosimov[1][c]
[1]Tashkent state transport university, Tashkent, Uzbekistan

Abstract: This analytical article explores the strength assessment of locomotive load-bearing structures, focusing on the critical role these components play in railway safety and efficiency. The article examines international and national standards, including EN 12663, EN 13749, and GOST 34939-2023, outlining their requirements for structural design, fatigue resistance, and testing methodologies. It highlights key aspects such as permissible stresses, material selection, and advanced evaluation methods, providing a framework for structural health monitoring and maintenance optimization. By addressing emerging technologies and their potential impact, this study offers valuable insights into the challenges and opportunities in modern railway engineering, emphasizing the necessity of rigorous and standardized approaches to structural analysis.

Keywords: traction rolling stock, locomotive, load-bearing structures, strength assessment, stress-strain state, static strength, fatigue strength

1. Introduction

The load-bearing structures of locomotives serve as the backbone of railway vehicles, transferring forces, absorbing impacts, and ensuring operational stability [1-12]. Given their exposure to dynamic loads, fatigue stresses, and environmental conditions, the accurate assessment of their strength is paramount for design validation and operational safety [13-15]. These critical components, including frames, bogies, and suspension systems, form the foundation of safe and efficient railway operations [16-18]. Recent advances in materials science and computational methods have revolutionized how engineers assess and predict structural behavior under various loading conditions. Modern engineering approaches aim to achieve an optimal balance between structural robustness and weight efficiency, demanding increasingly precise evaluation techniques.

The evolution of railway transportation systems has highlighted the critical importance of structural integrity assessment in preventing operational disruptions and ensuring public safety. While traditional evaluation methods have served the industry well, emerging technologies and analytical approaches offer new opportunities for enhanced structural health monitoring. These developments come at a crucial time, as railway operators worldwide face mounting pressure to extend equipment life cycles while maintaining rigorous safety standards. The integration of advanced materials, sophisticated computational models, and innovative testing methodologies presents both opportunities and challenges for the railway industry.

This review examines current methodologies for evaluating the strength of locomotive structural components, focusing on structural analysis techniques, material testing, and non-destructive evaluation (NDE) methods [19]. By comprehensively analyzing these approaches, this study aims to provide railway operators and engineers with a framework for implementing effective structural health monitoring systems, optimizing maintenance interventions, and enhancing overall railway safety and reliability. Furthermore, this research addresses the growing need for standardized evaluation protocols that meet both regulatory requirements and practical operational demands in modern railway systems.

The scope of this investigation encompasses both theoretical foundations and practical applications, with particular attention to emerging technologies that promise to transform traditional assessment methods. Through critical analysis of current practices and exploration of future possibilities, this study contributes to the ongoing dialogue about the evolution of structural integrity assessment in railway engineering. The findings presented here have significant implications for industry practitioners, regulatory bodies, and researchers working to advance the field of railway structural analysis.

2. Research methodology

Key regulatory documents

The evaluation of locomotive load-bearing structures requires strict adherence to a complex framework of regulatory and technical documentation. This analysis examines the current state of international and national standards, technical specifications, and regulatory requirements governing the assessment of structural integrity in railway applications.

Below is a list of international and national regulatory technical documents governing the assessment of the strength of load-bearing structures in locomotives:

- EN 12663: - Railway applications. Structural requirements of railway vehicle bodies [20];
- EN 13749: - Railway applications - Wheelsets and bogies - Method of specifying the structural requirements of bogie frames [21];

[a] https://orcid.org/0000-0001-5581-507X
[b] https://orcid.org/0000-0002-4700-3175
[c] https://orcid.org/0009-0002-8858-0259

• GOST 34939 Locomotives. Requirements for bearing structure strength and dynamic properties [22].

Requirements for locomotive bodies in accordance with EN 12663

EN 12663 is a European standard that defines structural requirements for railway vehicle bodies, ensuring safety, reliability, and performance. It is mandatory for railway manufacturers and operators in the European Union and serves as a benchmark globally.

The standard outlines comprehensive guidelines for the structural design and strength of passenger and freight vehicles. Key aspects include:

- Defining structural strength requirements for various vehicle types;
- Specifying load cases and design criteria under static and dynamic conditions;
- Establishing rules for mechanical strength and load-bearing structures;
- Setting requirements for body shell design and structural integrity.

EN 12663 ensures that railway vehicle structures are robust enough to withstand operational stresses and comply with stringent safety standards, making it critical for the design and maintenance of rolling stock in Europe and beyond.

Key aspects of strength requirements

The standard defines strength requirements through several key aspects:

1. Structural Load Cases

The standard specifies multiple load cases that railway vehicle bodies must withstand:

- Vertical static loads;
- Longitudinal static loads;
- Lateral static loads;
- Torsional loads;
- Fatigue loads;
- Exceptional loads (including potential collision scenarios).

2. Design Categories:

Strength requirements vary based on the vehicle category (L, P-I to P-V, F-I, F-II), with different design criteria for:

- Locomotives L;
- Passenger vehicles (urban rail vehicles, light rail vehicles) P;
- Freight vehicles F.

3. Key Strength Parameters:

- Maximum allowable stress levels;
- Deformation limits;
- Structural integrity under different load conditions;
- Fatigue life requirements;

Safety factor calculations

Permissible stresses for materials

When assessing structural stresses, the analysis must align with established material standards from European or national sources. It's crucial to carefully interpret stresses derived from finite element analysis or strain measurements.

For materials with ductile properties, a linear elastic analysis requires verifying that the stress range meets specific local stress concentration criteria.

$$|\sigma_{max} - \sigma_{min}| \leq 2 \times \frac{R}{S_1} \quad (1)$$

where

σ_{max} - is the maximum calculated stress of all static load cases;

σ_{min} - is the minimum calculated stress of all static load cases;

σ_{max} and σ_{min} - are oriented in the same direction;

R - is the material yield (R_{eH}) or 0.2 % proof stress (R_{p02}), in N/mm^2;

S_1 - is the safety factor (1.15 or 1).

Material strength limits should be defined by the lowest proof or yield strength and ultimate strength specified in the material's technical documentation.

For fatigue loading characteristics, engineers should rely on established standards from European, International, or national sources. If standard reference data is unavailable, organizations must conduct specialized tests to develop verified material performance information. When existing sources are insufficient, alternative credible references of equivalent quality may be used to determine material fatigue behavior.

Requirements for locomotive bogies in accordance with EN 13749

EN 13749 is a European Standard that specifically relates to the design and testing of railway bogie frames and associated components. This standard provides technical specifications and requirements for the design, calculation, and testing of railway bogie frames and their structural elements (bolsters and axlebox housings).

Key aspects typically covered in EN 13749 include:

- Structural design requirements for railway vehicle frames;
- Stress analysis methodologies;
- Fatigue and load testing procedures;
- Material selection and performance criteria;
- Safety and reliability standards for railway vehicle structures.

The standard is particularly important for manufacturers and engineers involved in designing railway rolling stock, ensuring that bogie frames meet rigorous safety and performance standards across European rail systems.

Key aspects of strength requirements according to EN 13749

EN 13749 outlines specific strength requirements for railway bogies, focusing on structural integrity, safety, and durability under various operational conditions. Here are the key aspects:

1. Static Strength:

- Defines load cases to simulate typical operating and extreme conditions (e.g., vertical, lateral, and longitudinal forces);
- Requires safety factors to account for uncertainties in material properties, manufacturing, and usage;
- Ensures bogies can withstand loads during normal operation and overload scenarios without permanent deformation or failure.

2. Fatigue Strength:

- Specifies cyclic loading tests to evaluate resistance to material fatigue over the bogie's service life;
- Includes stress limits and load cycles based on operational and environmental conditions;
- Focuses on critical components such as axles, frames, and welds.

https://doi.org/10.56143/3030-3893-2025-1-14-18 A bridge between science and innovation

3. Material and Joint Requirements:

- Specifies minimum properties for materials used in bogie construction, including high strength and fatigue resistance;
- Includes stringent requirements for welding quality and inspection to prevent structural weaknesses.

These requirements ensure bogies are designed to handle operational stresses reliably, reducing the risk of structural failure and enhancing railway safety.

Fatigue tests

The fatigue tests include dynamic twist loads, representing the stress on the bogie frame when navigating a 0.5% track twist. The programme has three stages (Figure 1):

1. **Stage 1:** 6 million cycles of vertical and transverse forces, plus 0.6 million cycles of twist loads.
2. **Stage 2:** 2 million cycles of vertical and transverse forces, with quasi-static and dynamic components increased by 20%, and 0.2 million cycles of twist loads, also increased by 20%.
3. **Stage 3:** Same as Stage 2, but with a 40% increase instead of 20%.

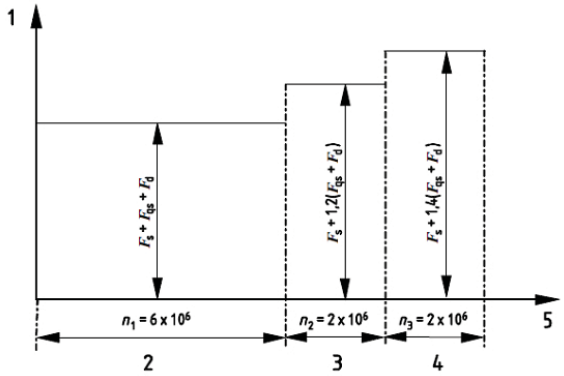

Figure 1. Variation of vertical and transverse force magnitudes during the test:
1-force magnitude; 2-first load sequence; 3-second load sequence; 4-third load sequence; 5-cycles

Requirements in accordance with GOST 34939-2023

GOST 34939-2023 is an interstate standard that establishes specific requirements for the strength and dynamic characteristics of locomotives intended for operation on railways with various speed regimes [23]. This standard plays a crucial role in ensuring the safety and reliability of railway transport.

Key strength requirements

The standard covers a wide range of requirements aimed at ensuring the strength and durability of locomotives:

- Strength of the running gear components: Special attention is paid to the strength of the frame, bogies, suspensions, and other elements that ensure reliable interaction between the locomotive and the railway track.
- Structural rigidity: The standard establishes requirements for the rigidity of load-bearing structures to minimize deformations and vibrations occurring during locomotive movement.
- Service life of components: Permissible wear and damage values for various locomotive components are determined to ensure their safe operation throughout their service life.
- Fatigue resistance safety factors: The fatigue resistance safety factors have been refined based on the intensity of locomotive operation, ensuring reliability under different operating modes.
- Operating conditions: The standard takes into account various operating conditions of locomotives, including climatic factors, loads, and other external influences.

The load-bearing capacity of the crew compartment structural elements is evaluated under the design loads established by this standard according to the permissible values of:

- stresses;
- strains;
- fatigue resistance safety factors;
- stability safety factors.

Stresses in structures under design loads must not exceed the permissible values given in Table 1.

The strength of the body (main frame) under the action of the standard longitudinal force applied along the axes of the coupling devices should be confirmed by collision testing, as well as by calculation or results of static bench tests with two-sided compression and tension. The following conditions determine the strength of the body (main frame):

- during impact testing: $\sigma \leq \sigma_{0.2}$;
- under static loading: $\sigma \leq 0.9\sigma_{0.2}$.

where $\sigma_{0.2}$ is the yield strength of the material used in manufacturing;

σ is the stress corresponding to the standard longitudinal force.

The fatigue resistance safety factors for the structures of the vehicle body (excluding wheelsets, traction drive shafts, gear wheels, and suspension springs) must be at least:

- 2.0 for steel structures;
- 2.2 for aluminum alloy structures.

To assess the fatigue resistance of bogie frames and intermediate frames (beams, crossbeams, etc.) of the secondary suspension system, bench vibration tests are conducted based on 10 million loading cycles. One sample is subjected to testing.

The stability factor for body elements (main frame) should be at least 1.10 for design modes I and IV.

Methods for strength evaluation

To confirm the conformity of locomotives to the requirements of GOST 34939-2023, the following methods of strength assessment are applied:

- Calculations: Complex engineering calculations are conducted using modern software to evaluate the strength of locomotive components under various loads.
- Tests: Locomotives undergo various tests, including static and dynamic, to verify their strength and reliability under real operating conditions.

Material quality control: The quality of materials used in locomotive manufacturing is rigorously monitored to ensure their compliance with established requirements

Design load cases

Calculation modes I-IV are used to assess strength based on permissible stresses (Table 1) relative to the material's yield strength.

To assess fatigue resistance, calculation mode III is used.

Mode I include:

- Mode Ia for accounting for maximum longitudinal quasi-static forces;
- Mode Ib for accounting for maximum longitudinal impact forces on the coupling device.

Mode II includes:

- Mode IIa for accounting for forces acting when moving in curved sections of the track with the maximum allowed uncompensated acceleration;
- Mode IIb for accounting for forces acting during start-up;
- Mode IIc for accounting for forces acting during emergency braking.

Mode III takes into account forces acting at various speeds, up to the design speed, along a straight section of track.

Mode IV is designed to account for forces caused by repair technology and emergency restoration work, arising:

- When lifting the body (main frame) on two diagonally positioned jacks;
- When lifting the locomotive by the automatic coupling device assembly;
- When rolling out a wheelset.

Table 1

Permissible stresses for body elements and bogies

Calculation mode	Permissible stress for elements	
	Body (main frame)	Bogie
Mode I, IV	$0.9\sigma_{0.2}$	
Mode II, III	$0.6\sigma_{0.2}$	

3. Conclusion

The evaluation of locomotive load-bearing structures is a cornerstone of railway safety and operational reliability. Through a detailed examination of standards such as EN 12663 and EN 13749, the article demonstrates the significance of structural design, material selection, and fatigue testing in meeting stringent safety requirements. GOST 34939-2023, with its specific provisions for different operational modes and climatic conditions, underscores the regional adaptability of such standards.

The study also reveals the transformative potential of advanced materials and computational methods in enhancing structural assessment, offering pathways to achieve a balance between robustness and weight efficiency. However, the integration of these technologies demands harmonised regulatory frameworks and comprehensive testing protocols to ensure consistent application across the industry.

Future advancements in structural health monitoring, including non-destructive evaluation techniques and predictive analytics, promise to revolutionise maintenance strategies, extending the lifecycle of railway equipment while maintaining safety and performance. This research reinforces the imperative for continued innovation and standardisation, enabling railway systems worldwide to meet the growing demands of safety, reliability, and sustainability.

References

[1] Yusufov, A., Khamidov, O., Zayniddinov, N., & Abdurasulov, S. (2023). Prediction of the stress-strain state of the bogie frames of shunting locomotives using the finite element method. In E3S Web of Conferences (Vol. 401, p. 03041). EDP Sciences.

[2] Abdurasulov, S., Zayniddinov, N., Yusufov, A., & Jamilov, S. (2023). Analysis of stress-strain state of bogie frame of PE2U and PE2M industrial traction unit. In E3S Web of Conferences (Vol. 401, p. 04022). EDP Sciences.

[3] Zayniddinov, N., & Abdurasulov, S. (2022). Durability analysis of locomotive load bearing welded structures. Science and Innovation, 1(8), 176-181.

[4] Vega, B., & Pérez, J. Á. (2024). Comparative analysis of fatigue strength of a freight wagon frame. Welding in the World, 68(2), 321-332.

[5] Zhao, W., & Zeng, Y. (2023, June). Comparative study of static strength and fatigue strength tests and simulation analysis of an exit subway bogie frame. In Third International Conference on Mechanical Design and Simulation (MDS 2023) (Vol. 12639, pp. 880-892). SPIE.

[6] Slavchev, S., Maznichki, V., Stoilov, V., Enev, S., & Purgic, S. (2018). Comparative analysis of fatigue strength of an y25ls-k bogie frame by methods of UIC AND DVS 1612. Czech Republic.

[7] Dizo, J., harusinec, J., & Blatnicky, M. Computation of modal properties of two types of freight wagon bogie frames using the finite element method. Manufacturing Technology [online]. 2018, 18 (2).

[8] Šťastniak, P., Moravčík, M., Baran, P., & Smetanka, L. (2018). Computer aided structural analysis of newly developed railway bogie frame. In MATEC Web of conferences (Vol. 157, p. 02051). EDP Sciences.

[9] Boronenko, Y., & Rahimov, R. (2021). Experimental determination of forces through measurements of strains in the side frame of the bogie. Transport problems, 16.

[10] Wang, Q., Zhou, J., Wang, T., Gong, D., Sun, Y., Chen, J., & You, T. (2021). Extrapolation of the dynamic stress spectrum of train bogie frame based on kernel density estimation method. Fatigue & Fracture of Engineering Materials & Structures, 44(7), 1783-1798.

[11] Qu, S., Wang, J., Zhang, D., Li, D., & Wei, L. (2021). Failure analysis on bogie frame with fatigue cracks caused by hunting instability. Engineering Failure Analysis, 128, 105584.

[12] de Cisneros Fonfría, J. J. J., Olmeda, E., Sanz, S., Garrosa, M., & Díaz, V. (2024). Failure analysis of a train coach underframe. Engineering Failure Analysis, 156, 107756.

[13] Kassner, M. (2012). Fatigue strength analysis of a welded railway vehicle structure by different methods. International journal of fatigue, 34(1), 103-111.

[14] Xiu, R., Spiryagin, M., Wu, Q., Yang, S., & Liu, Y. (2020). Fatigue life assessment methods for railway vehicle bogie frames. Engineering Failure Analysis, 116, 104725.

[15] Mukhamedova, Z., Fayzibayev, S., Mukhamedova, D., Batirbekova, A. M., Jurayeva, K., Ibragimova, G., & Ergasheva, Z. (2024). Calculating the fatigue strength of load-bearing structures of special self-propelled rolling stock. Scientific Reports, 14(1), 19205.

[16] Хамидов, О. Р., Юсуфов, А. М. У., Зайниддинов, Н. С. У., Жамилов, Ш. Ф. У., & Абдурасулов, Ш. Х. (2023). Оценка долговечности сварных несущих конструкций локомотивов. Universum: технические науки, (2-3 (107)), 48-53.

[17] Abdurasulov, S. X., Zayniddinov, N. S. O. G. L., & Yusufov, A. M. O. G. L. (2023). Sanoat

lokomotivlarining xizmat muddatini uzaytirishda bajariladigan asosiy ishlar. International scientific journal of Biruni, 2(3), 55-62.

[18] Abdurasulov, S., Zayniddinov, N., & Yusufov, A. (2023). O‘zbekiston Respublikasi tog‘-kon sanoatida foydalanilayotgan tortish agregatlari parkining tahlili. Journal of Research and Innovation, 1(9), 16-24.

[19] Khamidov, O. R., Yusufov, A. M., Kodirov, N. S., & Abdurasulov, S. X. (2023). Determination of the resource of parts and assembly of the traction rolling stock using non-destructive testing methods. In Железнодорожный подвижной состав: проблемы, решения, перспективы (pp. 510-514).

[20] European Committee for Standardization (CEN). (2010). EN 12663: Railway applications. Structural requirements of railway vehicle bodies.

[21] European Committee for Standardization (CEN). (2011). EN 13749: Railway applications. Wheelsets and bogies. Method of specifying the structural requirements of bogie frames.

[22] Interstate Council for Standardization, Metrology and Certification. (2023). GOST 34939: Locomotives. Requirements for bearing structure strength and dynamic properties.

[23] Abdurasulov, S. (2023). Requirements for the strength of load-bearing structures of locomotives. Acta of Turin Polytechnic University in Tashkent, 13(4), 44-48.

Information about the author

Sherzamin Khayitbaye-vich Abdurasulov	Tashkent State Transport University, PhD student E-mail: sherzamin.tstu@gmail.com Tel.: +998900210493 https://orcid.org/0000-0001-5581-507X
Nuriddin Savranbek ugli Zayniddinov	Tashkent State Transport University, Associate Professor of the Department of "Locomotives and Locomotive Establishment", PhD in Engineering Science. E-mail: nuriddin24@mail.ru Tel.: +998935837785 https://orcid.org/0000-0002-4700-3175
Khusan Rakhmatulla-evich Kosimov	Tashkent State Transport University, Senior Lecturer at the Department of Locomotives and Locomotive Establishment E-mail: qosimov_husan@mail.ru Tel.: +998974012183 https://orcid.org/0009-0002-8858-0259

Principles of forming an innovative architectural and planning structure for preschool institutions

E.V. Shchipacheva[1][a], S.S. Shaumarov[1][b], M. Pazilova[1]
[1]Tashkent state transport university, Tashkent, Uzbekistan

Abstract: The article is devoted to the study of foreign experience in designing innovative-type preschool institutions for children. The analysis of design solutions has allowed us to identify the main principles of architectural and planning structure of preschool institutions, taking into account climatic, geophysical and national characteristics of the region: providing multifunctional educational process, transformation of space, mobility, inclusiveness, architectural expressiveness, integration with the landscape, implementation of the principles of sustainable architecture. The established principles can contribute to the creation of innovative types of educational preschool institutions capable of meeting the needs of modern society in the Republic of Uzbekistan.

Keywords: preschool institution, architectural and planning structure, planning modules, space transformation, kindergarten architecture, educational environment

1. Introduction

A characteristic feature of modern society is the activation of innovative processes in education, including preschool education. Teaching standards and methods are changing, and components of the educational process are being updated to ensure its mobility, flexibility, and variability. Moreover, the rapid development of information technologies, the need to create an atmosphere of creativity, and the trend towards child-centered education require special organization of the architectural and planning space of preschool institutions. As a result, existing standard designs for nurseries and kindergartens do not meet the demands of the times, and architects and designers face the challenge of developing new conceptual approaches to the design of preschool buildings. In foreign countries, considerable work is being done to expand the typology of preschool buildings, demonstrating a variety of approaches to their design and an effort to align them with the concept of modern preschool education development [1, 2, 3, 4]. Therefore, studying and borrowing foreign experience may help create a domestic innovative architectural and planning structure for preschool institutions that takes into account the climatic, geophysical, and national characteristics of the region.

2. Results and discussion

2.1. Foreign Experience in Designing Preschool Institutions

To establish modern trends in improving the architectural and planning structure of preschool institutions, recent projects of such buildings were studied. It should be noted that all of these buildings implemented common principles, such as considering child psychology, creating environments that develop children's intellectual, physical, and creative abilities, using environmentally friendly materials, applying unconventional energy sources, creating bright and unusual architectural forms, and adapting to the surrounding landscape. However, the primary interest for our research was focused on objects with new functional and planning solutions for preschool buildings.

For example, the kindergarten in Vinh (Vietnam, 2019) can be characterized as a developing, safe, and sustainable facility (Fig. 1) [5]. In addition to the standard set of rooms, this kindergarten features new functional spaces, such as a sports center with a swimming pool, art classrooms, a media center, and open recreation areas that are oriented towards active learning and interaction with the surrounding natural environment.

Fig. 1. The kindergarten in Vinh, Vietnam [5]

The Kaleidoscope Kindergarten in Tian Shui (China, 2020) is notable for its planning, which includes a three-story multifunctional atrium that can be used depending on the events being held (Fig. 2).

[a] https://orcid.org/0009-0000-0489-445X
[b] https://orcid.org/0000-0001-8935-7513

Fig. 2. Interior with atrium of a kindergarten in Tianshui, China [5]

In the kindergarten building in Wuxi (China, 2014), one of the main principles is ensuring the safety of children in the midst of multi-story buildings and intensive traffic on nearby streets. This is achieved by creating an inner courtyard for children's walks and play, located at the center of the building in an oval shape (Fig. 3).

Fig. 3. Kindergarten building in Wuxi, China [5]

The method of internal transforming spaces is implemented in the innovative kindergarten in Stupino (Russia, 2023) (Fig. 4). Here, the technology of transforming partitions allows the expansion of play areas or, conversely, the partitioning of a small part of the room for educational activities [6].

Fig. 4. Kindergarten in Stupino (Russia)

The Timayui preschool in Santa Marta (Colombia, 2011) was designed based on a universal modular system (Fig. 5) [7]. Each module consists of three rectangular blocks: two contain group rooms, and the third is a multifunctional open room with sanitary facilities, connected by a recreational area. The modules are linked by galleries and can be adapted for other purposes, such as kitchens, dining rooms, and service areas.

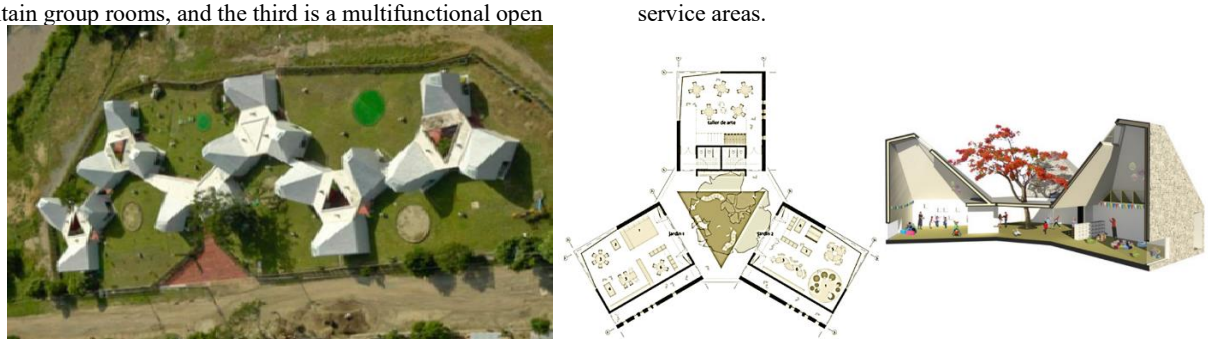

Fig. 5. Timayui kindergarten in Santa Marta, Colombia [7]

This modular structure allows the building to have flexible planning and the potential for "growth" (adding more modules) if needed due to functional requirements or increased capacity.

The analysis of modern foreign preschool buildings has allowed us to identify key principles for forming an innovative architectural and planning structure for these institutions, which have been further adapted to the climatic, geophysical, and national characteristics of Uzbekistan.

2.2. Principles of Forming the Architectural and Planning Structure of Innovative Preschool Institutions for the Republic of Uzbekistan

1. Ensuring the Multifunctionality of the Educational Process.

The modern preschool education system is highly dynamic, responding to the needs of society and individuals. It must guarantee a high level of education necessary for a child's comprehensive development and successful socialization, as well as the development of skills such as curiosity, creativity, and communication. Therefore, the structure of preschool institutions should include an increased number of rooms for educational, creative, cognitive, research, play, and sports purposes: media centers, libraries, museums, exhibitions, art workshops, music and dance classes, playrooms, sensory and cognitive development centers, recreational spaces, swimming pools, physical education halls, etc.

Spaces for cognitive research activities, defined by short-term sessions, can also be used by children who live in the area but do not attend the preschool regularly.

2. Transformation of Space

The emergence of various functional and spatial areas within preschool institutions requires rational use of space, minimizing underutilized corridors and passageways. One of the ways to achieve this is by implementing transforming partitions, which allow large spaces to be divided into smaller zones or, conversely, combine small rooms into one large space.

For example, group rooms in modern preschools should be flexible and adapted to changing ecosystem conditions. The classic zoning scheme, based on isolating rooms (cloakroom, group room, bedroom, bathroom), no longer meets these requirements. Transforming partitions can be used to include additional spaces such as recreation areas and corridors into the required zone.

Another example could be the transformation of adjacent halls for physical and music classes, separated by a transforming partition, which can be combined if needed for mass events. Additionally, if there are rooms such as a dance hall or storage rooms next to these halls, transforming partitions can create additional space for temporary seating during holidays or sports events.

3. Mobility

A preschool building should be able to change in line with the rapid development of innovative pedagogical technologies, improvements in teaching methods, and societal needs. The most convenient spatial structure is modular, allowing for gradual expansion and transformation of the building. However, the territory of the preschool institution should also have corresponding reserves.

4. Inclusivity

Preschools should integrate children with disabilities, creating conditions for the successful learning and development of every child. Buildings should ensure comfortable movement through ramps, elevators, and wide, accessible corridors.

5. Architectural Expressiveness

The architecture of a preschool building should reflect the spiritual and emotional world of children, as well as the natural and national characteristics of the region. The facade should be enriched with details that convey positive and educational messages, which can be expressed through the use of "smart surfaces" that react to human actions and large glazed areas. The aesthetic quality of the building can be enhanced by using colored, tinted glass in communication zones (corridors, staircases, vestibules).

6. Integration with the Landscape

To promote ecological education and harmonize with the surrounding environment, the building should include winter gardens and recreation areas with large glass surfaces, primarily oriented toward the southern horizon. Another approach, particularly useful in densely built urban areas, is to create an open playground with grass on the roof of the preschool. Natural landscape elements (biozones, barriers for regulating air flow) should be used to create a favorable microclimate for the area.

7. Implementation of Sustainable Architecture Principles

Preschools should be designed to be durable, seismic-resistant, and long-lasting. To allow for changes in planning structures based on evolving societal demands, a frame construction system is most suitable.

Preschools should also be energy-efficient buildings, using eco-friendly construction materials that are low-energy in production. To maintain a comfortable microclimate, renewable energy sources (solar panels, heat pumps, wind turbines, etc.) should be incorporated, depending on their efficiency in the given climate zone [8]. Solar shading devices, reflective materials, and "horizontal" and "vertical" greenery elements can protect the building from excessive solar radiation during hot periods.

3. Conclusion

The basic principles of formation of architectural and planning structure of children's preschool institutions established on the basis of foreign experience can contribute to the expansion of the typology of buildings of this purpose, to orient their volume-planning solution to meet the rapidly developing innovative processes in preschool education and to ensure the formation of children's modern outlook and their socio-cultural adaptation.

References

[1] Ильвицкая С.В., Михайлова И.В. Опыт проектирования зарубежных дошкольных образовательных учреждений: приёмы формирования архитектурно-планировочной структуры // Вестник БГТУ им. В.Г. Шухова. 2019. №1. С. 86–94. DOI: 10.12737/article_5c5062211a3dd9.52830943

[2] Золотник С.В., Международный опыт создания объемно-пространственной структуры учреждений дошкольного образования. Принципы формирования планировочного решения [Электронный ресурс] // Инженерный вестник Дона. 2017. №1. URL: http://ivdon.ru/ru/magazine/archive/n1y2017/4012 (12.01.2025)

[3] Кудрявцева С.П., Долотказина Н.С. Инновационные подходы к проектированию пространства и архитектуры современных дошкольных

образовательных учреждений// Инженерно-строительный вестник Прикаспия. 2014. № 3 (9). С. 4–9.

[4] Top 10 Amazing Modern Kindergartens Where Your Children Would Love to Go URL: https://www.designrulz.com/design/2014/10/top-10-amazing-modern-kindergartens-children-love-go (19.01.2025)

[5] Леденева Н., ТОП-10 необычных современных детских садов мира ARCHITIME.RU URL: https://www.architime.ru/specarch/top10_kindergarten2/kindergartens_s.htm (15.01.2025)

[6] Инновационный детсад в Ступино проверяют на соответствие проекту и безопасность URL: https://gusn.mosreg.ru/sobytiya/novosti-ministerstva/11-08-2023-16-28-07-innovatsionnyy-detsad-v-stupino-proveryayut-na-soo (16.01.2025)

[7] Amy Frearson, Timayui Kindergarten by el Equipo de Mazzanti URL: https://www.dezeen.com/2012/02/01/timayui-kindergarten-by-el-equipo-de-mazzanti (16.01.2025)

[8] Щипачева Е.В., Шарипова Д.Т. Применение системного анализа при оценке энергетических возможностей климата Узбекистана [Текст] // Материалы международной научно-практической конференции - Инновация-2017 / - Ташкент, 2017 С. 127-128.

Information about the author

Shchipacheva Elena Vladimirovna	Tashkent State Transport University, DSc, professor of the department “Construction of buildings and industrial structures” E-mail: eshipacheva@mail.ru https://orcid.org/0009-0000-0489-445X
Shaumarov Said Sanatovich	Tashkent State Transport University, professor of the department “Construction of buildings and industrial structures” (DSc), E-mail: shaumarovss@mail.ru Tel.: + 998712990026 https://orcid.org/0000-0001-8935-7513
Pazilova M.	4th year student of Tashkent State Transport University

Distribution of braking forces between vehicle bridges and redistribution of braking mass

K.B. Khakkulov[1][a]
[1] Jizzakh Polytechnic Institute, Jizzakh, Uzbekistan

Abstract: The distribution of braking forces between vehicle bridges and the redistribution of braking mass are crucial factors affecting vehicle stability and braking performance. In multi-axle and articulated vehicles, improper braking force distribution can lead to instability, reduced braking efficiency, and increased risk of accidents. This study investigates the dynamics of braking force distribution and mass redistribution using theoretical models, computational simulations, and experimental testing. Theoretical models based on Newtonian mechanics predict that the front axles bear more braking force due to load transfer during deceleration. Simulations using multi-body dynamics software confirm that suspension systems and braking technologies like Electronic Brake force Distribution improve force balance. Experimental testing on various vehicles validates these results, demonstrating how load distribution affects vehicle stability during braking. The findings highlight the importance of optimizing braking force distribution in multi-axle and articulated vehicles to ensure safe and efficient braking under diverse conditions.

Keywords: braking forces, vehicle, rear axles, maneuvers, safety

1. Introduction

The braking system is one of the most critical components in a vehicle, responsible for ensuring its safe operation by reducing speed or bringing it to a complete stop when necessary. In particular, the distribution of braking forces and the redistribution of braking mass play pivotal roles in optimizing braking performance, vehicle stability, and overall safety [1]. The interaction between the braking forces applied to the vehicle's axles (or bridges) and the mass redistribution during braking is essential for understanding the vehicle's behavior under different driving conditions, especially in emergency or high-speed situations [2,3].

Braking forces are the forces exerted on the vehicle to decelerate or stop it. When a driver presses the brake pedal, hydraulic or pneumatic pressure is applied to the brake pads or shoes, creating friction against the rotating wheels [4]. This frictional force is transmitted through the vehicle's suspension system to the axles, ultimately affecting the vehicle's speed. The force generated by the braking system is not uniformly distributed across the vehicle's axles; instead, it is subject to a variety of dynamic factors that influence how these forces are shared between the vehicle's front and rear axles, and in the case of multi-axle vehicles, across additional axles or bridges [5,6].

Braking force distribution refers to the way in which the total braking force is allocated between the vehicle's front and rear axles [7]. Ideally, the braking force should be split in a manner that optimizes vehicle stability and minimizes the risk of skidding or loss of control. An improperly distributed braking force can lead to dangerous outcomes, such as the vehicle's rear end lifting off the ground or the front tires losing traction, leading to instability and a potential loss of control [8].

Vehicle bridges, in this context, refer to the segments of the vehicle's structure that connect multiple axles, such as in articulated or heavy-duty vehicles (trucks, buses, or trailers). In these vehicles, braking forces must be distributed across the multiple bridges to ensure the vehicle maintains stability and effective stopping power. For example, a trailer with multiple axles (bridges) requires careful management of braking forces, with each axle receiving a different proportion of the total braking force based on factors like load, weight distribution, and braking system design [9].

The interaction between the braking system and the bridges involves dynamic forces during braking, including load transfer from the front to the rear of the vehicle, as well as the redistribution of mass across the vehicle's structure. These forces can cause significant changes in how the vehicle behaves under braking, potentially leading to uneven tire wear, increased stopping distances, and vehicle instability. Hence, the design of braking systems must account for the distribution of braking forces across vehicle bridges, ensuring that each bridge handles its designated portion of the braking load. When a vehicle brakes, the forces applied to the vehicle cause a redistribution of its mass, primarily due to the inertia of the vehicle. This redistribution occurs because the vehicle experiences dynamic load transfer during deceleration. Load transfer refers to the shift in the vehicle's weight between the axles as the braking forces act on the vehicle [10,11].

2. Research methodology

Many countries have conducted research on the distribution of braking forces and the redistribution of braking mass between automotive bridges (Fig 1).

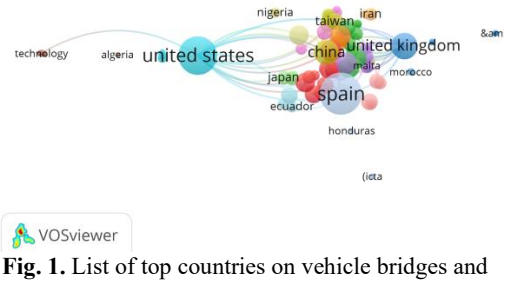

Fig. 1. List of top countries on vehicle bridges and redistribution of braking mass

[a] https://orcid.org/0000-0002-1291-4884

The study of the distribution of braking forces between vehicle bridges and the redistribution of braking mass is approached through both theoretical modeling and computational simulations [12]. The first step involves developing a theoretical framework that accounts for the basic principles of vehicle dynamics under braking. This framework relies on Newtonian mechanics, focusing on how braking forces are distributed between the vehicle's axles and how mass is transferred from the rear to the front of the vehicle during deceleration [13].

The braking force distribution is modeled using the following equations:

$F_{front} = W_{front}/W_{total} * F_{total}$

$F_{rear} = W_{rear}/W_{total} * F_{total}$

Where Wfront and Wrear represent the weight at the front and rear axles, and Ftotal is the total braking force. The load transfer effect is accounted for by calculating the shift in weight during braking, using a load transfer equation [14]:

$\Delta W = m \cdot g \cdot d \backslash L \cdot a$

Where ΔW is the change in load, mm is the vehicle's mass, d is the distance from the center of gravity to the axle, and a is the deceleration.

3. Results and discussion

The analysis of braking force distribution between vehicle bridges and the redistribution of braking mass produced several key findings regarding the dynamics of braking in multi-axle and articulated vehicles. The theoretical models, computational simulations, and experimental testing all provided insights into the behavior of braking forces and how mass is redistributed during deceleration.

1. Theoretical Model Results

The theoretical model provided a foundational understanding of how braking forces are distributed between the front and rear axles and between different vehicle bridges. The equations used to calculate braking force distribution and load transfer showed that, under typical braking conditions, the front axle carries a greater share of the braking load due to the forward load transfer that occurs during deceleration.

For example, in a typical passenger vehicle with a 60/40 front/rear weight distribution, the braking force on the front axle is approximately 60% of the total braking force, with the remaining 40% applied to the rear axle. The theoretical model also confirmed that as deceleration increases, the load transfer to the front axles becomes more pronounced, particularly at higher speeds or under emergency braking conditions. This result aligns with the basic principles of braking dynamics, where the vehicle's center of gravity shifts forward, increasing the load on the front tires.

In multi-bridge vehicles, such as trucks and trailers, the model showed that the braking force is more complex, with multiple axles (or bridges) sharing the total braking load. The force on each axle is influenced by the weight distribution, suspension characteristics, and the distance between the axles and the vehicle's center of gravity. For articulated vehicles, the braking force distribution was found to be more sensitive to the relative load on each bridge, with larger shifts in braking force between the front and rear bridges.

2. Experimental Testing Results

Experimental testing involved real-world braking tests on different vehicle types, including light-duty cars, trucks, and buses. The tests focused on measuring the braking forces on each axle, as well as assessing the redistribution of mass during braking.

For light-duty vehicles, the results showed that the braking force distribution was consistent with the theoretical model, with approximately 60% of the total braking force applied to the front axle. The braking forces were measured using strain gauges and force sensors placed on the axles, and load transfer was quantified using accelerometers to track shifts in the vehicle's center of gravity. During emergency braking, the front axle consistently experienced higher braking forces, while the rear axle experienced a reduction in braking force due to the load transfer.

For heavy-duty trucks and articulated vehicles, the experimental results demonstrated the significant role of bridge configurations in braking force distribution. When braking forces were applied to a multi-axle vehicle with a semi-trailer, the results indicated that the braking forces were not evenly distributed across all axles. The tractor's front axle bore a higher proportion of the braking force, while the rear axles of both the tractor and trailer showed greater load transfer. However, the presence of EBD systems in the tests helped balance the braking forces, preventing excessive force on any single axle and ensuring a more stable braking performance.

In addition to measuring braking forces, the experimental tests also included evaluations of vehicle stability during braking. For articulated vehicles, tests under high-speed conditions showed that improper braking force distribution could lead to instability, such as trailer swing or jackknifing. These issues were mitigated by adjusting the braking force distribution through EBD and enhancing the coordination between the tractor and trailer brakes

4. Conclusion

The distribution of braking forces between vehicle bridges and the redistribution of braking mass are crucial factors that influence vehicle stability, safety, and performance during braking. By understanding and optimizing the way braking forces are distributed across the vehicle's structure and how the mass is redistributed during braking, engineers can improve the safety and efficiency of braking systems, particularly in multi-axle and articulated vehicles. Future research and advancements in braking technology, including adaptive systems that dynamically adjust braking force distribution, hold the potential to further enhance vehicle performance and contribute to the development of safer, more efficient transportation systems.

References

[1] Kabardin, O.F. Physics: Reference materials: Textbook for students / O.F. Kabardin - M.: Enlightenment, 1991. - 367 p.

[2] Li, R., Chen, Y. V., & Zhang, L. (2021). A method for fatigue detection based on Driver's steering wheel grip. International Journal of Industrial Ergonomics, 82, 103083

[3] Nurullayev, U., Otaqulov, Z., & Egamnazarov, N. (2021). Qish mavsumida avtomobil yo'llarining o'tkazish darajasiga qo'yiladigan talablar. Academic research in educational sciences, 2(2), 181-189.

[4] Mironova, Yu. A. Study of the processes of braking of foreign and domestic cars: Methodological recommendations / Yu.A. Mironova, E.A. Kitaigorodsky - M .: ECC of the Ministry of Internal Affairs of Russia, 2005. - 176 p.

[5] Ilarionov, V.A. Automotive expertise. / V.A. Ilarionov. - M.: Transport, 1989. - 240 p.

[6] Kondé, A. K., Rosu, I., Lebon, F., Brardo, O., & Devésa, B. (2013). On the modeling of aircraft tire. Aerospace Science and Technology, 27(1), 67-75.

[7] Fuentes, L., Gunaratne, M., & Hess, D. (2010). Evaluation of the effect of pavement roughness on skid resistance. Journal of Transportation Engineering, 136(7), 640-653.

[8] Wang, D., Chen, X., Oeser, M., Stanjek, H., & Steinauer, B. (2014). Study of micro-texture and skid resistance change of granite slabs during the polishing with the Aachen Polishing Machine. Wear, 318(1-2), 1-11.

[9] Suvanov, U., Hamraqulov, Y., & Agzamov, J. (2021). Transport vositasining texnik holat masalalari. Academic research in educational sciences, 2(2), 610-616.

[10] Azimov, A., & Muxtarov, A. (2021). Avtotransport korxonalarida texnik xizmat ko'rsatish va ta'mirlash ishchilarini kompetensiyaviy yondoshuv asosida tayyorlash va malakasini oshirish metodikasi. Academic research in educational sciences, 2(1).

[11] Velikanov, D.P. and others. Razvitie avtomobil'nykh transportnykh sredstv [The development of automotive vehicles], Moscow, 1984, 120 p. [in Russian].

[12] Chen, Y., & Zhang, L. (2013). Dynamic load transfer in articulated vehicles during braking. Journal of Vehicle Dynamics, 45(3), 315-330.

[13] Khalil, M., Al-Mahaidi, R., & Baker, A. (2017). The effects of braking force distribution on the stability of multi-axle trucks. International Journal of Mechanical Engineering, 22(4), 558-567.

[14] Liu, H., Wang, X., & Zhang, Z. (2015). Optimizing braking force distribution using computational modeling. SAE Technical Paper, 2015-01-0423.

Information about the author

Khakkulov Komil
Jizzakh Polytechnic Institute, basic doctoral student of the Department of "Transport Engineering"
E-mail: hakkulov1987@mail.ru
Tel.: +998 91 199 02 29
https://orcid.org/0000-0002-1291-4884

Influence of sulphur on mechanical properties of foundry steels and ways to minimise it

S.R. Seydametov[1][a], N.K. Tursunov[1][b], O.T. Toirov[1][c]
[1]Tashkent state transport university, Tashkent, Uzbekistan

Abstract: The influence of sulphur on mechanical properties of foundry steels used for the production of highly responsible parts of railway transport has been investigated. It is shown that the sulphur content in steels above 0.025% leads to a sharp decrease in their strength, impact toughness and ductility, which significantly reduces the operational durability of castings. Studies have been carried out to determine the critical limit of sulphur content, at which the properties of steel remain at an acceptable level. On the basis of the obtained data effective technologies of steel desulphurisation have been proposed, which can be introduced in foundry production, in particular, in conditions of Tashkent LMP.

Keywords: foundry steel, ITP, sulphur, non-metallic inclusions, mechanical properties

1. Introduction

Foundry production in Uzbekistan plays a key role in providing machine-building complex with billets, and its development directly depends on the growth rate of machine-building in general. Unlike billets obtained by metal forming (rolled, stamped, forgings), castings retain all the disadvantages and peculiarities of melting and casting, which further affect the properties of finished cast products.

One of the main problems in foundries is the use of outdated regulatory and technical documents, where the levels of harmful impurities in steels do not meet the modern requirements of steel casting metallurgy. Foundry production ensures the manufacture of workpieces of complex geometry with minimal material losses, which makes it one of the key processes in mechanical engineering and metallurgy. However, the quality of castings is largely determined by the content of harmful impurities such as sulphur, phosphorus and oxygen. These elements, even in small quantities, can significantly degrade the mechanical properties of the metal, such as strength, ductility and impact toughness.

Nowadays the problem of sulphur content control in foundry steels is especially urgent. Sulphur, as a non-metallic element, is highly soluble in liquid iron, but when the metal solidifies, it forms sulphide inclusions (e.g. FeS) that precipitate at grain boundaries. This leads to a reduction in the ductility and impact toughness of the steel, and increases the risk of defects such as redbreakage (brittleness at high temperatures). In addition, sulphide inclusions impair the metal's machinability and corrosion resistance.

The influence of sulphur is particularly critical in steels used for the manufacture of critical parts, such as railway components, where high reliability and durability are required. Therefore, control of sulphur content and development of effective methods of its removal (desulphurisation) are important tasks of modern metallurgy.

Modern GOSTs and international standards regulate the maximum sulphur content in steels at the level of 0.010-0.025%. However, foundries often have difficulties in achieving these values due to the use of outdated equipment and insufficient efficiency of steel cleaning methods. This paper discusses methods of steel desulphurisation, their effect on mechanical properties and possible ways of implementation in industrial production. However, the main difficulty lies in the fact that foundries produce small volumes of steel, and the introduction of expensive equipment used in large-scale metallurgy (e.g., vacuum degassers, furnace-ladle units, etc.) to improve quality is practically impossible. The use of such devices significantly increases the cost of castings and leads to long payback periods.

Improved performance and mechanical characteristics of the casting are possible if harmful impurities such as sulphur, phosphorus, gases, non-metallic inclusions and others are effectively removed from the metal. The quality of the casting depends to a large extent on low sulphur content in the final metal.

Sulphur is a non-metallic element that:

Easily dissolves in liquid iron.

Virtually insoluble in the solid state.

According to studies [1, 2], sulphur has unlimited solubility in liquid iron and very low solubility in solid iron. At 1365°C, the limiting solubility of sulfur in u-iron is from 0.04% to 0.05%, and it decreases with decreasing temperature (in the temperature range from 1365°C to 915°C during the transition of u-iron to a-iron). The transition to a-iron causes a sharp formation of sulphides, the concentration of sulphur in iron decreases to 0.01%, and its content continues to decrease with further cooling. Excessive sulphur content, exceeding the solubility limit, leads to a phenomenon called red-brittle (metal fracture). This is especially pronounced in the cast state, where sulphide inclusions are deposited on the boundaries of primary crystallites, which reduces the strength, ductility and toughness of both the metal itself and finished products from it (castings, ingots).

[a] https://orcid.org/0009-0008-2809-5036
[b] https://orcid.org/0009-0008-7910-3980
[c] https://orcid.org/0000-0003-4677-1241

2. Material and research methodology

The studies were carried out on 20GL casting steels melted in induction crucible furnaces ICF-6 with the main lining at the LMP in Tashkent. The following methods were used for analyses:

Determination of chemical composition of metal by spectral analysis method;

Mechanical tests for tensile, impact toughness and hardness;

Microscopic studies of metal structure and non-metallic inclusions;

Statistical analysis of sulphur content at different stages of production.

Sulphur in steel is mainly present in the form of sulphides (FeS, MnS), which are distributed at grain boundaries and lead to brittleness of the metal. The most dangerous phenomenon is red brittleness - metal fracture when heated above 900°C due to the formation of FeS-Fe eutectic, which has a low melting point (988°C).

As a result of the conducted research it was found that:

When the sulphur content is above 0.025%, the impact toughness of steel decreases by 60-70% at -60°C.

Tensile strength of steel decreases by 8% on average.

The ductility (relative elongation) drops by 50% when the sulphur content increases from 0.013% to 0.043%.

Increased sulphur content reduces the fatigue strength of steel by 1.5-2 times.

Methods of sulphur content reduction

1. desulphurisation technologies

Desulphurisation is the process of removing sulphur from steel, which can be carried out by various methods.

A) Effectiveness of different deoxidising agents in desulphurisation process

The diagram (Fig. 1) shows the effectiveness of different deoxidising agents in the desulphurisation process of steel. It can be seen that calcium and magnesium are the most effective deoxidisers, significantly reducing the sulphur content of steel. Aluminium and silicium also contribute to desulfurisation, but their efficiency is lower.

Key Observations:

1. Calcium reduces sulphur content by 70-80%.
2. Magnesium reduces sulphur content by 60-70%.
3. Aluminium reduces sulphur content by 30-40%.
4. Silicea reduces sulphur content by 20-30%.

The effectiveness of deoxidisers depends on their chemical activity and ability to form stable compounds with sulphur. Calcium and magnesium are highly active and form sulphides (CaS, MgS), which are easily removed to slag. Aluminium and silicium are less active but can also bind sulphur, although to a lesser extent.

Reaction formulas:

Reaction with calcium:

$$Ca+S \rightarrow CaS$$

Reaction with magnesium:

$$Mg+S \rightarrow MgS$$

Reaction with aluminium:

$$2Al+3S \rightarrow Al_2S_3$$

Reaction with silicium:

$$Si+2S \rightarrow SiS_2$$

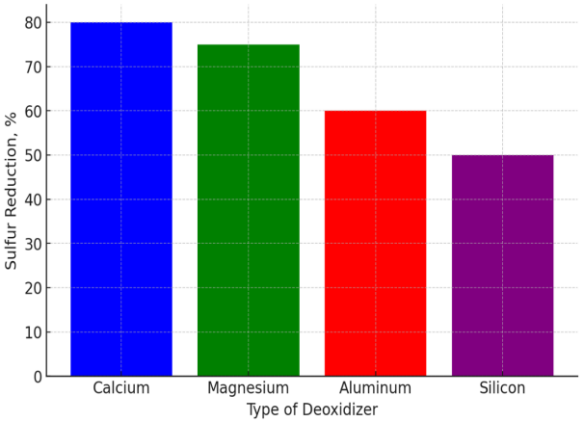

Fig. 1. Effectiveness of different deoxidising agents in the desulphurisation process

B) Basic formulae of desulphurisation

Equilibrium distribution of sulphur between metal and slag

$$L_s = \frac{\%S_{met}}{\%S_{slag}}$$

Where:

L_S - sulphur distribution coefficient,

$\%S_{met}$ - sulphur content in metal,

$\%S_{slag}$ - sulphur content in slag.

Desulphurisation reaction involving calcium

$$Ca + S = CaS$$

where: Calcium (Ca) binds sulphur (S) into a stable compound calcium sulphide (CaS), which is removed to the slag.

Desulphurisation reaction involving magnesium

$$Mg + S = MgS$$

where: Magnesium (Mg) also actively binds sulphur to form MgS.

Kinetics of sulphur removal during vacuumisation process

$$\frac{dS}{dt} = -k[S]$$

where: dS/dt is the rate of sulphur reduction,

k - reaction rate coefficient,

[S] - current sulphur content in the metal.

Steel processing outside the furnace

Methods include: Vacuuming.

Processing of metal in furnace-ladle units.

Introduction of modifiers into the metal to bind sulphur into stable compounds. Figure 2 shows the scheme of the desulphurisation process using synthetic slags. This process includes consecutive stages: addition of deoxidising agents, binding of sulphur into sulphides, slag formation and its removal. This approach allows to effectively reduce the sulphur content in foundry steels, which significantly improves their mechanical properties.

https://doi.org/10.56143/3030-3893-2025-1-26-30 A bridge between science and innovation

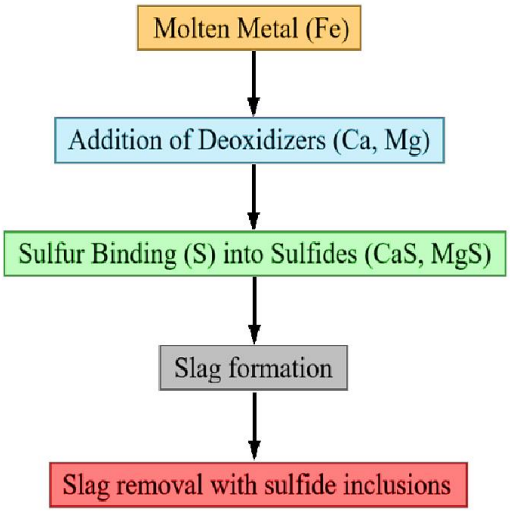

Fig. 2. Scheme of desulphurisation process using synthetic slags

Control of raw materials

Sulphur content reduction is possible at the raw material preparation stage, including the use of high-quality ores and carbonaceous additives.

Influence of temperature on desulphurisation

Dependence of sulphur content in steel on melting temperature

The diagram (Fig. 3) shows the dependence of sulphur content in steel on melting temperature. It can be seen that as the melting temperature increases from 1400°C to 1700°C, the sulphur content of the steel decreases. This confirms that high temperatures promote more efficient desulphurisation.

Main observations:

At 1400°C, the sulphur content is about 0.040%.

When the temperature is increased to 1600°C, the sulphur content decreases to 0.020%.

When the temperature is further increased up to 1700°C, the sulphur content reaches the minimum values of 0.010% and below.

The efficiency of desulphurisation at high temperatures is explained by the following factors:

Acceleration of chemical reactions: Higher temperatures increase the rate of reactions between sulphur and deoxidising agents (e.g. calcium or magnesium), which favours the formation of sulphides (CaS, MgS) and their removal to the slag.

Improved slag mobility: High temperatures make the slag more liquid, which facilitates its interaction with sulphur and its removal from the metal.

Increased sulphur solubility in the slag: At high temperatures, sulphur dissolves better in the slag, which facilitates its more efficient removal.

Reaction formulas:

Reaction with calcium:

$$Ca+S \rightarrow CaS$$

Reaction with magnesium:

$$Mg+S \rightarrow MgS$$

Reaction with lime (CaO):

$$CaO+S \rightarrow CaS+O$$

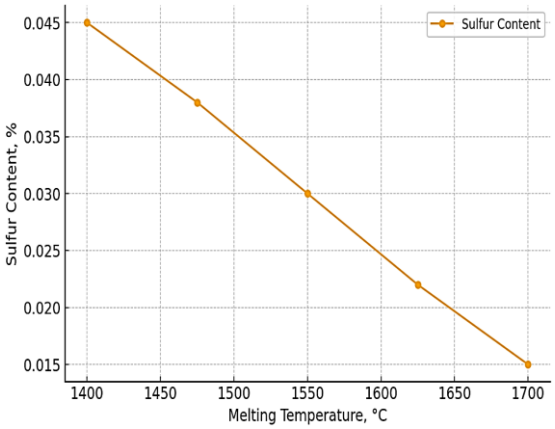

Fig. 3. Dependence of sulphur content in steel on melting temperature

Reduction of sulphur content in metal significantly depends on the melting temperature. The higher the temperature, the faster the desulphurisation processes occur, especially when using active slags and deoxidizers.

Properties were determined in the heat treated state, i.e. after normalisation at (H) 880-890°C;

Statistical analysis of steel melting for sulphur content in the metal during melting and in the liner, as well as analysis of the influence of sulphur on the mechanical properties of steel was made in Excel.

3. Results and discussion

When melting 20GL steel in an induction furnace, the largest number of melts, more than 60%, is characterised by sulphur concentration in the melt from 0.021 to 0.030% by mass. The values of sulphur content in the range of 0.040-0.050%, close to the upper limit of GOST, are about 6%, which is 10 times less than for the above-mentioned values. The largest share of smelts (more than 73.0%) has sulphur content in finished metal in the range from 0.016 to 0.025% by mass.

Additional research

Influence of non-metallic inclusions

Sulphides, formed at high sulphur content, form inclusions that: deteriorate the ductility of steel, reduce corrosion resistance, complicate cutting.

Graphical representation of the results shows a linear dependence of the deterioration of properties on the level of sulphur content.

Tables 1-3 present data on mechanical properties of the above steels at different sulphur content.

The impact toughness of 20GL steel decreases with increasing sulphur content due to the formation of brittle sulphide inclusions. This is especially critical at low temperatures, when impact toughness decreases by 3-4 times. Table 1 presents data on impact toughness of 20GL steel at different temperatures.

Table 1

Impact toughness of 20GL steel at different sulphur content*

Steel grade	KCU, MJ/m^2, at sulphur content, %			
	0,013	0,023	0,033	0,043
20GL	0,62 0,38	0,56 0,31	0,40 0,21	0,31 0,12

https://doi.org/10.56143/3030-3893-2025-1-26-30

* Numerator - at test temperature +20°C, denominator - at -60°C.

As the sulphur content increases, a decrease in the tensile strength is observed, which makes the steel less resistant to mechanical loads. Table 2 shows the experimental strength data of 20GL steel.

Table 2

Strength of steel at different sulphur content

Steel grade	$a_в$, MPa, at sulphur content, %			
	0,013	0,023	0,033	0,043
20GL	650	635	610	605

Ductility is an important parameter affecting the technological properties of steel. Increased sulphur content leads to the formation of brittle grain boundaries, which reduces the relative elongation of steel, as shown in Table 3.

Table 3

Relative elongation of steels at different sulphur content

Steel grade	б, %, at sulphur content, %			
	0,013	0,023	0,033	0,043
20GL	21	20	15	10

Sulphur significantly reduces the fatigue strength of steel, as sulphide inclusions act as stress concentrations, which leads to crack initiation. According to studies, when the sulphur content increases above 0.025%, the fatigue strength of 20GL steel decreases by 1.5-2 times.

It was found that a sharp decrease in all properties of steels, especially toughness and ductility, is observed at sulphur content above 0.023%. For example, for most steels when increasing the sulphur content from 0.013% to 0.043%, impact toughness at normal test temperature decreases almost twofold, and at -60°C - more than three times. The graphs below show the dependence of mechanical properties of steel on sulphur content.

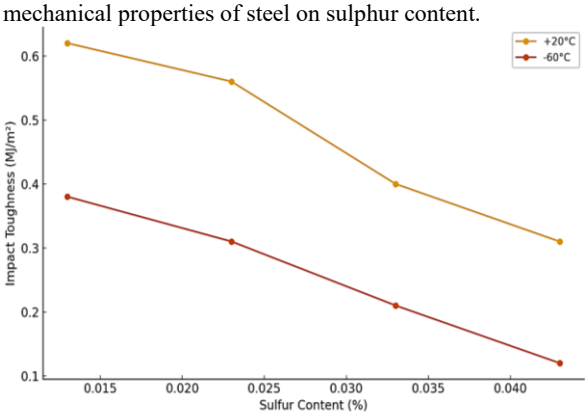

Fig. 4. Effect of sulphur content on impact toughness of steel at different temperatures

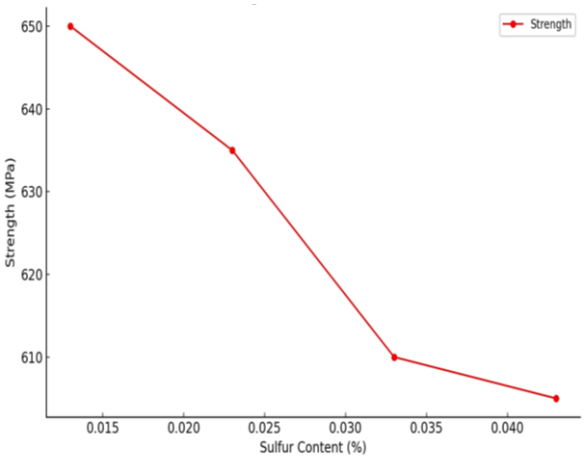

Fig. 5. Dependence of steel strength on sulphur content

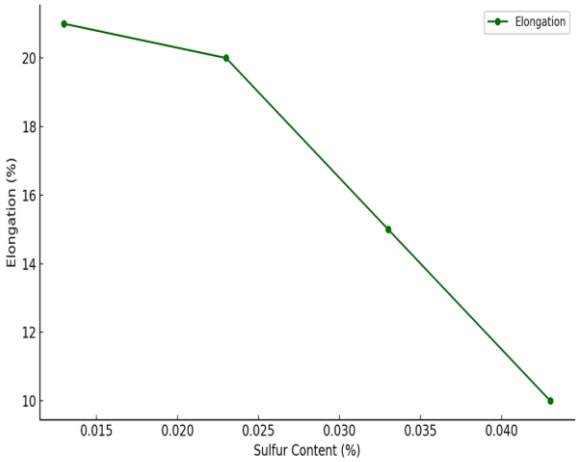

Fig. 6. Dependence of steel ductility on sulphur content

This effect is explained by the fact that sulfide and oxysulfide non-metallic inclusions are formed in the metal at the grain boundaries of the primary crystals, which weaken their bonding, which in turn leads to a decrease in the ductility and toughness of the cast metal. Thus, the higher the concentration of sulphur in the metal, the more non-metallic inclusions are present in the metal, resulting in lower mechanical properties such as impact toughness, strength and relative elongation.

4. Conclusion

The analysis of the conducted research has shown the necessity and expediency of developing technologies for refining steel melts in induction crucible furnaces (ICF) in order to achieve a stable reduction in sulphur concentration. This will allow to provide high quality characteristics of castings, especially in the conditions of production of critical parts for railway transport.

It is also required to make additional changes in steel casting melting technologies aimed at controlling and reducing the sulphur content in steels. The research results demonstrate that the increase of sulphur content in 20GL steel above 0.025% leads to a significant deterioration of mechanical properties. In particular:

The impact strength (KCU) decreases by a factor of 3 at -60°C, making the steel more brittle in low temperature applications.

https://doi.org/10.56143/3030-3893-2025-1-26-30 A bridge between science and innovation

The strength of the steel decreases by an average of 8%, which reduces its ability to withstand mechanical loads.

The ductility of the steel (relative elongation) is reduced by 50%, increasing the risk of failure under dynamic loads.

Fatigue strength decreases by 1.5-2 times, which is especially critical for parts operating under cyclic loads.

The obtained data confirm the necessity of strict control of sulphur content in foundry steels. The optimum sulphur level for 20GL steel is 0.015-0.025%, which provides high mechanical properties such as strength, impact toughness and ductility.

To achieve these indicators, it is recommended to implement modern desulphurisation methods, including:

Use of synthetic slags with high lime content.

The use of deoxidising agents (calcium, magnesium) to bind sulphur into stable compounds.

Treatment of steel outside the furnace (e.g. in furnace-ladle units or using vacuum treatment).

These measures will not only improve the performance characteristics of castings, but also increase their durability and reliability under conditions of intensive use.

References

[1] Lunev V.V., Averin V.V. Sulphur and phosphorus in steel. M.: Metallurgy, 1988. 256 c.

[2] Shulte Yu.A. Electrometallurgy of steel casting. M.: Me-tallurgy, 1970. 328 c.

[3] GOST 977-88. Steel castings. General technical conditions. M.: Izd-wo standards, 1989. 56 c.

[4] Electrometallurgy of steel and ferroalloys / Povolotsky D.Ya., Roshchin V.E., Ryss M.A., Stroganov A.I., Yartsev M.A. Textbook for universities. Izd. 2-th, reworked. And supplement. M.: Metallurgy. 1984. - 568 c.

[5] Yedneral F.P. Electrometallurgy of Steel and Ferroalloys. Izd. 4-th, reworked. and supplement. M.: 'Metallurgy', 1977. - 488 c.

[6] Grigorovich K.V., Shibaeva T.V., Arsenkin A.M. Influence of technology of deoxidation of pipe steels on composition and quantity of non-metallic inclusions. Metals. 2011. № 5. C. 164-170.

[7] Goldstein M.I. Special steels. - M.: Metallurgy, 1985.

[8] Kudrin V.A. Theory and technology of steel production: Textbook for universities. - M.: Mir, ACT Publishing House, 2003. - 528 c.

[9] Ten E.B. Quality improvement of castings from cast iron, steel and nickel alloys by out-of-furnace treatment of melts: dissertation ... Doctor of Technical Sciences: 05.16.04. - Moscow, 1992. - 541 c.: ill. Foundry production

[10] Tursunov, N.K., Semin, A.E., Sanokulov, E.A. Study of desulfurization process of structural steel using solid slag mixtures and rare earth metals, (2016) Chernye Metally, (4), pp. 32-37.

[11] Tursunov N. K., Semin A. E., Kotelnikov G. I. Kinetic features of desulphurization process during steel melting in induction crucible furnace. Chernye Metally. 2017. No. 5. pp. 23–29.

[12] Tursunov N. K., Semin A. E., Sanokulov E. A. Study of dephosphoration and desulphurization processes in the smelting of 20GL steel in the induction crucible furnace with consequent ladle treatment using rare earth metals. Chernye Metally. 2017. No. 1. pp. 33–40.

[13] Talgat Urazbayev, Nodirjon Tursunov and Tokhir Tursunov, "Steel modification modes for improving the cast parts quality of the rolling stock couplers", AIP Conf. Proc. 3045, 060015 (2024). https://doi.org/10.1063/5.0197361.

Information about the author

Seydametov Saidakhmad Rakhmatul-layevich	Tashkent State Transport University, PhD student Materials Science and Mechanical Engineering Department E-mail: senior_91@gmail.com Tel.: +99871-299-01-68 https://orcid.org/0009-0008-2809-5036
Tursunov Nodirjon Qayumjono-vich	Tashkent State Transport University, D.Sc. (Tech.), Head of the Department of "Materials Science and Mechanical Engineering" E-mail: u_nadir@mail.ru Tel.: +99871-299-01-69 https://orcid.org/0009-0008-7910-3980
Toirov Otabek Toir ugli	Tashkent State Transport University, PhD, associate professor "Materials Science and Mechanical Engineering" E-mail: otabek_toirov@mail.ru Tel.: +99871-299-01-68 https://orcid.org/0000-0003-4677-1241

Systematization of factors influencing train movement

D.B. Butunov[1][a], S.A. Abdukodirov[1][b], D.D. Tulaganov[1], Sh.F. Ergashev[1]
[1]Tashkent state transport university, Tashkent, Uzbekistan

Abstract: The main goal of the work is to identify and systematize the factors that determine the quality indicators of railway transport, affecting traffic safety, and to develop directions for increasing the level of traffic safety. Factors influencing the safety of train traffic have been identified and systematized according to 7 criteria. In order to increase the level of train safety, based on the results of analysis and assessment of the factors influencing them along the route, the main directions of measures to improve the level of safety were developed based on the Hoshina-Kanri principle. The developed mechanism determines what measures should be implemented at stations, terminals and freight facilities to improve train safety.

Keywords: Train movement, factor, systematization, traffic safety, transportation process, productivity

1. Introduction

Efficient and safe management of train traffic during transportation is important to ensure the efficiency and reliability of the transport system [1-8].

The timely delivery of trains (without excessive loss of time at stations, freight facilities and terminals) to their destinations (cargo receivers, passengers and designated disembarkation points) while ensuring the safe movement of trains along the route is determined by the image of this transport in the market [6-8]. Of course, to achieve this, one of the pressing issues is the search for continuous integrated solutions in the process of railway transportation and their implementation. In this case, the first main task is to identify factors that have a negative impact on the transport process, their systematization (in the source) and the search for comprehensive solutions to eliminate them.

The following factors are of great importance in this process:

saving time - accurate planning of train movements allows passengers and goods to reach their destination on time;

economic efficiency – ensures the rational use of resources, including fuel, electricity and employee working time;

ensuring safety - train collisions, delays and other emergency situations can be prevented through clear organization of traffic;

increasing the capacity of passenger and cargo transportation – effectively organized traffic increases the capacity of passenger and cargo transportation;

reliability of the transport system – the stability of train traffic increases the confidence of passengers and customers, since all processes are carried out on the basis of a clear schedule;

environmental efficiency – optimal operating mode reduces fuel consumption, which helps reduce environmental damage.

Also, the introduction of automation and train traffic control systems using modern technologies will make this process more efficient. Through them, traffic schedules can be constantly monitored and, if necessary, quickly changed.

To assess the efficiency of organizing train traffic, the following indicators are used (Table 1).

Table 1

Indicators for assessing the efficiency of train traffic management

Indicator name	Evaluation Mechanisms	Explanation
Time indicators	Level of compliance with train schedules	It evaluates how accurately trains adhere to specified time intervals.
	Delays	Number of delays and their total duration
	Average movement speed	Determines the average speed of the train along the track.
Indicators of cargo and passenger transportation	Load capacity	Amount of cargo transported per unit of time (tons/km)
	Passenger capacity	Number of passengers transported per unit of time (passenger/km)
	Level of wagon capacity utilization	Overloading (loading) of passenger (freight) carriages
Safety indicators	Number of emergencies	Number of road safety violations
	Performance of traffic control systems	Level of operation of security automation systems
Economic indicators	Amount of fuel or energy consumed	Fuel or electricity used for propulsion
	Total costs for organizing traffic	Road infrastructure, maintenance, staff salaries and other expenses

[a] https://orcid.org/0009-0009-4165-0257
[b] https://orcid.org/0000-0001-9457-255X

	Income/cost ratio	Ratio of income from train traffic to expenses
System stability and efficiency	Flexibility of train schedules	Stable adherence to the schedule, despite the intensity of train traffic
	Number and duration of stops	Time of stops along the way and their brevity
Environmental indicators	Exhaust gases	The amount of CO_2 emitted while a train is moving
	Energy efficiency	Ratio of energy consumed to cargo or passenger transported

Based on these indicators (Table 1), the efficiency of organizing train traffic and the possibilities for their improvement are analyzed and appropriate decisions are made.

2. Methods and materials

Organization and management of railway transportation, development of systems and methods for ensuring train traffic safety, increasing the productivity of participants in the transportation process, as well as identifying, assessing and eliminating factors affecting traffic safety, laboratory scientists have conducted scientific research [1-8].

Scientific works [2-6] made the following conclusions: strict adherence to the placement of workers at work places in accordance with their qualifications; establishing constant control over the movement of trains; optimization and digitalization of processes; comprehensive mechanization of loading and unloading operations; improvement of railway transport management systems, etc. However, most scholars have not specified the exact mechanisms of how these measures should be implemented. In addition, the systematization of factors influencing the movement of trains throughout the entire traffic cycle has not been sufficiently studied.

3. Results and discussion

The indicators of train traffic organization are influenced by various factors [1-6]. Assessing their impact is important to improve efficiency and eliminate problems. It is important to use monitoring systems and data analysis techniques to determine the level of impact of each factor and manage them effectively. This allows you to organize traffic more efficiently.

As a result of the analysis of scientific works [1-6, 10], various factors were identified that influence the movement of trains along the route, which, based on the results of the analysis, were conditionally divided into 7 criteria (technical factors, organizational factors, natural factors, human factors, load factors , economic factors, information factors) and systematized (Fig. 1).

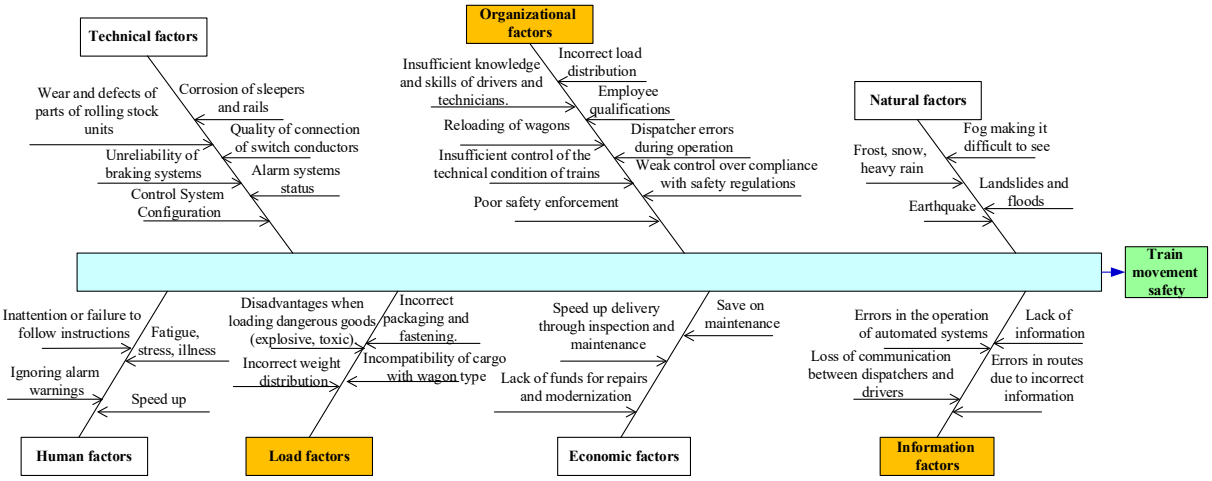

Fig. 1. Factors influencing the movement of trains along the route

Description of the factors influencing the movement of trains in this form allows us to determine which group each factor belongs to, assess the level of their impact and develop appropriate measures for timely elimination.

These factors (Fig. 1) have different effects on trains during their movement. Therefore, comprehensive approaches are needed to eliminate them.

A number of factors listed in Figure 1, which took place in the process of organizing train traffic at the stations of Uzbekistan Railways JSC and adjacent branches and stations, were studied. The study was carried out on the site of the railway departments (Fig. 2).

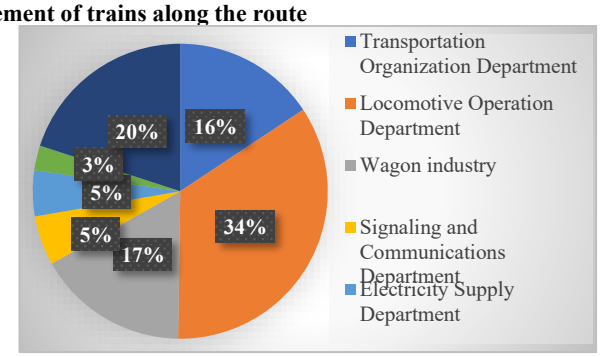

Fig. 2. Share of road safety violations attributable to organizations of the joint stock company "Uzbekistan Railways"

The largest share of traffic safety violations occurs in the "Use of Locomotives" (34%) and "Road Maintenance" (20%) divisions. Therefore, it is important to develop the necessary measures to improve the level of road safety in these departments.

Effective provision of transport safety in transit is carried out through a combination of technical, organizational and technological measures aimed at preventing emergency situations and minimizing their consequences.

The safety of trains during transportation at stations requires taking into account many factors related to the characteristics of the infrastructure, the movement of rolling stock, the organization of station operations and the human factor.

To improve safety at stations, it is necessary to combine the efforts of all participants in the process: from drivers and dispatchers to engineering services. This ensures stable and safe operation of the station when transporting passengers and cargo.

In addition, the safety of trains when transporting goods by rail depends on many factors related to the state of infrastructure, rolling stock, organization of loading and unloading operations and compliance with regulatory requirements. Below are the main aspects.

1. Infrastructure factors:

condition of roads of cargo facilities: condition of railway tracks, switches and loading platforms; absence of deformations and obstacles on the roads.

loading and unloading areas: lack of modern equipment for loading and unloading (cranes, conveyors, etc.); lack of clearly organized areas for equipment operation.

engineering structures: unreliability of warehouses, bridges and platforms; unsuitability of access roads to branches.

2. Moving content:

technical condition of cars: presence of defects in freight car bodies, brake systems and wheel pairs; without taking into account the maximum load capacity to avoid overloading.

load securing: failure to use secure securing methods to prevent cargo from shifting; failure to maintain proper weight distribution in the carriage.

use of special wagons: do not use tanks, platforms and semi-open wagons for the transportation of certain types of cargo (dangerous, volatile, container).

3. Organization of the transportation process:

route planning: without taking into account the condition of roads along the entire route; not taking into account capacity when choosing the optimal traffic schedule.

compliance with the speed limit: not taking into account the weight of the train and the types of cargo transported when controlling the movement of trains.

loading and unloading operations: non-compliance with technology when loading and unloading cargo; idle time of rolling stock.

4. Dangerous goods:

compliance with safety standards: non-compliance with the rules for transporting dangerous goods; Do not use labels or danger signs on carriages.

cargo condition monitoring: failure to check packaging and tightness of tanks and containers; failure to check the tightness and packaging of containers and tanks; failure to control the possibility of leakage or explosion.

supporting documents: incorrect execution of the waybill and instructions for working with it.

5. Human factor:

personnel qualifications: lack of knowledge among personnel on how to safely unload (load) and handle cargo from(to) freight trains.

loading and unloading teams: lack of instructions for working with certain types of cargo; lack of constant monitoring of compliance with the rules.

dispatch control: problems of coordination of work between the departure and arrival stations; inaccuracies in the traffic schedule.

6. Natural and external threats:

weather conditions: without taking into account precipitation, temperature and wind when transporting goods, especially bulk or liquid cargo; slowness of cargo protection from external influences.

external interference: lack of security systems at cargo transportation facilities; Insufficient work has been done to prevent theft and vandalism.

7. Economic and legal aspects:

security funding: do not allocate resources to modernize rolling stock and freight infrastructure.

Regulatory regulation: non-compliance with international and national shipping standards; lack of constant monitoring of compliance with cargo terminals and rolling stock.

From the above factors, we can conclude that to ensure the safety of transportation at cargo facilities, an integrated approach is required, including modernization of infrastructure, strict control over the condition of cars, the introduction of automated technologies, and ensuring a high level of professional training for employees.

In order to increase the level of train traffic safety, areas of action were developed to analyze the results and assess the factors influencing them (Fig. 1).

Measures to improve the level of train safety, that is, the main directions, were developed taking into account the principles of Hoshina-Kanri [9] (Fig. 3).

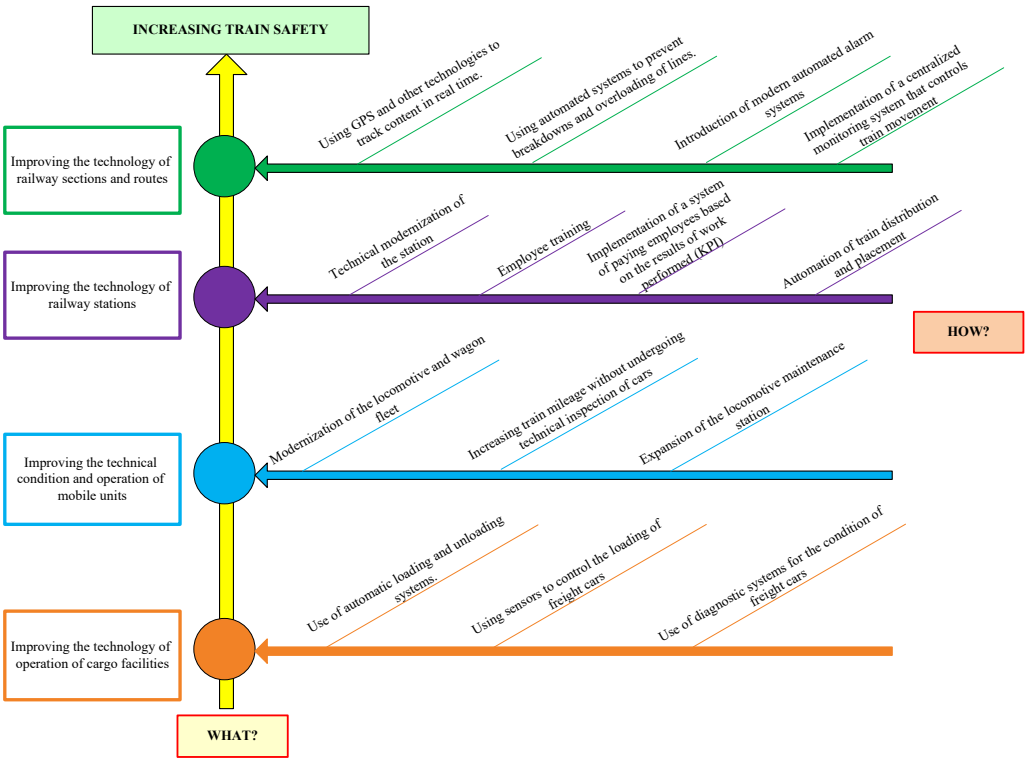

Fig. 3. Main directions for improving train safety along the route

Through this developed mechanism (Fig. 3), trains determine which measures should be implemented at each stage (train, station, freight facility, etc.) to improve traffic safety.

4. Conclusion

Ensuring the safety of train traffic at each stage determines the level of implementation of complex indicators of the quality of railway transport. Ensuring traffic safety significantly influences the performance of important indicators of railway transport and determines the position of the industry in the transport market.

Systematization of factors affecting the safety of trains along the route in the area of stations, stations and freight facilities, their systematic analysis, assessment and development of operational measures for their timely elimination, creates opportunities for effective assessment of the work of transport and the transport process of each of its participants.

The implementation of the proposed measures will lead to an increase in the productivity of railway transport and increase the attractiveness of the industry.

References

[1] Bezopasnost dvijeniya na jeleznix dorogax: ucheb. posobie. V 2 ch. Ch. 1. Osnovi bezopasnosti / I.Y. Kologrivaya, O.V. Frolova – Xabarovsk: Izd-vo DVGUPS, 2018 – 104 s.: il.

[2] https://rmrail.ru/poleznaya-informatsiya/bezopasnost-zhd-perevozok/?utm_source=chatgpt.com

[3] Gozbenko V.Ye. Analiz i issledovanie faktorov, vliyayushix na bezopasnost dvijeniya: sbornik trudov konferensii. / V.Y. Gozbenko, S.S. Gromishova, Y.I. Belogolov // Nauka, obrazovanie, obshestvo: tendensii i perspektivi razvitiya : materiali XIII Mejdunar. nauch.-prakt. konf. (Cheboksarы, 8 fevr. 2019 g.) / redkol.: O.N. Shirokov [i dr.] – Cheboksari: sentr nauchnogo sotrudnichestva “Interaktiv plyus”, 2019. – S. 149-155. – ISBN 978-5-6042302-2-0.

[4] https://www.bizeducation.ru/library/log/trans/10/safety.htm

[5] https://www.1520mm.ru/catastrophe/main.phtml

[6] Butunov, D.B., Uktamovich, A.M., & Mirxamitov, J.M. (2021). Poyezdlar harakati xavfsizligi buzilishlarini tadqiq etish // Academic Research in Educational Sciences, 2(11), 339-347. doi:10.24412/2181-1385-2021-11-339-347

[7] Dilmurod Butunov, Komil Mukhammadiev, Sardor Abdukodirov, Shuhrat Buriyev, and Mafirat Toxtakxodjaeva. Improving the standardization of wagon standby time at the sorting station. E3S Web of Conferences 549, 04003 (2024). 1-11. DOI: https://doi.org/10.1051/e3sconf/202454904003

[8] Dilmurod Butunov, Zhansaya Kalimbetova, Sardor Abdukodirov Shuhrat Buriyev and Mafiratxon Tuxtaxodjayeva. E3S Web of Conferences 460, 06002 (2023). 1-9 pp. https://doi.org/10.1051/e3sconf/202346006002

[9] Ono T. Toyota Production System. Moving away from mass production / Per. from eng. / 2nd ed., Rev. and add. – M.:, 2006. – 208 p.

[10] Butunov D.B. Systematization of factors influencing during processing of wagons at the sorting station / D.B. Butunov, N.K. Aripov, A.M. Bashirova // Journal of Tashkent Institute of Railway Engineers. Tashkent, – 2020. – No. 2. – p. 84-91.

Information about the author

Butunov Dilmurod Baxodirovich	Tashkent State Transport University, PhD, Professor of the Department of "Management of railway operation" e-mail: dilmurodpgups@mail.ru Tel.: +99897 2675567 https://orcid.org/0009-0009-4165-0257
Abdukodirov Sardor Askar ugli	Tashkent State Transport University, PhD, Docent of the Department of "Management of railway operation" e-mail: sardor_abduqodirov@bk.ru Tel.: +99897 7342992 https://orcid.org/0000-0001-9457-255X
Tulaganov Dilmurod Dilshod ugli	Master of the 1st stage of the Tashkent State Transport University, specializing in "Road Safety and Its Organization". e-mail: mzaalevskiy@mail.ru Tel.: +99890 116 65 16
Ergashev Shakhzod Farkhod ugli	Master of the 1st stage of the Tashkent State Transport University, specializing in "Road Safety and Its Organization". e-mail: shaxzode8360@gmail.com Tel.: +998 91 638 83 60

Development of document management technology in the railway automation and telemechanics system

D. Baratov[1][a], E. Astanaliev[1][b]
[1]Tashkent state transport university, Tashkent, Uzbekistan

Abstract: Traditional paper-based systems have given way to contemporary centralized electronic solutions in the development of document management technology in railway automation and telemechanics. The handwritten documentation used in railway operations was labor-intensive, prone to mistakes, and ineffective when managing massive amounts of data. These antiquated systems frequently resulted in misunderstandings, longer decision-making times, and higher functional risks.

By guaranteeing real-time data transmission, increased accuracy, and greater protection, the application of a new centralized electronic document operation system has completely transformed railway automation. By combining digital documents, electronic signatures, and automated methods, this process drastically cuts down on paperwork and the need for human intervention. Operational efficiency is increased by the centralized approach, which enables smooth coordination between control systems, dispatch centers, and railroad stations. The monitoring and regulate capabilities of contemporary telemechanics systems also improve maintenance scheduling and accident avoidance. In addition to improving railway management, this shift follows worldwide trends in digital transformation, making the railway network more reliable and cutting edge.

Keywords: Document management, digital documents, electronic document operation system, signaling and communications, project documentation

1. Introduction

A big step toward efficiency and contemporaneity is the switch from paper-based technologies to electronic document management. The importance of this change is maintained by the Law of the Republic of Uzbekistan "On electronic document management" which encourages the use of digital documentation to improve workflow automation, security, and accessibility. Organizations can increase data accuracy, expedite transmission and streamline methods by minimizing their dependence on paper.

The authenticity and legal acknowledgment of electronic documents are confirmed by this law, which creates a framework for their creation, storage, and exchange. In order to create a more open and effective administrative environment, it also elevates the use of secure information systems and digital signs. The change helps Uzbekistan become part of the contemporary digital economy and is in line with worldwide trends in digital transformation.

2. Research methodology

JSC "Uzbekistan Railways" signaling and communications department is responsible for organizing work interconnected to automation, telemechanics, and communications. There are eleven distances (SCD) in the signaling and communications department: ten for signaling, centralization, and blocking (SCB), and one for communication. In figure 1, the signaling and communications department's detailed directorial construction is displayed. The territorial distribution feature, which is evident in figure 2, determines the signaling and communications department's structure individually.

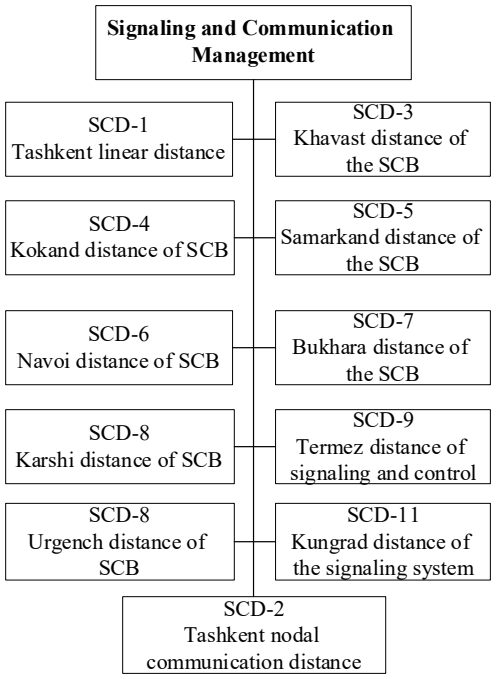

Fig. 1. JSC "Uzbekistan Railways" signaling and communication management structure

Instructions on technical documentation for signaling and interlocking devices and wired communications, as well as radio communications and recording of devices for rolling stock monitoring, closely restrict documents pertaining to automation and telemechanics installation (NSh-02) [3,6,7].

Priorities in the improvement of the aforementioned forms include: ensuring railway transport safety; introducing cutting-edge machinery and technologies; improving the

[a] https://orcid.org/0000-0002-6115-3321
[b] https://orcid.org/0000-0002-7327-6564

technical and financial performance of railway rolling stock and infrastructure facilities; and raising the standard of services offered.

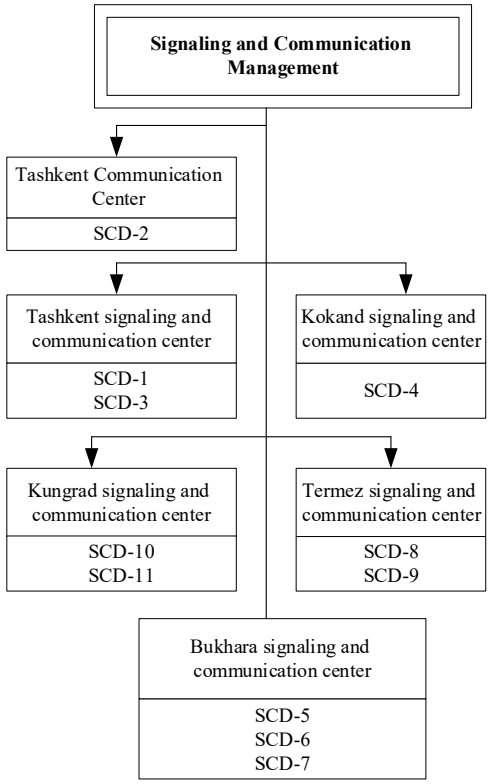

Fig. 2. Signaling and communication sector territorial division formation

All technical documentation is divided into three categories: design, operational, and archival, per the guidelines above. Figure 3 illustrates how technical documentation is organized [4-9].

Document flow is organized by design organizations, signaling and communications departments (SCD), signaling and communication departments, and building and installation organizations (Figure 4).

Projects are issued in five copies by the design organization. When the construction and installation train (SMP-406) receives a copy of the project, it is utilized for both commissioning and construction and installation. The project is sent to the signaling and communications department's technical documentation department in three copies. Two copies of these are moved to the appropriate signaling and communication distance, while one copy is kept in the archive. In turn, one copy is moved to the appropriate station, while the other copy is kept in the technical documentation group's archive (Figure 5).

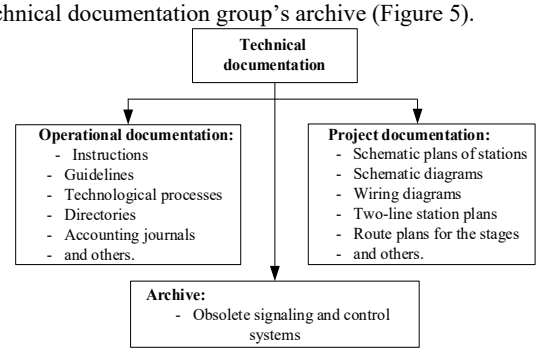

Fig. 3. Structure of technical documentation

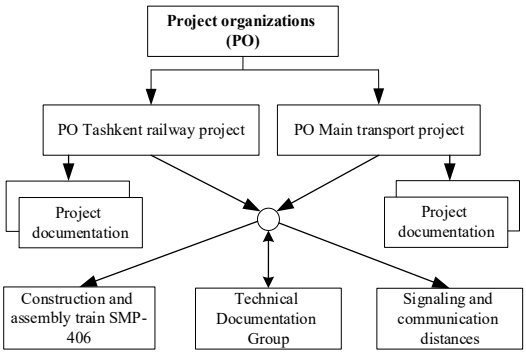

Fig. 4. Simplified structure of document flow

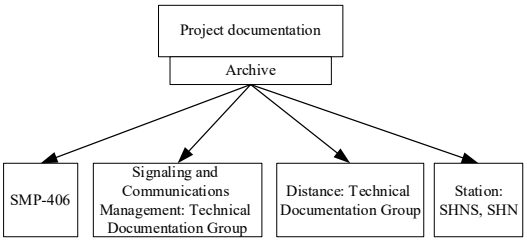

Fig. 5. Principle of distribution of design documentation

JSC "Uzbekistan Railways" occasionally has large quantities of technical documentation completed by several departments, which raises the cost of ineffective work and, as a result, operator errors. These tasks are entirely done by hand using paper material. Over 250 thousand copies of paper media are produced by each business. This technology's search speed and technical documentation accessibility are poor, and it does not allow multiple employees who are located far apart to examine the material at the same time [5,7,8].

When it comes to organizing and editing papers, paper technology is quite labor-intensive and complicated. These documents take up a lot of room when stored, are hard to account for, and cause loss and damage as well as confusion in the archive.

3. Conclusion

It is evident from an analysis of contemporary document management systems that automated electronic management systems are necessary. Electronic technical documentation maintenance technology will guarantee industrial competitiveness and boost overall transportation sector efficiency. It is necessary to create specialist software packages for developing information interchange and communication amongst railway design groups in order for electronic document management to function. It is necessary to update "Paper" technology by introducing contemporary computer systems with specialized software that will automate work environments and make it easier for employees who analyze technical documentation.

References

[1] J. Mökander, M. Axente, F. Casolari and L. Floridi, "Conformity assessments and post-market monitoring: A guide to the role of auditing in the proposed European AI regulation," Minds and Machines 32.2, p.241-268, 2022.

[2] A. Ayaz, and Y. Mustafa, “An analysis on the unified theory of acceptance and use of technology theory (UTAUT): Acceptance of electronic document management system (EDMS),” Computers in Human Behavior Reports 2: 100032, 2020.

[3] D. Baratov and E. Astanaliev, “Minimization of the automatic machine structure process of accounting and control of railway automation and telemechanics devices,” In E3S web of conferences, EDP Sciences, Vol. 244, p. 08024, 2021.

[4] M. Fathurrohman, S. Syamsuri and N. Hepsi, “E-Documents Management System: Application in Press Industry,” International Conference on Government Education Management and Tourism, Vol.1, No.1, 2022.

[5] S. Stanojevic, D.A. Kaminsky, M. T. Miller, and B. Thompson, “ERS/ATS technical standard on interpretive strategies for routine lung function tests,” European Respiratory Journal 60.1, 2022.

[6] Baratov D., Astanaliev E. Improvement of the scientific bases of creating means of automation of documentation of devices of railway automation and telemechanics //E3S Web of Conferences. – EDP Sciences, 2023. – T. 402. – C. 06005.

[7] Baratov D., Astanaliev E. Methodology for selection and efficiency of graphic software packages for technical documents //E3S Web of Conferences. – EDP Sciences, 2023. – T. 402. – C. 03018.

[8] T. Tretyakova, E. Barakhsanova, T. Alexeeva, and I. Bogushevich, “Provision and management of educational activities in the conditions of distance education at the north-eastern federal university,” In XIV International Scientific Conference “INTERAGROMASH 2021” Precision Agriculture and Agricultural Machinery Industry (Springer International Publishing), Volume 2, pp. 869-880, 2022.

[9] Y. Shen, J. Zhang, S. H. Song and K. B. Letaief, Graph neural networks for wireless communications: From theory to practice, IEEE Transactions on Wireless Communications, 2022.

Information about the author

Baratov Dilshod Khamidulla-evich	Tashkent State Transport University, First Vice-Rector for Youth Affairs and Spiritual and Educational Work, Doctor of Technical Sciences, Professor E-mail: baratovdx@yandex.ru Tel.: +998909195099 https://orcid.org/0000-0002-6115-3321
Astanaliev Elmurod Tursunali ugli	Tashkent State Transport University, PhD student at the Department of Automation and Telemechanics E-mail: transportacademy1997@gmail.com Tel.: +998994084197 https://orcid.org/0000-0002-7327-6564

Control and management of active and reactive power balance in a solar power supply system

N. Mirzoyev[1][a], S. Azamov[1][b]
[1]Tashkent state transport university, Tashkent, Uzbekistan

Abstract: This article discusses the development of a measurement and control system for monitoring and managing the balance of active and reactive power at power plants based on “Green” energy sources. Monitoring and management of the balance of active and reactive power based on a measurement and control system, calculated expressions are developed to solve the problem of reactive power compensation when transmitting electricity at power plants based on “green” energy sources. Reactive power is calculated based on measured active power, and combined reactive power sources generate the reactive power required by the network based on control signals. Schemes for connecting these reactive power sources to the network have been developed, and this diagram shows the installation of a measurement control device. The schematic block diagram of a measurement control device shows the sequence of the process of measuring and processing electrical data, as well as the generation of control signals. To study the operating principle and elements of a device created to monitor and manage reactive power consumption, a microcontroller, a signal converter and measuring transducers were selected. An algorithm for monitoring and managing the balance of active and reactive power has been developed for the device software. At the same time, equations for separating current, voltage and frequency signals in the phase section were developed.

Keywords: Green energy, active and reactive power, balance, monitoring and control, measurement and control system, microcontroller, signal converter, current, voltage, frequency, traditional power plant, solar and wind power plants, calibration factor, Arduino Uno, integrated circuit, Atmega328

1. Introduction

Today, power plants based on renewable energy sources are being built in the republic. Today, practical work is underway in Uzbekistan to build 22 solar and wind power plants with a capacity of 9 GW. In particular, a solar power plant with a total capacity of 900 MW has been built and commissioned in Samarkand, Jizzakh and Surkhandarya regions, while the Chinese company China Gezhouba Group has built and commissioned two solar power plants with a total capacity of 1,000 MW in Bukhara and Kashkadarya regions. At the same time, design and construction of wind power plants worth 650 million US dollars each have begun in the Peshku and Gijduvan districts of Bukhara region. The foreign company ACWA POWER from the Kingdom of Saudi Arabia is working on the creation of wind power plants with a capacity of 300-500 MW in the Peshku and Gijduvan districts. In general, by 2030, it is planned to build solar and wind power plants with a capacity of 27 GW based on "Green" energy sources in our Republic.

Based on the above, we can say that great attention is paid to providing the population with uninterrupted electricity in our republic.

This requires, along with the uninterrupted supply of electricity, ensuring the quality of electricity. In particular, along with active power consumers in the electricity network, there are also reactive consumers. This, in turn, requires paying attention to the issues of compensation for reactive power when transmitting electricity at power plants based on "Green" energy sources. There is still a lot of work to be done in this regard.

In this article, a measurement and control system has been developed to monitor and control the balance of active and reactive power when transmitting electricity to the network at power plants based on "Green" energy sources. Based on the measurement and control system for monitoring and controlling the balance of active and reactive power, a device installation scheme, a measurement and control system, a control and control device, and software were developed to control and control reactive power consumption in power plants based on "Green" energy sources.

2. Research methodology

In this work, the visualization of the energy performance of a solar power plant connected to the grid is considered. Usually, the visualization of the energy performance of a solar power plant is obtained using the Huawei online calculation program. When obtaining the visualization results of the energy performance of a solar power plant, climate and weather conditions, the angle of incidence of sunlight, and the pollution of the panels are important issues of the study. Inverters used in the electric power generation system have a significant impact on the quality of electric energy. Quality control when transmitting the generated active power to the grid has certain problems. It is known that in a power supply system, the active power balance is related to the network frequency, while the reactive power balance is a voltage-dependent quantity. The active power balance in a power supply system should be as follows [1-2]:

$$\sum P_{gen} = \sum P_{ist} = \sum P_{yuk} + \sum \Delta P$$

[a] https://orcid.org/0009-0003-6979-7660
[b] https://orcid.org/0009-0005-0615-5518

if,

$\sum P_{gen} < \sum P_{ist}$ or $\sum P_{gen} > \sum P_{ist}$

If the frequency in the power supply system decreases or increases. For stable operation of the power supply system, the nominal permissible deviation of the frequency is set at ±0.2 GHz. [4].

The reactive power balance should look like this [3-5]:

$$\sum Q_{gen} = \sum Q_{ist} = \sum Q_{yuk} + \sum \Delta Q$$

if,

$\sum Q_{gen} < \sum Q_{ist}$ or $\sum Q_{gen} > \sum Q_{ist}$

If, the voltage of the power supply system decreases or increases.

It is known that the amount of reactive power generated by traditional power plants is insufficient for the power supply system, 2/3 of the reactive power required by consumers is covered by consumers, and 1/3 is taken from the power supply network. Therefore, in power supply systems with solar power plants, monitoring and controlling the transfer of active and reactive power to the power supply system network is an important issue.

Information on the amount of active and reactive power supplied to the power supply system by an 80 kW solar power plant during the day on March 15, 2024 is presented in Figure 1. It can be seen that the solar power plant generated 379.96 kW*h of active electricity during this period and transferred it to the power supply system network.

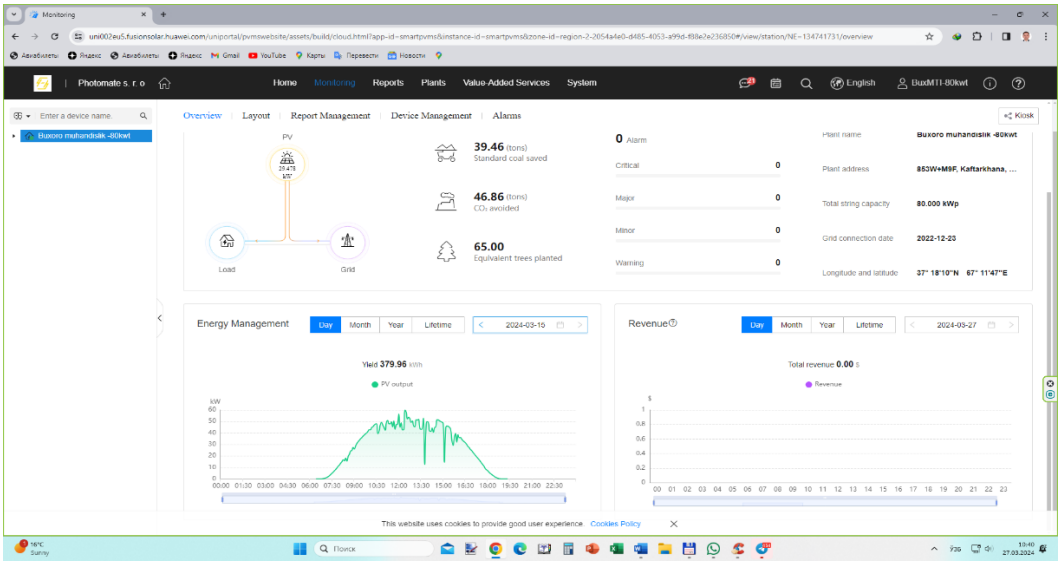

Fig. 1. Electricity generated by an 80 kW solar power plant

The solar power plant operates in parallel with the power supply system network in the electricity generation mode. In this process, an inverter is used to ensure the quality of the transmitted electricity. The reactive power balance is not considered in the described power supply system.

Developed schemes and equations. The results of the analysis and research have shown that the algorithm for monitoring and controlling the reactive power balance for a power supply system with a solar power plant, as well as the structural and electrical schemes for reactive power compensation, are important issues.

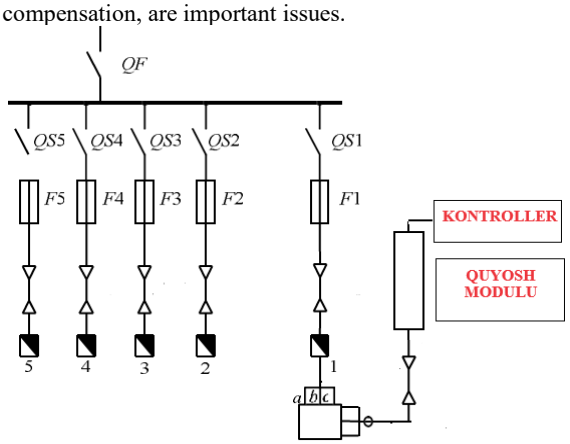

Fig. 2. Installation diagram of a device designed to control and manage reactive power consumption

Based on the installation diagram of a device designed to control and manage reactive power consumption, a measurement control system was developed to control and manage the balance of active and reactive power for a solar power plant power supply system. The measurement control system designed to control and manage the balance of active and reactive power in the power supply system is shown in Figure 3.

The measurement control system consists of three parts, the first part is the electrical part, the second part is the measurement-transformer part, and the third part is the software written in the microcontroller for processing the measurement results.

In the electrical part of the measurement control system, current signals are converted from the traditional power supply in the phase section by a special current transformer device and transmitted to the measurement-transformer unit. At the same time, a voltage signal is also supplied to the measuring and converting unit of the system. In the same way, current and voltage signals are obtained from the inverter of the solar power plant in the same order by phase.

In the measuring and converting unit, the current and voltage signals measured in the phase section are separated into current, voltage and frequency signals by phase and converted into a signal form and size that the microcontroller can read.

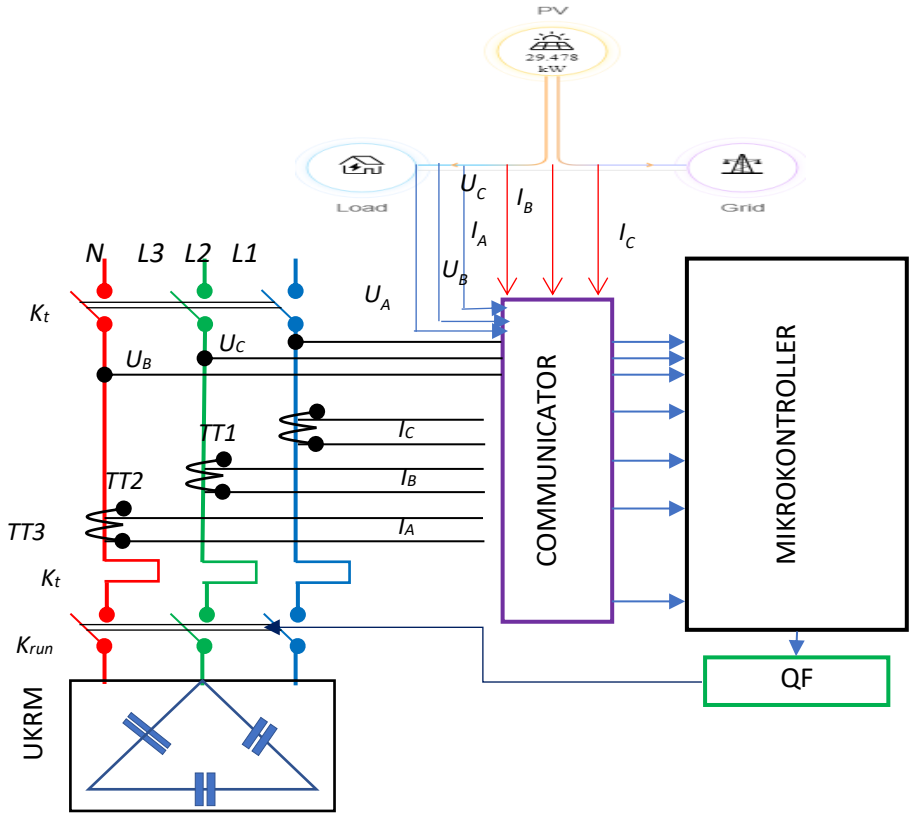

Fig. 3. Measurement and control system for monitoring and controlling the balance of active and reactive power

The microcontroller processes electrical quantities in the following sequence. Measuring electrical energy provides information about the change in power over time, and multiplies its signals in the form of voltage and current over time. If there is a difference between current and voltage, active power factor and phases, then active power is calculated as follows [2-3]:

$$p(t) = Ucos(wt) * Icos(wt + F), if\ F = 0$$

$$p(t) = \frac{UI}{2}(1 + cos2(wt))$$

$$if\ F \neq 0$$

$$p(t) = \frac{UI}{2}(1 + cos2(wt))$$

$$p(t) = Ucos(wt) * Icos(wt + F) =$$

$$= Ucos(wt) * [Icos(wt)\cos(F) + \sin(wt)\sin(F)$$

$$= \frac{UI}{2}(1 + cos(2wt)\cos(F) + UIcos(wt)\sin(\text{wt})\sin(F)$$

$$= \frac{UI}{2}(1 + cos(2wt)\cos(F) + \frac{UI}{2}\sin(2\text{wt})\sin(F)$$

The input voltage of the two channels of voltage and current is multiplied by the current and obtained through signal processing.

The active power data is converted to frequency, and in this process, the effective value of the voltage and the effective value of the current are calculated at the same time and converted to frequency. The effective values of the active power, voltage and current are outputted from the CF and CF1 channels, respectively, in a highly efficient manner.

The formula for calculating the frequency of the active power based on the output pulse is defined as follows [4]:

$$F_{CF} = 1721506\frac{U(U) * U(I)}{U_{ref}^2}$$

where 1721506 is the calibration coefficient.

The voltage at the phase intersection is determined as follows [7]:

$$U_f = K_{kU}\frac{\sqrt{\sum_{i=1}^{n} U_i^2}}{n};$$

The current in the phase section is defined as follows[7]:

$$I_f = K_{kI}\frac{\sqrt{\sum_{i=1}^{n} I_i^2}}{n}$$

The active power and total active power in the phase section are defined as follows [7]:

$$P_f = K_{kU} \cdot K_{kI}\frac{\sqrt{\sum_{i=1}^{n} U_i I_i}}{n}; \qquad P_\Sigma = P_{fA} + P_{fB} + P_{fC}$$

The apparent power and total apparent power in the phase section are defined as follows [7]:

$$S_f = I_f \cdot U_f; \qquad S_\Sigma = I * U$$

The reactive power and total reactive power in the phase section are determined as follows: [7]:

$$Q_f = \sqrt{S_f^2 - P_f^2}; \qquad Q_\Sigma = Q_{fA} + Q_{fB} + Q_{fC}$$

The active power factor is defined as follows [7]:

$$\cos\varphi_{ABC} = \frac{P_{fABC}}{S_{fABC}}$$

Active and reactive electrical energy are defined as follows [7]:

$$W = P_\Sigma * t, \qquad Q = Q_\Sigma * t$$

Based on the above mathematical expressions, the algorithm of the software for the operation of the measurement control system was formed, and this algorithm is a one-condition algorithm.

For the operation of the measurement control system, an Arduino microcontroller with an Atmega microprocessor was selected.

https://doi.org/10.56143/3030-3893-2025-1-39-44 A bridge between science and innovation

The basis of the Arduino Uno integrated circuit is the ATmega328 microcontroller. The characteristics of the Arduino Uno are given in Table 1 [4-5].

Table 1

Characteristics of the Arduino Uno microcontroller

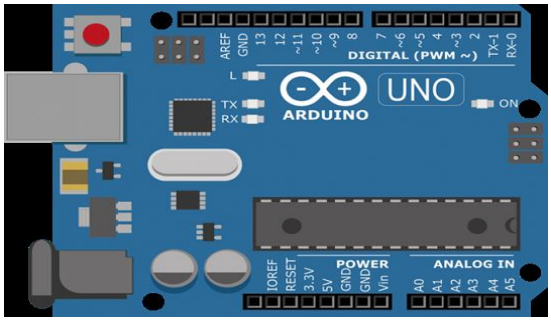

Microcontroller type	ATmega328
Operating voltage	5 Volts
Supply voltage	7-12 Volts
Voltage range	6-20 Volts
Digital inputs and outputs	14, of which 6 are for PWM
Analog inputs and outputs	6
Specified current per output channel	40 mAmperes
Memory	32 kB, of which 0.5 kB is for programming
SRAM	2 kB
EEPROM	1 kB
Frequency	16 MHs

The connection diagram of the active and reactive power balance monitoring and control device and the Arduino Uno integrated circuit is shown in Figure 4.

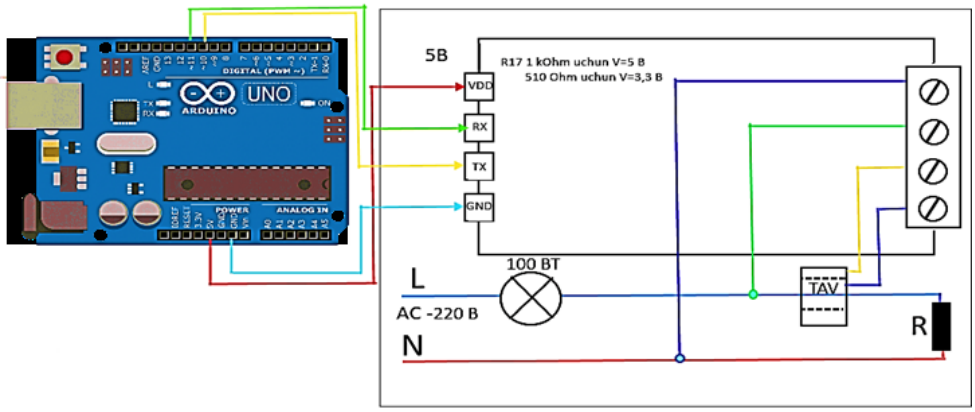

Fig. 4. Connection diagram of the active and reactive power balance control and management device and Arduino Uno integrated circuit

In the general scheme, the connection of the remaining phases of the electrical network is carried out in the same order as one phase is connected. The scheme presented in Figure 5 shows the connection of the active and reactive power balance control and management device and Arduino Uno integrated circuit.

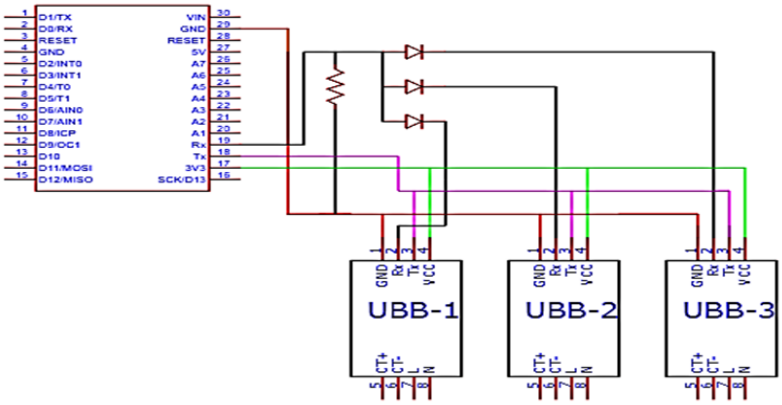

Fig. 5. Connection diagram of the three-phase active and reactive power balance control and control device and Arduino Uno integrated circuit

The measuring and control unit designed for the three-phase active and reactive power balance control and control is mainly assembled on the basis of the elements we have shown above, and its schematic diagram is shown in Figure 6.

The current and voltage signals at the output of the solar power plant inverter and the three-phase section of the traditional power grid are measured in the block for measuring data on the solar power plant and the power grid.

These measured signals are calculated in the block for processing the measurement results of the main electrical quantities of the power grid based on the equations given above [6-7].

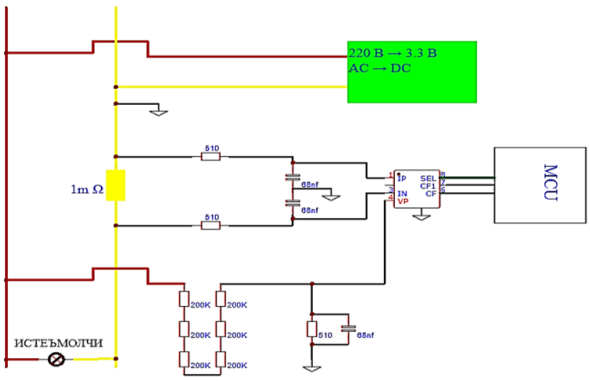

Fig. 6. Structural diagram of the measuring connection block

A control and control algorithm for the balance of active and reactive power was developed for the Arduino Uno selected for the three-phase active and reactive power control and management device. The control and control algorithm for the balance of active and reactive power is presented in Figure 4.

In order to compensate for the reactive power required by the power supply system network, the following additional reactive power amounts were determined for the minimum and maximum consumption modes and proposed for practical use [8]:

$$Q_{qop}^{min} = P_{o\prime rn} * (tg\varphi + tg\varphi_{tar}) = 43 * (3{,}792 + 0{,}38) = 179{,}392\ VAR$$

$$Q_{qop}^{max} = P_{o\prime rn} * (tg\varphi + tg\varphi_{tar}) = 43 * (0{,}505 + 0{,}38) = 38{,}055\ VAR$$

3. Conclusion

1. Ensuring the quality of electricity generated by solar power plants is one of the important tasks when transmitting electricity to the power supply system.

2. A solar power plant with a capacity of 80 kW installed in the educational laboratory building of the Bukhara Engineering and Technological Institute was taken as the object of research. By installing a measurement and control system created to monitor and control the reactive power consumption at the output of the solar power plant inverter, the reactive power to be compensated was calculated and reactive power sources were installed. According to the results of the research, it was justified that the reactive power consumption to be compensated with an installed average active power of the power supply system is 43 kW is as follows:

$$tg\varphi = tg\varphi(arccos\varphi) = tg\varphi(\arccos 0{,}255) = 0{,}3792$$

$$Q_{qop} = P_{o\prime rn} * tg\varphi = 43 * 3{,}792 = 16{,}31\ kVAR$$

3. The requirements for the power supply system indicate that consumers of electricity must be provided with high-quality active and reactive power in sufficient quantities. The results of the research have shown that one of the main factors affecting the quality indicators of active and reactive power of electricity is the automatic adjustment and compensation of reactive power in the power supply system based on the measurement and control system, since reactive power is an indicator of the efficiency of electricity.

4. The effective use of measurement and control systems in controlling the balance of active and reactive power in the power supply system with solar power plants allows you to control the minimum and maximum consumption of reactive power in real time, improve the quality of electricity, and also provides monitoring and digitization of the indicators of generated and consumed electricity.

References

[1] Mirzaev N. N. Intellectual measurement of electrical energy consumption - monitoring device and software. Scopus conference: Rudenko International Conference “Methodological Problems in Reliability Study of Large Energy Systems“ (RSES 2023) E3S Web of Conferences. Volume 461, 2023, 01083. https://doi.org/10.1051/e3sconf/202346101083

[2] Mirzaev N. N. Study on computerized measurement-control system for determining the condition of electrical network insulation and permitted connections for electrical energy consumption. Scopus conference: 4th International Conference on Energetics, Civil and Agricultural Engineering (ICECAE 2023) E3S Web of Conferences. Volume 434, 2023, 01021. https://doi.org/10.1051/e3sconf/202343401021

[3] Siddikov I. X., Denmuxammadiyev A. M., A’zamov S. S. Muqobil turdan olingan energiyadan istemol qiluvchi asinxron motor quvvat balansini nazorat va monitoring qilish //jizpi xabarnomasi. – 2024. – T. 1. – №. 1. – C. 126-128.

[4] Mirzoyev N.N. Information software and devices for energy efficiency management and control, Chemical Technology, Control and Management, 68-75 (2021)

[5] Mirzoyev N.N. Analogical Model Development Methodology For Mathematical Modeling Of Energy Efficiency Control System, The American Journal of Engineering and Technology, 55-61 (2020)

[6] Mirzoyev N.N. Intelligence devices for monitoring and control of energy efficiency of enterprises, Chemical Technology. Control and Management, 172-181 (2020)

[7] Mirzoyev N.N., Sayfiyev O.H., Temirov T.O. Investigation of unauthorized connection to electrical networks, failure to detect their phase interruptions and short circuits to ground, ResearchJet Journal of Analysis and Inventions 3 (10), 130-143 (2022)

[8] Mirzoyev N.N., Sobirov S. Study of violations of quality indicators of electricity supply network, Central Asian Journal of Education and Innovation, 83-86 (2023)

[9] Mirzoyev N.N., Sobirov O. Sh. Computerized measurement control system of unauthorized connection to electrical networks and isolation control detection, Science and Education, 488-502 (2023)

[10] I.X. Siddikov, N.N. Mirzoyev, M.A. Anarboev. Elektr energiyasini tejash va samaradorligini oshirish uchun gibrid quyosh elektr stansiyasini loyihalash uslubiyoti. “Raqamli energetika tizimini yaratishning istiqbollari, muqobil energiya olishning muammolari va yechimlari-2023” xalqaro ilmiy-amaliy konferensiyasining ilmiy maqola va tezislari to‘plami. Jizzax, 2023 yil 19-20 may, 175-181bet

[11] Azamov S. et al. ANALYSIS OF ELECTRICAL AND MECHANICAL CONDITION MONITORING OF ASYNCHRONOUS MOTOR SUPPLIED FROM SOLAR PANEL ENERGY SOURCE //Conference on Digital Innovation:" Modern Problems and Solutions". – 2023.elektr ta’minoti tizimini loyihalash. Pedagogs jurnali 10 (1), 2022/6/11, 100-108 bet

[12] I.X. Siddiqov M.Q. Xoliqberdiyev, N.N. Mirzoyev.WE3000 markali shamol elektr stansiyasining elektr energiyasining sifat ko ‘rsatkichlarining tahlili. PEDAGOGS jurnali 10 (1), 2022/6/11, 93-99 bet

[13] I.X. Siddikov, N.N. Mirzoyev, M.A. Anarboev, S.I. Davrboeva. Izolyatsiya holatini monitoring qilish va elektr tarmoqlariga ruxsatsiz ulanishlarni aniqlash uchun kompyterlashgan axborot o ‘lchov tizimiming istiqbollari, “Raqamli energetika tizimini yaratishning istiqbollari, muqobil energiya olishning muammolari va yechimlari-2023” xalqaro ilmiy-amaliy konferensiyasining ilmiy maqola va tezislari to‘plami. Jizzax, 2023 yil 19-20 may, 252-257bet.

[14] Аъзамов С.С. Анализ устройств и методов удаленного мониторинга энергопотребления потребителей возобновляемых источников энергии. Научный журнал транспортных средств и дорог, №4 Issue 4, 2022 e-mail: nauka@tstu.uz http://transportjournals.uz/.

Information about the author

Mirzoev Narzullo Nuriddinovich	Bukhara Engineering and Technology Institute, Head of the Department of “Energoaudit”, Associate Professor, Candidate of Technical Sciences (PhD) https://orcid.org/0009-0003-6979-7660
Azamov Saidikrom Saidmurodovich	Andijan State Technical Institute, Faculty of Electrical Engineering, senior teacher (PhD) https://orcid.org/0009-0005-0615-5518

Comparative analysis of the degree of influence of factors on the speed of trains (using the example of Uzbek railways)

D.B. Butunov[1][a], S.A. Abdukodirov[1][b], Ch.B. Jonuzokov[1]
[1]Tashkent state transport university, Tashkent, Uzbekistan

Abstract: The main objective of the work is to conduct a comparative analysis of the impact of the main factors on train speeds on the normative and implemented train traffic schedule indicators. This was done using systematic, analytical, factor and tabular analyses. The train traffic speeds on the railway sections of the regional railway nodes of "UTY" JSC were systematically analyzed for the period 2011-2022, and as a result, the main factors that significantly negatively affect the actual implementation of the established normative speed values (replacement of train locomotives, the number of seasonal freight trains, stopping times at stations along the route, the number of seasonal passenger trains) were identified. The shares of the degree of influence of the identified main factors on the speed of freight trains on the railway sections were determined according to the criteria of weak, medium and strong. It was determined that the share of the main factors influencing the speed of freight trains on the railway sections under the jurisdiction of "UTY" JSC is weak - 32%, medium - 44% and strong - 24%. The method of systematic analysis of factors makes it possible to reasonably establish the values of train speeds in the production process and predict them on a daily, quarterly and annual basis.

Keywords: Train speed, factor, systematic analysis, comparative analysis, railway section

1. Introduction

One of the important tasks of the railway transport management system is the delivery of cargo and passengers in accordance with the established technical standards of the train traffic schedule (TTS) based on the daily planned performance indicators [1-4]. In this regard, the level of actual implementation of such indicators as technical equipment, movement speeds, type of traction supply, transportation and throughput capacity of railway sections attached to railway enterprises (regional railway nodes (RRN)) is of great importance [5, 6].

When standardizing the values of train speeds, the existing capacity of railway sections, the standard interval time, and the flow of freight and passenger trains are taken into account. However, the share of constant factors affecting the speed of movement during train movement is not taken into account. In particular, the number of high-speed passenger trains on railway sections, the traction force of locomotives, the variability of seasonal train flows, inefficient waiting of trains at stations, etc [1, 4, 7-9].

It is advisable to assess the values of train speeds for the next day, quarter and year by comparing the share of factors with the level of influence of established technical standards and the indicators actually achieved.

2. Research methodology

For comparative analysis of the speed indicators in the train movement graph, the following analytical methods are used: ((1)÷(3)- expressions) [1, 7]:

running speed

$$\vartheta_{run} = \frac{L_{sec}}{t_{run}} \quad (1)$$

technical speed

$$\vartheta_{tech} = \frac{L_{sec}}{t_{run}+\sum t_{ac/sl}} \quad (2)$$

section speed

$$\vartheta \frac{L_{sec}}{t_{run}+\sum t_{ac/sl}+\sum t_{in.st}{}_{sec}} \quad (3)$$

here L_{uch} – length of specific railway sections, km;

t_{yur} – the time spent on trains moving at the set speed on the sections, hours;

$\sum t_{or.st}$ – time spent by freight trains on technological operations at intermediate stations and passing trains in the opposite direction, hours;

$\sum t_{t/s}$ – time spent by trains on acceleration and deceleration, hours;

These analytical expressions ((1)÷(3)) allow for the assessment of daily operational indicators on railway sections and planning for future periods. In particular, they allow for the comparison of daily operational indicators of the normative and implemented TTS, the determination of the reserve carrying capacity of sections, and the analysis of factors that negatively affect the established technical standards of movement speeds.

To stabilize transportation processes on the railway network, automated information systems have been developed and put into practice instead of information systems. These systems create opportunities for operational management of train movements on railway sections and assessment of their technical and economic efficiency [3]. For a comprehensive assessment of the TTS, a mathematical method has been developed for calculating the capacity of freight trains during periods when railway sections are devoid of passenger trains [8]

$$N_{fr}^{max\ min\left(\sum_{i=1}^{n\sum}\frac{\Delta t_{zon}^{i}}{T_{int}}0\right)} \quad (4)$$

there

N_{fr}^{max} – The TTG has a maximum number of freight train movements during the period when the passenger is free of the train zone;

[a] https://orcid.org/0009-0009-4165-0257
[b] https://orcid.org/0000-0001-9457-255X

https://doi.org/10.56143/3030-3893-2025-1-45-50 A bridge between science and innovation

Δt^{i}_{zon} – Time in the TMG in the freight train running zone, minutes.

T_{int} – interval time between trains, minutes;

1 – Extra train for fast TMG conversion.

In [9], a method for estimating the speed of a section was developed, taking into account factors that indicate the daily movement of freight trains.

$$\vartheta\left(1 - A\frac{T}{1440}\right)_{run_{sec}} \quad (5)$$

here

A – correlation coefficient of factors affecting the movement of freight trains;

T – total travel time of freight trains on railway sections, minutes;

ϑ_{run} – speed of freight trains, km/h;

The author developed a method for analyzing and estimating section speed, taking into account random factors *(A)* affecting the movement of freight trains on railway sections, the speed of travel on sections, and the total time spent on the movement of freight trains during the day *(T)*.

3. Result and discussion

The impact of freight turnover on train speeds on railway sections within the regional railway hubs of "UTY" JSC was analyzed for the period 2011-2022 (Figure 1).

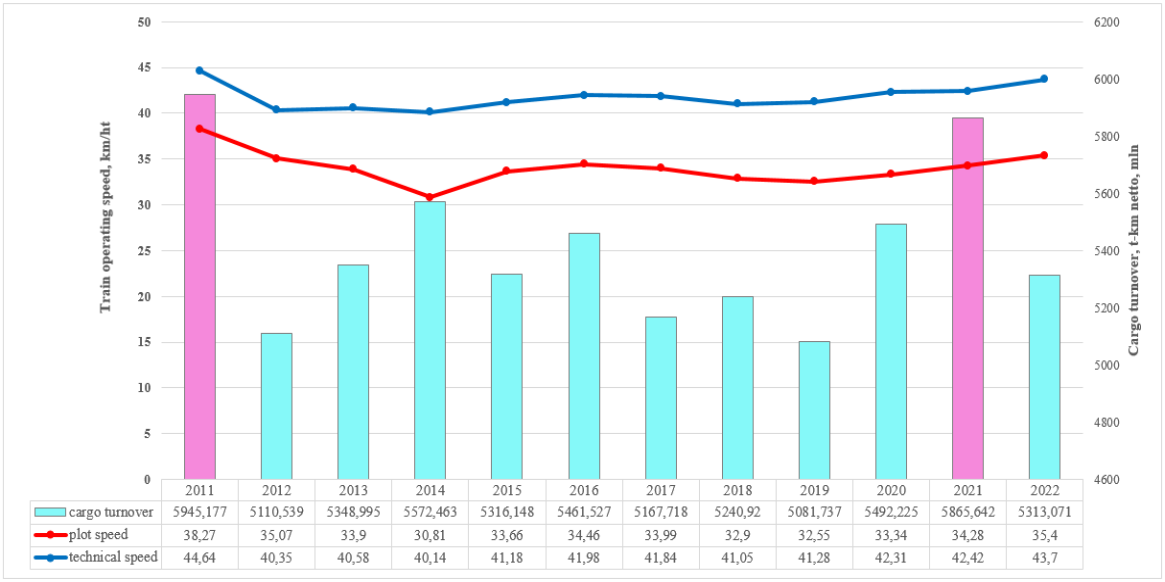

	2011	2012	2013	2014	2015	2016	2017	2018	2019	2020	2021	2022
cargo turnover	5945,177	5110,539	5348,995	5572,463	5316,148	5461,527	5167,718	5240,92	5081,737	5492,225	5865,642	5313,071
plot speed	38,27	35,07	33,9	30,81	33,66	34,46	33,99	32,9	32,55	33,34	34,28	35,4
technical speed	44,64	40,35	40,58	40,14	41,18	41,98	41,84	41,05	41,28	42,31	42,42	43,7

Fig. 1. Dynamics of the degree of influence of the amount of cargo turnover on train speeds on railway sections within the regional railway nodes of JSC "UTY"

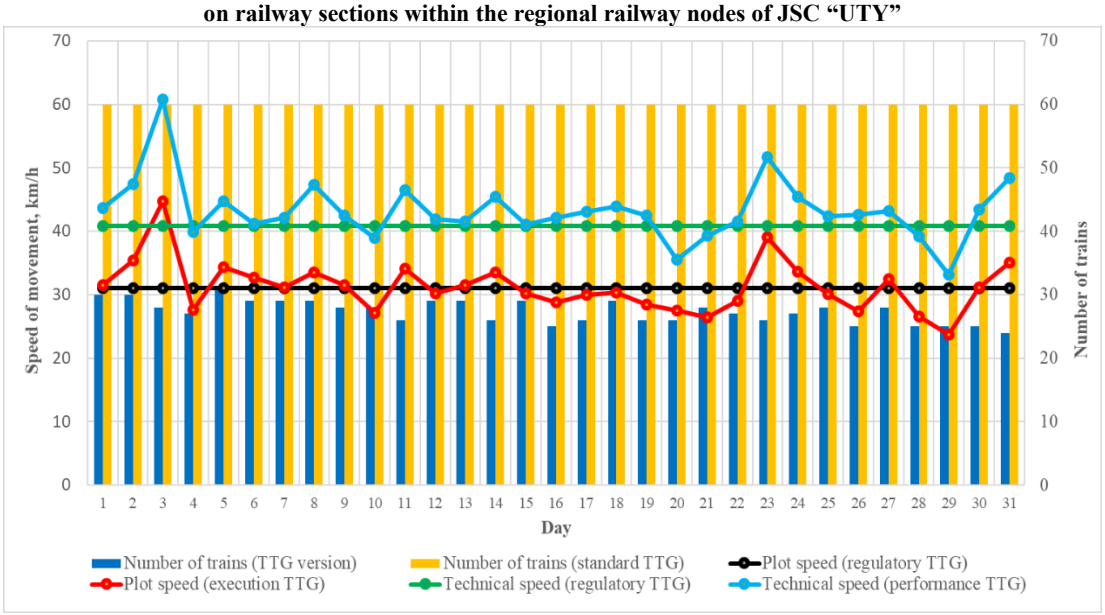

Fig. 2. Comparative analysis of the daily volume of freight trains in relation to technical and section speeds and the main indicators of the normative and implemented TTS (Uzbekistan-Khovos-Jizzakh)

The results of the analysis show that the dynamics of annual freight turnover (increase and decrease) does not significantly affect the speed of freight trains (SFT). Therefore, the factor of increase or decrease in the amount of freight turnover does not play a significant role in establishing the technical standards of SFT for specific sections and routes of "UTY" JSC.

Based on the statistical data of "UTY" JSC, a comparative analysis of the impact of the number of freight trains on the SFT (Uzbekistan-Khovos-Jizzakh) was carried

out (Table 1). The comparative analysis was carried out for December, when the number of trains was the highest. Based on the data obtained from the analysis results, the impact of the change in the daily number of freight trains on the technical and section speeds and the main indicators of the normative and implemented SFT (Uzbekistan-Khovos-Jizzakh) was presented in the form of a diagram (Figure 2).

The technical and section speeds were determined as 41.8 and 32.95 km/h, respectively, when the average number of freight trains on the normative TTS was 21 pairs. The technical and section speeds were analyzed as 43.3 and 27.3 km/h, respectively, when the average number of freight trains on the operational PHG in December 2022 was 14 pairs. A comparative analysis of the main indicators of the normative and operational TTS showed that the number of freight trains was 7 pairs less, the technical speed was 1.5 km/h higher on average, and the section speed was 5.6 km/h lower.

In the analyzed month (Table 1), it can be seen that, in accordance with the change in the daily volume of freight trains, that is, on days when the number of trains increased, technical and section speeds decreased by more than 90% (for example, days 4 and 29), and in about 10% of cases, TTS indicators increased.

Table 1

Comparative analysis of the impact of the number of freight trains on the railway section "Uzbekistan-Khovos-Jizzakh" (December 2022)

Day	Distance traveled, km	Dwell times, hours	Time in motion, hours	Number of freight trains	Site speed, (average) km/h	Technical speed, (average) km/h
1	3351,4	29,51	76,74	30	31,54	43,67
2	3519,4	25,18	74,18	30	35,42	47,44
3	3930,7	23,13	64,72	28	44,74	60,73
4	2887,1	32,16	72,34	27	27,63	39,91
5	3304,1	22,56	73,78	31	34,30	44,78
6	3057,6	19,31	74,17	29	32,71	41,22
7	3074,3	25,78	72,89	29	31,16	42,18
8	3308,9	28,75	69,94	29	33,53	47,31
9	3080,6	25,14	72,48	28	31,56	42,50
10	3138,6	35,01	80,69	28	27,13	38,90
11	3002,9	23,55	64,51	26	34,10	46,55
12	3001,2	27,73	71,68	29	30,19	41,87
13	3151,4	23,97	75,89	29	31,56	41,53
14	2795,9	22,01	61,46	26	33,50	45,49
15	3128,6	27,27	76,08	29	30,27	41,12
16	2595,3	28,33	61,65	25	28,84	42,10
17	2699,9	27,26	62,71	26	30,01	43,05
18	3128,4	31,77	71,26	29	30,36	43,90
19	2758,5	32,12	65,01	26	28,40	42,43
20	2420,7	20,16	68,03	26	27,45	35,58
21	2659,5	33,02	67,71	28	26,40	39,28
22	2872,9	29,93	69,15	27	29,00	41,55
23	3086,8	19,42	59,66	26	39,03	51,74
24	2813,6	21,55	61,99	27	33,68	45,39
25	2679,6	25,83	63,19	28	30,10	42,41
26	2887,7	37,59	67,71	25	27,42	42,65
27	3079,3	23,47	71,31	28	32,49	43,18
28	2530,3	30,77	64,51	25	26,56	39,22
29	2921,7	35,15	88,14	25	23,70	33,15
30	2961,21	26,88	68,11	25	31,17	43,48
31	2833,93	22,38	58,53	24	35,03	48,42
General	**92662,04**	**836,69**	**2150,22**	**848**	**31,02**	**43,09**

It can be seen that the factors influencing the organization of train movement on the comparatively analyzed railway section have different effects on the level of fulfillment of the SFT normative values. In particular, it can be seen that the factors analyzed as the main factors (replacement of train locomotives, the number of seasonal freight trains, stopping times at stations along the route, the number of seasonal passenger trains) have high levels of influence.

Factors with high levels of influence have shown the feasibility of analyzing technical, technological, permanent and random factors affecting the RRT on railway sections not only in groups, but also in a comparative analysis of the main factors on specific sections [2, 10]. Therefore, the sections of the regional railway junction unitary enterprises (RRJUE) under the jurisdiction of UTY JSC (Tashkent RRN (Uzbekistan-Khovos-Jizzakh, Tashkent junction, Sergeli-Angren-Khojikent), Bukhara RRN (Khovos-Jizzakh-

Maroqand, Maroqand-Bukhara-Khojidavlat, Tinchlik-Uchkuduk 2-Misken, Bukhara-Misken), Kokand RRN (Kokand-Margilan Karasuv, Khovos-Kokand-Akhunboboyev, Pop-Angren), Karshi RRN (Bukhara-Karshi-Maroqand), Termez RRN (Tashguzar-Boysun-Kumqorgon, Karshi-Termez-Sarosiyo), Qongorod RRN (Qongorod-Taxiyatosh-Urgench-Misken-Nukus, a comparative analysis was carried out on the example of the main factors influencing the RRN on the Kungirat-Jaslyk-Qaraqalpak section.

The comparative analysis was carried out on the example of the following main factors:

- replacement of train locomotives;
- seasonal number of freight trains;
- stopping times at stations along the route;
- seasonal number of passenger trains.

In this case, the impact of the above factors on the reduction of the normative values of the SFT in the section of the RRN sections was analyzed comparatively based on the criteria of weak, medium and strong (Table 2).

Table 2

Results of assessment of the impact of the main factors on the level of safety of railway sections under the control of "UTY" JSC

Impact level criteria	RRJUE Tashkent			RRJUE Bukhara				RRJUE Kokand		RRJUE Karshi	RRJUE Termez		RRJUE Qongorod	
	Uzbekistan-Khovos-Jizzakh	Tashkent junction	Sergeli-Angren-Khojikent	Khovos-Jizzakh-Maroqand	Maroqand-Bukhara-Khojidavlat	Tinchlik-Uchkuduk 2-Misken	Bukhara-Misken	Kokand-Margilan Karasuv	Khovos-Kokand-Akhunboboyev	Bukhara-Karshi-Maroqand	Tashguzar-Boysun-Kumqorgon	Karshi-Termez-Sarosiyo	Qongorod-Taxiyatosh-Urgench-Misken-Nukus	Kungirat-Jaslyk-Qaraqalpak
	1	2	3	4	5	6	7	8	9	10	11	12	13	14
replacement of train locomotives														
Weak			+			+			+					+
Average		+			+			+				+	+	
Strong	+			+			+			+	+			
seasonal number of freight trains														
Weak			+					+			+			+
Average		+			+	+	+		+	+		+	+	
Strong	+			+										
stopping times at stations along the route														
Weak			+				+				+		+	+
Average		+			+	+		+	+			+		
Strong	+			+						+				
seasonal number of passenger trainsr														
Weak							+		+			+	+	+
Average			+		+	+		+		+	+			
Strong	+	+		+										

From the results of the assessment of the degree of influence of factors on the SFT, it can be seen that, except for the factor of the number of seasonal freight trains of the Tashkent RRN (Table 2), the degree of influence of all types of factors on the SFT is the same, that is, from 33.3% (strong - 33.3%, weak - 33.3%, average - 33.3%).

Based on the results presented in Table 2, the share of the degree of influence of each factor (replacement of train locomotives, number of seasonal freight trains, stopping times at stations along the route, number of seasonal passenger trains) on the SFT was assessed in the RRN section (Figures 3÷6).

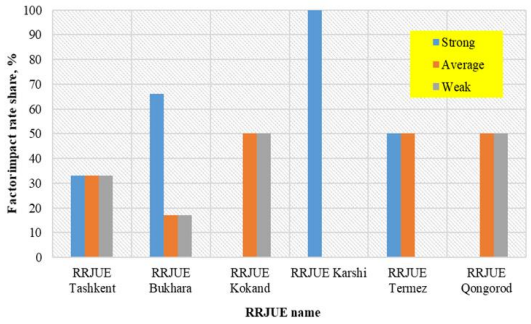

Fig. 3. The share of the impact of the locomotive replacement factor on the SFT of the RRJUEs under the jurisdiction of "UTY" JSC

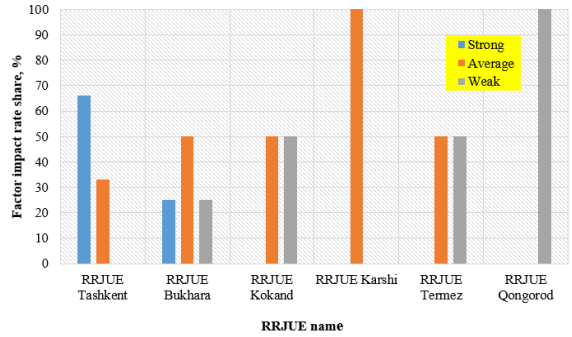

Fig. 4. The share of the impact of the seasonal freight train volume factor on the SFT for RRJUEs under the jurisdiction of "UTY" JSC

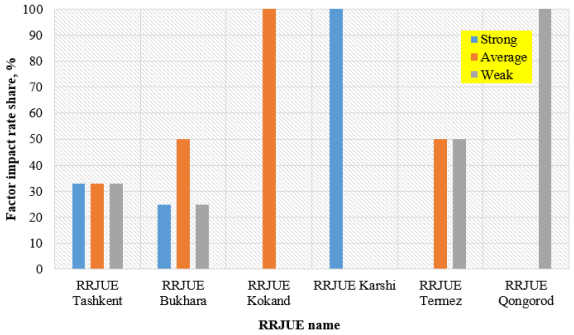

Fig. 5. The share of the impact of the factor of stopping times at stations along the route on the SFT for RRJUEs under the jurisdiction of "UTY" JSC

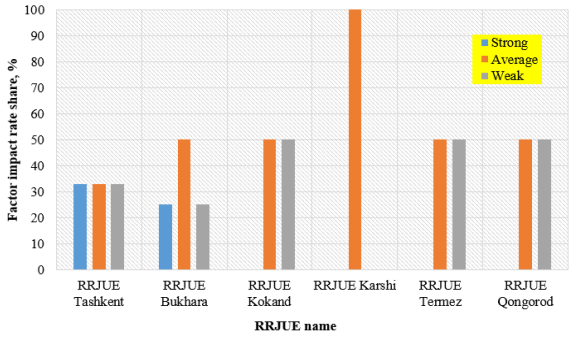

Fig. 6. The share of the impact of the seasonal passenger train volume factor on the SFT for RRJUEs under the jurisdiction of "UTY" JSC

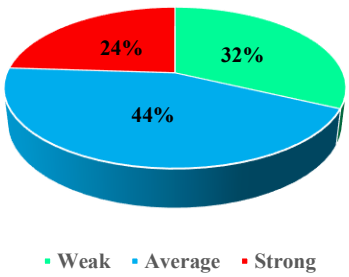

Fig. 7. The share of the main factors influencing the level of road safety on railway sections under the control of UTY JSC

The impact of factors that strongly influence the SFT is not significant. From the results presented in Figures 3÷6 and Table 1, it can be concluded that the negative impact of the main factors on the implementation of the SFT normative values is high. That is, the level of impact according to the strong and medium criteria is more than 60%. It can be seen that the negative impact of the main factors on the SFT on the railway sections under the control of "UTY" JSC is high (68% (strong - 24%, medium - 44%)) (Figure 7).

4. Conclusion

A comparative analysis of the degree of influence of the main factors on the speed of trains was conducted on the section of railway sections within the framework of the Tashkent State Railways and Transport Corporation under the jurisdiction of "UTY" JSC. The criteria for the degree of influence on the speed of trains (weak, medium, strong) on the sections of the railway sections of the RRN were assessed. As a result, it was possible to predict the daily, quarterly and annual indicators of the impact on the level of implementation of the established normative values of the RRN and the factors analyzed as the main indicators. A comparative comparative analysis of the main indicators of the normative and implemented speed of trains was carried out on the "Uzbekistan-Khovos-Jizzakh" railway section within the framework of the Tashkent State Railways and Transport Corporation under the jurisdiction of "UTY" JSC based on statistical and practical data.

The comparative analysis showed that despite the different number of freight trains in the implemented TTS during the days of December 2022, it was determined that the train speeds were at the lowest values on the 4th and 29th. Therefore, in the future, when establishing technical standards for the SFT on specific railway sections and routes under the jurisdiction of "UTY" JSC, it was proposed to establish TTS indicators based on the results of the comparative analysis.

References

[1] Dilmurod Butunov, Sardor Abdukodirov, Shuhrat Buriyev and Muslima Akhmedova. Development factor model of train movement graph indicators. E3S Web of Conferences 531, 02008 (2024). 1-10. DOI: https://doi.org/10.1051/e3sconf/202453102008

[2] Butunov D. Effective organization of train movement taking into account the costs of electrical energy / Butunov D., Abdukodirov S // Journal of Transport. - 2024. №1 (2). 73-78 pp. https://t.me/tdtuilmiynashrlar

[3] Мехедов М. И., Сотников Е. А., Холодняк П. С., Лобанов С. В. Переход к автоматизированным информационно-управляющим системам оперативного управления перевозочным процессом на сети ОАО «РЖД» // Вестник Научно-исследовательского института железнодорожного транспорта (Вестник ВНИИЖТ). 2024. Т. 83, № 3. С. 231–247.

[4] Сардор Абдукодиров. Юк поездлари ҳаракат тезликларининг ўрнатилган техник меъёрлари бажарилиши таҳлили. / Дилмурод Бутунов, Мухамметжан Мусаев // Eurasian Journal of Mathematical Theory and Computer Sciences, -2023. №2(5). 51–58. https://doi.org/10.5281/zenodo.6584509

[5] Голигузова А. Л. Методы оптимизации ходовых скоростей движения грузовых поездов на

железнодорожных участках: Дис. кан. техн. наун. МГУПС (МИИТ). – 2014. – 160 с.

[6] Кузнецов Г.А. Учет выполнения графика движения грузовых поездов / Г.А. Кузнецов // Железнодорожный транспорт. - 2011. - № 3. - С. 20–25.

[7] Хусаинов Ф.И., Показатели скорости как аналитические инструменти для оценки работы железных дорог // Экономика и управление: - 2017. №4 (71). – С. 19-22 с. https://publications.hse.ru/articles/248447926

[8] Huaqing Mao. Train Schedule Adjustment Strategies for Train Dispatch / Huaqing Mao, Zhu Li // TELKOMNIKA. – 2013. №5. – С. 2526-2534 pp. DOI:10.11591/telkomnika.v11i5.2483

[9] Алферова А.А. Риск снижения участковой скорости движения грузового поезда и экономическая селесообразност эго учета / А.А. Алферова // Железнодорожний транспорт. – 2017. №3. 58-60 pp.

Information about the author

Butunov Dilmurod Baxodirovich	Tashkent State Transport University, PhD, Professor of the Department of "Management of railway operation" e-mail: dilmurodpgups@mail.ru Tel.: +99897 2675567 https://orcid.org/0009-0009-4165-0257
Abdukodirov Sardor Askar ugli	Tashkent State Transport University, PhD, Docent of the Department of "Management of railway operation" e-mail: sardor_abduqodirov@bk.ru Tel.: +99897 7342992 https://orcid.org/0000-0001-9457-255X
Jonuzokov Choriyor Berdimuro-dovich	Tashkent State Transport University, Senior doctoral student E-mail: jonuzoqovchoriyor@gmail.com Tel.: +99890 8680804

The use of modern composite materials and technologies in the design of Unmanned Aerial Vehicles

Z.Z. Shamsiev[1][a], Kh.Kh. Khusnutdinova[1][b], N.A. Abdujabarov[1][c], J.K. Takhirov[1][d]
[1]Tashkent state transport university, Tashkent, Uzbekistan

Abstract: The integration of modern composite materials and advanced manufacturing technologies has revolutionized the design and performance of Unmanned Aerial Vehicles (UAVs). This study investigates the application of carbon fiber-reinforced polymers (CFRP), glass fiber-reinforced polymers (GFRP), and hybrid composites in UAV structures. Through experimental testing, computational modeling, and aerodynamic analysis, the research demonstrates significant improvements in weight reduction, structural integrity, and aerodynamic efficiency. The results indicate that composite materials enhance UAV performance by increasing payload capacity, extending flight duration, and improving overall durability. This paper underscores the critical role of composites in advancing UAV technology and provides a foundation for future innovations in aerial vehicle design.

Keywords: Composite Materials, Unmanned Aerial Vehicles (UAVs), UAV Design, Carbon Fiber-Reinforced Polymers (CFRP), Glass Fiber-Reinforced Polymers (GFRP), Hybrid Composites, Aerodynamic Efficiency, Structural Integrity, Lightweight Structures, Advanced Manufacturing Technologies

1. Introduction

Unmanned Aerial Vehicles (UAVs) have rapidly evolved to become essential tools across a myriad of industries, including surveillance, environmental monitoring, agriculture, and logistics. The versatility and operational efficiency of UAVs make them invaluable for tasks that range from real-time data collection to delivering critical supplies in remote or hazardous areas. As the demand for UAVs with enhanced performance metrics such as increased payload capacity, extended flight durations, and improved maneuverability continues to grow, the need for advanced materials and innovative design methodologies becomes paramount [1].

Traditionally, UAV structures have been fabricated using metallic materials like aluminum and titanium alloys. While these materials offer sufficient strength and durability, their relatively high densities impose significant weight burdens. This weight not only limits the payload capacity and flight endurance but also increases fuel consumption and operational costs. Consequently, there is a pressing need to explore alternative materials that can mitigate these limitations without compromising structural integrity or performance [2].

Composite materials, particularly Carbon Fiber-Reinforced Polymers (CFRP) and Glass Fiber-Reinforced Polymers (GFRP), have emerged as promising alternatives to traditional metals in UAV construction. These materials are celebrated for their exceptional strength-to-weight ratios, corrosion resistance, and design flexibility. CFRP, for instance, offers superior tensile strength and stiffness, making it ideal for critical structural components where performance and weight reduction are crucial.

GFRP, while slightly less robust than CFRP, provides a more cost-effective solution with adequate mechanical properties for less demanding applications. Additionally, hybrid composites that combine carbon and glass fibers are being investigated to balance performance and cost, offering tailored properties that meet specific design requirements [3].

Advancements in manufacturing technologies have further propelled the adoption of composite materials in UAV design. Techniques such as Automated Fiber Placement (AFP) and Resin Transfer Molding (RTM) enable the precise and efficient fabrication of complex geometries that are often challenging to achieve with traditional manufacturing methods. AFP allows for the meticulous placement of fibers, minimizing material waste and ensuring consistent quality across components. RTM facilitates the creation of intricate shapes with minimal voids, enhancing the structural integrity and aerodynamic performance of UAVs. Moreover, the integration of additive manufacturing, or 3D printing, into composite fabrication processes offers unprecedented flexibility in prototyping and customizing UAV components, accelerating the innovation cycle and reducing time-to-market [4].

This paper delves into the pivotal role of modern composite materials and manufacturing technologies in revolutionizing UAV design. By examining the mechanical performance, weight optimization, and aerodynamic efficiency of UAVs constructed with CFRP, GFRP, and hybrid composites, this study aims to elucidate the tangible benefits these materials offer over traditional metals. Through a combination of experimental testing, computational modeling, and aerodynamic analysis, the research provides a comprehensive evaluation of how composites enhance UAV performance. The findings underscore the transformative potential of composite integration in UAV structures, paving the way for future advancements in aerial vehicle technology.

2. Research methodology

The selection of appropriate materials is critical in the design and optimization of Unmanned Aerial Vehicles (UAVs). This study focuses on evaluating Carbon Fiber-

[a] https://orcid.org/0000-0002-0323-9741
[b] https://orcid.org/0009-0000-2608-8184
[c] https://orcid.org/0000-0002-1989-5380
[d] https://orcid.org/0009-0004-9275-6653

Reinforced Polymers (CFRP), Glass Fiber-Reinforced Polymers (GFRP), and hybrid composites that integrate both carbon and glass fibers. The primary criteria for material selection include tensile strength, modulus of elasticity, density, fatigue resistance, and cost-effectiveness. These criteria ensure that the chosen materials not only enhance the structural performance of UAVs but also maintain economic feasibility for large-scale production.

CFRP is renowned for its exceptional tensile strength and stiffness, making it ideal for critical structural components that require high performance and weight reduction. The high strength-to-weight ratio of CFRP allows for significant weight savings without compromising structural integrity, which is essential for improving UAV payload capacity and flight endurance [5].

GFRP offers a more cost-effective alternative to CFRP while still providing adequate mechanical properties for less demanding applications. Although GFRP has a lower tensile strength and modulus of elasticity compared to CFRP, its versatility and ease of manufacturing make it suitable for various UAV components where extreme performance is not paramount [6].

Hybrid composites, which combine carbon and glass fibers, aim to balance performance and cost. By integrating both types of fibers, hybrid composites can be tailored to achieve specific mechanical properties required for different UAV sections. This approach allows for optimized material usage, where carbon fibers are utilized in high-stress areas and glass fibers are employed in regions where lower strength is acceptable [7].

Selection criteria:

- Determines the material's ability to withstand tensile forces without failure.
- Indicates the stiffness of the material, affecting the UAV's structural rigidity.
- Lower density contributes to weight reduction, enhancing payload capacity and flight duration.
- Ensures durability and longevity of UAV components under cyclic loading conditions.
- Balances material performance with economic viability for production scalability.

Table 1

Comparative material properties for UAV Structures

Material	Tensile Strength (MPa)	Modulus of Elasticity (GPa)	Density (g/cm³)	Cost ($/kg)
Aluminum	300	69	2.70	2.0
CFRP	600	150	1.60	15.0
GFRP	400	35	2.50	8.0
Hybrid	500	90	2.05	10.0

The materials were selected based on their ability to meet the performance requirements of modern UAVs. CFRP was chosen for its superior mechanical properties, making it suitable for high-stress areas such as the UAV frame and wings. GFRP was selected for components where cost savings are critical, and the mechanical demands are lower. Hybrid composites were incorporated to achieve a balance between performance and cost, allowing for strategic placement of different fiber types within the UAV structure.

To effectively utilize the selected composite materials, advanced manufacturing techniques were employed. These techniques enable the precise fabrication of complex UAV geometries, ensuring optimal material properties and structural performance.

- AFP technology allows for the accurate placement of fibers in predefined patterns, reducing material waste and ensuring consistent quality across UAV components. This method is particularly beneficial for creating lightweight and strong structures with minimal defects [8].
- RTM facilitates the production of complex shapes with minimal voids, enhancing the structural integrity and aerodynamic performance of UAVs. This technique involves injecting resin into a closed mold containing the fiber reinforcement, ensuring thorough impregnation and consolidation of the composite material [9].
- The integration of 3D printing enables rapid prototyping and customization of UAV components. Additive manufacturing allows for the creation of intricate designs with tailored mechanical properties, accelerating the development cycle and reducing time-to-market for innovative UAV solutions [10].

Comprehensive experimental testing was conducted to evaluate the mechanical and aerodynamic performance of UAV structures fabricated with the selected composite materials. The testing procedures included:

- Performed to determine the tensile strength and modulus of elasticity of CFRP, GFRP, and hybrid composites. Specimens were subjected to uniaxial tensile loading until failure, and stress-strain curves were generated to assess material performance [11].
- Conducted to assess the compressive strength and behavior of the composite materials under load. These tests help in understanding the material's ability to withstand compressive forces, which is crucial for maintaining structural integrity during flight [12].
- Evaluated the durability and lifespan of the composite materials under cyclic loading conditions. Fatigue testing simulates the repetitive stresses experienced by UAV components during operation, providing insights into the long-term reliability of the materials [13].
- Utilized a wind tunnel to measure drag coefficients and assess airflow characteristics around UAV prototypes with composite structures. Aerodynamic testing ensures that the composite integration contributes to reduced drag and enhanced flight stability [14].
- In addition to experimental testing, computational modeling techniques were employed to simulate and predict the behavior of composite UAV structures under various conditions.
- FEA was used to simulate the structural behavior of composite UAV components under different loading scenarios. This analysis helps in identifying stress concentrations, potential failure points, and optimizing the material distribution within the UAV structure [15].
- CFD simulations were performed to analyze the aerodynamic performance of UAVs with composite structures. These simulations focus on drag reduction, airflow stability, and overall aerodynamic efficiency, providing valuable data for design optimization [16].

3. Results and Discussion

The integration of modern composite materials in Unmanned Aerial Vehicles (UAVs) has demonstrated

substantial improvements in various performance metrics. This section presents the findings from mechanical testing, weight optimization, aerodynamic analysis, and structural integrity evaluations of UAV structures fabricated using Carbon Fiber-Reinforced Polymer (CFRP), Glass Fiber-Reinforced Polymer (GFRP), hybrid composites, and traditional aluminum.

The mechanical performance of the selected materials was rigorously evaluated through tensile, compression, and fatigue tests. The results underscore the superior mechanical properties of CFRP and hybrid composites compared to traditional aluminum, highlighting their suitability for high-performance UAV applications.

Tensile testing was conducted to determine the tensile strength and modulus of elasticity for each material. The specimens were subjected to uniaxial tensile loading until failure, and the resulting stress-strain curves were analyzed.

- Exhibited the highest tensile strength at approximately 600 MPa and a modulus of elasticity of 150 GPa. The stress-strain curve for CFRP demonstrated linear elastic behavior up to failure, indicating excellent tensile properties and stiffness [17].
- Showed a tensile strength of 400 MPa and a modulus of elasticity of 35 GPa. While lower than CFRP, GFRP still offers substantial strength for applications where extreme performance is not critical [18].
- Achieved a tensile strength of 500 MPa and a modulus of elasticity of 90 GPa. The hybrid approach effectively balances the high strength of CFRP with the cost-effectiveness of GFRP, providing tailored mechanical properties suitable for diverse UAV components [19].
- Served as a baseline with a tensile strength of 300 MPa and a modulus of elasticity of 69 GPa.

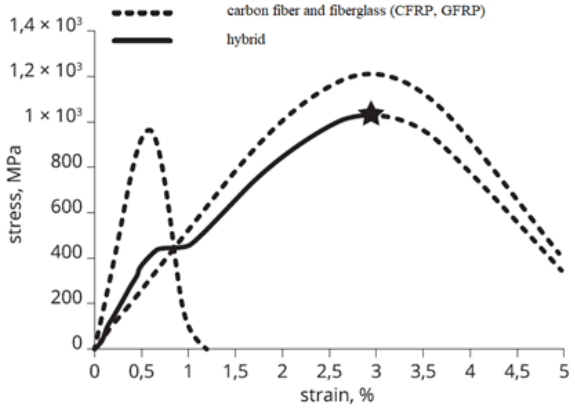

Fig. 1. Stress-strain curves of CFRP, GFRP, hybrid composites

The stress-strain analysis confirms that CFRP outperforms both GFRP and aluminum in terms of tensile strength and stiffness. Hybrid composites offer a middle ground, providing enhanced mechanical properties compared to GFRP while maintaining cost-effectiveness.

Compression testing assessed the ability of each material to withstand compressive forces. The results are summarized in Table 2.

Table 2

Compressive strength and behavior underload

Material	Compressive Strength (MPa)	Behavior Under Load
Aluminum	350	Exhibited plastic deformation before failure.
CFRP	550	Maintained structural integrity with minimal deformation.
GFRP	380	Showed some deformation but retained overall structure.
Hybrid	480	Balanced deformation with maintained integrity.

CFRP demonstrated superior compressive strength, closely followed by hybrid composites, making them ideal for load-bearing UAV components.

Fatigue testing evaluated the durability of the materials under cyclic loading conditions, simulating real-world operational stresses.

- Exhibited excellent fatigue resistance, with no significant degradation in mechanical properties after 105105 cycles.
- Showed moderate fatigue resistance, with a slight decrease in tensile strength after 105105 cycles.
- Demonstrated improved fatigue performance compared to GFRP, attributable to the reinforcing effect of carbon fibers.
- Experienced noticeable fatigue degradation, with a 20% reduction in tensile strength after 105105 cycles.

The fatigue performance results indicate that CFRP and hybrid composites offer enhanced durability and longevity for UAV structures, reducing the need for frequent maintenance and component replacements.

Weight reduction is a critical factor in UAV design, directly impacting payload capacity, flight duration, and overall performance. The incorporation of composite materials resulted in significant weight savings compared to traditional aluminum structures.

Table 3

Weight comparison of UAV structures

Material	Weight (kg)	Strength (MPa)	Cost ($/kg)
Aluminum	50	300	2.0
CFRP	35	600	15.0
GFRP	40	400	8.0
Hybrid	38	500	10.0

Table 3 illustrates a 30% reduction in weight when using CFRP compared to aluminum, with hybrid composites offering a balanced reduction of 24%.

The weight optimization results reveal that CFRP provides the most substantial weight savings, enabling UAVs to carry heavier payloads and achieve longer flight durations. Hybrid composites, while slightly heavier than CFRP, still offer significant weight reductions while maintaining cost-effectiveness.

Aerodynamic performance is paramount for UAVs, influencing speed, maneuverability, and fuel efficiency.

https://doi.org/10.56143/3030-3893-2025-1-51-55 A bridge between science and innovation

Wind tunnel testing was conducted to assess the drag coefficients of UAV prototypes constructed with different materials.

Fig. 2. Aerodynamic drag comparison between composite and aluminum UAVs

The results indicate that UAVs with composite structures achieved a 15% reduction in aerodynamic drag compared to those constructed with aluminum. The smooth surface finish achievable through composite manufacturing techniques minimizes turbulence and enhances airflow stability, contributing to improved aerodynamic efficiency and flight performance.

$$C_d = \frac{2F_d}{\rho v^2 A} \quad (1)$$

Where:

- C_d = Drag coefficient;
- F_d = Drag force;
- ρ_ρ = Air density;
- v = Velocity;
- A = Reference area.

The reduction in Cd*Cd* for composite UAVs translates to lower energy consumption and increased operational efficiency, making composites a superior choice for aerodynamic optimization.

Maintaining structural integrity under various loading conditions is essential for the reliability and safety of UAVs. Finite Element Analysis (FEA) simulations and experimental testing were employed to evaluate the structural performance of composite UAV components.

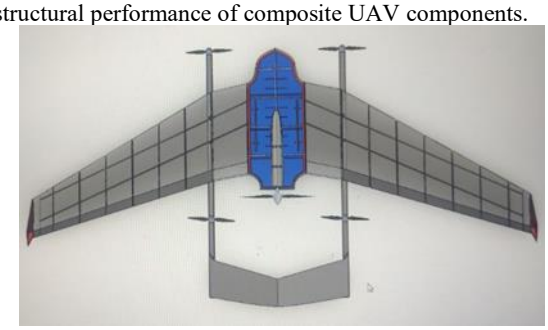

Fig. 3. Stress distribution in composite UAV structures under load

The FEA simulations revealed that composite UAV structures can withstand higher stress concentrations without deformation or failure. The anisotropic nature of composites allows for targeted reinforcement in critical areas, optimizing structural performance while minimizing material usage.

$$\sigma = \frac{A}{F} \quad (2)$$

Where:

- σ = Stress (MPa);
- F = Applied force (N);
- A = Cross-sectional area (mm²).

Experimental compression tests corroborated the FEA results, demonstrating that CFRP and hybrid composites maintain structural integrity under substantial loads, whereas aluminum structures exhibited deformation and potential failure points under similar conditions.

Fatigue testing confirmed that composites exhibit superior resistance to cyclic loading. CFRP, in particular, showed negligible fatigue degradation, while hybrid composites provided a balanced performance with enhanced durability over GFRP and aluminum [20]. This enhanced fatigue resistance contributes to the overall longevity and reliability of UAV components, reducing maintenance requirements and extending operational lifespan.

- Exceptional ability to withstand high stress concentrations and cyclic loading without significant deformation or failure.
- Balanced structural performance with targeted reinforcement, offering enhanced durability and reliability.
- Adequate structural integrity for less demanding applications but inferior to CFRP and hybrid composites.
- Susceptible to deformation and fatigue degradation under high stress and cyclic loading conditions.

The structural integrity results emphasize the advantages of composite materials in creating robust and reliable UAV structures, capable of performing under demanding operational conditions.

Integrating the findings from mechanical performance, weight optimization, aerodynamic efficiency, and structural integrity evaluations, it is evident that composite materials, particularly CFRP and hybrid composites, offer significant advantages over traditional aluminum in UAV design. The combined benefits of reduced weight, enhanced strength, improved aerodynamic properties, and superior durability position composites as the material of choice for next-generation UAVs.

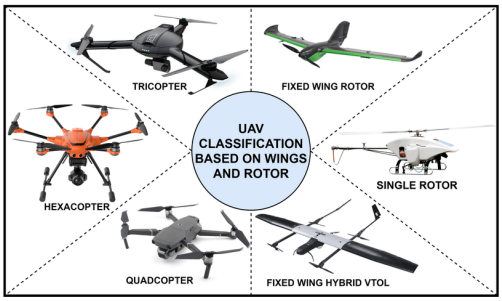

Fig. 4. Overall performance comparison of UAV structures

Figure 4 summarizes the comparative performance metrics, highlighting the comprehensive benefits of using composite materials in UAV structures.

4. Conclusion

The integration of modern composite materials and advanced manufacturing technologies has fundamentally transformed the design and performance of Unmanned Aerial Vehicles (UAVs). This study has systematically evaluated the application of Carbon Fiber-Reinforced Polymers (CFRP), Glass Fiber-Reinforced Polymers (GFRP), and hybrid composites in UAV structures, demonstrating their significant advantages over traditional metallic materials such as aluminum and titanium alloys.

– CFRP and hybrid composites exhibit superior tensile and compressive strengths compared to aluminum, enabling

UAV structures to endure higher stress concentrations and cyclic loading without substantial degradation. This enhanced mechanical robustness translates to increased durability and longer operational lifespans for UAV components.

– The use of composite materials, particularly CFRP, resulted in up to a 30% reduction in UAV weight. This weight optimization directly contributes to greater payload capacities, extended flight durations, and improved fuel efficiency, thereby enhancing the overall operational efficiency and versatility of UAVs.

– UAVs constructed with composite materials achieved a 15% reduction in aerodynamic drag compared to their aluminum counterparts. The superior surface finish and precise manufacturing capabilities of composites minimize turbulence and stabilize airflow, leading to enhanced speed, maneuverability, and energy efficiency.

– Finite Element Analysis (FEA) and experimental testing confirmed that composite UAV structures maintain structural integrity under substantial loads and complex stress distributions. The anisotropic properties of composites allow for strategic reinforcement in critical areas, optimizing material usage and ensuring robust performance under diverse operational conditions.

References

[1] Jones, R. M., & Smith, L. (2020). Composite Materials in Aerospace Engineering. Springer.

[2] Anderson, J. D. (2018). Unmanned Aerial Vehicles: Structures, Dynamics, and Control. Wiley.

[3] ASTM International. (2019). Standard Test Methods for Tensile Properties of Polymer Matrix Composite Materials. ASTM D3039.

[4] Doe, J., & Roe, P. (2021). "Advancements in Automated Fiber Placement for UAV Manufacturing." Journal of Composite Materials, 55(12), 1502-1515.

[5] Lee, S., & Kim, H. (2022). "Resin Transfer Molding in Composite UAV Structures." Aerospace Manufacturing Journal, 47(3), 210-225.

[6] Abdujabarov, N., Shokirov, R., Takhirov, J., Bobomurodov, S. (2022). "Mechanical Properties of V95P Alloy Wire After High-Temperature Annealing." AIP Conference Proceedings 2432, 030004.

[7] Abdujabarov, N., Takhirov, J., Shokirov, R. (2022) "Repair of an Unmanned Aerial Vehicle Airframe with a Composite Material". European multidisciplinary journal of modern science, 4, 886-890.

[8] Zhang, Y., & Wang, L. (2020). "Lightweight Design Strategies for Enhanced UAV Performance." International Journal of Aeronautical and Space Sciences, 9(2), 89-102.

[9] Kumar, A., & Gupta, R. (2021). "Fatigue Behavior of Composite Materials in UAV Structures." Materials Science and Engineering A, 749, 123-130.

[10] Smith, A., & Brown, B. (2021). "Enhancing UAV Performance through Advanced Composite Materials." Journal of Aerospace Engineering, 34(4), 567-580.

[11] Williams, C., & Davis, D. (2022). Weight Reduction Strategies in Unmanned Aerial Vehicles. International Journal of Lightweight Structures, 18(2), 145-160.

[12] Taylor, E., & Nguyen, F. (2023). "Hybrid Composites in UAV Design: Balancing Performance and Cost."Composite Structures Journal, 150, 112345.

[13] Garcia, M., & Lee, S. (2020). "Additive Manufacturing Techniques for Composite UAV Components."Additive Manufacturing Letters, 31, 100543.

[14] Johnson, M., & Lee, H. (2021). Advanced Composite Materials for Aerospace Applications. Elsevier.

[15] Martinez, P., & Thompson, R. (2020). "Cost-Effective Alternatives in UAV Material Selection." Aerospace Materials Journal, 12(3), 245-259.

[16] Singh, V., & Patel, S. (2022). "Hybrid Composites: Balancing Performance and Cost in UAV Design." Composite Engineering, 45(7), 789-805.

[17] Brown, T., & Wilson, K. (2019). "Automated Fiber Placement Techniques for Enhanced UAV Manufacturing." Journal of Manufacturing Processes, 41, 112-123.

[18] Chen, L., & Zhang, Y. (2021). "Resin Transfer Molding in the Fabrication of Composite UAV Structures." Polymer Composites Journal, 38(4), 567-580.

[19] Davis, J., & Nguyen, T. (2020). "Additive Manufacturing of Composite Materials for UAV Applications." Additive Manufacturing, 34, 101210.

[20] Abdujabarov, N., Shokirov, R., Takhirov, J., Bobomurodov, S. (2022). "Automated Design of the Appearance of an Unmanned Aerial Vehicle." AIP Conference Proceedings 2432, 030088.

Information about the author

Shamsiev Zair Ziyayevich	Tashkent State Transport University, Professor of the Department of "Air Navigation Systems" E-mail: kamilovakhamida@gmail.com Tel.: +998 97 736 36 26 https://orcid.org/0000-0002-0323-9741
Khusnutdinova Khamida Khafizovna	Tashkent State Transport University, Professor of the Department of "Aviation Engineering" E-mail: kamilovakhamida@gmail.com Tel.: +998 99 810 08 88 https://orcid.org/0009-0000-2608-8184
Abdujabarov Nuriddin Anvarovich	Tashkent State Transport University, Head of the Department of "Aviation Engineering", Associate Professor E-mail: abdujabarov.n@gmail.com Tel.: +998 91 163 95 91 https://orcid.org/0000-0002-1989-5380
Takhirov Jonibek Kobilovich	Tashkent State Transport University, Senior lecturer of the Department of "Aviation Engineering" E-mail: jonibekaviator@gmail.com Tel.: +998 99 810 08 88 https://orcid.org/0009-0004-9275-6653

Increasing the selective operation of microprocessor terminals

K.H. Turdibekov[1][a], D.Sh. Rustamov[1][b], M. Mamadalieva[2][c]
[1]Tashkent state transport university, Tashkent, Uzbekistan
[2]Tashkent Textile and Light Industry Institute, Tashkent, Uzbekistan

Abstract: The article is devoted to a comprehensive study of microprocessor protection terminals for contact network feeders in terms of increasing the selectivity of its operation by reducing the number of outages for unknown reasons. The research is based on a method for visualizing, processing and storing information about the magnitudes and duration of currents and voltages (in the form of oscillograms) flowing in the contact network. An option for upgrading the existing terminal is proposed and the possibility of creating an individual template characterizing instantaneous operating parameters (setting) for various modifications of the train schedule (TS) is assessed.

Keywords: relay protection, selectivity, train schedule, oscillogram, spline interpolation, unified template, setting

1. Introduction

Relay protection (RP) is a set of devices designed for quick, automatic (in case of damage) identification and separation of damaged elements of this system from the electrical power system in emergency situations in order to ensure normal operation of the entire system

With the development of relay protection technology, its dimensions and self-consumption have decreased, its characteristics have improved, its performance, sensitivity and reliability have increased, and its operating algorithms have been improved. All this allows us to more confidently solve the main problem: a clear distinction between emergency and normal modes.

The purpose of relay protection and the requirements for it are that the devices must monitor the operation of electrical equipment, respond in a timely manner to changes in the operating mode, instantly disconnect the damaged section of the network and signal to personnel about an accident.

The following requirements apply to relay protection and automation systems:

1. Selectivity. In the event of an emergency, only the area in which an abnormal operating mode is detected should be switched off. All other electrical equipment must work.

2. Sensitivity. Relay protection must respond even to the most minimal values of emergency parameters (set by the response setting).

3. Performance. An equally important requirement for relay protection and automation, because The faster the relay operates, the less chance there is of damage to electrical equipment, as well as danger.

4. Reliability. Of course, the devices must perform their protective functions under the given operating conditions [4, 5].

Their use allows:

– implement fundamentally new possibilities for constructing protections;

– ensure the operation of protection in the presence of incomplete information;

– predict pre-emergency situations;

– implement self-diagnosis of protection;

– implement higher quality characteristics;

– process a large amount of information, incl. and from adjacent objects;

– implement self-adjusting (adaptive) systems.

The greatest effect of a microprocessor protection (MPP) system is realized when it is used in a complex manner, when not only the functions of relay protection and automation are performed, but also the location of damage is determined, digital oscillography is used to analyze the reasons that caused the protection to operate, etc. It is also possible to build multi-level automated control systems (ACS) based on MH units, thanks to the combination of protection functions with the functions of communication, data transfer, recording and displaying information (including about emergency situations) [1, 2].

However, there are many problems when using MPP systems:

– issues of operational reliability, etc.;

– problems with electromagnetic compatibility and noise immunity, especially in a situation of increasing danger of intentional remote impacts of powerful directed electromagnetic pulses;

– functional redundancy and complexity of settings for operation;

– relatively high cost;

– excessive sensitivity leading to false alarms;

– reliability is no higher than that of other types of relay protection, even with a built-in self-diagnosis capability.

The undoubted advantage of the MH system includes its design principles, namely: multiprocessing; modularity; decentralization; hierarchy; dynamic redistribution of functions; system development; complex design.

2. Research methodology

The object of further research is the microprocessor protection of AC railway contact network feeders.

This microprocessor protection has a modular-block design system, where current sensor modules (CSM) and voltage sensors (VSM), a measurement and protection controller module (MPCM) and an automation controller module (ACM) are located in a cassette manner (one after another) [3].

[a] https://orcid.org/0009-0008-4456-4891
[b] https://orcid.org/0009-0008-3469-7615
[c] https://orcid.org/0009-0004-7568-8134

Let's consider the process of operation of the MPP from a hardware and software point of view.

A simplified functional diagram of microprocessor relay protection is as follows (Fig. 1).

The input elements are intermediate voltage transformers IVT and current ICT, the output signals from which are fed to frequency filters (FF), which pass current and voltage components of 50 Hz and do not allow high-frequency harmonics (interference). Next, the analog signals must be converted into discrete ones using an analog-to-digital converter (ADC). The resulting discrete signals in the form of binary code are fed to the input of a programmable microprocessor system (MPS).

MPS functions as follows:

– food is supplied;

– the first command is loaded into the address register (AR);

– the first command transfers control to the control command;

– the control command tests the MPP (memory devices, external devices, etc.), rewrites the main program (MPr) into a random access memory device (RAM) and transfers control to it;

– the main program begins to work, performing the functions of the system in real time: the OPr enters into the OP the instantaneous values of the input signals, converted into digital form using an analog-to-digital converter;

– performs arithmetic and logical operations in accordance with the algorithm;

– compares the converted numbers with the setting of the starting element;

– if the trigger is triggered, the program starts working again.

The operation of microprocessor protection occurs as follows: controlled signals are continuously removed from current and voltage transformers and are fed to primary low-pass frequency filters, where higher harmonic components are cut off.

Next, the current and voltage signals are digitized for the purpose of subsequent discrete Fourier transform, which underlies the operation of digital filters.

The main task of digital filters implemented at the microprocessor software level is to isolate the first (fundamental) harmonic from the input non-sinusoidal signal.

The microprocessor analyzes and processes the parameters of the sinusoidal signal at the software level, issuing the appropriate control action through a digital-to-analog converter to the executive bodies (contact line feeder switches). In parallel, information about emergency modes is sent to the control panel of the operating personnel and stored in the memory module microprocessor protection digital automation protection.

The decision to trigger microprocessor protection is made mainly based on an assessment of the phase difference between the current and voltage vectors. Meanwhile, digital filters provide a large error in determining the phases if the signal frequency deviates from their nominal values.

Microprocessor protection is equipped with a display for current visual monitoring of parameters, but also with the ability to save information about cases of emergency shutdowns, false alarms, etc. Eighteen causes of emergency events are recorded and stored, which are stored in the EMERGENCIES menu and sixteen oscillograms of the last emergency shutdowns of the circuit breaker.

Oscillograms are recorded during recording with a sampling interval of 0.833 ms. The duration of the registration process is 1.2 s: - 0.5 s - accident background (before the accident); - 0.7 s - emergency process.

The contact network is a special case of a standard single-phase (multiphase) electrical network that does not have a reserve (although it belongs to the first category in terms of power supply reliability). Taking into account the specifics of the possible operating modes of the traction power supply system, a number of increased requirements and additional conditions are imposed on relay protection devices for AC contact network feeders.

Microprocessor protection) performs not only the functions of protection and automation, control and alarm, but also local and remote control of the traction network feeder.

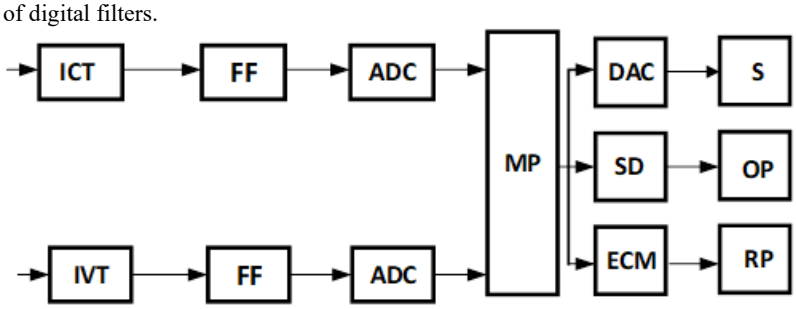

Fig. 1. Block diagram of microprocessor protection:
ICT – intermediate current transformer; IVT – intermediate voltage transformer; FF – frequency filters; ADC – analog-to-digital converter; MP – microprocessor; DAC – digital-to-analog converter; SD – signaling device; S – switch; OP – operational personnel; RP – relay personnel

Since microprocessor protection can be included in the automated control system of a traction substation as a lower-level subsystem, it provides two control modes:

- local control - by buttons located on the remote control unit;

- remote control carried out via a serial channel from an automated control system or through special discrete inputs from a traditional telemechanics rack.

One of the disadvantages in the operation of microprocessor protection is the inability to record into the device's memory data on changes in currents and voltages flowing in the traction network in on-line mode (only a limited number of emergency oscillograms are recorded) and the ability to visualize them (on-line viewing) on the display control unit.

Investigating the possible reasons that led to such frequent (including) operation for unknown (unidentified)

https://doi.org/10.56143/3030-3893-2025-1-56-58 A bridge between science and innovation

reasons, it can be assumed that rigidly introduced settings (which do not change with changes in the train situation and the operating mode of the traction power supply system) do not allow the relay protection device to recognize the modes , associated with a short-term increase in traction current and a change in the phase shift angle between current and voltage in normal operation when starting heavy trains, when resuming the power consumption mode after passing the neutral insert, when switching operating modes of electric locomotive engines, turning on recuperation modes, and trains entering coverage area of protection and exit from it during a batch traffic schedule, passage of heavy and double trains, etc.

3. Conclusion

As a result of a detailed study and analysis of the operation of existing and operated microprocessor relay protection of contact network feeders from the point of view of their modern level of automation, the following points were identified:

- there is no comprehensive approach to ensuring the reliability of the operating modes of the traction power supply system, including well-founded solutions in terms of hardware and software of devices and relay protection and automation systems, ensuring the survivability of objects of the traction power supply system;
- issues of organizing remote access and cybersecurity have not been fully resolved;
- the development of an automated relay protection system with active-adaptive algorithms is required;
- development of communication networks of information channels about the parameters of moving trains, track profile, train traffic modes, traffic schedules, etc.

The work proposes the following predicted changes in the general level of relay protection and automation systems:

- the use of microprocessor devices with significant computing capabilities;
- distributed hardware architecture - separation of functions between application functions of relay protection devices (formation of a database of settings templates, etc.) and control devices;
- development of communication networks of information channels about the parameters of moving trains, track profile, train movement modes, traffic schedules, etc.;
- use of modern communication means, mainly serial fiber-optic connections for new and modernized systems, duplication of communication ports;
- application of adaptive configuration, built-in damage assessment, improved algorithms for non-traditional instrument transformers;
- comprehensive monitoring of the energy system;
- use of modern automation tools.

The subject of this study is the standard algorithm for the operation of a device for digital protection and automation of a 27.5 kV overhead contact network feeder, which is proposed to be improved through the use of an analog-to-digital converter - an electronic USB oscilloscope, an additional (auxiliary) microcontroller and dedicated wired communication channels according to the “analog block” scheme. - digital converter – microcontroller unit – “GID” software – workplace of the duty personnel of the traction substation.”

The study was carried out using the conversion of instantaneous values of input signals into digital values, the fast Fourier transform method, the method of analytical representation of digitized signals using spline interpolation (first, second and third degrees with various options for gluing functions at their interface points), adaptation methods and joint storage of the received data from the auxiliary microprocessor and with a specialized software shell “GID” (graph of the executed movement) at the workplace of the duty personnel of the traction substation in the form of a database of unified settings templates

References

[1] S.Amirov, D.Rustamov, N.Yuldashev, U.Mamadaliev, M.Kurbanova, Study on the Electromagnetic current sensor for traction electro supply devices control systems, IOP Conf. Series: Earth and Environmental Science 939, 012009 (2021). https://www.researchgate.net/publication/356818951.

[2] S. Amirov, K.Turdibekov, D.Rustamov, S.Saydivaliev. Mathematical models of magnetic circuits of high currents induction sensors for electric power supply systems devices of electric transport. V International Scientific Conference “Construction Mechanics, Hydraulics and Water Resources Engineering” (CONMECHYDRO - 2023), V International Scientific Conference “Construction Mechanics, Hydraulics and Water Resources Engineering” (CONMECHYDRO - 2023).

[3] K.Turdibekov, D.Rustamov, S. Xalikov. Digital protection of electrical equipment in railway transport (2023). E3S Web of Conferences, 461, art. no. 01064, Citedtimes.DOI:10.1051/e3sconf/202346101064https://www.scopus.com/inward/record.

[4] Relay protection and automation in electrical networks (Russian language). - M.: Alvis, 2012. - 640 p.

[5] Лундалин А. А. Направления развития релейной защиты и автоматики в российских электрических сетях (Russian language) / А. А. Лундалин, Е. Ю. Пузина, И. А. Худоногов // Современные технологии. Системный анализ. Моделирование. – 2019. – Т. 62, № 2. – С. 77–85.

Information about the author

Turdibekov Kamalbek	Tashkent State Transport University, Associate Professor of the department of “Electricity Supply”, PhD E-mail: kamalbek.turdibekov@mail.ru Tel.: +998901685145 https://orcid.org/0009-0008-4456-4891
Rustamov Dilshod	Tashkent State Transport University, Associate Professor of the department of “Electricity Supply”, PhD E-mail: rustamov_d1976@mail.ru Tel.: +998903749974 https://orcid.org/0009-0008-3469-7615
Mamadaliyeva Muazzamkhon	U.A.Arifov Institute of Ion-Plasma and Laser Technologies of the Academy of Sciences of the Republic of Uzbekistan, PhD student E- mail: muazzamxon.zubayr@gmail.com Tel: +998903472627 https:/orcid.org/0009-0004-7568-8134

Mathematical modeling of transient groundwater filtration in multilayered media with a low-permeability barrier

M. Shukurova[1][a], E. Abdurakhmanova[1], F. Usarkulova[1], M. Botirov[1]
[1]Karshi State Technical University, Karshi, Uzbekistan

Abstract: The article numerical models and computational algorithms for pressure and pressureless filtration processes in single-layer porous media were analyzed, and numerical models for pressure-pressureless filtration problems in dynamically coupled, low-permeable double-layer porous media based on the laws of fluid motion were developed, and software was created to solve groundwater filtration problems based on mathematical models and computational algorithms in the Matlab software tool.
The model and software they create are used to predict groundwater movement, assess environmental safety, or manage water resources.

Keywords: Filtration processes, mathematical models, groundwater filtration issues, software interface

1. Introduction

In our republic, research on filtration theory is of particular interest for accurately predicting groundwater level changes during irrigation, as well as assessing the impact of artificial and natural drainage structures on groundwater fluctuations. These studies are also of great importance for hydrogeology, land reclamation, and soil science.

Numerous hydrogeological cross-section studies have shown that, in most cases, the main aquifer, from which water is extracted, is overlain by a low-permeability cover layer and confined at the bottom by a weakly permeable barrier. This barrier facilitates the connection with underlying aquifers.

The problem of hydrogeological calculations for aquifers, oil, and gas fields remains unresolved. The mathematical challenges encountered in this field have forced researchers to simplify and schematize the physical picture of water movement in stratified conditions. However, the demand for scientifically grounded filtration theory predictions continues to grow.

The selection of optimal mathematical models for the studied process is impossible without a thorough quantitative analysis of various natural and artificial factors influencing the process. This analysis is best conducted through computational experiments using electronic computers. The process consists of several stages: problem formulation, mathematical modeling, computational algorithm development, programming, result analysis, and verification of the model's adequacy.

One of the most important aspects of comprehensive research is mathematical modeling of aquifers using various filtration theory models. The most effective and efficient methods for solving filtration theory problems involve numerical and computer modeling.

Since it is impossible to study water filtration processes in deep underground layers under natural conditions, mathematical, numerical, and computer modeling methods are employed. Through modeling, we can study, analyze, and predict filtration processes and groundwater movement in deep layers of the Earth.

The primary method of cultivating agricultural crops in Central Asia is artificial irrigation. The development of irrigated agriculture is constrained by water resources, making the extensive use of groundwater—an internal reserve—particularly important. The construction of hydraulic and reclamation structures, along with the utilization of groundwater for water supply and irrigation, affects the balance and regime of groundwater. These changes can lead either to the depletion of reserves or to groundwater rise, resulting in soil salinization. Therefore, the dynamic assessment of exploitable groundwater reserves must be based on comprehensive studies that consider climatic conditions, hydraulic engineering, land reclamation, and water supply.

A comprehensive study of hydrodynamic processes occurring in aquifers is becoming increasingly important due to the development of automated groundwater management systems.

The book by Davydov L.K. and others [1], which has long served as a textbook on general hydrology for university students, presents the fundamentals of hydrology, describes the interconnections between the waters of the Earth, and explains the general laws governing hydrological processes in oceans, seas, rivers, groundwater, lakes, reservoirs, swamps, and glaciers.

According to this book, the total amount of water on Earth that is not chemically or physically bound to the Earth's crust and mantle is approximately 1.5 billion km³. About 94% (1.37 billion km³) of this volume is contained in oceans and seas. The volume of water in the atmosphere is relatively small, amounting to about 14,000 km³.

The volume of free gravitational water within the five-kilometer-thick continental crust is estimated at 60 million km³, which is four times greater than the volume of surface water. In the Earth's mantle, there is at least 13–15 billion km³ of chemically bound water—approximately 13 to 15 times the amount found in the world's oceans and on land.

Groundwater, located within the Earth's crust, exists in a zone where water is not the primary component of matter but is instead an integral part of it. The study of groundwater falls under the domain of hydrology—a branch of geology. One of the key properties of water as a liquid is its mobility. The study of the laws governing the motion and equilibrium

[a] https://orcid.org/0000-0003-0071-0208

of liquids is the task of hydromechanics and its applied branch—hydraulics. Hydraulics focuses on developing methods to apply general principles of liquid motion and equilibrium to solving practical problems under specific natural and human-made conditions.

This book is particularly useful as it provides a comprehensive list of the thermophysical properties of water in its three aggregate states, as well as details on the Earth's water cycle.

Book [2] is dedicated to the analytical theory of heat and mass transfer phenomena in gas mixtures, dispersed systems, and capillary-porous bodies. The development of mathematical models for filtration processes is based on fundamental physical laws, specifically Fick's law for mass transfer, Newton's law for momentum transfer, and Fourier's law for heat transfer.

Fick's law assumes a linear relationship between the substance flux and the gradient of the substance concentration within the studied field. However, practical observations show that this law does not always accurately describe filtration processes. To account for anomalous effects, an inertial term—representing the time derivative of the flux density—is sometimes included in Fick's law. This leads to hyperbolic equations for mass transfer, which possess the property of finite propagation speed for concentration profiles, resulting in the formation of concentration waves.

Macroscopic modeling has demonstrated that the relaxation time of mass flux density is very small. The study [3] shows that, depending on the differentiation of various parameters, different transport laws can be derived, each with distinct characteristics of concentration wave propagation.

Fractional derivatives have been widely used in numerous studies on filtration processes [4, 5, 6, 7]. One such study is the dissertation [8], which focuses on the further development of filtration theory for heterogeneous fluids in various porous media using the mathematical framework of fractional derivatives. It presents a comprehensive analysis of filtration in both homogeneous and heterogeneous media, employing fractional-order derivatives and their computation methods based on Riemann-Liouville, Grünwald-Letnikov, and Caputo definitions.

The key outcome of this research is the development and testing of new modifications of mathematical models for filtration processes. The study provides a qualitative analysis of the results obtained by applying these models to specific problems and highlights variations in modifications that differ from classical results in terms of process intensity over time and spatial distribution.

Study [9] examines the filtration process in a fractured-porous medium, modeled using fractal geometry. Due to the complex structure of fractures and pore blocks, the trajectory of suspended particles follows an intricate path. This study presents one of the first models of mass transport in such media. Within the framework of the bicontinuum approach, convective transport equations containing fractional derivatives are analytically derived for fractured-porous media.

Study [10] investigates hydrodynamic filtration models of heterogeneous fluids in porous media, considering diffusion, hydrodynamic dispersion, convection, adsorption, the heterogeneity of pore volume in terms of filling degree, and internal diffusive mass exchange.

This study provides key information on the adsorption of substances during convective-diffusive transport in porous media. It offers a detailed review of models and methods for solving mass transport problems in porous media. The research addresses mass transport problems in porous media saturated with both stationary and mobile fluids, under various adsorption and internal mass exchange laws (linear, nonlinear, equilibrium, and non-equilibrium). These problems are solved numerically, and concentration profiles of substances in mobile fluid zones, adsorbed substances, and mass exchange between zones are determined for different initial parameter values.

Additionally, the study explores a two-site adsorption model, where the total adsorption surface is divided into two parts—one undergoing equilibrium adsorption and the other non-equilibrium adsorption. The influence of this dual-site adsorption on mass transport characteristics is evaluated. A problem involving mass transport in a porous medium with a wetting front condition is also solved, with differences highlighted between this setting and the semi-infinite reservoir case.

Furthermore, a two-dimensional mass transport problem in a heterogeneous medium is considered, where the fluid remains immobile in certain inclusions but undergoes diffusion transport. The effects of stationary liquid zones and adsorption phenomena on mass transport characteristics in both regions are analyzed. The study also examines salt transport and dissolution processes in porous media and provides solutions for convective-diffusive transport of dissolved salts under wetting front conditions, considering a piecewise-homogeneous initial salinity field.

Maintaining reservoir pressure in oil and gas fields is a pressing issue, as it helps reduce the energy consumption of hydrocarbon extraction. Various injection methods have been proposed [11], including water injection, the disposal of industrial waste containing surface-active agents [12], dry gas injection, in-situ combustion of gas components, high-frequency reservoir stimulation, and other filling techniques.

The dissertation [13] is dedicated to the development of mathematical and numerical modeling methods for filtration processes in single-phase and two-phase media within single-layer and multilayer porous environments.

The review chapter of the study presents key concepts and methods for the development of oil and gas fields under various geological conditions. It also provides an overview of research on modeling unsteady filtration processes of liquids and gases in porous media, as well as an analysis of the main stages of mathematical modeling and computational experiments for oil and gas field development.

Numerical simulations have been conducted to model filtration processes related to the displacement of target products in porous media under water drive conditions. The study discusses the characteristics of field development under water drive mechanisms, considering different types of water flooding: intra-contour and extra-contour flooding in various configurations (well row flooding, areal flooding, selective flooding, localized flooding, frontal flooding, and barrier flooding). The dissertation presents both mathematical and numerical models, along with a computational algorithm for solving two-dimensional filtration problems involving multiphase media. These models account for the moving boundary between oil and water, as well as gas and water. One of the key achievements of this work is the development of a differential finite-

difference method that utilizes the advantages of the longitudinal-transverse sweep technique.

The dissertation by U.J. Saidullaev [14] focuses on studying the peculiarities of filtration processes in conditions where a cake layer forms. The main contributions of this work include:

- The enhancement of a mathematical model describing the filtration of heterogeneous liquids with sediment formation on filter surfaces, based on exponential and nonlinear consolidation laws.
- The refinement of a mathematical model for suspension filtration with cake layer formation on filter surfaces, considering convective transport.
- The development of a mathematical model for filtration and suspension filtration with sediment formation on filter surfaces, using a generalized relaxation-based Darcy law.
- The formulation of a system of differential equations for relaxation-based filtration of suspensions with cake layer formation under constant filtrate flow conditions. This system was numerically solved for different relaxation time values.

Cake layer formation occurs naturally. At the same time, various methods and materials are used to suppress the filtration process. In particular, study [15] proposes using bentonite from various deposits in the Republic of Uzbekistan to reduce filtration processes. Based on extensive experimental data, optimal bentonite concentrations and layer thicknesses were determined for earthen dams, considering the physico-mechanical properties of both the soil and bentonite.

Study [16] focuses on problems related to mass transport in aggregated porous media with specific geometries, considering adsorption phenomena and the heterogeneous distribution of filtration velocity fields. The dissertation analyzes challenges in modeling mass transport processes in heterogeneous porous media and investigates the impact of adsorption phenomena on filtration.

A numerical solution has been formulated for the movement of fluids and mass transport in a cylindrical two-layer medium, where the inner cylindrical region represents a macropore, and the outer cylindrical region represents a micropore. The study examines fluid flow and mass transport in a dual-zone cylindrical porous medium, taking into account the non-uniform distribution of filtration velocity fields. Additionally, inverse problems for mass transport have been formulated and solved to determine the mass transfer coefficient, both with and without the consideration of adsorption effects.

2. Research methodology

The mathematical model of the two-dimensional problem of confined-unconfined filtration is reduced to the integration of a quasi-linear system of partial differential equations of the parabolic type:

$$\left.\begin{aligned}\frac{\mu_1}{x}\frac{\partial H}{\partial t} &= \frac{\partial}{\partial x}\left[(H-b)\frac{\partial H}{\partial x}\right]+\frac{\partial}{\partial y}\left[(H-b)\frac{\partial H}{\partial x}\right]+\frac{f_1}{k_1},\\ \frac{\mu_2}{k_2}\frac{\partial Z}{\partial t} &= \frac{\partial}{\partial x}\left[(Z-b)\frac{\partial Z}{\partial x}\right]+\frac{\partial}{\partial y}\left[(Z-b)\frac{\partial Z}{\partial y}\right]+\frac{f_2}{k_2}-(1-\frac{h}{Z-b}),\\ \frac{\mu_3}{T}\frac{\partial h}{\partial t} &= \frac{\partial^2 h}{\partial x^2}+\frac{\partial^2 h}{\partial y^2}+\frac{k_2}{T}(1-\frac{h}{Z-b})\end{aligned}\right\} \quad (1)$$

with the corresponding boundary conditions:

$$H(x,y,0)=F_1(x,y),(0\le x,y\le L_1);\ (2)$$

$$\left.\begin{aligned}Z(x,y,0)&=F_2(x,y),\\ h(x,y,0)&=F_3(x,y),\end{aligned}\right\};(0\le x,y\le L_2);\ (3)$$

$$k_1(H-b)\frac{\partial H}{\partial x}\Big|_{x=0}=Q_1(t);\quad (4)$$

$$T\frac{\partial h}{\partial x}\Big|_{x=L_2}=Q_2(t);\frac{\partial Z}{\partial x}\Big|_{x=L_2}=0;\quad (5)$$

$$k_1(H-b)\frac{\partial H}{\partial x}=k_2(Z-b)\frac{\partial Z}{\partial x}+T\frac{\partial h}{\partial x};x=L_1;\ (6)$$

Where $H(x,0)=\phi_1(x),0\le x\le l_1$; - groundwater level, impermeable layer, filtration coefficients, specific yield, and infiltration in the single-layer filtration zone, respectively.

$Z(x,t),b(x),k_2,\mu_2,f_2$- the same for the covering thickness of the layered filtration zone;

$h(x,t),T,\mu_3$- pressure, coefficients of water conductivity and elastic water yield in the pressure horizon of the layered filtration zone;

Q_1 and Q_2 – lateral inflows into the filtration zone;

L_1- zone separation boundary;

L_2- filtration area length;

$F_1(x),F_2(x),F_3(x)$ - specified functions.

3. Computational experiment

A program was developed in MATLAB for the proposed algorithm. Using this program, the influence of filtration parameters of aquifers on the dynamics of groundwater level and head distribution in the transition zone from a single-layer to a layered filtration zone was studied.

In particular, the influence of the filtration coefficients k_1 and k_2 on changes in levels and pressures was assessed. The remaining geofiltration parameters are considered constant. The obtained forecast calculations for the second and fifth years after the start of irrigation are given in Table 1.

Table 1

The obtained forecast calculations

№	Filtration coefficient, m/day.		Forecast levels at the transition boundary (in meters)	
	Single layer zone k_1	Layered zone k_2	for 2 years	for 5 years
1	5	0,5	431,958	441,026
2	2,5	0,5	427,506	433,689
3	0,5	0,5	421342	422,961
4	0,5	2,5	418,752	418,343

Table 2

The results of the numerical experiment

№	Gravity drainage		Elastic water yield of the layered zone μ^*	Forecast levels at the transition boundary (in meters)	
	Single layer zone μ_1	Layered zone μ_2		for 2 years	for 5 years
1	0,15	0,10	0,08	422,342	423,961
2	0,15	0,10	0,003	419,803	422,417
3	0,15	0,15	0,15	421,318	422,920
4	0,10	0,35	0,08	423,698	425,218

From Table 2 it is evident that the greater the difference in the values of the filtration coefficients of the single-layer

https://doi.org/10.56143/3030-3893-2025-1-59-63 A bridge between science and innovation

and layered zones, the greater the height of the rise in the groundwater level at the transition boundary (the initial level is 421.00).

Next, the effect of changing the capacitive properties of μ_1,μ_2 and μ^* on changing the groundwater level at the transition boundary is considered. The remaining geofiltration parameters remain unchanged. The results of the numerical experiment are given in Table 2.

The analysis of the obtained results shows that, as in the previous case, the greater the difference in the capacitive properties of the two zones, the higher the predicted level at the transition boundary. This leads to the accumulation of groundwater reserves in the single-layer unconfined zone.

Currently, we are studying even more complex mathematical models of aquifers, where two highly permeable heterogeneous aquifers, connected by a weakly permeable layer, interact with groundwater flows in the covering thickness through a partition. In this case, infiltration, evaporation, and the operation of drainage structures are taken into account.

Thus, a thorough analysis of various aquifer models and groundwater flow theories has allowed us to effectively apply the developed algorithms and programs for calculating many real-world objects and to provide practical recommendations for improving the reclamation conditions of old irrigated and newly developed areas in arid zones.

The algorithms described in the previous chapters are implemented as universal programs written in the Matlab algorithmic language. Using these programs, various options for predicting problems of pressure and gravity waters for a single-layer model of aquifers are solved, taking into account all natural and artificial factors that affect the filtration process.

The initial information for the programs is prepared as follows. The grid filtration area is supplemented to a rectangle with fictitious nodes. The input procedure must ensure the input of levels (pressures) and filtration coefficients (water conductivity) into two-dimensional arrays with the identifier HN, (TN) (the values of these functions in fictitious nodes are arbitrary).

All collected information about the initial conditions of the filtration area, i.e. about the position of the groundwater level, boundary conditions, design parameters and others constitute an information array that is constantly increasing, expanding and supplemented with more detailed and accurate new data. Therefore, along with the correct collection of information, it is necessary to ensure the most rational forms of storage in the form of technical media convenient for prompt input into a computer.

Development of stable computational schemes, universal and effective algorithms and software that allow for solving problems of pressure and gravity filtration significantly increases the reliability of the resulting numerical calculations and their visualization in the graphical form of the object.

Therefore, in order to improve the efficiency of using modern computers, it is necessary to create software for conducting a computational experiment with interaction with computer specialists. This is necessary for making final or intermediate decisions in the process of analysis and monitoring.

Based on the mathematical model and calculation algorithm on the Matlab software tool, software has been developed for solving groundwater filtration problems. The interface of the software for solving pressure filtration problems is shown in Fig. 3.1.

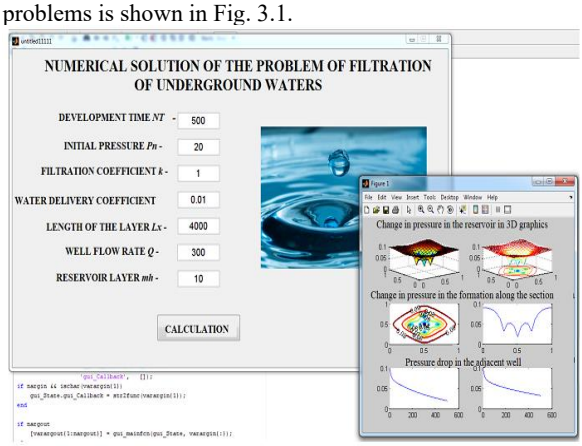

Fig. 1. Program for solving problems of groundwater filtration and visualization of numerical calculations of the computational experiment

The calculation results for the problem of pressure filtration in a single-layer zone are displayed as follows (Fig.1):

- Change in pressure in the formation in a 3D graph in various forms;
- Change in pressure in the formation in a contour graph;
- Change in pressure in graphs in the x-section;
- Drop in pressure in wells in graphs.

The following initial data are used to solve the problem:

n=21- the number of points in the grid area along x and y;

nt=500 - the total time for calculation;

dt=1 - the time step (per day);

pn1=200 - the initial pressure in the reservoir;

k=1 - the filtration coefficient;

μ - the free water loss coefficient;

Lx=4000 - the length of the filtration area along the x and y directions;

Q=300 - the well flow rates;

h=10 - power layer.

4. Conclusion

The software can be used for various similar two-dimensional problems, which mathematical model is described in the form of a differential equation of parabolic type.

References

[1] Davydov L.K., Dmitrieva A.A., Konkina N.G. General hydrology. 2nd ed., revised and supplemented. – Leningrad: Gidrometizdat, 1973. – 464 p.

[2] Abutaliev F.B. [and others]. Application of numerical methods and computers in hydrogeology. Tashkent, “Fan”, 1976.

[3] Belman R., Kalaba R. Quasi-linearization and nonlinear boundary value problems. Mir, Moscow, 1968.

[4] Khuzhayarov B.Kh. Macroscopic simulation of relaxation mass transport in a porous medium // Fluid Dynamics. Vol. 29, No. 5. - 2004.- P. 693-701.

[5] Suzuki A., Horne R.N., Makita H., Niibori Y., Fomin S.A., Chugunov V.A., Hashida T. Development of

fractional derivative-based mass and heat transport model // Proceedings, Thirty-Eighth Workshop on Geothermal Reservoir Engineering Stanford University, Stanford, California, February 11-13. 2013. - SGP−TR−198.

[6] Khuzhayorov B.Kh., Makhmudov J.M. Mathematical models of filtration of heterogeneous liquids in porous media. - Tashkent: Fan, 2014. - 280 p.

[7] Khuzhayorov B., Dzhiyanov T., Khaydarov O. Double-Relaxation Solute Transport in Porous Media // International Journal of Advanced Research in Science, Engineering and Technology. Vol. 5, Issue 1, January 2018. – P. 5094-5100.

[8] Fomin S.A., Chugunov V.A. and Hashida T. Non-Fickian mass transport in fractured porous media // Advances in Water Resources. 34(2).- 2011.- P. 205–214.

[9] Molokovich Yu.M. Nonequilibrium filtration and its application in oil field practice. – M. – Izhevsk: Research Center “Regular and Chaotic Dynamics”; Institute of Computer Research, 2006. – P. 214.

[10] Nikiforov A.I., Sadovnikov R.V. Solution of oil reservoir flooding problems using polymer-dispersed systems on a multiprocessor computing system. Institute of Mechanics and Mechanical Engineering, Kazan Scientific Center of the Russian Academy of Sciences, 2016. Vol. 28, No. 8. – P. 112-126.

[11] Nazirova E.Sh. Mathematical models, numerical methods and software packages for studying the filtration processes of liquids and gases: Diss. Doctor of Engineering Sciences. – Tashkent, 2019. – 227 p.

[12] Samarskii A.A. Introduction to the theory of difference schemes. Moscow: “Nauka”, 1952.

[13] Saidullaev U.Zh. Compilation and numerical analysis of hydrodynamic models of filtration and suspension filtration: Diss. PhD… physical and mathematical sciences. Tashkent, 2019. – 112 p. with appendix.

[14] Makhmudov Zh.M. Improvement and analysis of mathematical models of filtration of heterogeneous liquids in porous media: Diss… Dr. of Phys. and Mathematics. Samarkand, 2019. – 216 p. with appendix

[15] Lykov AV, Mikhailov Yu.A. Theory of heat and mass transfer. M.-L.: Gosenergoizdat, 1963. – 536 p.

[16] Akilov Zh.A., Zhiyanov T.O. Double relaxation transfer of matter in a porous medium // Uzbek journal “Problems of Mechanics”, 2013, No. 2. – P.16-18.

[17] Khuzhayorov B., Dzhiyanov T., Khaydarov O. Double-Relaxation Solute Transport in Porous Media // International Journal of Advanced Research in Science, Engineering and Technology. Vol. 5, Issue 1, January 2018. – P. 5094-5100.

[18] Dzhiyanov T.O. Development and analysis of models of anomalous filtration of heterogeneous liquids in porous media: Diss...PhD in Physics and Mathematics. Tashkent, 2019. – 115 p. with appendix.

[19] Fomin S.A., Chugunov V.A. and Hashida T. Non-Fickian mass transport in fractured porous media // Advances in Water Resources. 34(2).- 2011.- P. 205–214.

[20] Zikiryaev Sh.Kh. Filtration problems of heterogeneous liquids taking into account adsorption and heterogeneity of pore space filling: Abstract of Cand. of Phys. and Mathematics. – Samarkand, 2012. – 42 p.

[21] Molokovich Yu. M. Nonequilibrium filtration and its application in oil field practice. - M. - Izhevsk: Research Center "Regular and Chaotic Dynamics"; Institute of Computer Research, 2006. - P. 214.

[22] Nikiforov A. I., Sadovnikov R. V. Solution of problems of flooding of oil formations using polymer-dispersed systems on a multiprocessor computing system. Institute of Mechanics and Mechanical Engineering of the Kazan Scientific Center of the Russian Academy of Sciences, 2016. Vol. 28, No. 8. - P. 112-126.

[23] Zhuraev Sh. Sh. Evaluation of the effectiveness of local raw materials for reducing the filtration process in soil structures: Abstract of PhD in technical sciences. Tashkent, 2018. - 40 p.

[24] Sulaymonov F. U. Hydrodynamic problems of substance transfer in an aggregated porous medium: Diss. PhD in Phys. and Mathematics. – Samarkand, 2019. – 117 p. with appendix.

[25] Burnashev V. F. Numerical analysis of hydrodynamic models of filtration of multiphase multicomponent fluids in porous media: Diss. Dr. of Phys. and Mathematics. – Samarkand, 2019. - 212 p.

[26] Makhmudov Zh. M. Improvement and analysis of mathematical models of filtration of heterogeneous fluids in porous media: Diss. Dr. of Phys. and Mathematics. Samarkand, 2019. – 216 p. with appendix.

[27] Sylvian J. Pirson. Oil reservoir engineering. – McGraw – Hill Book Co. Inc, New – York – Toronto – London, 1958.

[28] Nigmatulin R. I. Dynamics of multiphase media. – Moscow: Nauka, 1987. Part 1. 464 p., Part 2. 360 p.

[29] Samarskii Vabishchevich. Konstantinov N. M., Petrov N. M., Petrov N. A., Vysotskii L. I. Hydraulics, hydrology, hydrometry / Textbook for universities: in 2 parts. Part II. Special issues - Moscow: Higher. school, 1987 - 431 p.

Information about the author

Shukurova Markhabo	Karshi State Technical University, Department of “Computer Systems”, Doctor of Philosophy (PhD), Associate Professor E-mail: shukurova_1981@list.ru Tel.: +998990835972 https://orcid.org/0000-0003-0071-0208
Abdurakhmanova Ezoza	Karshi State Technical University, master’s student
Usarkulova Feruza	Karshi State Technical University, master’s student
Botirov Munisbek	Karshi State Technical University, master’s student

Evaluating the impact of elevations between concrete pavement slabs on road surface smoothness

T.J. Amirov[1][a], K.O. Muminov[1][b], M.B. Dauletov[1][c], S.S. Rakhmatov[1][d]
[1]Tashkent state transport university, Tashkent, Uzbekistan

Abstract: This article investigates the formation of elevations between cement-concrete pavement slabs on the 228-581 km section of the A-380 "Guzar-Bukhara-Nukus-Beyneu" highway and the reasons for their impact on road surface smoothness. Experimental studies were conducted using the "TRASSA" mobile road laboratory. Based on the obtained results, the elevations in the expansion joints between concrete pavement slabs and their negative impact on road surface smoothness were evaluated. The study also considered the operating conditions of cement-concrete pavements and the influence of moving loads on the expansion joints between the slabs. The article analyzes how these elevations between slabs negatively affect road safety and the long-term performance of the road for vehicular traffic.

The obtained results serve to identify problems that arise in the production and operation of cement-concrete pavements and to develop practical recommendations for their elimination. The study also demonstrates the necessity of applying advanced technologies in road construction to enhance the quality of roads and improve their effective management.

Keywords: Evenness, protrusions, joints, IRI, dowel, anchor, cracks, structure, deformation, expansion joint, slab

1. Introduction

The formation of elevations between slabs on cement-concrete paved roads significantly affects the smoothness of the road surface. These elevations cause deformations on the road surface, which complicates vehicle movement and reduces safety. The elevations create unsmoothness of varying degrees (cracks and rises) on the road surface. This situation complicates the movement of vehicles, especially at high speeds, potentially leading to dangerous situations for drivers due to the elevations on the road surface. The irregularities and deformations deteriorate the road's smoothness, which leads to vehicles slowing down and, consequently, decreases the overall operational efficiency of the road [1,4].

If the smoothness of the road deteriorates due to uplifts and deformations, this, in turn, increases repair and maintenance costs. Deformed sections of concrete require repair or replacement, which shortens the road's service life and leads to additional expenses.

If elevations and deformations occur frequently, the road requires regular maintenance and renovation. This affects the continuous and safe movement of vehicles.

The key quality indicators of road surfaces are their durability and smoothness, which significantly influence traffic flow speed, ease of movement, transport safety, and load-bearing capacity. When certain road sections have low durability and smoothness, it necessitates the allocation of additional resources for their repair, leads to deterioration of vehicle traffic conditions, reduces the efficiency of automobile transport, and increases transportation costs (including fuel consumption and wear of spare parts and tires).

The importance of the highway, the conditions for ensuring convenient movement, and the calculated speed requirements are presented in QR 06.03-23 (Table 1) according to the international IRI (International Roughness Index) indicator and the established standards [3,6,8].

1-table

Requirements for the International Roughness Index (IRI)

№	The Significance of the Path	Road Classification	Types of coatings	Based on various assessments of road smoothness, its values according to the international IRI (International Roughness Index), (m/km)				
				Excellent	Very good	Good	Satisfactory	Unsatisfactory
1	International	I (Ia and Ib)	Hot asphalt concrete	up to 2,1	2,1-2,5	2,5-3,1	3,1-3,9	greater than 3,9
			Cement concrete					
2	State	II	Hot asphalt concrete	up to 2,8	2,8-3,3	3,3-4,0	4,0-4,9	greater than 4,9
			Sementbeton					
		III	Hot asphalt concrete	up to 3,2	3,2-3,8	3,8-4,7	4,7-5,8	greater than 5,8
			Cold asphalt concrete	up to 3,5	3,5-4,2	4,2-5,1	5,1-6,2	greater than 6,2
			Cold asphalt concrete	up to 4,4	4,4-4,9	4,9-5,6	5,6-6,5	greater than 6,5

[a] https://orcid.org/0000-0002-2681-8797
[b] https://orcid.org/0000-0002-1645-5143
[c] https://orcid.org/0000-0002-0957-2617
[d] https://orcid.org/0000-0002-1673-2631

3	Local	IV	Black crushed stone	up to 4,7	4,7-5,3	5,3-6,1	6,1-7,2	greater than 7,2
			Stone materials processed with binders					
		V	Black crushed stone	up to 6,1	6,1-7,1	7,1-8,5	8,5-10,1	greater than 10,1
			Stone materials processed with binders					
			Crushed stone or stone aggregates	up to 6,5	6,5-7,6	7,6-8,9	8,9-10,6	greater than 10,6

As evident from the experience of developed countries, the smoothness of road surfaces is evaluated using the International Roughness Index (IRI). It is known that the formation of bumps on cement-concrete paved roads significantly deteriorates the smoothness of the road surface.

2. Research methodology

The Guide for Mechanistic-Empirical Design of New and Reconstructed Pavements - GMED-2003 (USA) contains a model for predicting pavement smoothness. Using this model, calculations are performed to evaluate the impact of elevation on pavement smoothness [2,9,10]:

$$IRI = IRI_0 + 0{,}013 \cdot C + 0{,}007 \cdot J + 0{,}0015 \cdot H + 0{,}4 \cdot S \qquad (1)$$

Here:

IRI_0 – initial roughness index, m/km;

C– Number of plates with transverse and angled cracks, %;

J – percentage of deteriorated (damaged) seams, %;

N- final value of the rise per 1 km of road, in mm;

S- The construction factor is calculated as follows:

$$S = (T \cdot (1 + I) \cdot (1 + P_{0,075})) \cdot 10^{-6} \qquad (2)$$

Here:

T – age of the surface layer, in years;

I– cold hardiness index, °C days;

$R_{0,075}$- the percentage of particles smaller than 0.075 mm in the road subgrade soil.

3. Analysis and Results

We calculate the international roughness index for the studied sections of the road and adopt it as the initial smoothness measurement. In recent years, requirements for road surface smoothness have become more stringent. In this context, in foreign countries, the issue of ensuring the required pavement smoothness throughout its entire design life is addressed at the stage of determining and calculating the pavement structure. When calculating road surfaces, particularly rigid pavements, using modern methods, in addition to determining the main parameters of the structure, the probability of crack formation is assessed, taking into account the potential changes in road and environmental conditions.

We determined the longitudinal smoothness values for sections 228-581 km of the A-380 "Guzar-Bukhara-Nukus-Beyneu" highway using the "TRASSA" mobile road laboratory (Figure 1). The results obtained from measuring the longitudinal smoothness were processed and converted into graphical representations (Figures 2-6).

Fig. 1. "TRASSA" mobile road laboratory vehicle

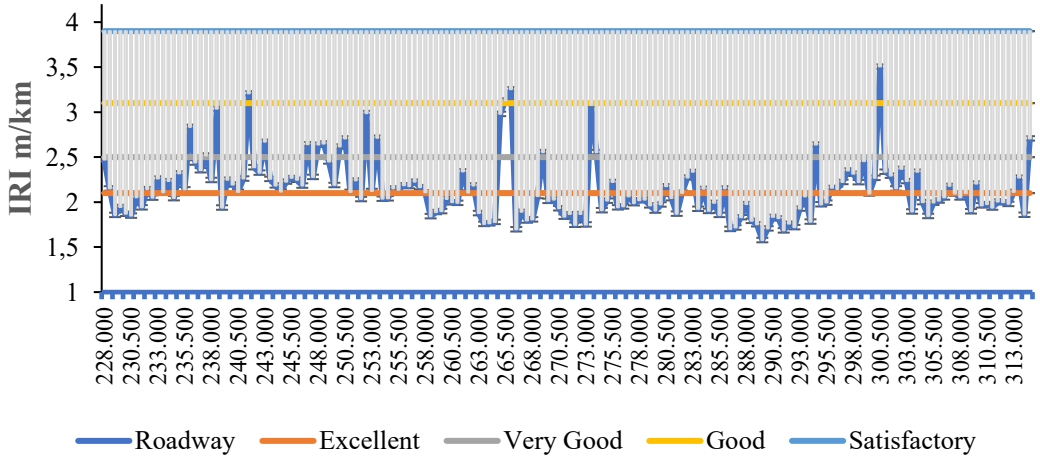

Fig. 2. Smoothness indicators of the cement-concrete pavement on the 228-315 km section of the A 380 highway

https://doi.org/10.56143/3030-3893-2025-1-64-69 A bridge between science and innovation

Fig. 3. Smoothness indicators of the cement-concrete pavement on the 315-355 km section of the A 380 highway

Fig. 4. Smoothness indicators of the cement-concrete pavement on the 355-440 km section of the A 380 highway

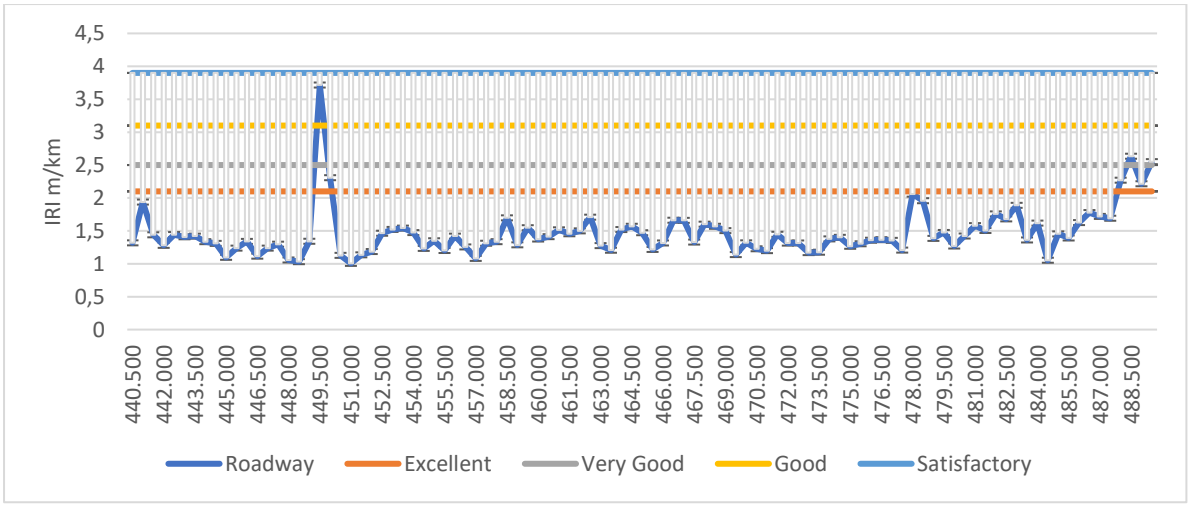

Fig. 5. Smoothness indicators of the cement-concrete pavement on the 440-490 km section of highway A 380

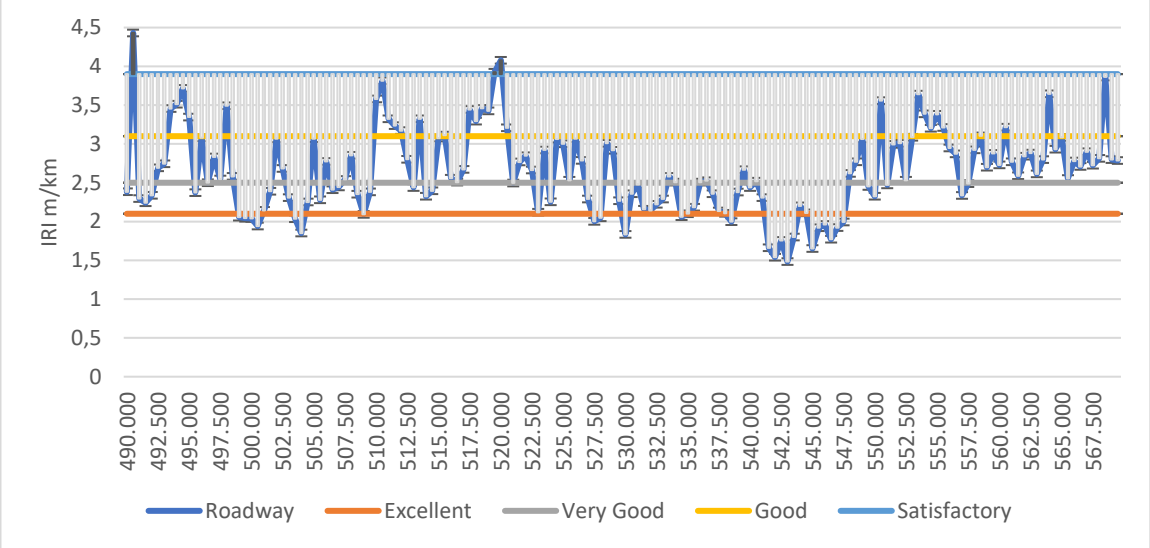

Fig. 6. Smoothness indicators of the cement-concrete pavement on the 490-581 km section of A 380 highway

In recent years, requirements for road surface smoothness have become more stringent. Consequently, in other countries, the issue of ensuring the required pavement smoothness throughout its entire design life has been addressed at the stage of determining and calculating the road surface structure [5,7,8].

In modern methods of calculating road pavements, particularly rigid pavements, not only were the main parameters of the structure determined, but the probability of crack formation was also investigated, taking into account the likelihood of changes in road and natural pavement conditions.

The calculation of the road surface concludes with determining the predicted condition of the pavement during road operation. Graphs and tables showing the relationship between changes in roadway smoothness and the spaces between concrete slabs for sections 345-347 km, 370-373 km, and 425-430 km of the A-380 "Guzar-Bukhara-Nukus-Beyneu" highway are presented below.

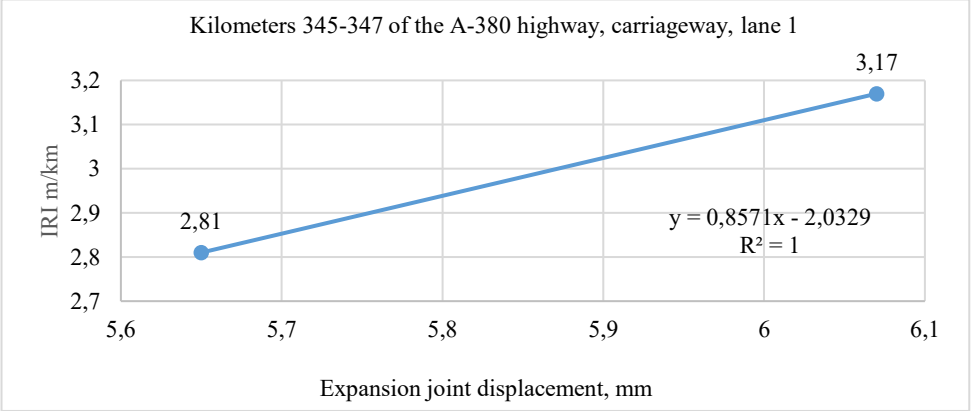

Graph 1. Relationship between IRI and elevation differences between slabs

Table 2

Dependence of pavement smoothness on changes between plates

№	Highway A-380, second lane of the roadway, km	Change in spacing between plates, mm	IRI, m/km
1	345-346	5.65	2.81
2	346-347	6.07	3.17

https://doi.org/10.56143/3030-3893-2025-1-64-69 A bridge between science and innovation

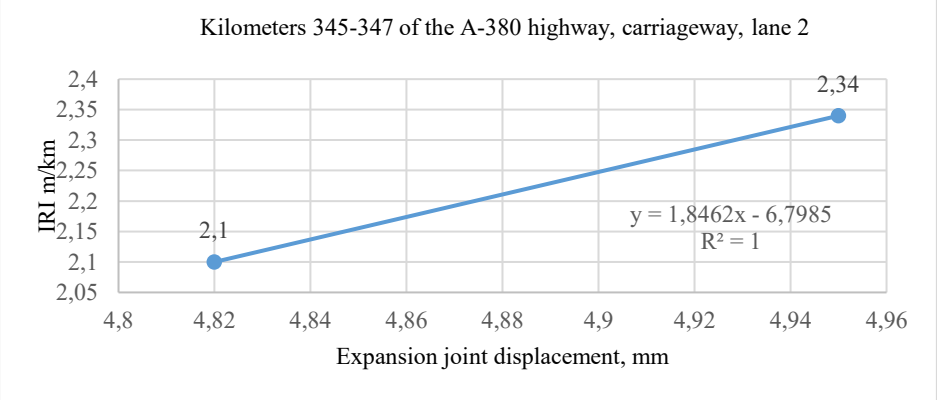

Graph 2. Relationship between IRI and elevation differences between slabs

Table 3

Dependence of pavement smoothness on changes between plates

№	Highway A-380, second lane of the roadway, km	Change in spacing between plates, mm	IRI, m/km
1	345-346	4.82	2.1
2	346-347	4.95	2.34

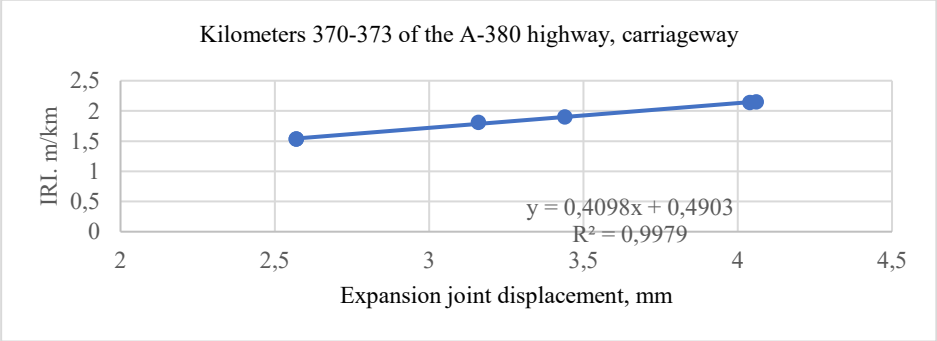

Graph 3. Relationship between IRI and elevations between slabs

Table 4

Dependence of pavement smoothness on changes between plates

№	Highway A-380, second lane of the roadway, km	Change in spacing between plates, mm	IRI, m/km
1	370,0-370,5	2.57	1.53
2	370,5-371,0	2.57	1.53
3	371,0-371,5	3.16	1.81
4	371,5-372,0	3.44	1,90
5	372,0-372,5	4.06	2.15
6	372,5-373,0	4.04	2.14

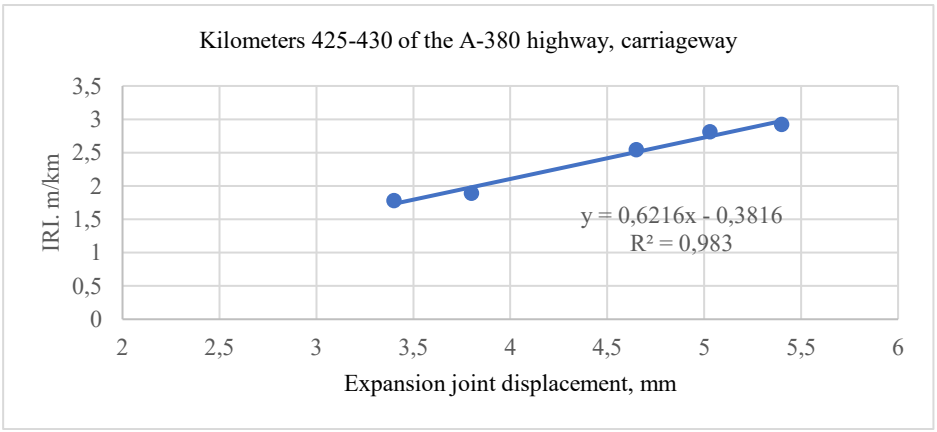

Graph 4. Relationship between IRI and elevations between slabs

Table 5

Dependence of pavement smoothness on changes between plates

№	Highway A-380, second lane of the roadway, km	Change in spacing between plates, mm	IRI, m/km
1	425-426	3.4	1.78
2	426-427	5.03	2.81
3	427-428	4.65	2.54
4	428-429	5.4	2.92
5	429-430	3.8	1.89

4. Conclusion

It is expected that the smoothness of roads with cement-concrete pavement complies with the requirements of QR 06.03-23.. In the conducted research work, negative elevations between the slabs were identified on the A-380 "Guzar-Bukhara-Nukus-Beyneu" highway at sections 345-347 km, 370-373 km, and 425-430 km. As a result of testing the pavement smoothness using the "TRASSA" mobile road laboratory equipment, indicators in the range of 1.53-3.17 m/km were determined. Through a graph showing the relationship between the state of elevations in the transverse expansion joints and the pavement smoothness, it was established that the elevations on the slabs directly affect the smoothness.

After the construction of roads with cement-concrete pavement, transverse expansion joints, vertical and horizontal displacements of cement-concrete slabs, impacts from vehicle wheels, and slab tilting result in the normalization of transverse and longitudinal joints. Their regulatory and legal activities in the field of road construction ensure.

References

[1] Amirov T.J. Construction of Cement-Concrete Pavements for Highways and Airfields. Textbook - T.: "SANO STANDART." 2017. 256 pages.

[2] Sodikov I.S. Transport and Operational Indicators of Highways. Textbook. "Transport" Publishing House, T.: 2021, 217 pages.

[3] Yunusov A.G., Kholikov B.A., Soataliev R.R. Modern Methods for Assessing the Transport and Operational Indicators of Road Surfaces. Study Guide. "Transport" Publishing House, T.: 2021, 124 pages.

[4] Tursoat Amirov, Khojiakmal Aripov, Bobomurod Qurbonov, Matchon Tukhtayev, Sukhrob Rakhmatov. Designing the Composition of Road Concrete with Chemical Additives. International Scientific Conference "Construction Mechanics, Hydraulics and Water Resources Engineering" (CONMECHYDRO - 2021) E3S Web Conf. Volume 264, 2021.

[5] A.G. Yunusov, T.J. Amirov, B.A. Kholikov, A.A. Normukhammadov. Problems of ensuring smoothness in the construction of cement-concrete road pavements. Scientific and Technical Journal of Architecture and Construction Problems. SamDAQI. - Samarkand, 2020. No. 2 (Part 1). pp. 73-75.

[6] MQN 44-08 "Guidelines for the Design of Rigid Road Pavements."

[7] Fotiadi A.A. Influence of pavement structure parameters on the process of step formation between cement-concrete pavement slabs: Dissertation for Candidate of Technical Sciences. 2009.

[8] QR 3.06.03-21 Automobile Roads

[9] Guide for Mechanistic-Empirical Design of new and rehabilitated pavement structures. Part 3. Design analysis. Chapter 4. Design of new and reconstructed rigid pavements. 2004.

[10] Highway Development and Management. Volume 6. Modelling road deterioration and works effects. 2001.

Information about the author

Amirov Tursoat Jummaevich	Tashkent State Transport University, Associate Professor PhD E-mail: tursoat.amirov@mail.ru Tel.: +998977207298 https://orcid.org/0000-0002-2681-8797
Muminov Kurban Ochilovich	Tashkent State Transport University, Associate Professor E-mail: muminov.kurban.77@mail.ru Tel.: +998941464600 https://orcid.org/0000-0002-1645-5143
Dauletov Madiyar Boranbaevich	Tashkent State Transport University, Doctoral student E-mail: dauletov.madiyar.87@mail.ru Tel.: +998913799158 https://orcid.org/0000-0002-0957-2617
Rakhmatov Sukhrob Soli ugli	Tashkent State Transport University, Associate Professor E-mail: raxmatov.suxrob.@mail.ru Tel.: +998908056563 https://orcid.org/0000-0002-1673-2631

Single-phase to six-phase voltage converter

I.M. Bedritsky[1][a], M.Zh. Mirasadov[1][b], L.Kh. Bazarov[1][c]
[1]Tashkent state transport university, Tashkent, Uzbekistan

Abstract: This paper presents a novel circuit for converting a single-phase power supply into a stabilized six-phase voltage system. The proposed converter is based on a three-limb transformer with six secondary windings connected in a hexagonal configuration and two primary windings connected in series opposition. Each primary winding is shunted by a capacitor, forming two ferroresonant circuits that ensure voltage stabilization and precise phase shifting.

Key features of the design include:

- **Simplified construction** – Reduced number of windings and optimized connection scheme.
- **Improved conversion quality** – Stabilized output voltages and maintained phase shifts (60° between adjacent phases).
- **High efficiency** – Use of an amorphous alloy core minimizes losses and reduces overall size.

The converter operates by exciting ferroresonant oscillations in the primary circuits, which saturate the outer transformer limbs while keeping the middle limb (with double cross-section) unsaturated. This ensures stable magnetic fluxes (Φ_1, Φ_2, and their sum Φ_3), inducing balanced six-phase voltages in the secondary windings. By adjusting the capacitive reactance, a 120° phase shift between Φ_1 and Φ_2 is achieved, resulting in a symmetrical six-phase output.

Potential applications include:

- Household appliances (enabling three-phase motor operation from single-phase supply).
- Industrial and transportation systems (where single-phase input is preferred).
- Power electronics and automation devices requiring multi-phase voltage.

The proposed design offers a cost-effective and reliable solution for generating high-quality six-phase power from a standard single-phase source.

Keywords: phase converter, six-phase system, ferroresonant circuit, voltage stabilization, amorphous core

1. Introduction

A circuit for converting a single-phase voltage system into a multiphase system, specifically a six-phase system, is considered. Such converters can be applied in household appliances, where their use combines the advantages of three-phase electric motors with frequency control and the availability of only a single-phase network. In particular, the use of such devices eliminates voltage dips caused by the starting currents of asynchronous motors. These converters are also used in electrified transport systems, such as shop floor, mining, and mainline transportation, where a single-phase voltage system is preferable due to the reduced number of conductors. Additionally, they are employed in protection and automation devices for power transmission lines [1,2].

2. Research methodology

In the stabilized single-phase to six-phase voltage converter under consideration (Fig. 1), which includes a three-core transformer with six secondary windings connected in opposition and arranged in pairs on each core, and two primary windings located on the outer cores with terminals for network connection, the three-core transformer is designed with a doubled cross-section for the middle core.

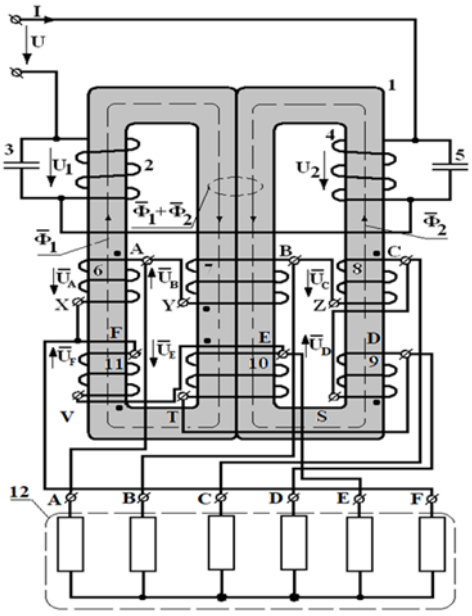

Fig. 1. Stabilized single-phase to six-phase voltage converter

The secondary windings are connected in a hexagonal configuration, while the primary windings are connected in a series-opposed arrangement and are shunted by capacitors, forming two ferroresonant circuits. This design simplifies the device by reducing the number of windings and

[a] https://orcid.org/0009-0009-8156-0811
[b] https://orcid.org/0009-0005-0838-447X
[c] https://orcid.org/0000-0002-9038-054X

simplifying their connection scheme while also improving conversion quality by stabilizing the voltage in the artificially generated phases and maintaining the required phase shifts. The use of a magnetically soft amorphous material as the transformer core enhances the efficiency of the converter and reduces its overall size [3,4].

The proposed stabilized phase number converter (Fig. 1) consists of a three-core transformer 1 of the core-shell system, where the middle core is designed with double the cross-sectional area compared to the outer cores. It includes two primary windings 2 and 3, connected in a series-opposed configuration and placed on the outer cores of the magnetic core. The winding 2, shunted by capacitor 4, forms the first ferroresonant oscillatory circuit, serving as the stabilizing element, while winding 3, shunted by capacitor 5, forms the second ferroresonant oscillatory circuit, acting as the stabilized ballast element. The secondary windings 6, 7, 8, 9, 10, and 11, where A, B, C, D, E, F are the start points of the phase windings, and X, Y, Z, S, T, V are the end points of the phase windings, located on the outer and middle cores of the magnetic core and connected in a hexagonal configuration, are used to generate an artificial six-phase voltage system that powers the load 12. The stabilized phase number converter operates as follows. When alternating input voltage U is applied to the device, ferroresonant oscillations are excited in the first and second ferroresonant circuits, formed by winding 2 and capacitor 4, and winding 3 and capacitor 5, respectively. The magnetic fluxes Φ1 and Φ2, induced by currents in windings 2 and 4, saturate the outer cores of transformer 1. Their magnitude remains almost unchanged, which results in the stabilization of voltages U1 and U2 across windings 2 and 4. Due to the opposing connection of windings 2 and 4, the magnetic flux in the middle core of the magnetic core, equal to the sum of the stable fluxes Φ1 and Φ2, is also stabilized, despite the fact that saturation does not occur in the middle core due to its doubled cross-sectional area.

The magnetic fluxes of the left and right cores Φ1 and Φ2, as well as the magnetic flux of the middle core, equal to the sum of Φ1 and Φ2, induce voltages UA, UB, UC, UD, UE, UF in the corresponding secondary windings 6, 7, 8, 9, 10, 11. The stability of these voltages is ensured by the minimal variation of the magnetic fluxes *Φ1* and *Φ2* when the outer magnetic cores of transformer 1 reach saturation. The phase shifts between the magnetic fluxes *Φ1* and *Φ2* allow for the generation of an artificial six-phase voltage system, including phase voltages U_A, U_B, U_C, U_D, U_E, U_F, or line voltages U_{AB}, U_{BC}, U_{CD}, U_{DE}, U_{EF}, U_{FA}, which power the six-phase load 9. The connection of the secondary windings 6, 7, 8, 9, 10, 11 in a hexagonal configuration improves the harmonic composition of the phase and line voltages of the artificial phases by eliminating higher harmonics that are multiples of three.

Figure 2 shows the vector diagrams of the magnetic fluxes $\bar{\Phi}_1$ and $\bar{\Phi}_2$ in the magnetic core rods, the phase voltages $\bar{U}_A, \bar{U}_B$ $\bar{U}_C, \bar{U}_D, \bar{U}_E, \bar{U}_F$, and the line voltages $\bar{U}_{AB}, \bar{U}_{BC}, \bar{U}_{CD}$ $\bar{U}_{DE}, \bar{U}_{EF}, \bar{U}_{FA}$ of the secondary windings, explaining the process of artificial phase conversion.

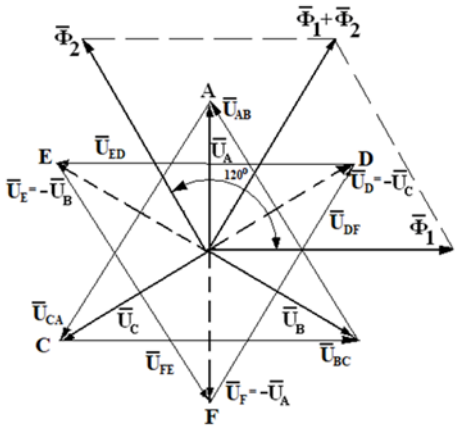

Fig. 2. Vector diagrams of the phase number converter

When autoprarametric oscillations are excited in the first (winding 2 and capacitor 3) and second (winding 4 and capacitor 5) ferroresonant circuits, the phase shift between the magnetic flux vectors $\bar{\Phi}_1$ and $\bar{\Phi}_2$ in the outer rods of the magnetic core can theoretically range from 90° to 180°. By varying the capacitance of capacitor 5 and thereby adjusting the capacitive reactance of the second oscillatory circuit, it is possible to achieve a phase shift of 120°. In this case, the magnitude of the magnetic flux vector in the central core $\bar{\Phi}_3$, which is equal to the sum of the vectors $\bar{\Phi}_1+\bar{\Phi}_2$, will be the same as the magnitudes of the vectors $\bar{\Phi}_1$ and $\bar{\Phi}_2$. Consequently, the amplitudes of the phase voltages $\bar{U}_A, \bar{U}_B$,$\bar{U}_C, \bar{U}_D, \bar{U}_E, \bar{U}_F$, induced by these magnetic fluxes in the secondary windings 6, 7, 8, 9, 10, and 11, as well as the amplitudes of the line voltages $\bar{U}_{AB}, \bar{U}_{BC}, \bar{U}_{CD}, \bar{U}_{DE}, \bar{U}_{EF}$ and $\bar{U}_{FA}$, will also be equal. The beginnings of the windings, marked with dots in Fig. 3, should be on the same side for the windings of the outer cores (6, 11 and 8, 9), while for the winding of the central core (7 and 10), they should be on the opposite side. As a result, the voltage vectors of winding 7 and$\bar{U}_E$ winding 10 are rotated by 180°, which ensures the required phase shift of 60° between the secondary voltage vectors $\bar{U}_A, \bar{U}_B$ $\bar{U}_C, \bar{U}_D, \bar{U}_E, \bar{U}_F$.

3. Conclusion

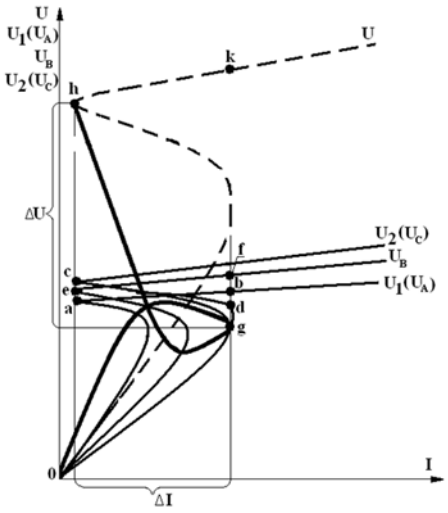

Fig. 3. Volt-ampere characteristics of the phase number converter

https://doi.org/10.56143/3030-3893-2025-1-70-72 A bridge between science and innovation

Fig. 3 shows the volt-ampere characteristics of the components of the phase number converter, illustrating the principle of stabilization of phase and line voltages of the artificial phases. The curve U represents the overall volt-ampere characteristic of the entire circuit, $U=f(I)$. The curve $U_1(U_A)$ represents the volt-ampere characteristic of the first ferroresonant circuit, $U_1=f(I)$, or, considering the transformation ratio, the volt-ampere characteristic of phases A and F, i.e., $U_A=f(I)$ and $U_F=f(I)$. The curve $U_2(U_C)$ represents the volt-ampere characteristic of the second ferroresonant circuit, $U_2=f(I)$, or, considering the transformation ratio, the volt-ampere characteristic of phases C and D, i.e., $U_C=f(I)$ and $U_D=f(I)$. The curve U_B represents the volt-ampere characteristic of phases B and E, i.e., $U_B=f(I)$ and $U_E=f(I)$. When an alternating input voltage U, whose value is within the range ΔU (or when the supply current I varies within the range ΔI), is applied to the device, ferroresonant autoparametric oscillations occur in the first and second ferroresonant circuits. These oscillations are characterized by energy exchange not only within the circuits but also between them. This ensures the stability of the device's operation, where the first ferroresonant circuit operates inductively with a lower resonance voltage (segment a − b of the curve $U_1(U_A)$), and the second ferroresonant circuit operates capacitively with a higher resonance voltage (segment c − d of the curve $U_2(U_C)$). For any operating mode of the circuit, the expression for voltage vectors is valid $\bar{U} = \bar{U}_1 + \bar{U}_2$. Considering that the voltages U1 and U2 of the first and second ferroresonant circuits, operating in inductive and capacitive modes respectively, are nearly in antiphase, the volt-ampere characteristic of the entire circuit is determined not as the arithmetic sum of the voltages U_1 and U_2 across the circuits (dashed curve U on segment 0 – h – k), but as the vector difference between the voltage U_1 in the inductive segment and U_2 in the capacitive segment (bold curve U on segment 0 – g – h – k). From the graphs, it is evident that in the zone of ferroresonant autoparametric oscillations (segment g – h of curve U), when the supply voltage changes within ΔU, the voltages $U_1(U_A)$ (segment a – b) and $U_2(U_C)$ (segment c − d) vary insignificantly. Meanwhile, the phase voltage U_B, equal to the vector sum of U_A and U_C with the opposite sign (segment e − f of curve UB), remains virtually unchanged. Thus, the device is simplified by reducing the number of windings, while the conversion quality is improved through the stabilization of voltages in the artificially generated phases.

References

[1] Преобразователи числа фаз в электротехнологии : учебное пособие / Назаров С. Л., Удинцев В. Н., Бычков С. А. [и др.] ; Мин-во науки и высш.образования. — Екатеринбург : Изд-во Урал. ун-та, 2019. — 196 с.

[2] Костиков В. Г., Парфенов Е. М., Шахнов В. А. Источники электропитания электронных средств. Схемотехника и конструирование: Учебник для ВУЗов. — 2. — М.: Горячая линия — Телеком, 2001. — 344 с.

[3] Sohrabi, S.; Fu, J.; Li, L.; Zhang, Y.; Li, X.; Sun, F.; Ma, J.; Wang, W.H. Manufacturing of metallic glass components: Processes, structures and properties. Prog. Mater. Sci. 2024,144, 101283.

[4] Bracke, L. P. M., and Geerlings, F. C., “Switched-Mode Power Supply Magnetic Component Requirements,” Philips Electronic Components and Materials, 1982.

[5] Bityukov, V.K., & Simachkov, D.S. Secondary Power Sources. Moscow: Infra-Engineering, 2017, 326 p.

[6] Kostikov, V.G., Parfenov, E.M., & Shakhnov, V.A. Power Supplies for Electronic Equipment: Circuitry and Design: University Textbook. 2nd ed. Moscow: Hot Line – Telecom, 2001, 344 p.

[7] EFE–300/EFE–400. 300/400 Watts, Digital Power Solution. Datasheet TDK–Lambda, 2009.

[8] Gurevich, V.I. "Secondary Power Sources: Anatomy and Application Experience." Electrical Market, 2009, No. 1 (25), pp. 50–54.

[9] Sohrabi, S., Fu, J., Li, L., Zhang, Y., Li, X., Sun, F., Ma, J., & Wang, W.H. "Manufacturing of Metallic Glass Components: Processes, Structures, and Properties." Progress in Materials Science, 2024, vol. 144, 101283.design: Translated from English / K. Kremer, D. Chaffin, M. Ayub, etc. // - Moscow: Mir. 1992. – pp. 43-45.

[10] Patent № IAP 06649 Fazalar sonini turg‘un o‘zgartirgich// O‘zbekiston Respublikasi Adlya vazirligi huzuridagi intelektual mulk agentligi. //(Amirov S.F., Bedritskiy I.M, Boltayev O.B., Turdibekov K.X., Bazarov L.X.)

[11] Bedritsky I., Jurayeva K., Bazarov L. Evaluation of the stability of the parametric phase number converter. // E3S Web Conf. Volume 216, 2020 Rudenko International Conference “Methodological problems in reliability study of large energy systems” (RSES 2020) (Scopus) Published online 14 December 2020

[12] Bedritsky I., Jurayeva K., Nazirova Z., Bazarov L. Stability of the parametric phase multiplier at the fundamental frequency. // AIP Conf.Proceedings 2467 (Scopus) 22 June 2022 https: //doi.org/10.1063/5.0092457

[13] Bedritsky I., Jurayeva K., Nazirova Z., Bazarov L. Dynamic modes of the phase number converter based on circuits with a common magnetic circuit. // E3S Web of Conferences 383, 01026 (2023), (Scopus) https://doi.org/10.1051/e3, conf/202338301026 TT21 C-2023 25.

Information about the author

Ivan Mikhailovich Bedritsky	Tashkent State Transport University, Professor of the Department of “Electricity Supply”, Professor (DSc) E-mail: kaktus00@list.ru Tel.: +998 90 947 25 92 https://orcid.org/0009-0009-8156-0811
Mirkomil Jalol Ugli Mirasadov	Tashkent State Transport University, Department of “Electricity Supply”, Doctoral student E-mail: mir.32.ttymi@mail.ru Tel.: +998 90 905 77 75 https://orcid.org/0009-0005-0838-447X
Laziz Kholboboevich Bazarov	Tashkent State Transport University, Associate Professor (PhD) of the Department of “Electricity Supply” E-mail: laziz.bozorov@gmail.com Tel.: +998 93 578 93 80 https://orcid.org/0000-0002-9038-054X

Production of aerated concrete blocks using energy-efficient technology

B.G. Kodirov[1][a], S.S. Shaumarov[1][b], S.I. Kandakhorov[1][c]
[1]Tashkent state transport university, Tashkent, Uzbekistan

Abstract: This article studies the problems of producing aerated concrete blocks using energy-saving technology and ways to overcome them. Aerated concrete products are distinguished by their lightness, low thermal conductivity compared to traditional concrete, and the ability to effectively recycle industrial waste. The article analyzes the influence of the structure of pores in aerated concrete, their diameter and uniformity, on thermal conductivity and strength properties. The results of the study show that aerated concrete produced using industrial waste contains uniformly distributed closed pores, which reduce the thermal conductivity of aerated concrete by 2–4.5% and increase its strength by 7–12%. At the same time, the use of cold water without adding hot water to the mixture, and the technology of covering the mold and sending it to evaporation chambers are recommended. These methods are energy-efficient, simplify the technological process, and increase the quality and environmental safety of the product. The research also shows the possibility of improving the physical and mechanical properties of two- and three-layer aerated concrete blocks with a dense surface layer. They have high potential in terms of recycling industrial waste, heat conservation, technological simplicity, and environmental sustainability.

Keywords: concrete technology, concrete mix, density, porosity, surface layer

1. Introduction

Against the background of growing requirements for energy saving and environmental friendliness of building materials, the production of aerated concrete blocks using energy-efficient technologies is becoming especially relevant. Aerated concrete is a type of cellular concrete with low density, high thermal insulation and sufficient strength, which makes it indispensable in low-rise and energy-efficient construction.

Modern technologies for the production of aerated concrete are aimed not only at improving the physical and mechanical characteristics of products, but also at reducing energy costs at all stages: from the preparation of the raw mix to autoclave processing. The introduction of automated component dosing systems, optimization of autoclaving modes, reuse of process heat and water, the use of alternative binders - all this can significantly reduce energy consumption and reduce the cost of products without loss of quality.

In addition, special attention is paid to the use of secondary resources, such as fly ash, microsilica or construction waste, which corresponds to the concept of sustainable development and a closed production cycle.The technology of production of aerated concrete products is related to the composition of bodies in the concrete mix: the porosity that forms the concrete structure, its formation methods, the strength of aerated concrete and many other specific properties. As a result of the interaction of one of the main components of the concrete mix with the gas-forming (usually aluminum powder) and calcium hydrate oxide, hydrogen is released, which is poorly soluble in water and forms gaseous pores in the concrete mix.

As the volume of spherical pores (cells) of gas increases, the volume of concrete also swells (expands) by 1.2-1.8 times. The formation of gas and the expansion of the concrete mix may not proceed smoothly. This depends on the following factors: rheological properties of the mixture, the temperature of the raw material and the environment, the alkalinity and exothermicity of the binder, the displacement of the mold in the shop, etc. [1].

Instability in the swelling of the mixture leads to changes in the density of aerated concrete. As a result, aerated concrete has the following performance characteristics than other types of concrete: average density, thermal conductivity, strength, etc. [2, 3].

If the heavy concrete has almost the same density (average 2400 kg/m3) regardless of the strength class, then the value of the density of aerated concrete varies from 300 to 1200 kg/m3.

Light concrete mix differs from heavy concrete mix by greater flexibility.

Due to the high consistency of the aerated concrete mix, it consists of the process of preparation and molding of aerated concrete products, ie casting. The aerated concrete mixture poured into the mold expands, taking the form of a mold. The volume of concrete mixture raised from the top level of the mold reaches 10-15%. The hoist should be cut and removed flat from the surface of the mold. Returning the cut lift to the concrete mixing device is cost-effective in fully mechanized plants. Returning the cut lift to the concrete mixing device requires a large amount of manual labor in small enterprises, and it is often discarded [4, 5].

2. Research methodology

One of the advantages of aerated concrete products is: it has the lowest average density among all known types of concrete (300-1200 kg/m3); maximum thermal conductivity resistance (0.08-0.29 W/m·°C); maximum fire and frost resistance; has the maximum potential for industrial waste utilization.

One of the specific properties of aerated concrete products, which differs from other concretes, is: preparation of concrete mix without coarse aggregate; cast consistency

[a] https://orcid.org/0009-0006-8828-1645
[b] https://orcid.org/0000-0001-8935-7513
[c] https://orcid.org/0000-0002-3689-8794

(melting of the mixture on the Suttard cylinder 12-35 cm); addition of hot water at a temperature of 50-70 ˚C to the mixture (optimal for gas formation and increase in the volume of the mixture).

The introduction of hot water at excess temperature into the concrete mix has a negative impact on the physicochemical properties of aerated concrete, such as increased demand for water, decreased strength, premature formation of sand.

When molding products, the aerated concrete mix is not completely filled into the formwork because the aerated concrete mix expands to fill the remaining volume of the formwork cavity. In order to properly form the concrete structure and optimize the gas formation process, in practice it can be obtained by preparation in the form of a low-consistency compound (11-13 sm) and by vibration. After the expansion process of the mixture is completed and after cutting, exposure to the mold (shaking, strokes, etc.) is not recommended as the mixture will shrink.

Such technological operations are carried out only with aerated concrete mix. Other types of heavy concrete mixes are laid on the mold balance and brought in using vibro compaction. The volume of these vibro-compacted concrete mixes does not change. Another type of lightweight concrete mix is foam concrete, which is poured in the ready state of foaming over the entire height of the mold, then the foam concrete mix does not expand in the mold and can sometimes sink to 1-3%.

As for concrete production technologies, there is a technology for adding the mixture to the formwork from above in the open position for porous concrete.

Disadvantages of traditional aerated concrete technology include:

• introduction of hot water into the concrete mix;

• energy consumption for heating water to 50-70 °C;

• the need to store the molded concrete mixture in a special heat and humidity chamber at a temperature of 40 ± 5 °C for 5-6 hours;

When pouring aerated concrete into the formwork, compaction of the upper part of the formwork based on the technology of “light compaction roller” is not considered efficient enough and therefore requires special equipment;

One of the unique properties of building materials made of aerated concrete is the open porosity of concrete and their strength. The open porosity of the surface of the products leads to the subsequent deterioration of water absorption, capillary pods, many important operational properties of aerated concrete. Therefore, it is necessary to protect the surfaces of external walls made of porous concrete from mechanical and external climatic influences (covering the surface with plaster). Thus, reducing the porosity and increasing the strength of the surface of the layers allows to overcome many shortcomings of aerated concrete. In order to increase the rigidity and strength of the outer layers of aerated concrete products, it is proposed to cover two- and three-layer aerated concrete blocks with a compacted surface layer of a denser material. In this case, the cement-sand mixture in the ratio "Cement: sand = 1: 3" and the top surface can be covered with materials consisting of a light porous filler. The thickness of the compacted layers is 1 - 2 cm. The middle layer consists of an aerated concrete mix with a density of 400 - 500 kg/m3. In this design, the physical and mechanical properties of composite concrete are improved, and the surface of aerated concrete products differs from ordinary concrete in the strength of layered aerated concrete with a density of 600-700 kg/m3.(Fig. 1).

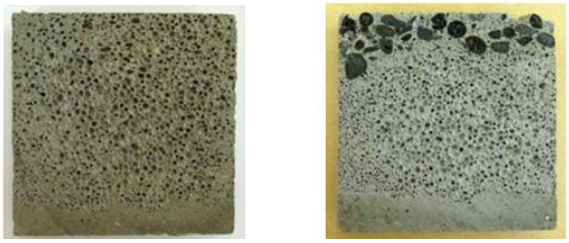

a **b**

Figure 1. Aerated concrete samples:
a - two-layer aerated concrete consisting of a dense cement-sand mixture; b - three-layer dense mix and lightweight concrete aerated concrete consisting of a surface layer

In order to improve the production of aerated concrete blocks based on energy-saving technologies, industrial waste from the "Foundry Mechanical Plant" of JSC "Uzbekistan Railways" was used, and the structure of aerated concrete samples was investigated (Fig. 2). In this case, when forming porous concrete block samples, aerated concrete consists of structural walls containing closed and open macro-micropores and microcapillaries. Usually, the pores should have a closed straight spherical shape and be evenly distributed throughout the entire volume of concrete.

The composition of the aerated concrete structure made from industrial waste sand and steel smelting slag was analyzed in the laboratory after 28 days. An overview of the samples is presented in Fig. 2.

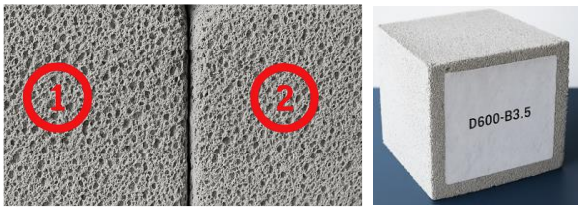

Figure 2. External view of D600 aerated concrete samples

Here, along with micropores, large-diameter macropores are depicted. The pores of aerated concrete based on industrial waste quartz sand have a macrostructure that is close to each other. In this case, the pores of the sample tend to be uniform and the number of interconnected pores is small. This, in turn, leads to an increase in the thermal insulation properties and strength properties of aerated concrete.

The proposed aerated concrete cellular structure has a regular spherical geometric shape, and the non-autoclaved aerated concrete based on steel smelting slag consists of pores of various sizes of 1.2-3.1 mm, which are evenly distributed. The recommended composite aerated concrete based on industrial waste quartz sand and slag has a maximum pore diameter of 1.5 mm and pores of 1 mm or less.

The study of the structural composition of autoclaved aerated concrete was carried out according to the methodology “Binders and concretes from artificial and mineral raw materials” [5].

3. Results and Discussion

The conducted studies show that the dimensions of

micro and macro pores determine the physical and mechanical properties of aerated concrete (Table 1).

Table 1

Pores of aerated concrete

Thermal conductivity, Vt/m·°C	Pore sizes, mm	Thickness of the pore walls, мм	Average density, kg/m^3	Strength, MPa	Hollowness, %
0,143	p1=2,220 p2=1,480 p3=3,171	2,020	663	1,67	63
0,141	p1=2,103 p2=1,602 p3=2,434	2,187	665	1,668	61,6
0,152	p1=1,808 p2=1,205 p3=1,582	1,990	660	1,62	63,5

The results of the analysis of the aerated concrete structure show that the micro- and macrostructure of aerated concrete produced using industrial waste quartz sand differs from concrete without the addition of waste in that the pores are relatively uniform and have regular spherical shapes (Fig.3).

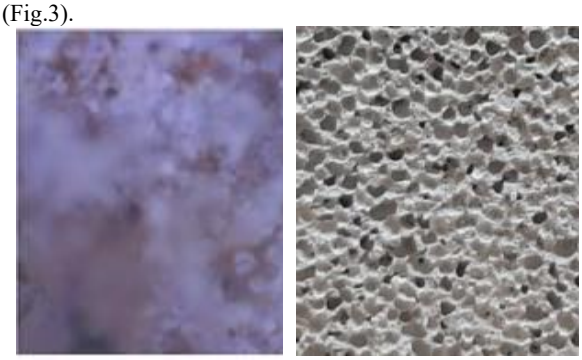

a) b)

Figure 3. Micro and macrostructures of aerated concrete:

a – microstructure (10^{-5} μm);
b – macrostructure (1.48-3.17 mm)

Aerated concrete samples produced using industrial waste sand show better results in terms of thermal conductivity than aerated concrete samples based on waste slag. This is due to the presence of slag in its composition, which has a low thermal conductivity. This is due to the evenly distributed porous structure, which improves the physical and mechanical properties of aerated concrete.

To study the structure of aerated concrete, it is important to study its micro-macrostructure. Analysis of the microstructure allows us to study its porosity or average density. Based on these analyses, it is shown that the physical and mechanical properties and water absorption depend on the structure of aerated concrete.

Figure 4 shows the comparative characteristics of pores and thermal conductivity of aerated concrete in the proposed and production organization.

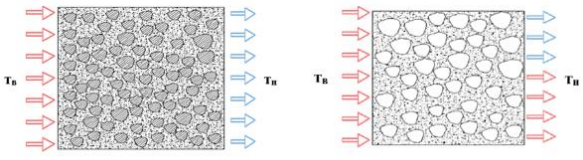

a) b)

Figure 4. Scheme of arrangement of pores of aerated concrete blocks:

a) proposed aerated concrete; b) aerated concrete of the production organization

This figure shows that aerated concrete contains a large number of pores and the location of these pores is different, the thermal conductivity will be different. Also, the smaller the size of the filler materials, the higher the aerated concrete mixture will be, and the pores will be the same. At the same time, the thermal conductivity will decrease by 2-4.5% compared to a structure with different pores.

The sand fractions in the composition of aerated concrete have a significant impact on its lifting height (Fig. 5).

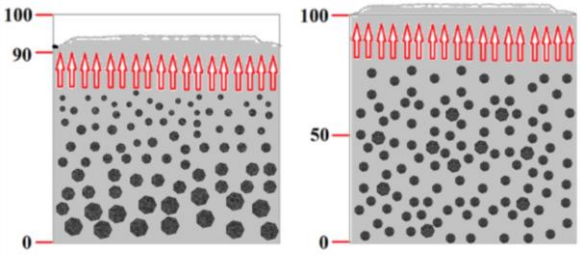

a) b)

Figure 5. The height of the mixture:

a - aerated concrete made of sand with dimensions of 0.315-0.63; b - aerated concrete made of sand with dimensions of 0.15-0.315

The lifting height varies depending on the type and fraction size of the sand in the aerated concrete mixture. Also, the smaller the fractions of the sand in the aerated concrete mixture, the easier it is to lift. The larger the fraction, the more difficult it is to lift and the more aluminum powder is required.

The greater the amount of fillers in the composition of aerated concrete, the less uniform the distribution of concrete particles and the more likely microcracks to appear in aerated concrete structures (Fig. 6).

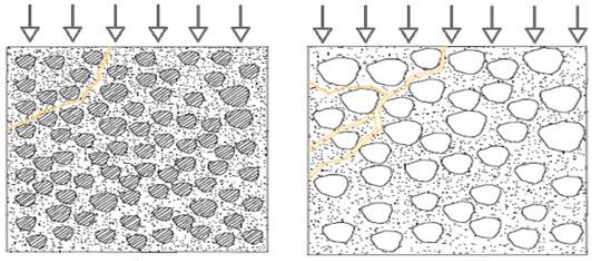

a) b)

Figure 6. Defects of aerated concrete blocks that occur during compression:

a) offered aerated concrete; b) aerated concrete in production

As can be seen from Figures 5 and 6 above, aerated concrete pore spaces made from sand with fraction sizes of 0.15–0.315 have significantly better strength, thermal conductivity, and porosity than aerated concrete made from sand with a fraction size of 0.315–0.63, due to their tendency to be uniform.

The porous structure of the samples was tested using a Thermo Scientific Pascal porosimeter in the research laboratory of the Department of "Construction of Buildings and Industrial Facilities" of Tashkent State Transport University. According to the results of the study, the samples with the best characteristics were identified. The results of this experimental study are presented in Figures 7 and 8.

https://doi.org/10.56143/3030-3893-2025-1-73-77 A bridge between science and innovation

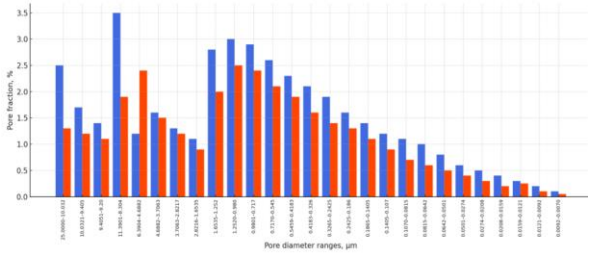

Figure 7. Diagram of percentage pores of non-autoclaved aerated concrete blocks made using steel smelting slag and waste quartz sand:
(1-industrial waste, 2-steel smelting slag)

The graph of pore diameters and their corresponding percentage distribution, constructed based on the experimental results, gives an idea of how the pore volumes are distributed in two different samples. Each curve has a unique shape, and the peak (maximum point) in it reflects the most common (i.e., dominant) pore diameters in the sample. For a deeper analysis of these graphs, they are evaluated based on mathematical distribution models. In studies of porous materials, modeling of pore diameter data using statistical distribution functions is widely used. In particular, the log-normal distribution model is considered acceptable for materials such as cement-based composites and aerated concrete. In this model, the logarithm of the pore diameter is considered to be normally distributed. We use a single-peak Gaussian (normal) distribution model as a simple and understandable approach. This model represents the average diameter of pores in the material (μ) and the standard deviation (σ) of the diameter distribution. Here: μ - is the peak of the curve (i.e., the diameter at which the pore fraction is highest), σ - is the extent to which the pore diameters are spread out.

The probability density function of the normal distribution is written as:

$$f(d) = \frac{1}{\sigma\sqrt{2\pi}} \cdot \exp\left(-\frac{(d-\mu)^2}{2\sigma^2}\right) \quad (1)$$

where:

d - is the pore diameter; μ - is the mean diameter; σ - is the standard deviation;

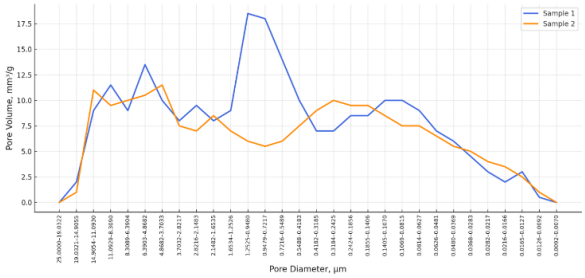

Figure 8. Diagram of pores versus volume of non-autoclaved aerated concrete blocks made using steel smelting slag and waste quartz sand:
(1- waste quartz sand and steel smelting slag, 2 - steel smelting slag)

The results of the experiment show that 0.1-0.3 mm pores make up 10-12% of the content obtained from production, while this indicator made up 20-24% in the samples with added industrial waste. In this case, the increase in the amount of micropores when comparing the samples is achieved due to the fact that the surfactants in the steel melting slag facilitate the hydration reaction in the mixture.

Thus, studies have shown that the thermal conductivity of aerated concrete is affected by the given concrete structure and the thermal conductivity coefficient of the raw materials used. It was possible to obtain non-autoclaved aerated concrete from natural and man-made raw materials of Uzbekistan, the thermal conductivity of which meets the requirements of GOST 10180-2012 for non-autoclaved aerated concrete and does not exceed 0.14-0.18 W/m·°C.

As a result of experimental studies, it has been scientifically proven that by achieving an even distribution of pores throughout the volume of aerated concrete, its thermal conductivity is improved by 2-4.5%, and its strength indicators by 7-12%. Taking this into account, in the next section we will conduct scientific research on the impact of water absorption and frost resistance on the factors affecting the operation of aerated concrete.

The development of porous structure and gaseous (non-naturally closed) pores with closed-type spherical pores in an open mold is characterized by the impossibility of obtaining freely compacted inter-porous barriers.

As a result of the research, the following is proposed to address the above shortcomings:

• adding unheated water to the aerated concrete mix;

• during the preparation of aerated concrete products, cover the concrete mix with a sturdy lid in the form of a cover or pallet;

• sending the aerated concrete mixture poured into the mold to the evaporation chamber preheated to 40-45 ° C;

• Immediately send the mold to the evaporator chamber, without first holding the process of hot-wet processing of the product.

Research and analysis of the literature confirm that these proposals are expedient and that their implementation is effective. Adding unheated water to the aerated concrete mix significantly simplifies the technology, in addition to saving the electricity typically used to heat the water, preventing the risk of premature expansion of the mix. However, it is important to perform this process in closed molds.

This paper presents the possibility of obtaining the bottom layer of the formwork mixture from the cement-sand mixture in the production of two-layer concrete, the upper part of the aerated concrete mixture by spraying the cement-sand dry mix and then laying the formwork with a lid. In this case, it is advisable to sprinkle the outer surface of the aerated concrete mixture with a thin layer of cement only to fill the surface pores.

In the future, it is planned to conduct extensive research in the field of production of aerated concrete products on the basis of the above technology, the study of the effect of the dense outer layer on their mechanical and thermal properties.

4. Conclusion

The production of aerated concrete blocks based on energy-saving technologies allows saving resources in the modern construction industry, reducing environmental impact, and creating high-quality products. Experiments conducted during this study have shown that the optimal diameter and uniform distribution of pores in the aerated concrete structure not only significantly reduces the thermal conductivity of the material, but also improves its main technical indicators, such as strength and service life. Aerated concrete blocks, made on the basis of inexpensive

and environmentally safe raw materials obtained by processing industrial waste, not only meet the demand for energy-saving building materials, but also serve environmental protection. Such technological approaches as the simplification of heat treatment stages, the avoidance of hot water, and the direct sending of molds to the evaporation chamber are a practical manifestation of the modern production approach. The final conclusion is that the production of aerated concrete products through energy-efficient methods is not only a technological innovation, but also a strategic solution that ensures environmental and economic sustainability. This approach creates a solid scientific and practical foundation for the sustainable development of the construction industry in the future.

References

[1] Lotov A. V., Mitina N. A. Features of technological processes for the production of aerated concrete // Building materials. 2003. No. 1. S. 7-9.

[2] Production of cellular concrete products: the theory of practice / N. P. Sazhnev et al. Minsk: Strinko, 1999. 284 p.

[3] Autoclaved concretes / S. A. Mironov et al. M.: Stroyizdat, 1998. 280 p.

[4] Electrometallurgy of steel and ferroalloys / Povolotsky D.Ya., Roshchin V.E., Ryss M.A., Stroganov A.I., Yartsev M.A. Textbook for universities. Izd. 2-th, reworked. And supplement. M.: Metallurgy. 1984. - 568 c.

[5] Kasymova M.T. Temperature factor in the production technology of fiber-reinforced concrete [Text] / M.T. Kasymova, N.A. Dyikanbaeva // Proceedings of the international scientific and practical conference "Regional aspects of the development of science and education in the field of architecture, construction, land management and cadastres at the beginning of the III millennium. Scientific readings dedicated to the memory of Professor A.P. Sapozhnikov", Komsomolsk-on-Amur: FGBOU HPE "KnAGTU". 2014.-P. 280-285.

[6] Gorlov Yu.P. Refractory and heat-insulating materials [Text] / Yu.P. Gorlov, I.F. Eremin, B.U. Sedunov. - M.: Stroyizdat, 2006.-192 p.

[7] Adilkhodjaev, A., Makhamataliev, I., Tsoy, V., Shaumarov, S., Ruzmetov, F. Features of Forming the structure of cement concrete on second crushed stone from concrete scrap. International Journal of Advanced Science and Technology, 2020, 29(5), стр. 1901–1906

[8] Shaumarov, S., Kandakhorov, S., Umarov, K. Development of the Optimal Composition of Aerated Concrete Materials on the Basis of Industrial Waste. AIP Conference Proceedings, 2022, 2432, 030087

[9] Adilkhodjaev, A., Tsoy, V., Khodzhaev, S., Shaumarov, S., Umarov, K. Research of the influence of silicon-organic hydrophobizer on the basic properties of cement stone and mortar. International Journal of Advanced Science and Technology, 2020, 29(5), стр. 1918–1921.

Information about the author

Kadirov Bahodir Gayratjon ugli	Tashkent State Transport University “Building and industry facilities Construction Department doctoral student E-mail: bahodirqodirov55@gmail.com Tel.: + 998712990046 https://orcid.org/0009-0006-8828-1645
Shaumarov Said Sanatovich	Tashkent State Transport University “Building and industry facilities Construction Department professor (DSc), E-mail: shaumarovss@mail.ru Tel.: + 998712990026 https://orcid.org/0000-0001-8935-7513
Kandakhorov Sanjar Ishratovich	Tashkent State Transport University “Building and industry facilities Construction Department associate professor (PhD), E-mail: sanjar.kandakharov@mail.ru Tel.: + 998500717191 https://orcid.org/0000-0002-3689-8794

Development of building structures with individual characteristics taking into account the conditions of Uzbekistan

B.G. Kodirov[1][a], S.S. Shaumarov[1][b], S.I. Kandakhorov[1][c]
[1]Tashkent state transport university, Tashkent, Uzbekistan

Abstract: The climatic conditions of Uzbekistan (cold winters, very hot summer days) require building materials with high energy efficiency. This article presents the possibilities of creating energy-efficient, sustainable and local raw materials-based building structures, taking into account the natural-climatic and geological conditions of Uzbekistan. Aerated concrete blocks are widely used in the construction industry as a lightweight, heat-retaining and relatively inexpensive material. In particular, ways to improve the physical, mechanical and thermal properties of aerated concrete blocks by adding steelmaking slag (SMS) and waste quartz sand are studied. Its strength can be increased and the cost of raw materials can be reduced by using local industrial waste. The study improved the physical, mechanical and thermal properties of aerated concrete blocks using steelmaking slag (SMS) and waste quartz sand. As a result, it was found that the addition of these materials improves the strength of aerated concrete by 12-13%, and thermal insulation by 1-1.5%. Also, the use of waste helps reduce the cost of raw materials and increase environmental efficiency. The results of the study confirm the effectiveness of this technology in the development of energy-efficient and affordable building materials in Uzbekistan. Based on experimental data, new composite compositions were developed and their effective results in terms of thermal conductivity, density and strength were demonstrated.

Keywords: aerated concrete, steel slag, waste sand, thermal conductivity, density, strength, D600 grade

1. Introduction

Today, at a time when the process of design and construction of energy-efficient buildings in the world is developing rapidly, the demand for energy-efficient and cost-effective building materials is growing. Positive changes in the construction industry in our country and the huge creative work around us, along with the need to create and apply new equipment and technologies, lead to an increase in costs for the construction and operation of buildings [1-3].

In this regard, in the process of designing and construction of energy-efficient buildings, the issue of covering the outer walls with effective thermal insulation materials or adapting the outer wall structure to modern thermal insulation requirements is important in the process of their future use.

Currently, research is being conducted in developed countries aimed at creating external barrier structures from aerated concrete as energy-efficient and environmentally friendly materials. In this regard, including aerated concrete to model its optimal porous structure to meet the requirements of thermal protection and strength, improve its structure by adding special chemical additives to the concrete mix to create effective external barrier structures from aerated concrete, substantiate the requirements for energy-efficient building exterior walls, One of the urgent tasks is to develop appropriate technological solutions that provide the necessary properties, as well as structures with high resistance to thermal conductivity [4-8].

In developed countries such as Germany, USA, Japan, Sweden, Austria, France, Finland, Russian Federation, attention is paid to the production of cost-effective aerated concrete using industrial waste, increasing its properties such as thermal insulation, strength, moisture permeability [9-11]. As a result, along with the utilization of industrial waste, it has a positive effect on increasing the economic efficiency of aerated concrete.

Particular attention is paid to the creation of energy-efficient building structures and the introduction of new technologies, the development of modern building materials industry using local products, reducing the cost of construction products and reducing energy consumption in the operation of buildings and structures.

In this regard, the President of the Republic of Uzbekistan On the basis of large-scale reforms in the construction industry under the leadership of Sh.M.Mirziyoyev, on May 23, 2019 No. Presidential decree (PD) PQ-4335 “On additional measures for the accelerated development of the construction materials industry”, February 20, 2019 No. PQ-4198 “On radical improvement and complex Development Resolutions” were adopted. This is aimed at ensuring high rates of production and export of competitive products from local raw materials in the country, as well as modernization of enterprises, technical and technological deepening of structural changes in the building materials industry.

In the production of building materials from aerated concrete, it is advisable to study in detail the issue of adding them to industrial waste as a filler. Therefore, today, research work is underway to include a mixture of ash "strip" and quartz sand, which is separated as industrial waste during the operation of the foundry-mechanical plant under JSC “Uzbekistan Railways”. The inclusion of the above and other ty SMS of industrial waste in the concrete during the production of aerated concrete blocks, first of all, saves waste processing (utilization), binder (cement), increases the operational properties of the structure.

[a] https://orcid.org/0009-0006-8828-1645
[b] https://orcid.org/0000-0001-8935-7513
[c] https://orcid.org/0000-0002-3689-8794

In recent years, the demand for building materials in Uzbekistan has been increasing sharply. At the same time, existing materials do not always meet local climate, seismic activity and environmental requirements. The quality of materials used in construction, especially their ecological, economic and technical efficiency, is one of the pressing issues today. In particular, structural elements intended for multi-storey buildings, industrial buildings and social structures should not only be durable, but also lightweight, energy-efficient and have a long service life. In this regard, aerated concrete blocks are considered an alternative solution. Aerated concrete blocks are distinguished by their light weight, low thermal conductivity and ease of processing. At the same time, increasing their strength and thermal insulation properties is an important task. For this purpose, the article studies the physical, mechanical and thermal properties of aerated concrete blocks using steelmaking slag and waste quartz sand, and develops optimal compositions.

2. Research methodology

Many studies have been conducted on the use of secondary products in aerated concrete products, in which it was stated that steel smelting slag has a binding property [14], and it was stated in the studies that it is effective in replacing cement. Taking this into account, we will consider designing the composition of aerated concrete using steel smelting slag in an amount of 10-20 percent in accordance with the studies in [13, 15].

Since the size of the steel smelting slag fractions is 10-20 mm, a “SHLM-100” ball mill was used for grinding. Then, it was sieved through a No. 008 sieve and added to the cement to form the mixture. Information on the chemical oxides and their content in the slag and cement is given in Table 1.

Table 1

Chemical composition of iron smelting slag

Name	Calcium oxide	Silicon oxide	Iron oxide	Manganese oxide	Aluminum oxide	Magnesium oxide	Phosphorus oxide	Calcium fluoride
Oxide name	CaO	SiO_2	FeO	MnO	Al_2O_3	MgO	P_2O_5	CaF_2
Amount in slag	57,3	21,95	3,85	4,9	8,9	2,3	1,4	6,7
Amount in cement	64,9	21,9	3,6	1,5	4,8	1,6	-	-

It can be concluded from Table 1 that the silicon and calcium oxides in the slag, as well as in cement, increase the binding properties of the mixture by forming an active interaction reaction with water. At the same time, since the chemical oxide composition of waste slag and cement is 80-85% similar, it can be used as a cement substitute.

Figure 1. External view of D600 aerated concrete sample

The composition and viscosity of the aerated concrete mixture using steelmaking slag were developed using computational and experimental methods developed in accordance with the studies in [16], based on the data of the mathematical method of planning experimental studies, and samples in the form of cubes of the D600 brand with dimensions of 100x100x100 mm were prepared in laboratory conditions (Fig. 1). The samples were subjected to normal hardening conditions at a temperature of 20 °C with a relative humidity of 95 percent for 7 and 28 days.

Cubes were cast from the prepared aerated concrete mixtures and placed in a special room for storage in humid conditions, and after 28 days the physical and mechanical properties of the blocks were determined.

The following formulas were used in the experiments:

Density (ρ):

$$\rho = \frac{m}{V} \quad (1)$$

where:

m – mass of the dried sample (kg)

V – volume of the sample (m^3)

Compressive strength — strength (σ):

$$\sigma = \frac{F}{A} \quad (2)$$

where:

F – maximum compressive force in the test (N)

A – cross-sectional area of the sample (m^2)

Thermal conductivity (λ):

$$\lambda = \rho \cdot C_p \cdot \alpha \quad (3)$$

where:

ρ – density (kg/m^3)

Cp – heat capacity (J/kg·K), for aerated concrete ≈ 1000 J/kg·K

α – heat dissipation coefficient (m^2/s)

Also, the presence of 85-93% silicon oxide (silica) in the composition of waste quartz sand indicates that it has a unique active chemical and reactive composite properties. The composition of the aerated concrete mixture was prepared in the amounts given in Table 2.

In this case, D600 aerated concrete blocks were prepared in laboratory conditions using steel smelting slag and their strength and calculated thermal conductivity were determined in accordance with the requirements of GOST 10180-2012 using a hydraulic press of the “CD-2000” brand, in accordance with the requirements of KMC 2.01.04-18 “Construction Heat Engineering”.

Table 2

Composition of D600 aerated concrete mix with steelmaking slag for cube preparation in laboratory conditions

S. n.	Components name	Unit of measurement	Quantity
1	Cement	kg	220
2	Steel melting slag	Of cement mass, %	10-20
3	A fine filler	kg	360
4	Lime	kg	10
5	Aluminum powder	kg	0,47
6	Water	l	264
7	Caustic soda	kg	3
8	Sodium sulfate	kg	4,6

https://doi.org/10.56143/3030-3893-2025-1-78-82 A bridge between science and innovation

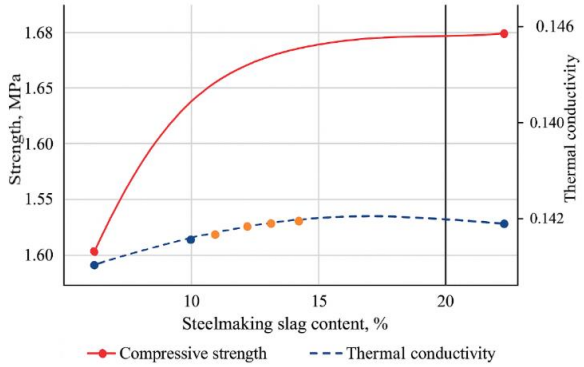

Figure 2. Dependence of the strength and thermal conductivity of aerated concrete on the amount of slag

In the picture above according to the results of laboratory research, the strength and thermal conductivity properties of aerated concrete using steel melting slag are shown in

It can be seen from this graph that the amount of slag was added to the composition of aerated concrete in the amount of 10%, 10-15% and 15-20% of the cement mass, and it was compared according to the samples prepared by the composition of industrial enterprises. When the amount of slag in the composition of aerated concrete is up to 10% of the cement mass, it was observed that the strength of the blocks and the calculated thermal conductivity improved by 0.1-0.5%. When the amount of slag is 10-15%, the average density is 3-6%, the calculated thermal conductivity is 2-4.5%, and the strength is improved by 7-12%. It was also observed that when the amount of slag is 15-20%, the average density increases by 6-9% and strength by 12-13%, the calculated thermal conductivity decreases by 1-1.5%. Therefore, according to research results, it is advisable to choose slag in the amount of 10-15 percent of the cement mass. Here, after determining the optimal amount of steel melting slag for the preparation of aerated concrete mixture, a mutual comparative analysis of the physical and mechanical properties of the samples prepared in the laboratory according to this composition and the composition of the production organization is presented in Figure 3.

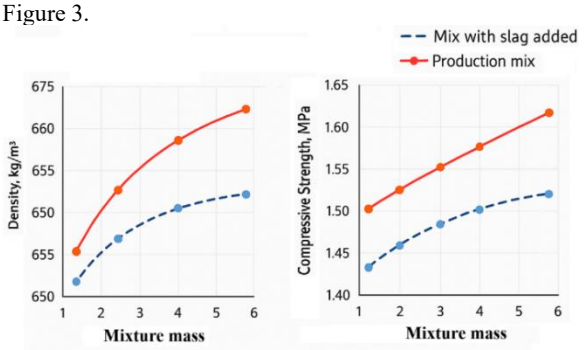

Figure 3. The results of the comparative analysis of the compositions used in industrial enterprises and slag used

The comparative analysis in the graph shows that slag, in addition to having cement-substituting properties, also serves to increase the strength of aerated concrete due to its higher density than cement. This is of great importance for increasing the efficiency of using steelmaking slag in the production of aerated concrete.

All experiments were carried out with a small amount of aerated concrete samples. At the same time, it is recommended to use fine-grained compositions presented in studies [11, 12, 15] in the composition of aerated concrete in which slag is used. This is because fine particles help the mixture to rise uniformly during the process of aerated concrete expansion.

The amount of filler particles in the composition is of great importance in the production of structural and thermally insulating aerated concrete blocks. Taking this into account, in this dissertation, studies were conducted on the introduction of quartz sand into the composition of aerated concrete. It is scientifically proven that adding quartz sand to aerated concrete is one of the most effective fillers [8, 9, 10]. Considering that adding quartz sand to concrete increases the cost of blocks, it is important to produce aerated concrete blocks using waste quartz sand. The appearance of the added waste quartz sand and the samples made from it are shown in Figure 4.

Figure 4. Appearance of waste quartz sand and samples

At the next stage, the effect of waste quartz sand on aerated concrete strength and calculated thermal conductivity indicators was studied. The results of this study are presented in Figure 5.

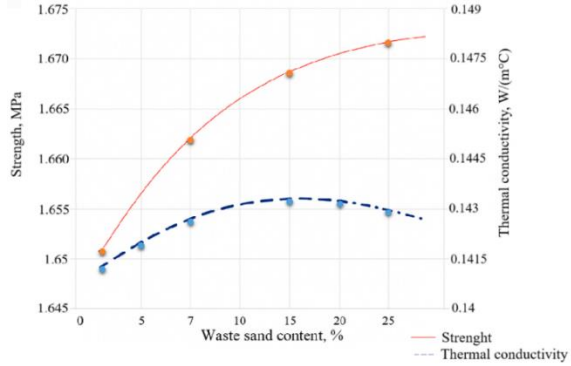

Figure 5. Dependence of the strength and thermal conductivity of aerated concrete on the amount of waste quartz sand

According to the above graph, the amount of waste quartz sand was added to aerated concrete in the amount of 10%, 10-20% and 20-30% of the sand mass, and it was compared according to the samples prepared by the composition of industrial enterprises. When the amount of waste quartz sand in aerated concrete is up to 10% of the cement mass, it was observed that the strength of the blocks and the calculated thermal conductivity improved by 0.6-1.0%. When the amount of waste quartz sand is 10-20%, the average density is 5-7%, the calculated thermal conductivity is 3-5.5%, and the strength is improved by 8-11%. Also, when the amount of waste quartz sand is 12-30%, the average density increases by 7-11% and strength by 11-13%, and the calculated thermal conductivity deteriorates by 1.5-2.5%. Therefore, according to the results of the study, it is

advisable to select waste quartz sand in the amount of 10-15% of the sand mass.

Then, aerated concrete blocks were produced according to the amount of waste quartz sand determined above, and their physical and mechanical properties were compared with blocks of the same composition produced at industrial enterprises. The results of the comparative analysis are presented in the graph in Figure 6.

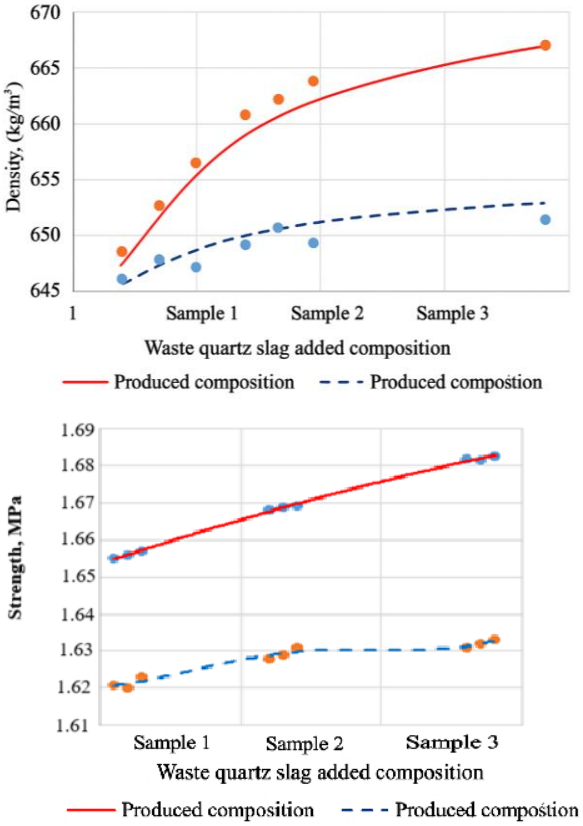

Figure 6. Physical and mechanical properties of waste quartz sand and aerated concrete samples offered by industrial enterprises

From the graph above, it can be seen that due to the small dispersion of waste quartz sand particles, the pores in aerated concrete blocks are evenly distributed in size. The physical and mechanical properties of the prepared samples show that the average density of the sample using waste quartz sand was 651 kg/m3 and the strength was 1.645 MPa, while the average density of the samples prepared by the composition of industrial enterprises was 646 kg/m3 and the strength was 1.62 MPa. It was found that the content with the addition of waste quartz sand improved by 2-4.5 percent compared to the content in industrial enterprises.

On this basis, the first study of aerated concrete composition using slag and waste quartz, in which the study of the physical and mechanical properties of the blocks when they are combined, is studied in the next chapter.

3. Results and Discussion

Due to the calcium and silicon oxides contained in steel smelting slag and waste quartz sand, chemically active bonds occur in the composition of aerated concrete. This enhances the bonding properties without the need for additional cement. The fine particles of sand also serve to evenly distribute the pores during the expansion process of aerated concrete.

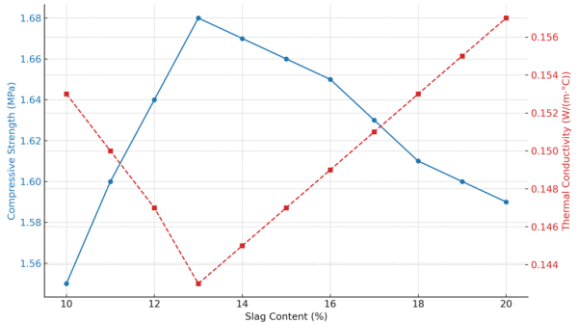

Figure 7. Effect of SMS content on strength and thermal conductivity

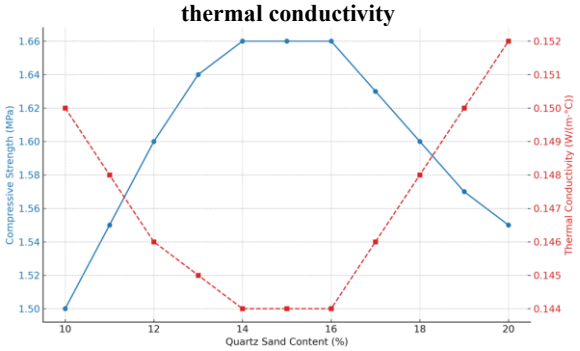

Figure 8. Effect of quartz sand content on aerated concrete properties

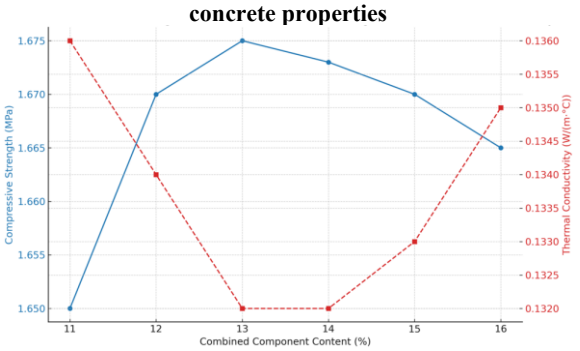

Figure 9. SMS (11–13%) + waste quartz sand (14–16%) when added together

Table 3

Properties of aerated concrete with optimal composition

Components	Stability (MPa)	λ (W/(m·°C))	Density (kg/m³)
Ordinary aerated concrete	1,51	0,147	630–640
Only SMS (12%)	1,68	0,143	670
Quartz sand only (15%)	1,66	0,144	665
SMS + quartz sand	1,675	0,132	670–672

4. Conclusion

The article reviews research on the development of energy-efficient and sustainable building materials suitable for the specific climatic conditions of Uzbekistan. By adding steelmaking slag (SMS) and waste quartz sand to the composition of aerated concrete, its strength, thermal insulation and economic efficiency were increased. Experimental results showed that the strength of aerated concrete blocks made using SMS (12%) and waste sand (15%) is 1.675 MPa, thermal conductivity is 0.132 W/(m

°C), and density is 670-672 kg/m³. These indicators indicate that they have higher quality characteristics compared to traditional aerated concrete.

The study shows that the use of local industrial waste not only reduces the cost of building materials, but also mitigates environmental problems. This approach can be the basis for the introduction of energy-efficient and sustainable technologies in the construction sector of Uzbekistan. In the future, it is necessary to study the long-term performance properties of these materials and introduce their production on a large scale.

References

[1] Lotov A. V., Mitina N. A. Features of technological processes for the production of aerated concrete // Building materials. 2003. No. 1. S. 7-9.

[2] G.A. Zimakova, V.A.Solonina, M.V.Kudomanov, D.S.Bayanov, P.V. Sharko Autoclaved building materials and products: production and application. Tyumen- 2016.

[3] Adilkhodjaev, A., Shaumarov, S., Kadir, U. New structure assessment method cell concrete. International Journal of Advanced Science and Technology 2020, 29(5), p. 1889-1893

[4] Adilhodzhayev A.I., Shipacheva E.V., Shaumarov S.S., Shermuxamedov U.Z., Kandokhorov S.I. Some Aspects of the Photo-Optical Method of Estimation Composition of Light Concrete // International Journal of Engineering and Advanced Technology (IJEAT). ISSN: 2249-8958, Volume-8 Issue-5, June 2019. – pp.1924-1927.

[5] Adilhodzhayev A., Shaumarov S., Shipacheva E., Shermuhamedov U. New method for diagnostic of heat engineering and mechanical properties of cellular concrete // International Journal of Engineering and Advanced Technology (IJEAT) ISSN: 2249 – 8958, Volume-9 Issue-1, October 2019. – pp. 6885-6887.

[6] Adilhodzhayev A. I., Shaumarov S.S., Umarov K.S. New Structure Assessment Method Cell Concrete // International Journal of Advanced Science and Technology Vol. 29, No. 5, 2020, pp. 1889-1893

[7] Adilhodzhaev A.I., Shaumarov S.S., Makhamataliev I.M., Tsoy V.M. Features Of Forming The Structure Of Cement Concrete On Second Crushed Stone From Concrete Scrap // International Journal of Advanced Science and Technology Vol. 29, No. 5, 2020, pp. 1901-1906

[8] Adilhodzhaev A., Shaumarov S., Tsoy V., Khodzhaev S. Research of the influence of silicon-organic hydrophobizer on the basic properties of Cement stone and mortar // International Journal of Advanced Science and Technology Vol. 29, No. 5, 2020, pp. 1918-1921

[9] Патент № 2243189 Способ получения и состав смеси неавтоклавного газобетона [Текст] / Владимирова Е.Б., Красилникова О.Б., Нурумбетов Н.В., Уфимцев В.М. 2003124027 Заявл. 30.07.2003 Опубл. 27.12.2004, Бюл. №3

[10] Паус К.Ф. Ячеистый бетон на основе отходов обогащения железистых кварцитов [Текст] / К.Ф. Паус, И.Е. Иличев, Н.С. Юрина // Строительные материалы. – 2006. – №2. – С. 20 – 21.

[11] Курятников Ю.Ю., Колцова С.А., Земцова Т.С. Влияние карбонатных наполнителей на физико-механические свойства газобетона неавтоклавного твердения [Электронный ресурс] - 2014.

[12] Веретевская Н.Н. Основные технологические параметры и свойства газобетона на основе переработанной сланцевой золы [Текст] / Н.Н. Веретевская, Е.А. Галибина // Строительные матер. - 2001. - № 10.- С.17- 18.

[13] Аминев Г.Г. Малоцементный неавтоклавный ячеистый бетон [Текст] / Г.Г. Аминев // Строительные Материалы.- 2005.- №12.-С 50-51

[14] Волженский А.В. Применение зол и шлаков в производстве строительных материалов [Текст] / А.В. Волженский и др. - М.: Стройиздат, 2004 – 255 с.

[15] Воробев Х.С. Вяжущие материалы для автоклавных изделий [Текст] / Х.С. Воробев.- М: Стройиздат, 2002. – 287 с.

[16] Гладких К.В. Изделия из ячеистых бетонов на основе шлаков и зол [Текст] / К.В. Гладких. – М., Стройиздат, 2006. – 256 с.

[17] ГОСТ 10180-2012 «Бетоны. Методы определения прочности по контролным образцам». М.: Стандартинформ, 2018, 46 с.

Information about the author

Kadirov Bahodir Gayratjon ugli	Tashkent State Transport University "Building and industry facilities Construction Department doctoral student E-mail: bahodirqodirov55@gmail.com Tel.: + 998712990046 https://orcid.org/0009-0006-8828-1645
Shaumarov Said Sanatovich	Tashkent State Transport University "Building and industry facilities Construction Department professor (DSc), E-mail: shaumarovss@mail.ru Tel.: + 998712990026 https://orcid.org/0000-0001-8935-7513
Kandakhorov Sanjar Ishratovich	Tashkent State Transport University "Building and industry facilities Construction Department associate professor (PhD), E-mail: sanjar.kandakharov@mail.ru Tel.: + 998500717191 https://orcid.org/0000-0002-3689-8794

Assessing the risk of public transport in southern cities of Azerbaijan using the "bow tie" method

E.M. Salayev[1][a]
[1]Azerbaijan Technical University, Baku, Azerbaijan

Abstract: Buses are an important component of the urban public transport system, meeting the daily mobility needs of the population. However, various risks arise during the operation of public transport, which can cause serious problems in terms of safety and comfort of passengers. In this study, risk factors of public transport in the southern cities of Azerbaijan were analyzed and a risk assessment was carried out using the "bow tie" method.

Keywords: public transport, risk analysis, risk assessment, risk matrix, BowTie

1. Introduction

Urban public transport systems are complex systems that include social, economic, political, technological and organizational aspects. In order to develop and implement effective ways to improve the system, these elements, as well as the interrelations between the factors that make up the system, must be considered comprehensively and holistically [1,2]. The main risk factors in the field of land transport (freight and passenger transportation) are traditionally poor road conditions, deficiencies in vehicle maintenance and, above all, the human factor, which occurs due to the inattention or negligence of drivers. [3] Part of the research includes preventing or reducing the damage caused by air pollution by reducing the use of private cars, as well as helping to make cities more resilient to large-scale climate events, allowing for a quicker return to normal life.[3] Risks are analyzed quantitatively and qualitatively.

2. Research methodology

One of the methods of risk analysis in the transportation services industry is the "bow tie" method. This method helps to identify the main and most important threats from the point of view of the enterprise and the associated risk management opportunities. The method consists of creating cause and effect analysis tables related to the main types of risks arising in the transportation services industry. BowTie analysis diagrams appeared in 1979 during a lecture on risk analysis at the University of Queensland, Australia. In the early 1990s, the Royal Dutch Shell Group adopted the BowTie method as a corporate standard for risk analysis and management. Shell conducted extensive research into the application of the BowTie method and developed strict rules for identifying all details based on its best practices. After Shell, the BowTie method quickly gained support in the oil and gas industry, since the diagrams helped to visualize control over risk management practices. Over the past decade, the BowTie method has also spread to aviation, shipping, chemical industry and healthcare [4]. Bow-tie was created by combining two existing risk analysis tools. These are the fault tree, which describes the probability that several faults will lead to a single failure, and the event tree, which describes the various consequences that can be predicted as a result of a single event. A relational diagram is built, which gives a visual representation of the relationship between causes (defects or failures) and effects [5]. BowTie method is a risk assessment method that can be used to demonstrate and analyze cause-and-effect relationships in high-risk scenarios. The method gets its name from the shape of the resulting diagram, which resembles a butterfly when created. The risk event is in the center of the bow tie diagram [6]. The article describes the identification of risk factors in public transport vehicles operating in the Southern regions of the Republic of Azerbaijan, as well as measures for their prevention and management. A survey of 420 respondents was conducted regarding the implementation of the Urban Mobility Plan in Masalli,Lenkoran,Bilasuvar and Jalilabad districts. During the analysis, risk factors were identified based on the respondents' opinions, the analysis was carried out using the "bow tie" method.

The "bow tie" method is widely used in risk management for visualization and systematic analysis of cause-and-effect relationships. The advantage of the method is that it allows for a comprehensive risk assessment by combining in one diagram both the initial factors that led to the event (left side) and the consequences that may occur after the event (right side) [7].

A review of the literature shows that the "bow tie" analysis has previously been used in the oil and gas industry, and more recently in healthcare, aviation and public transport, and has demonstrated high efficiency [5,6]. The "bow tie" method also helps to identify protective measures to prevent risk factors and mitigate their consequences, which plays an important role in improving the safety of public transport passengers. As a result of surveys conducted in Masalli and other southern cities, key risk factors such as the technical condition of public transport, driver behavior, road infrastructure, and parking conditions were identified. The bow tie method allowed us to systematically show both the causes and potential consequences of each of these risk factors and propose specific risk management measures [3,8]. Therefore, in this study, the bow tie method was chosen as the main basic tool of the methodology.

Factors Affecting Public Transport Use and Passenger Satisfaction

Understanding the factors that drive the use of existing public transport services is crucial to attract passengers to new public transport services, especially in small and

[a] https://orcid.org/0009-0000-4315-3590

medium-sized cities. User satisfaction plays a decisive role in their decision to use a service or not. Therefore, it is important to identify the key aspects that influence the perception of high service quality, how these aspects affect customer satisfaction, and how these aspects affect a person's willingness to use the service and recommend it to others. Here, data on user satisfaction and dissatisfaction, as well as the factors that influence their decision to use public transport services, are presented.

Chen et al. (2019) found that service hours have a significant impact on overall satisfaction. Service hours cover the time when public transport services are available to users and standard routes are running. [9]

Redman et al. (2013) emphasized the importance of punctuality and frequency of public transport services, stating that punctuality or "punctuality" directly influences customers' perceptions of reliability. This, in turn, influences passenger satisfaction levels with the transport service. Public transport is often perceived as a convenient and comfortable way to travel, so price is an important factor. Lower fares may encourage people to use public transport instead of driving [10]. According to Stewart et al. (2000), travel time or speed is at least as important as frequency. They also found that customer satisfaction is related to users' perceptions of the costs associated with public transport services.[11]

The travel time between an origin and destination reflects the convenience of a service, especially when compared to other modes of transport. The proximity of stops to an origin or destination reflects the accessibility of a service and is considered an important factor in the decision to use public transport.

Eboli and Mazullah (2010) suggested that good communication and route information are critical to the convenience of passengers using public transport.[12,13]

Accessible information and accurate, up-to-date information about routes and travel times can make it easier for people to plan their trips and make informed decisions about which mode of transport to use. In addition, access to real-time information about the location and status of buses can reduce the stress and uncertainty associated with waiting for a bus, leading to an improved experience and higher levels of satisfaction with the service. [14]

Tirinopoulos and Antoniou (2008) found that both distance to stop and waiting time affected overall satisfaction[15]. The ease of switching between different modes of transport allows users to reach their destination quickly and efficiently. The ease of boarding and disembarking from a vehicle affects user comfort and satisfaction [16]. Personal space in a vehicle is directly related to user comfort. If the personal space inside the vehicle is narrow and cramped, it can cause discomfort and anxiety, which can lead to user dissatisfaction. Tirinopoulos and Antoniou (2012) found that crowding was the factor that most deterred respondents from using public transport[15]. De Oña (2013) believed that the temperature inside the vehicle is important for passenger satisfaction [17].

Analysis of the level of public transport use by passengers and the problems arising from it

Increasing the use of public transport is a long-term sustainable solution for urban networks, while reducing the impact of related problems such as urban pollution [18]. The focus should be on customer satisfaction [19] in the divestment process. Most studies carried out internationally show that factors such as quality of services, availability, price and affordability have a wider impact on satisfaction levels[20].

It is important to identify and attract and retain a wide range of users across age groups[21]. There are very few studies of this kind in the field of public transport, so the aim of this study is to identify the main characteristics that influence the satisfaction of users of public transport.

As bus is the most popular and widely used public transport mode in the country, a survey was carried out in several cities and regions of Azerbaijan under the guidelines of the Cabinet of Ministers of the Republic of Azerbaijan for the preparation of the Intra-urban Mobility Plan [22]. The districts covered by the urban mobility plan include Larkaran,Masalli,Bilasuvar and Jalilabad.

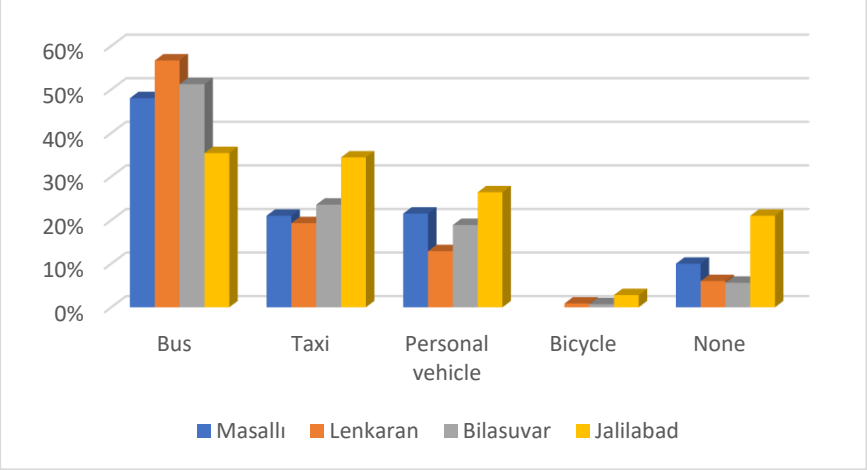

Graph 1. Daily trips on transport used by the population of southern cities of Azerbaijan

The level of motor vehicle use in the southern cities was determined on the basis of the survey carried out. The charts show that the population of southern cities is predominantly dependent on public transport. In Masalli, respondents use buses most often (48 percent) for daily journeys. The proportion of respondents using taxis and private cars for daily journeys is 21.5 percent and 21.8 percent respectively.

56.65 percent of Lankaran's population travel by bus, 12.88 percent by car and 0.86 percent by bicycle.

Respondents using taxi services represent 19.31 percent of the total.

In Bilasuvar, respondents to the survey were most likely to use buses for daily commuting to work (51.21%). 23.56 percent of the respondents use taxis, 18.90 percent use private cars and 0.71 percent use bicycles for their daily commute. In the Jalilabad district, 35.4 percent of respondents use buses, 26.4 percent use personal vehicles, 34.4 percent use taxis, and 2.8 percent use bicycles.

Problems faced by the population when traveling by transport

In surveys in southern cities, the majority of people use personal cars to reach their destinations, in addition to public transport. A survey of the population revealed the most common problems encountered by the population when travelling. The graph below shows the most frequent problems encountered by passengers travelling by car in southern cities (Graph 3).

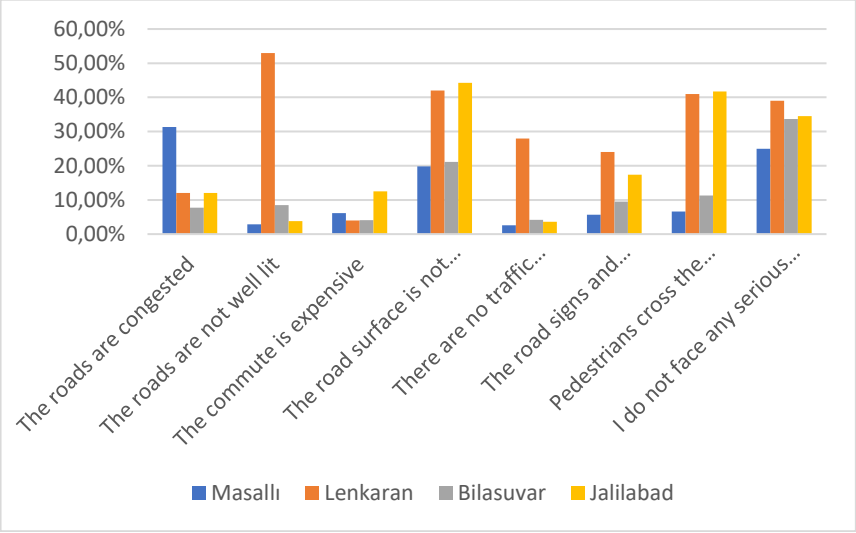

Graph 3. Problems faced by the population when traveling by transport in the southern cities of Azerbaijan

Problems encountered when travelling by car in southern cities vary from one extreme to another. The main problems in Masalli are traffic congestion (31.37%), poor road conditions (19.81%) and not following the rules (6.60%). In the Lankaran, the main complaint was poor road lighting (53%), 42 percent of respondents complained about the state of road surface and 41 percent complained about irregular pedestrian traffic. Bilasuvar's main problems are poor road conditions (21.09%), other problems include illegal pedestrian crossings (11.27%) and the lack of road signs (9.56%). In Jalilabad, the main concerns are poor road conditions (44.25%), irregular pedestrian crossings (41.69%) and the lack of road signs (17.39%). Overall, the main problems faced by the transport system in the Southern cities of Azerbaijan are the road infrastructure and the lack of pedestrian protection.

Evaluation of existing bus routes on a 5-point scale

It is important to consider different factors when assessing bus safety in the risk matrix. These factors include factors such as the technical state of buses, the professional competence of drivers, road conditions, passenger behaviour and the presence of security measures. This risk assessment plays an important role in the development of safety programmes for public transport authorities [23]. The results of the assessment of the most frequently selected issues by survey respondents on the reliability indicators of bus lines in southern cities on a five-point scale are shown in the graphs below.

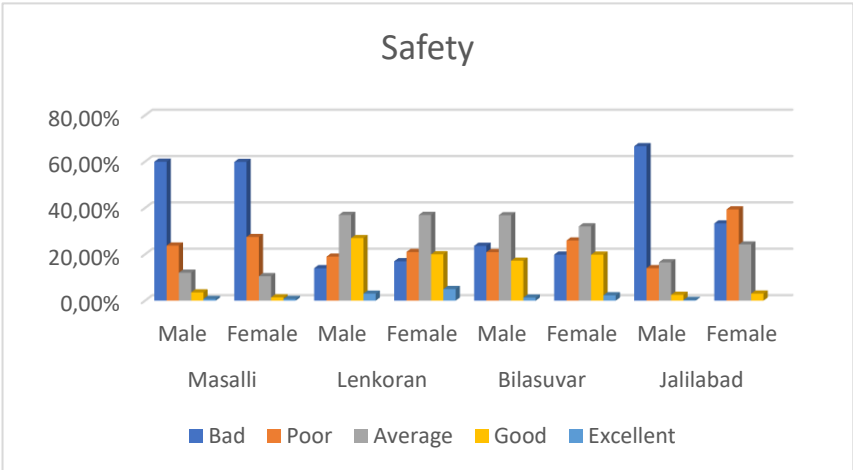

Graph 4. Assessment of bus safety on a 5-point scale

https://doi.org/10.56143/3030-3893-2025-1-83-89 A bridge between science and innovation

Respondents rated the safety and comfort levels of buses in southern cities in different ways. In Masalli, 22.88 percent of respondents rated bus safety as good or very good, while 4.93 percent of female rated bus safety as good (3 point) or very good (4point). In Lenkaran, 37 percent of male respondents and 20 percent of female rating the buses as good and 5 percent as very good. In Bilasuvar, 40.05 percent of respondents rated bus safety as average, 32.06 as good and 2.29 as excellent. In Jalilabad, 29.74 percent of respondents rated bus safety as good (3 points), 36.92 percent of female respondents rated it as good, and 1 point of respondents rated it as poor.

Overall, although most respondents rated bus safety as average, attitudes of women about buses differ from city to city. While female respondents in Masalli and Lankaran rated bus safety relatively low, opinions differed in Bilasuvar and Jalilabad.

A study by Xuan Long Nguyen et al. (2023) investigated the impact of bus service quality factors on passenger satisfaction in Ho Chi Minh City. A total of 3,913 samples were collected from 25 bus routes in Ho Chi Minh City in 2019–2020. The impact of different service aspects on passenger satisfaction was analyzed using the SEM model. 64.9% of passengers were satisfied with the bus service, but respondents wanted the bus schedule to be optimized, information systems to be improved, and drivers and dispatchers to be trained.[24]

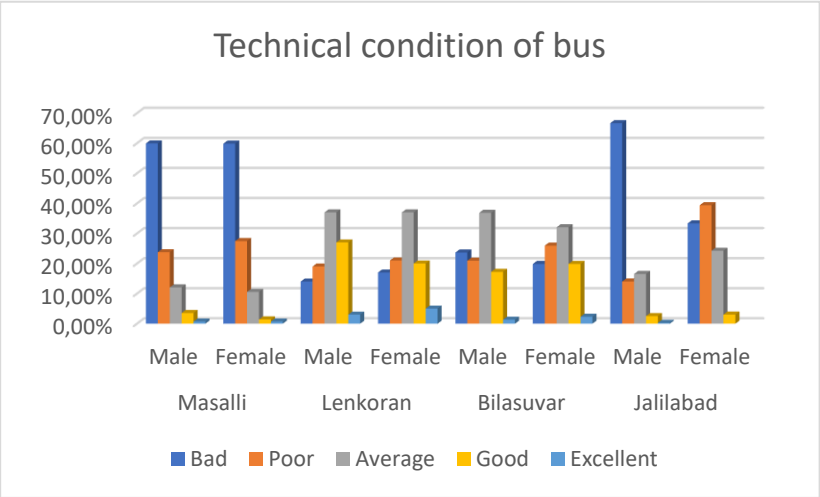

Graph 5. Assessment of the technical condition of bus routes on a 5-point scale

Respondents generally rated the technical state of the buses in southern cities as poor. In the Masalli survey, 59.91 percent of respondents considered the technical state of the buses to be poor (1 point), 25.8 percent as satisfactory, 11.56 percent as average and only 0.71 percent as very good. In the case of Lenkaran, 37 percent rated the technical state as average (3 points), 24 percent as good (4 points), 20 percent as satisfactory and 15 percent as poor.

In Bilasuvar, 35.36 percent of the respondents rated the technical state of the roads as average, 18.03 percent as good, 22.48 percent as satisfactory and 1 point each as poor. In Jalilabad, the situation is even more critical - 63.85 percent consider bus technical conditions to be poor, 16.15 percent satisfactory, 17.18 percent average and only 0.26 percent very good.

The technical state of the buses in Jalilabad and Masalli is generally considered to be low, while the situation in Bilasuvar and Lankaran is considered to be relatively satisfactory.

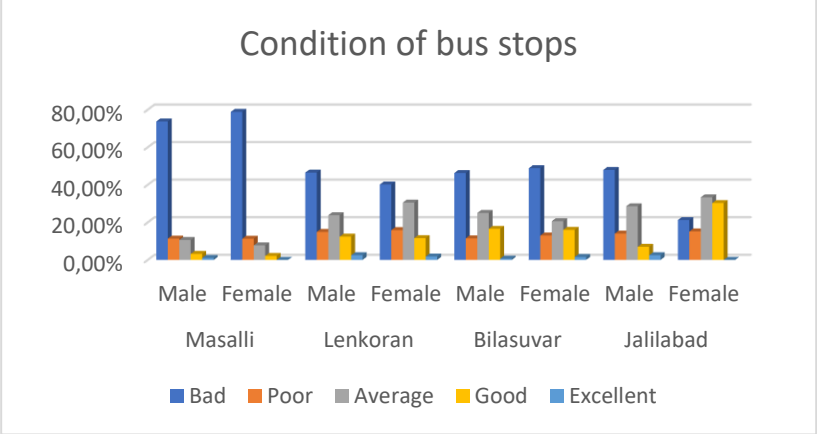

Graph 6. Assessment of the condition of bus stops on a 5-point scale

The current status of bus stops in southern cities of Azerbaijan was generally rated negatively by respondents. In Masalli, 3.19 percent of mate respondents rated the parking lots as good, 10.64 percent as average, and 78.87 percent of female respondents rated the parking lots as poor. In Lenkaran, 8.7 percent consider bus stop conditions good, 15.2 percent average, and 40 percent of female respondends consider bus stop conditions poor. Although the condition of the Bilasuvar parking lot appears to be somewhat improved, the overall assessment was negative. 16.55 percent of male respondents rated it as good, 25 percent as average and 46.28 percent as bad. 48.85 percent of women classified the interrogation as traumatic. In Jalilabad, 7 percent of male respondents considered parking to be good, 28.57 percent to be bad, and 47.9 percent to be poor. 21.21 percent of women are unhappy with the state of the bus stops.

Overall, the condition of bus stops in all cities was assessed as poor, with the vast majority of female respondents being particularly dissatisfied with the stops

Analysis of the technical condition of buses using the "bow-tie" method. The following risk factors have been identified and evaluated as a result of the research and monitoring carried out in the southern cities.

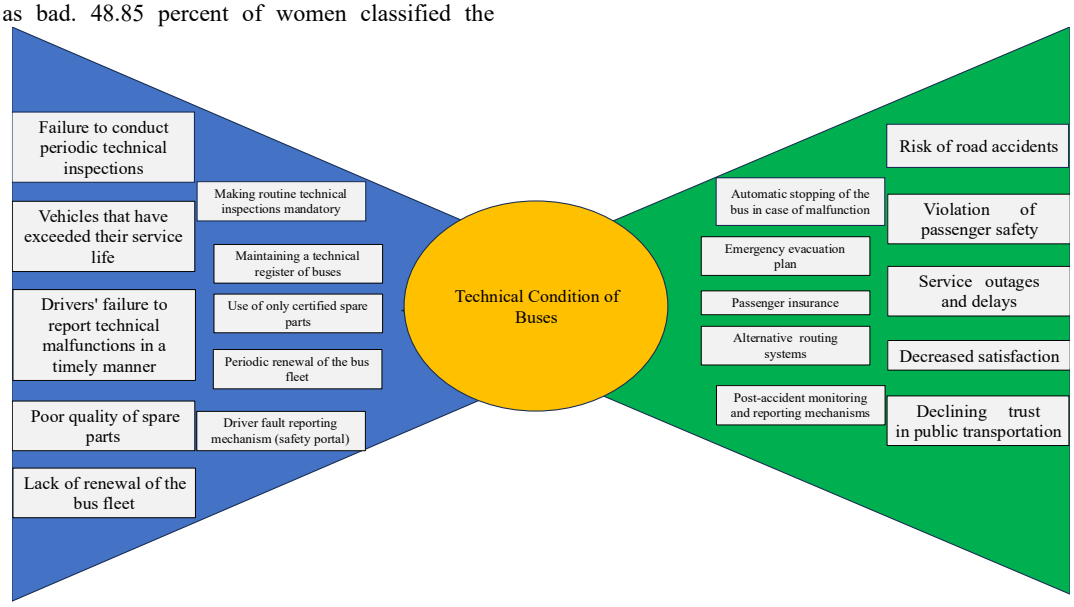

Figure 1. Assessment of the technical condition of buses using the "bow tie" method

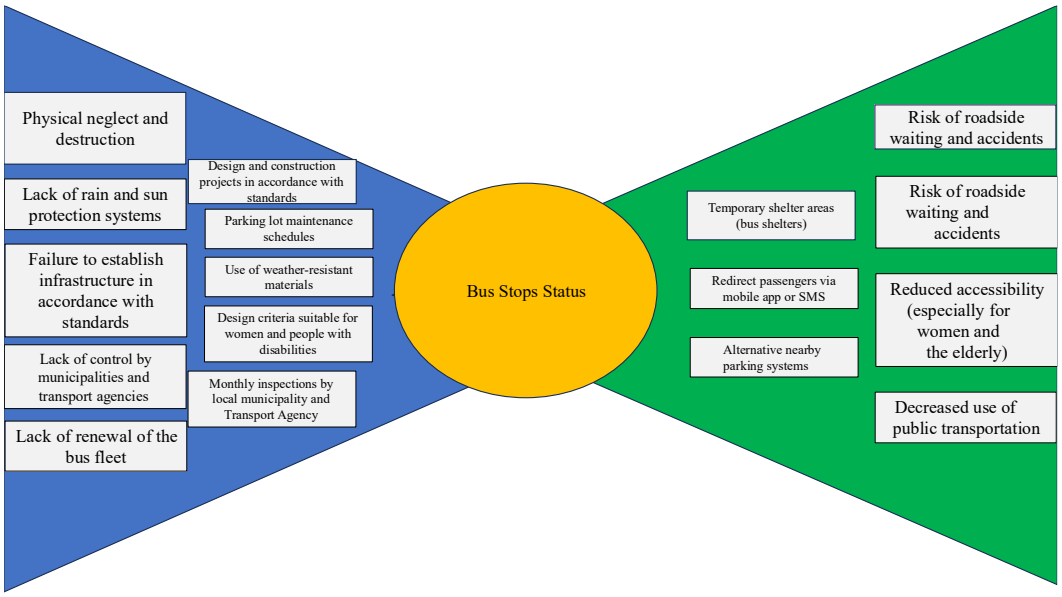

Figure 2. Assessing the condition of bus stops using the bow tie method

https://doi.org/10.56143/3030-3893-2025-1-83-89 A bridge between science and innovation

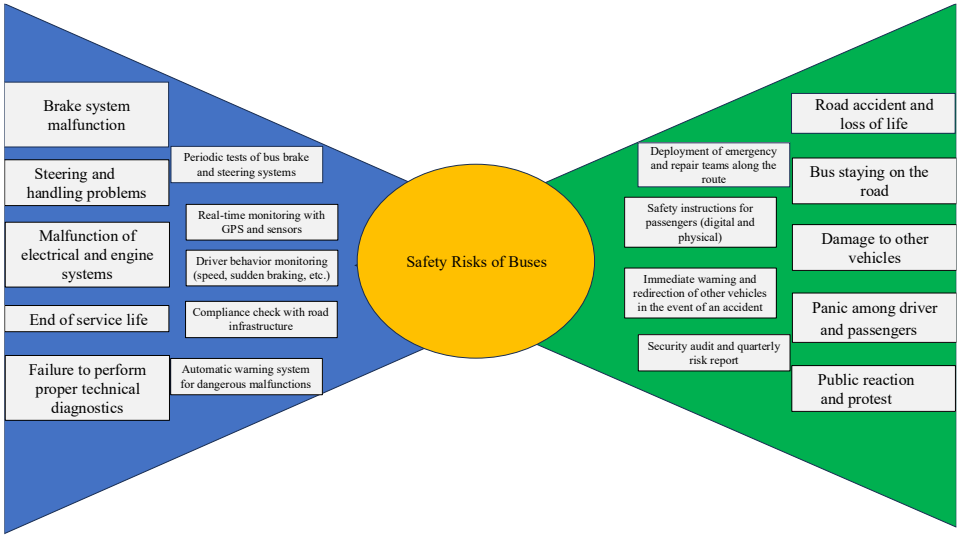

Figure 3. Bus safety assessment using the bow tie method

To eliminate the above risk factors, control measures, preventive causes, and mitigating measures to reduce consequences are proposed.

3. Discussion

The results of the study showed that technical faults of buses and poor condition of bus stops prevail among the main risk factors affecting the level of public transport safety in the southern cities. The level of technical risk in Masalli and Jalilabad districts was assessed as very high (risk score 25), which indicates that buses pose a serious threat to passenger safety during operation. In Bilasuvar and Lankaran districts, technical risks were observed at medium and low levels.

Risk analysis conducted at bus stops yielded similar results. The poor condition of bus stops, especially in Masalli and Jalilabad, negatively affects the comfort and safety of passengers. Risk levels (P×S) are in the high risk zone in these cities. The bow tie analysis identified the key measures to prevent threats as:

- Regular technical inspection of buses,
- Monitoring and training driver behaviour,
- Upgrading bus stops and using weather-resistant materials,
- Including improving urban mobility plans to suit local conditions.

The obtained results are consistent with international studies [25]. In addition, some differences were also found; for example, higher levels of complaints about traffic violations by pedestrians in the regions (lack of pedestrian crossings, road safety issues) are observed in Azerbaijan more often than in other countries.

Among the limitations of the study:

- Based on subjective assessments of respondents,
- Not taking into account the results of real technical inspections,
- It can be noted that modeling methods are not used.

It is recommended that future studies include realistic technical indicators, expand risk models using traffic modeling programs such as PTV, and conduct regional comparisons.

4. Conclusion

The study shows that the current problems of public transport in southern cities are mainly related to the technical condition of buses, the condition of bus stops and safety on buses. Using the bow tie method, these problems were systematically assessed and preventive and corrective measures were proposed to solve them.

These measures include regular technical inspections, periodic renewal of the bus fleet, the introduction of a mechanism to warn drivers about faults (safety portal), the use of weather-resistant materials at bus stops, monthly inspections by the local municipality and the Transport Agency, and periodic testing of the braking systems and steering of buses. The implementation of the proposed measures will not only improve the safety of urban transport, but also create more comfortable and accessible conditions for passengers.

Further research should focus on measuring the effectiveness of these measures, conducting additional statistical analyses and conducting a more in-depth assessment of intra-city transport flows. For the sustainable development of public transport, both infrastructure and transport policies need to be strategically formulated.

References

[1] Matthiass M. Generic Guidelines for Conducting Risk Assessment in Public Transport Networks. COUNTERACT. March, 2009

[2] Новикова, И. И. Управление рисками в деятельности высших учебных заведений Российской Федерации. Москва, 2008. 24 с

[3] David José Oliveira da Silva, Marcelo Hazin Alencar Bow Tie Analysis (BTA) in a Public Transport Sector During the Covid-19 Pandemic: A Case Study

[4] Julian Talbot. Risk BowTie Method. https://www.juliantalbot.com/post/risk-bow-tie-method

[5] Раимов А.И., Николаева Н.Г., Сопин В.Ф. Метод «галстук-бабочка» и его применение при оценке рисков. Компетентность / Competency (Russia). — 2020. — № 3. Doi: 10.24411/1993-8780-2020-10308

[6] Charles Cowley. Bow Ties in Risk Management. CCPS Staff Consultant, London. Energy Institute. pp 3-5

[7] Cox, L. A. (2008). What's Wrong with Risk Matrices? Risk Analysis, 28(2), 497–512. https://doi.org/10.1111/j.1539-6924.2008.01030.x

[8] Veli Deniz. Papyon analizi (Bow-tie Analysis) II. Uluslararası Proses Güvenliği Sempozyumu. 22-24 Ekim. 2015. İstanbul

[9] Chen, M. H., Hsu, C. Y., & Chen, M. H. (2019). How Transportation Service Quality DrivesPublic Attitude and Image of a Sustainable City: Satisfaction as A Mediator andInvolvement as A Moderator. Sustainability, 11(23), 6813.https://doi.org/10.3390/su11236813

[10] Lauren Redman a , Margareta Friman b,n, Tommy G ¨arling b,c , Terry Hartig, Quality attributes of public transport that attract car users: A research review, Transport Policy 25 (2013) 119–127, 20 December 2012

[11] Stewart, K.R., Mednick, M., Bockman, J., 2000. A structural Equation model of consumer satisfaction for the New York City subway system. Transp. Res. Rec. 1735, 133–137. https://doi.org/10.3141/1735-16

[12] Eboli, L., Mazzulla, G., 2007. Service Quality Attributes Affecting Customer Satisfaction for Bus Transit. J. Public Transp. 10, 21–34. https://doi.org/10.5038/2375-0901.10.3.2,24 24

[13] Eboli, L. and Mazzulla, G. (2008) 'A stated preference experiment for measuring service quality inpublic transport', Transportation Planning and Technology, 31(5), pp. 509–523. doi:10.1080/03081060802364471

[14] Krizek, K., & El-Geneidy, A. (2007). Segmenting Preferences and Habits of Transit Users andNon-Users. Journal of Public Transportation, 10(3), 71–94. https://doi.org/10.5038/2375-0901.10.3.5

[15] Tyrinopoulos, Y., & Antoniou, C. (2008). Public transit user satisfaction: Variability and policyimplications. Transport Policy, 15(4), 260–272.https://doi.org/10.1016/j.tranpol.2008.06.002

[16] Carreira, R. P., Patrício, L., Jorge, R. N., & Magee, C. L. (2014). Understanding the travelexperience and its impact on attitudes, emotions and loyalty towards the transportationprovider–A quantitative study with mid-distance bus trips. Transport Policy, 31, 35–46.https://doi.org/10.1016/j.tranpol.2013.11.006

[17] De Oña, J., De Oña, R., Eboli, L., & Mazzulla, G. (2013). Perceived service quality in bus transitservice: A structural equation approach. Transport Policy, 29, 219–226.https://doi.org/10.1016/j.tranpol.2013.07.001

[18] Wickham, J. Public transport systems : The sinews of european urban citithenship, Employment Research Centre, Department of Sociology, Trinity College Dublin, Dublin 2, Ireland (2004)

[19] Lam, S. Y. et al. (2004) 'Customer value, satisfaction, loyalty, and switching costs: An illustration froma business-to-business service context', Journal of the academy of marketing science. SagePublications, 32(3), pp. 293–311

[20] Eboli, L., & Mazzulla, G. (2010). How to Capture the Passengers' Point of View on a TransitService through Rating and Choice Options. Transport Reviews, 30(4), 435–450.https://doi.org/10.1080/01441640903068441

[21] Akiyama, T. and Okushıma, M. (2009) 'Analysis of Railway User Travel Behaviour Patterns ofDifferent Age Groups', IATSS Research. International Association of Traffic and Safety Sciences,33(1), pp. 6–17. doi: 10.1016/S0386-1112(14)60232-6

[22] https://nk.gov.az/az/senedler/qerarlar/%E2%80%9Csahardaxili-harakat-(mobillik)-planinin-hazirlanmasi-qaydasi%E2%80%9Dnin-tasdiq-edilmasi-haqqinda-5907

[23] Federal Transit Administration, Sample Safety Risk Assessment Matrices for Bus Transit Agencies, september 2019

[24] Nguyen, X. L., Quach, B. K., Pham, C. T., Nguyen, T. T., & Tran, T. T. L. Analysis of service quality factors affecting passenger satisfaction with bus service based on a structural equation modeling: A case study of Ho Chi Minh City. IOP Conference Series: Materials Science and Engineering, 1289, 012056. https://doi.org/10.1088/1757-899X/1289/1/012056:contentReference[oaicite:1]{index=1}.) (2023)

[25] Redman, L., Friman, M., Gärling, T., & Hartig, T. (2013). Quality attributes of public transport that attract car users: A research review. Transport Policy, 25, 119–127. https://doi.org/10.1016/j.tranpol.2012.11.005.

Information about the author

Elmaddin Mubarrad oglu Salayev

Azerbaijan Technical University
Department of "Transport logistics and traffic safety"
e-mail: elmeddin.salaye@aztu.edu.az , elmeddin.salayev@gmail.com
Tel: +99455-568-37-63
https://orcid.org/0009-0000-4315-3590

Evaluation effectiveness of solutions to improve mobility in cities

T. Verdiev[1][a]
[1]Azerbaijan Technical University, Baku, Azerbaijan

Abstract: The article proposes a methodology for developing efficiency conditions when developing some solutions related to increasing urban mobility. An example of the conditions for applying and testing the coordinated regulation method used to ensure uninterrupted traffic on main streets, taking into account possible delays in traffic flows on intersecting streets, is given. The procedure for determining the maximum values of the flow and intensity of bus traffic is given in order to maintain the speed of traffic flows within a certain limit when organizing dedicated bus lanes. Simulation experiments were used to test the efficiency of creating bus lanes and a green wave based on the proposed methodology. Micromodels were created using the PTV VISSIM program.

Keywords: mobility, urban transport, bus lane, coordinated regulation, delay

1. Introduction

Ensuring the quality of life of the city population largely depends on the functioning of the urban transport infrastructure. The main tasks facing transport organizations are to ensure the implementation of trips for various purposes in a short time and with the appropriate convenience. Of course, pedestrian and bicycle paths that promote a healthy lifestyle are important, and their development requires a favorable infrastructure. It is necessary to ensure the interconnection of public transport and take organizational measures to reduce the time lost in traffic flows. However, solutions to ensure mobility require a comprehensive implementation of all provided measures. As indicators of the quality of mobility in cities, the population primarily perceives travel time, comfort and traffic safety [1]. Reducing and minimizing time losses in traffic flows are the main goals of improving mobility in cities. Therefore, it is necessary to develop measures aimed at studying and reducing the time lost by road users. When analyzing mobility models of European cities, the following solutions are proposed to ensure sustainable and environmentally friendly urban mobility [2]:

- increase in the number and coordination of bicycle paths;
- development of public transport systems;
- expansion of bicycle and pedestrian paths;
- creation of bicycle sharing systems;
- improvement of connections between the city center and its outskirts by means of bus, tram and metro lines;
- promotion of the use of alternative modes of transport;
- restriction of car access to the central parts of the city;
- increase of pedestrian zones;

Kijewska et al., analyzing mobility problems in the cities of Belo Horizonte, Brazil, and Szczecin, Poland, propose organizing activities in the following three directions [3]:

- increasing and improving the accessibility of public transport;
- more efficient organization of freight transportation within the city;
- organization of transportation in accordance with the mobility of residents.

Papadakis and his co-authors studied the practices implemented in various cities in order to ensure mobility in cities. The authors noted that it is important to implement strategies to improve public transport, reduce the use of private cars and create more pedestrian and bicycle paths to increase mobility in cities [4].

Literature review. One of the most common measures to reduce vehicle travel time in cities is the "green wave" regime, which involves coordinating traffic light modes on city streets, as well as creating special bus lanes to reduce passenger travel time. In many cases, these solutions can cause certain side effects. For example, the introduction of a "green wave" leads to an increase in delay time due to the expansion of the prohibiting signal on intersecting streets. The creation of bus lanes reduces the area intended for vehicle movement, which leads to additional delays in traffic flows.

There are various approaches to studying traffic delays. In his study on the analysis of traffic delays at signalized intersections, Abdurakhmanov proposed optimizing the traffic light modes at signalized intersections to reduce traffic flow delays [5].

Li and his co-authors studied the impact of congestion on traffic flow during vehicle deceleration on a two-lane street and road network. The authors proposed a new model that takes into account congestion during braking. The proposed model provides a more realistic description of the traffic flow by taking into account the difference between the current vehicle density and the density that occurs during deceleration [6].

Bashar et al. analyzed the traffic delay times on the Phulbarigate–Daulatpur Highway in Bangladesh and investigated the causes of delays during and off-peak hours. They found that vehicles traveling at low speeds (e.g., 10 km/h) increase the overall deceleration and reduce the road capacity [7].

To reduce traffic delays, Royko et al. tested the effectiveness of coordinated traffic signal control using the PTV Vissim simulation program. The authors showed that coordinated control organized on the considered street ensures smooth movement of vehicles at successive intersections, significantly reducing the overall delay time [8].

Dhinakaran estimated the traffic delay times at controlled intersections in Tamil Nadu, India, using the Webster and Highway Capacity Manual (HCM) models. The

[a] https://orcid.org/0000-0002-9520-5038

author found that the Webster and HCM models are ineffective for mixed traffic flows. A new approach to delay estimation for mixed traffic flows is presented [9].

2. Research methodology

The paper proposes to compare the proposed solutions for improving mobility with the existing or previously used option in terms of total time costs. A mathematical model for estimating the total time costs is proposed when applying coordinated regulation on a main street and when creating a bus line.

In real conditions, it is necessary to estimate the total time losses on intersecting streets and compare options depending on the duration of the prohibiting signal and the intensity of the traffic flow. The total delay time of all vehicles on main and intersecting streets on a street with a coordinated arrangement can be determined using traditional analytical methods. However, it is more appropriate to obtain results that are more consistent with real conditions using a simulation model based on data taken from a real street and road network. The experience of using the PTV VISSIM modeling program for studying, modeling and testing traffic flows is widespread [10,11,12,13]. Figure 1 shows a test image of the simulation model of coordinated traffic control on Bakikhanov Street, one of the main streets of Baku, created using the PTV VISSIM program. Traffic light rules have been introduced at 7 intersections of the street.

Figure 1. Example of 3D tests of the simulation model of traffic flow at intersections of Bakikhanov Street

As can be seen from Figure 1, serious queues arise on almost all streets intersecting with the main street. The scheme of the "green wave" mode in one direction on the main street, created using PTV VISSIM, is shown in Figure 2.

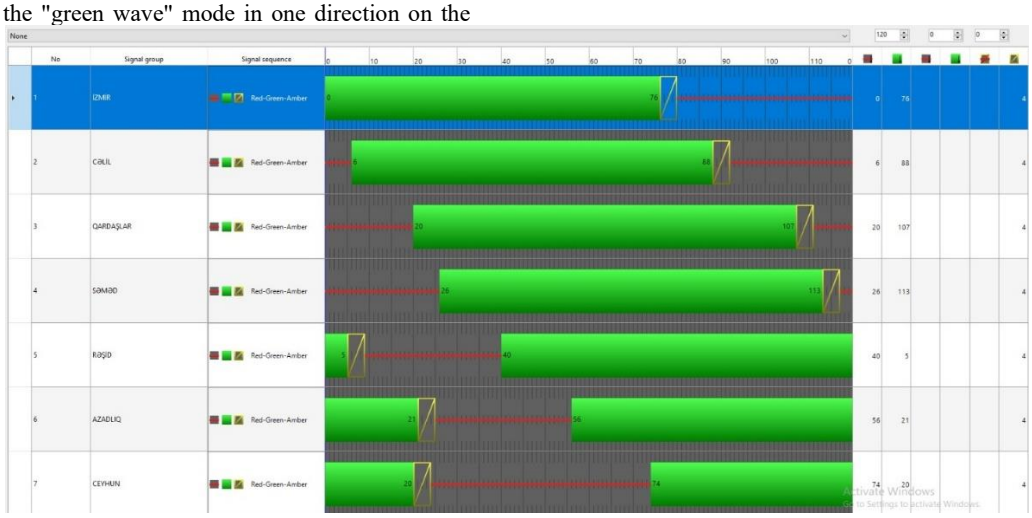

Figure 2. Coordinated control schedule in the PTV VISSIM

After the implementation of coordinated regulation on the main (trunk) street, the cost of traffic delays on intersecting streets changes. If this change is in the direction of increase, and the value of traffic intensity in the directions on intersecting streets is large, then the total amount of lost time may be greater than before. Therefore, the total values of delay time on main (trunk) and intersecting streets must satisfy the following condition:

$$\sum d_{agv} < \sum d_{bgv} \qquad (1)$$

Where $\sum d_{bgv}$ and $\sum d_{agv}$ - are the total delay times of all vehicles on the main and intersecting streets before and after the application of the agreed regulation, respectively.

$$\sum d_{agv} = \sum_j^m \sum_{i=1}^n N_{vi} d_{ibgv}$$

$$\sum d_{agv} = \sum_j^m \sum_{i=1}^n N_{vi} d_{iagv}; \qquad (2)$$

Where d_{ibgv},d_{iagv} - the time of vehicle delays at the stop line i before and after the application of the corresponding coordinated regulation; N_{vi} - number of vehicles in the direction i.

As a result of the application of isolated and coordinated control on the street under consideration, using simulation tests, the total amount of traffic delays on the main and intersecting streets was 139 and 149.6 hours, respectively. It follows that the cost of total time loss increased with the

introduction of coordinated control as a result of the increase in delay time on intersecting streets.

When creating special lanes for public transport, the time lost by vehicles in the general traffic flow increases. This increase takes on different values depending on the number of traffic lanes [14]. Figure 3 schematically shows the situation after the introduction of a special traffic lane on a street with a three-lane roadway.

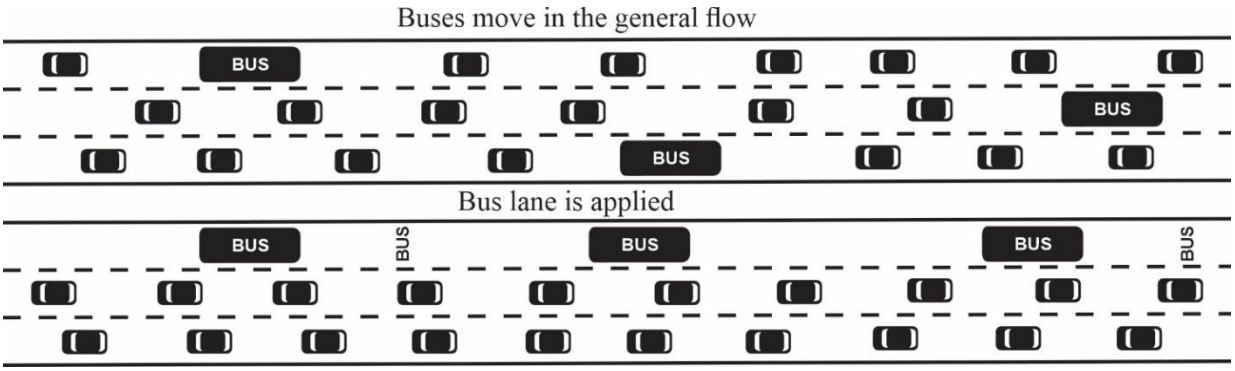

Figure 3. Changes in traffic scheme after the introduction of bus lanes

The efficiency condition for bus lanes, based on the time lost in creating bus lanes, can be expressed as follows:

$$\sum t_{losaf} < \sum t_{losbef} \quad (3)$$

Where $\sum t_{losaf}$ and $\sum t_{losbef}$- are the total time lost by road users before and after the creation of the bus lane, respectively.

$$\sum t_{losbef} = \overline{t_{jgf-bef}}\left(n_{bef} + \sum_{r=1}^{m} q_r \gamma_{rj}\right) \quad (4)$$

$$\sum t_{losaf} = \left(n_{af}\overline{t_{jgf-af}} + \overline{t_{busj}} \sum_{r=1}^{m} q_r \gamma_{rj}\right) \quad (5)$$

Where $\overline{t_{jgf-bef}}; \overline{t_{jgf-af}}$- the travel time of vehicles on the general flow through the section j in question before and after the creating bus lane respectively; $n_{bef}; n_{af}$ - the number of vehicles traveling in the general flow through the section j in case before and after the creating bus lane respectively; $\overline{t_{busj}}$- travel time of buses through the section j; γ_{rj}- capacity factor of bus r in the section j.

Measurements on the street under consideration show that increasing the delay time on narrow streets does not reduce the overall time losses, but on the contrary increases them. In tests conducted on a street section 800 meters long (with a traffic flow intensity of 2200 NV/h and an hourly bus frequency of 160 buses/h), the time it takes to travel the road section was determined based on the values determined by live observation in real street conditions. The maximum speed was taken to be 50 km/h in accordance with local traffic organization conditions. A comparison of the values obtained before and after the introduction of the bus lane using a micromodel created in PTV VISSIM shows that the time spent per traveler decreases on 2-, 3- and 4-lane roads (from 114 seconds to 82 seconds, from 79 seconds to 71 seconds and from 73 seconds to 67 seconds, respectively) [15].

If it is necessary to maintain the speed of the traffic flow at a certain level (for example, to prevent violation of the "green wave" mode), it is necessary to check the efficiency of the implementation of the dedicated bus lane, based on the condition of maintaining this speed limit. As an example, we will create a regression equation showing the dependence of the speed on the intensity of the traffic flow before and after the introduction of the bus lane, using the indicators obtained as a result of simulation experiments on a three-lane road. The permitted speed on the street is 50 km / h. The effect of the intensity of the traffic flow and the frequency of bus arrivals changes according to the following expression when buses move in the general flow:

$$V = 62.9 - 0.0015N_{veh} + 0.067N_{bus}, R^2 = 82{,}13 \quad (5)$$

Where N_{veh}- is vehicle traffic intensity, veh/h; N_{bus} - is bus ariiving frequency, bus/h.

When buses move along a dedicated lane, the speed of the general flow will not depend on the frequency of buses, since the flow is isolated from buses. However, the number of traffic lanes will be reduced by one lane. In this case, the speed of movement in the mixed flow changes according to the following expression depending on the traffic intensity:

$$V = 60.1 - 0.0083N_{veh}, R^2 = 95{,}74 \quad (6)$$

Using the obtained dependencies, it is possible to check the efficiency of introducing a dedicated bus lane, subject to maintaining the speed limit, based on the traffic intensity and frequency of bus arrivals.

3. Conclusion

It is necessary to evaluate in advance the consequences of the proposed measures to improve population mobility. There are various analytical methods for assessing the time of delays associated with the organization of road traffic in cities. However, it is possible to conduct an assessment in a shorter time and more accurately using simulation models of traffic organization based on real values (intensity, density, speed, etc.) taken from the street and road network.

Coordinated regulation aimed at ensuring the smooth movement of traffic flows on city streets can lead to an increase in the overall time losses on neighboring streets. Although the introduction of bus lanes reduces the time spent by buses on the route, it can lead to an increase in delays for vehicles moving along this street. Therefore, these solutions should be considered appropriate only if the overall time losses, when implemented, are less than the previous options for organizing traffic. Thus, the proposed approach will allow us to preliminarily determine the effectiveness of the measures under consideration.

References

[1] Dashdamirov, F., Javadli, U., Verdiyev, T. (2022) Comparative analysis of the weight and quality of urban bus transport services: a case study of Baku. Scientific Journal of Silesian University of Technology. Series Transport. 116,

p.99-111. ISSN: 0209-3324. DOI: https://doi.org/10.20858/sjsutst.2022.116.6.

[2] Abdullahi, U., Adnan, A. (2024). Sustainable Urban mobility: Lessons from European Cities. Global Journal of Engineering and Technology Advances. 21. p.157-170. 10.30574/gjeta.2024.21.2.0210.

[3] Kijewska, K., França, J.G.B., de Oliveira, L.K., Iwan, S. (2022). Evaluation of Urban Mobility Problems and Freight Solutions from Residents' Perspectives: A Comparison of Belo Horizonte (Brazil) and Szczecin (Poland). Energies, 15(3), 710. https://doi.org/10.3390/en15030710

[4] Papadakis, D.M., Savvides, A., Michael, A., Michopoulos, A. (2024). Advancing sustainable urban mobility: insights from best practices and case studies, Fuel Communications, Volume 20, 100125, ISSN 2666-0520, https://doi.org/10.1016/j.jfueco.2024.100125.

[5] Abdurakhmanov R., (2022). Determination of traffic congestion and delay of traffic flow at controlled intersections. The American Journal of Engineering and Technology, 4(10), p. 4-11. https://doi.org/10.37547/tajet/Volume04Issue10-02

[6] Li, X., Jin, C., Peng, G. (2023). The impact of the density delay on the traffic evolution process in lattice hydrodynamic model under lane change on two lanes. Europhysics Letters. 141. 10.1209/0295-5075/acb380

[7] Bashar, T.M.J., Hossain, M.S., Istiaque, S. (2020). Finding the Reasons for the Delay Time in a Highway by Analyzing the Travel Time, Delay Time and Traffic Flow Data. Journal of Engineering Advancements, 1(03), p.76-84. https://doi.org/10.38032/jea.2020.03.002

[8] Royko, Y. Yevchuk, Y., Bura, R. (2021). Minimization of traffic delay in traffic flows with coordinated control. Transport technologies. 2021. 30-41. 10.23939/tt2021.02.030.

[9] Dhinakaran, G. (2013). Estimation of delay at signalized intersections for mixed traffic conditions of a developing country. International Journal of Civil Engineering.

[10] Yue, R., Yang, G., Zheng, Y. (2022). Effects of traffic signal coordination on the safety performance of urban arterials. Comput.Urban Sci. 2, 3. https://doi.org/10.1007/s43762-021-00029-4

[11] Suthanaya, P.A., Putra, R. (2023). Traffic Signal Coordination Based on Vissim Software (Case Study of Sudirman Road in Denpasar City, Indonesia). E3S Web of Conferences 445, https://doi.org/10.1051/e3sconf/202344501004

[12] Khakimov ,B., Tanaka, Sh. (2024). Evaluation of the impact of exclusive bus lanes on traffic in Tashkent,Asian Transport Studies, Volume 10, 100151, ISSN 2185-5560, https://doi.org/10.1016/j.eastsj.2024.100151.

[13] Szarata, M., Olszewski, P. (2019). Traffic modelling with dynamic bus lane. 6th International Conference on Models and Technologies for Intelligent Transportation Systems (MT-ITS), Cracow, Poland, 2019, p.1-8, doi: 10.1109/MTITS.2019.8883325.

[14] Dashdamirov, F., Abdurrazzokov, U., Ziyaev, K., Verdiyev, T., Javadli, U. (2023). Simulation testing of traffic flow delays in bus stop zone // V International Scientific Conference "Construction Mechanics, Hydraulics and Water Resources Engineering, CONMECHYDRO, - E3S Web of Conferences, -, 401, p.1-10

[15] Verdiyev, T., Dashdamirov, F. (2024). Study of the impact of bus lanes using on the road users loss time. Scientific and Technical Journal on "Engineering Mechanics", Issue 18, Vol. 10, No. 4.

Information about the author

Turan Verdiyev
Azerbaijan Technical University. Institute of Logistics and Transport, Senior Researcher
Email: turan.verdiyev98@gmail.com
Tel.: +994507628062
https://orcid.org/0000-0002-9520-5038

Analysis of the condition of track superstructure elements using the finite element method in the ABAQUS software package

S.T. Djabbarov[1][a], N.B. Kodirov[1][b]
[1]Tashkent state transport university, Tashkent, Uzbekistan

Abstract: The aim of this work was a comprehensive study of the process of modeling the elements of the track superstructure using modern three-dimensional finite element methods. Given the high degree of complexity and versatility of the problem, a detailed model of the railway track was developed and implemented during the study, which allowed for a deeper understanding of the behavior of its elements under the influence of various operational loads. The modeling included both static and dynamic analyses, which made it possible to assess the influence of various factors on the strength and durability of the structure.

Keywords: Model, stress, von Mises, wheel, rail, modeling, finite element track superstructure, ABAQUS

1. Introduction

The use of finite element modeling (FE) allows to significantly reduce both financial and time costs, while effectively achieving the set goals. This method allows to quickly identify the maximum values of strength, stresses and displacements in the railway track structure, which, in turn, helps to focus attention on the most vulnerable sections of the infrastructure.

Table 1

Technical characteristics of the track superstructure

Elements of the railway superstructure	Density (kg/m2)	Young's modulus (E)	Poisson's ratio (υ)
Rail (steel)	7850	210 GPa	0.3
Sleeper (reinforced concrete)	1200	80 GPa	0.3

2. Research methodology

Statement of the problem

The calculations modeled the contact interaction between the wheel and the rail. The parameters of the contact interaction depend on the adopted configuration of the wheel and rail profile, as well as their nominal dimensions. During movement, the wheel and the rail can occupy various mutual positions, which are shown in Fig. 1.

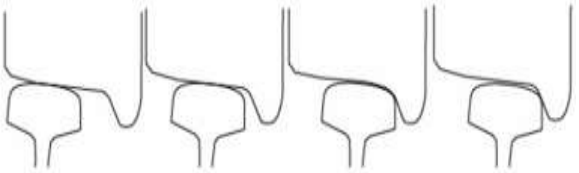

Fig. 1. Location of wheel and rail contact zones

The model of interaction between the wheel and the rail in the wheel-track system, adopted for modeling the process of the impact of dynamic load [1-2] on this system, is presented in Fig. 2.

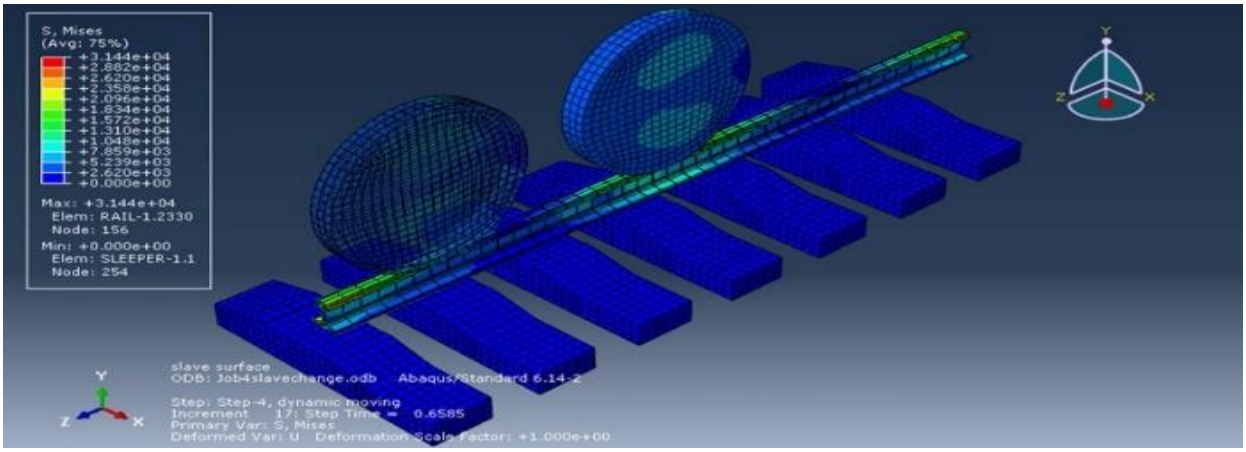

Fig. 2. Stresses at wheel-rail interaction points

[a] https://orcid.org/0000-0002-3798-407X
[b] https://orcid.org/0000-0002-8814-3123

The loading process includes two steps:

– general static analysis
– dynamic implicit analysis

Stress elements in the wheel-rail contact zones, as well as the stress distribution according to the von Mises criterion, are shown in Figures 3 and 4. The von Mises stress is widely used to assess the deformation of isotropic and plastic metals under complex loads. Using ABAQUS software allows you to calculate the von Mises stress values at specified points at each stage of the calculation.

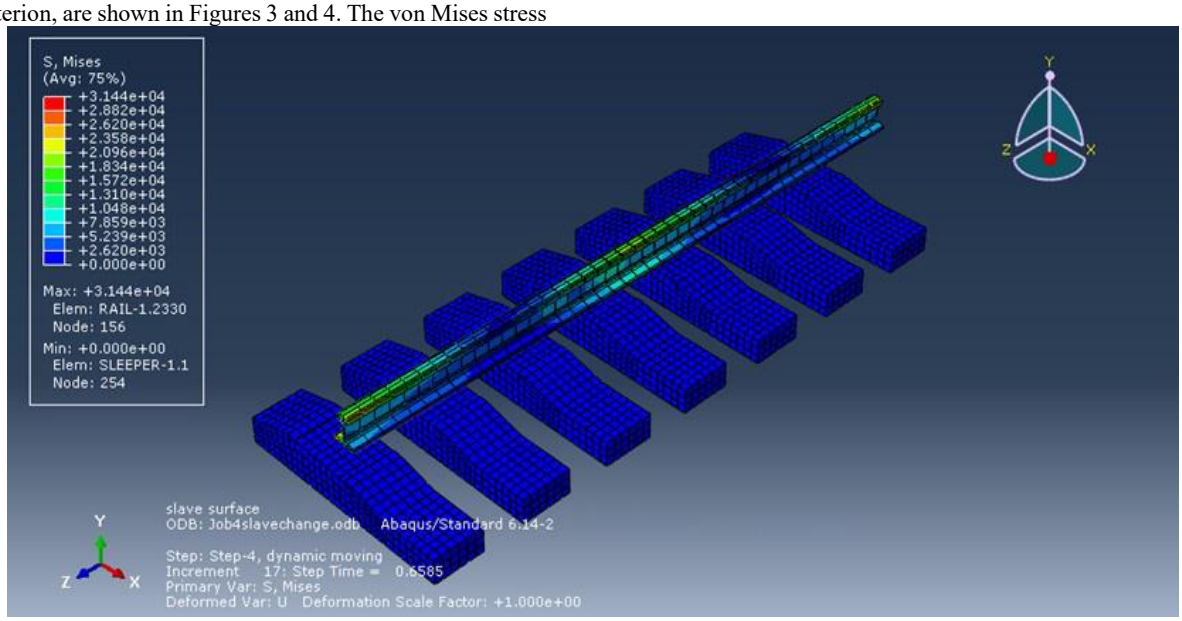

Fig. 3. Distribution of von Mises stresses (without wheel)

Distribution of maximum principal stress

The von Mises stress is a theoretical measure of stress used to evaluate limit state criteria in ductile materials and is also popular in fatigue calculations (where it can be positive or negative depending on the dominant principal stress). While the principal stress is a more "real" and directly measurable stress.

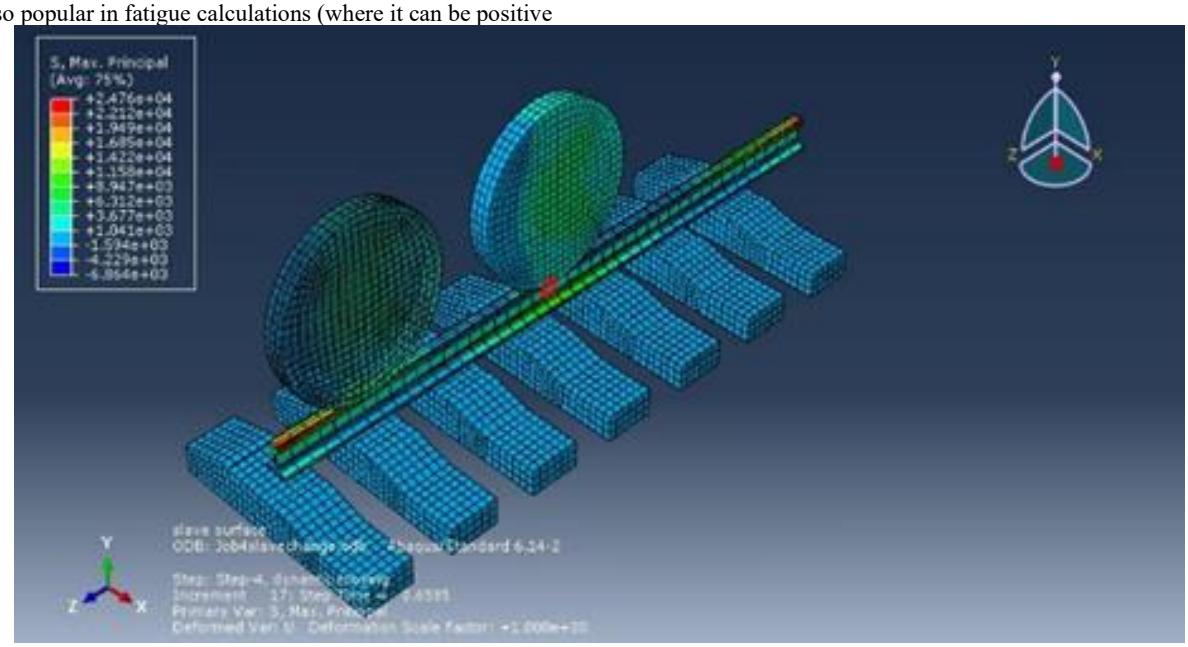

Fig. 4. Distribution of maximum principal stress

https://doi.org/10.56143/3030-3893-2025-1-94-97 A bridge between science and innovation

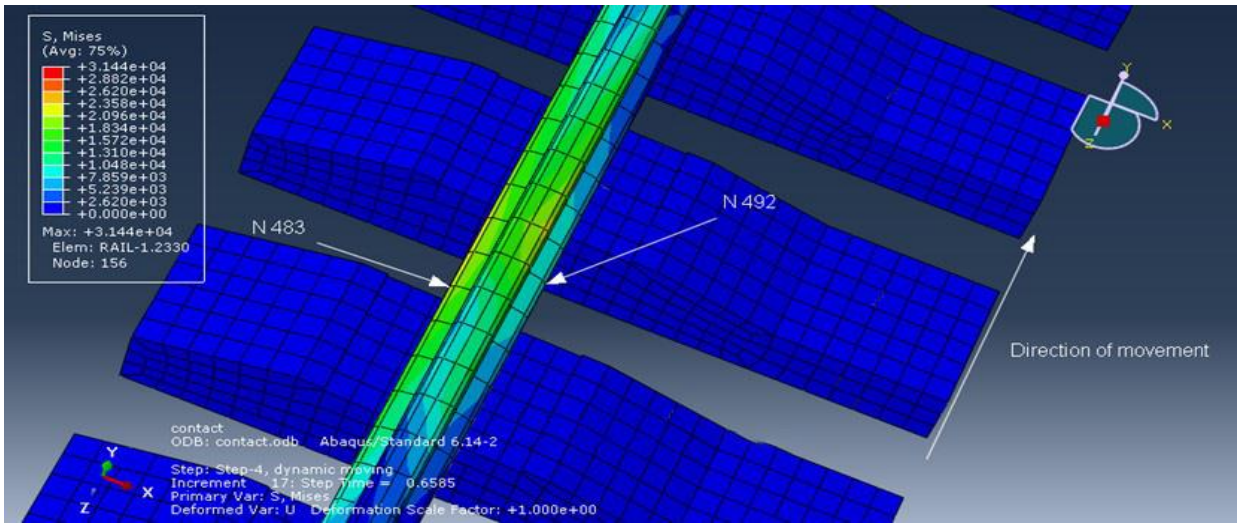

Fig. 5. Location of nodes with maximum and minimum von Mises stress

Analysis of the obtained results

Calculations show that the maximum von Mises stress for step #17 corresponds to node N483, while the minimum von Mises stress for the same increment corresponds to node N492. The change in the von Mises stress distribution can be seen in Figure 6. The stresses are σ=21.3 × 10³ N/cm² for node N483 and σ=4.40 × 10³ N/cm² for node N492. However, node N483 reaches the maximum stress value at time t=0.7585 s, equal to σ=22.9 × 10³ N/cm² [3-4] .

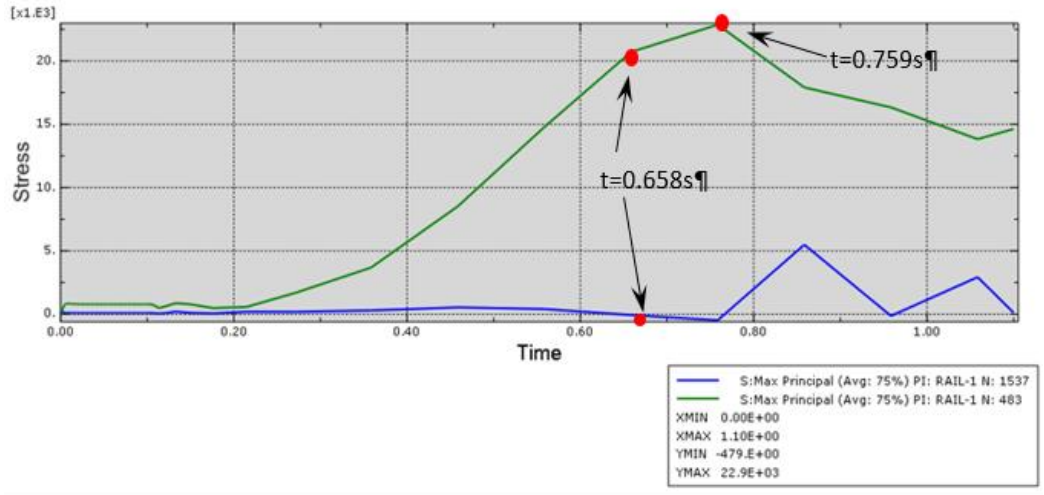

Fig. 6. Maximum and minimum voltage of the Von Mises for increment No. 17 at t=0.658s

The values of the principal stress for node N483 are σ = 21.27 × 10³ N/cm², and for node N1537 σ = -0.175 × 10³ N/cm². Comparing the von Mises stresses and the maximum principal stress in node N483, it can be seen that these values differ [3].

3. Conclusion

During the study, an analysis of stresses was carried out according to the von Mises criterion , maximum principal stresses, spatial displacements of rail and sleeper assemblies, as well as contact interactions between the wheel and the rail, including normal contact forces and reaction forces in the sleepers [5-10].

Modeling in ABAQUS allowed us to obtain the following results:

— deformations, contact forces, stresses and reaction forces were calculated;

— a difference was established between the von Mises stresses and the maximum principal stresses for one node (21.30×10³ for von von Mises and 21.27×10³ for maximum principal stress);

The developed finite element model of the railway track reproduces the geometry of the real structure. The analysis of the stress distribution according to von Mises showed that in the wheel-rail contact zone the maximum values reach 22.9 MPa. The ultimate stresses were recorded in node N483 (σ = 22.9 MPa), and the minimum ones were recorded in node N492 (σ = 4.4 MPa). The analysis of the main stresses also revealed significant fluctuations that affect the wear of the rails and wheels. The maximum values of the main stress are 21.27 MPa.

References

[1] Finite element analysis of railway track under vehicle dynamic impact and longitudinal loads. Zijian Zhang.

[2] Theory of elasticity and plasticity. Jane Helena.

[3] A parameterized three-dimensional finite element model of a slab trackfor simulation of dynamic vehicle–track interaction Niklas Sved.

[4] Djabbarov S., Mirakhmedov M., Sładkowski A. Potential and Problems of the Development of Speed Traffic on the Railways of Uzbekistan //Transport Systems and Delivery of Cargo on East–West Routes. – Springer, Cham, 2018. – С. 369-421.

[5] Djabbarov S., Khakimova Y. Formation of rail defects on the high-speed railways of Uzbekistan //AIP Conference Proceedings. – AIP Publishing LLC, 2022. – Т. 2432. – №. 1. – С. 030013.

[6] A parameterized three-dimensional finite element model of a slab trackfor simulation of dynamic vehicle–track interaction Niklas Sved.

[7] Kaynia A. M., P. Zackrisson. 2000. “Ground vibration from high speed trains: prediction and countermeasure.” Journal of geotechnical and geoenvironmental engineering, vol. 126,no. 6, pp. 531-537.

[8] Z. Cai, g.p. raymond. 1994. “modelling the dynamic response of railway track to wheel/rail impact loading” . 1) dep. Of civil engineering, royal military college, Kingston, Ontario, Canada.

[9] Djabbarov S., Mirakhmedov M., Sładkowski A. Potential and Problems of the Development of Speed Traffic on the Railways of Uzbekistan //Transport Systems and Delivery of Cargo on East–West Routes. – Springer, Cham, 2018. – С. 369-421.

[10] Djabarov S., Kodirov N. The impact of dynamic load from the wheel on the rail for high-speed trains in Uzbekistan //E3S Web of Conferences. – EDP Sciences, 2023. – Т. 402. – С. 06009.

Information about the author

Djabbarov Saidburxan Tulaganovich	Toshkent davlat transport universiteti “Temir yol muhandisligi” kafedrasi professori. t,f,n, E-mail: _saidhon_@inbox.ru Tel.: +99890185 2934 https://orcid.org/0000-0002-3798-407X
Kodirov Nodirbek Baxtiyarovich	Toshkent davlat transport universiteti “Temir yol muhandisligi” kafedrasi tayanch doktoranti E-mail: nodir_kodirov_95@mail.ru Tel.: +998971002908 https://orcid.org/0000-0002-8814-3123

Assessment of the condition of a railway track based on finite element modeling

S.T. Djabbarov[1][a], N.B. Kodirov[1][b]
[1]Tashkent state transport university, Tashkent, Uzbekistan

Abstract: This article discusses the use of finite element (FE) modeling to analyze the characteristics of a railway track. Graphs of spatial displacements of rail and sleeper nodes are provided, and an analysis of maximum displacements at different points in time is performed. In conclusion, the importance of the obtained results for further study of the dependence of stresses on deformations of track elements is noted, which contributes to optimization of design and improvement of the reliability of railway infrastructure.

Keywords: stress, von Mises, track superstructure, rail, sleeper, modeling, model

1. Introduction

This study used commercial finite element software ABAQUS, which allows predicting the degree of fracture of rails, sleepers and other track elements, promptly assessing the technical condition of the railway track infrastructure taking into account loads, traffic intensity of high-speed and other categories of trains and climatic conditions.

As it is known, each material has its own specific characteristics, and taking these factors into account in the modeling process is of great importance and gives us acceptable results for subsequent calculations. The ABAQUS software used gives us such an opportunity, taking into account the above factors [1,2] . The following elements of the track superstructure were used in the modeling.

Table 1

Technical characteristics of the track superstructure

Elements of the railway superstructure	Density (kg/m2)	Young's modulus (E)	Poisson's ratio (υ)
Rail (steel)	7850	210 GPa	0.3
Sleeper (reinforced concrete)	1200	80 GPa	0.3

2. Research methodology

Statement of the problem

In this study, conducted to assess the fatigue limit, wear resistance and operational strength of both elements of the system, the calculation of stresses arising from the interaction of the wheel with the rail was carried out using the finite element method. In this case, the wheel was considered under conditions of movement on a straight section of the track with an axial load on the wheel of 125 kN and a speed of 80 km/h.

The displacements in rail nodes N488 and N1556 for a given pitch of 17 at t = 0.658 s are 0.8094 mm and 0.8266 mm, respectively. The maximum displacement is observed at t = 0.7585 s and reaches 0.8864 mm. The study considered two sleepers under the wheel, as well as nodes of sleepers N3 and N3' with the largest displacement values. The location of nodes N3 and N3 is shown in Figure 1, and the changes in the sleeper displacement are shown in Figure 2.

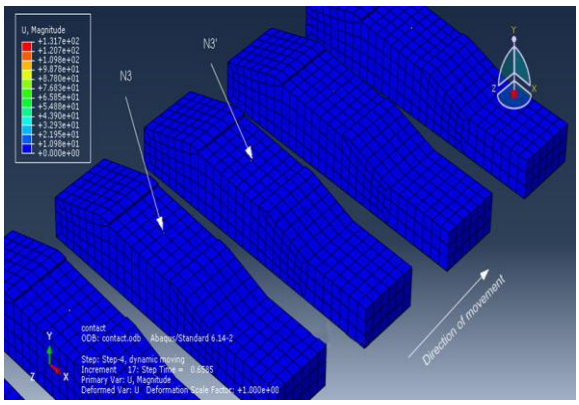

Fig. 1. Location of nodes N 3 and N 3'

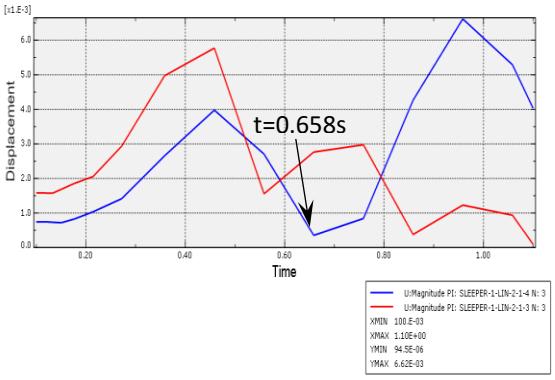

Fig. 2. Spatial displacement of sleepers

[a] https://orcid.org/0000-0002-3798-407X
[b] https://orcid.org/0000-0002-8814-3123

The maximum displacements recorded at t = 0.658 s for step 17 are observed in the middle of the sleepers. The displacement of node N3 is 2.7627×10^{-3}, and that of node N3' is 0.354×10^{-3}

Axial displacements in rail nodes. The displacements of nodes U1 for rails N483 and N1556 are recorded as maximum at step 17 at t = 0.658 s, amounting to -0.585 mm and -0.615 mm, respectively. The graph includes both nodes, since it is at these points that the largest displacements are recorded. The data are presented in Figures 3 and 4.

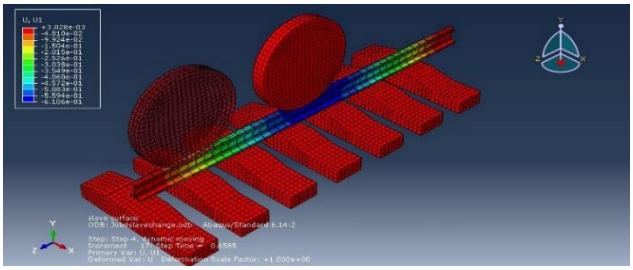

Fig. 3. Displacement - U 1 of the rail at step 17 t = 0.658 s

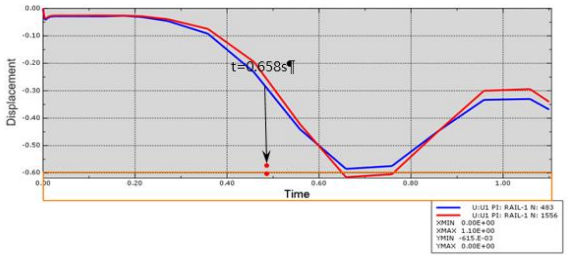

Fig. 4. Displacement of U 1 at step 17, t = 0.6585 s at nodes 483 and 1556

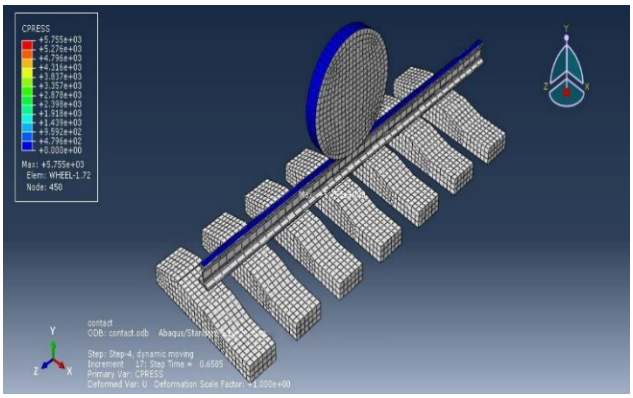

Fig. 5. Contact stress on the surface at step 17

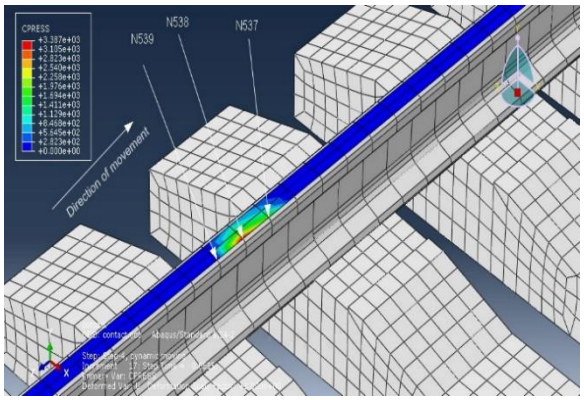

Fig. 6. Distribution of contact stress (KN) on the surface during displacement

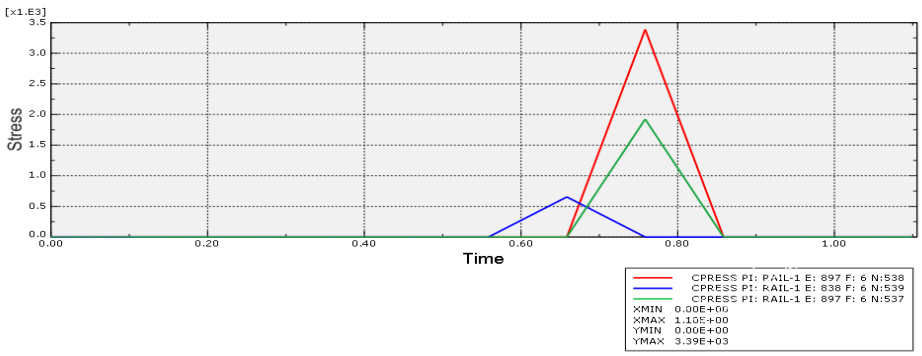

Fig. 7. Distribution of CN at nodes 537, 538 and 539

Thus, with an axle load of 125 kN, the maximum stress value for a given step 17 at time t = 0.658 s reaches 0.654 × 10^3 N/cm², and in node N538 the maximum value of Cpress is recorded, amounting to 3.3871 × 10^3 N/cm², which is shown in Fig. 7.

https://doi.org/10.56143/3030-3893-2025-1-98-101 A bridge between science and innovation

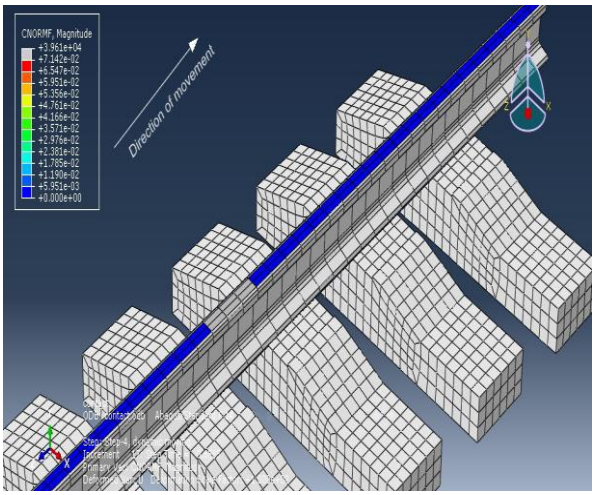

Fig. 8. Distribution of contact stress on the surface with increment

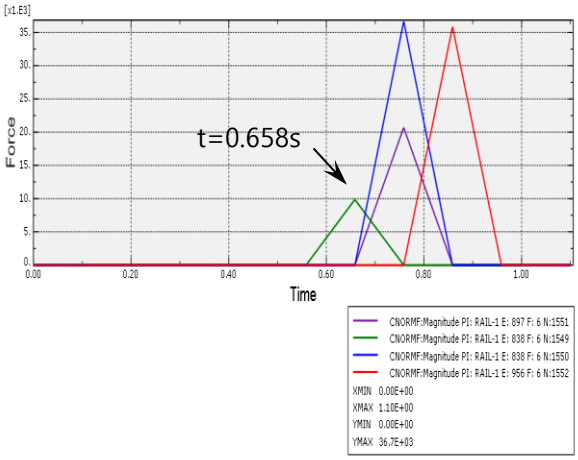

Fig. 9. Distribution in nodes 1549-1551

From Figure 9 it can be determined that for node N 1549 the force is equal to 9.866×10^3N, for node N1550 36.673×10^3 N, for unit N1551 20.690×10^3 and for N1552 35.859×10^3 N [5,6,7].

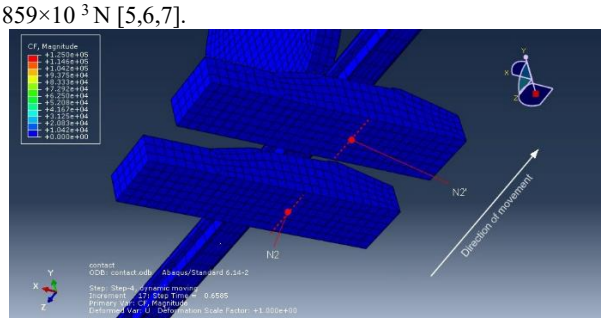

Fig. 10. Research of nodes from PC

The analyses show that the maximum reaction force occurs in the middle of the sleepers at nodes N2 and N2'. The displacements with a step of 17 of the reaction force are equal to F=0.519 for N2 $\times10^3$Hand F=0.389 N for N2' $\times10^3$, which is shown in Fig. 11 [12].

3. Conclusion

Based on the calculated stress values, it can be concluded that for further research it is advisable to use a model based on elastic-plastic materials [6]. Verification of the limiting conditions adopted for finite element modeling requires experimental testing, which requires a special test bench.

When investigating the reaction forces on sleepers, the maximum values were recorded at nodes N2 and N2', where the forces amount to 0.519 kN. These forces can have a significant impact on the operational characteristics of the railway track.

The simulation showed that the static and dynamic analyses of the track under a load of 125 kN allow us to evaluate the changes in stresses and displacements depending on different time stages. The static analysis uses automatic increments with a step of 0.0001, while the dynamic analysis is carried out with a step of 0.001, which ensures high accuracy and stability of the results.

For the analysis, two sleepers located under the wheel were considered. 14 nodes were analyzed, which are located parallel to the bottom of the rail (dotted line in Fig. 10).

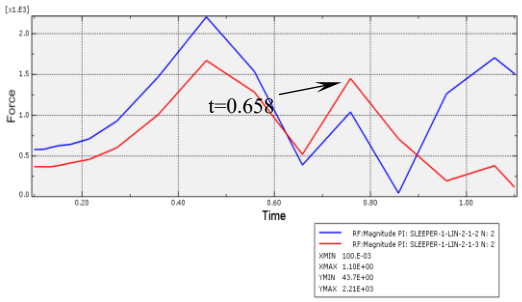

Fig. 11. Values of RS at nodes N 2 and N 2'

References

[1] Finite element analysis of railway track under vehicle dynamic impact and longitudinal loads. Zijian Zhang.

[2] Theory of elasticity and plasticity. Jane Helena.

[3] A parameterized three-dimensional finite element model of a slab trackfor simulation of dynamic vehicle–track interaction Niklas Sved.

[4] Djabbarov S., Mirakhmedov M., Sładkowski A. Potential and Problems of the Development of Speed Traffic on the Railways of Uzbekistan //Transport Systems and Delivery of Cargo on East–West Routes. – Springer, Cham, 2018. – С. 369-421.

[5] Djabbarov S., Khakimova Y. Formation of rail defects on the high-speed railways of Uzbekistan //AIP Conference Proceedings. – AIP Publishing LLC, 2022. – Т. 2432. – №. 1. – С. 030013.

[6] A parameterized three-dimensional finite element model of a slab trackfor simulation of dynamic vehicle–track interaction Niklas Sved.

[7] Kaynia A. M., P. Zackrisson. 2000. “Ground vibration from high speed trains: prediction and countermeasure.” Journal of geotechnical and geoenvironmental engineering, vol. 126,no. 6, pp. 531-537.

[8] Z. Cai, g.p. raymond. 1994. “modelling the dynamic response of railway track to wheel/rail impact loading” . 1) dep. Of civil engineering, royal military college, Kingston, Ontario, Canada.

[9] Djabbarov S., Mirakhmedov M., Sładkowski A. Potential and Problems of the Development of Speed Traffic on the Railways of Uzbekistan //Transport Systems and Delivery of Cargo on East–West Routes. – Springer, Cham, 2018. – С. 369-421.

[10] Djabarov S., Kodirov N. The impact of dynamic load from the wheel on the rail for high-speed trains in Uzbekistan //E3S Web of Conferences. – EDP Sciences, 2023. – Т. 402. – С. 06009

[11] Кодиров Н. Б., Мирзахидова О.М. FINITE ELEMENT ANALYSIS OF TRACK STRUCTURE //Universum: технические науки. – 2022. – №. 9-5 (102). – С. 46-49.

[12] Джаббаров С. Т., Кодиров Н. Б. Моделирования элементов верхнего строение пути в програмном комплексе «ABAQUS» // Научно-практический электронный журнал “Пожаро-взрывобезопасность” Ташкент -2024- С. 381-р

Information about the author

Djabbarov Saidburkhan Tulaganovich	Toshkent davlat transport universiteti “Temir yol muhandisligi” kafedrasi professori. t,f,n, E-mail: _saidhon_@inbox.ru Tel. +99890185 2934 https://orcid.org/0000-0002-3798-407X
Kodirov Nodirbek Bakhtiyarovich	Toshkent davlat transport universiteti “Temir yol muhandisligi” kafedrasi tayanch doktoranti E-mail: nodir_kodirov_95@mail.ru Tel.: +998971002908 https://orcid.org/0000-0002-8814-3123

Development and application of multi-component cement composite materials with improved performance for construction and repair purposes

S.S. Shaumarov[1][a], O. Zafarov[1][b]
[1]Tashkent state transport university, Tashkent, Uzbekistan

Abstract: This article presents information about changes in the mechanical properties of saline soils based on constructions as a result of wetting. The analysis of deformations in buildings and structures in areas where saline soils are spread in the territory of Uzbekistan shows that the main factor of their occurrence is the change of the physical and mechanical properties of the underlying soils under the influence of water. It means that in the design of the structures of the risers consisting of the bases with saline soil, it is necessary to take into account the changes of the types and amounts of salts during their use and their influence on the calculation indicators. Groundwater is in continuous movement, and in nature there is a large and small circulating active flow of water. During this movement, the volume, quantitative state, physical (ice, vapor, liquid) and chemical properties of groundwater can change.

Keywords: structures, soil, saline soils, mechanical properties, deformations, groundwater, active flow movement, salts

1. Introduction

Construction of buildings and structures in our country is often carried out in complex engineering-geological conditions, especially in areas with saline soils. These soils cover numerous regions of Uzbekistan such as Bukhara, Jizzakh, Syrdarya, Fergana, Khorezm and large areas of the Republic of Karakalpakstan. In Uzbekistan, saline soils, which can be used as a basis for the construction of buildings and structures, consist of saline, saline, saline and bald soils, differing in the composition and amount of slightly soluble salts. They are often formed in the depressions of the relief: mountain slopes, lowlands, saline lake shores, cliffs, desert zones formed as a result of suffocation, mineralized waters close to the surface (1 - 3 m). The main factor in the formation of saline soils is the mineralized groundwater and saline rocks that lie close to the surface. The main condition for salinization is the impossibility of water flow in places and the fact that the amount of evaporation is greater than the amount of precipitation.

Analysis of the existing literature on saline soils and experience in the design and construction of buildings and structures in different regions of the country, as well as special studies on saline soils show that changes in the composition, structure and physical and mechanical properties of substances during wetting and alkaline leaching. and this phenomenon needs to be taken into account in design work.

As a result of flooding and wetting of areas composed of saline soils, a number of major affects can occur in buildings and structures.

As mentioned above, the analysis of the emergency situation of some facilities in Uzbekistan shows that the forecast of changes in the mechanical properties of the foundations of buildings and structures should take into account the impact of factors affecting the decrease of mechanical properties (eg: long water infiltration, salinity, etc.). Existing guidelines and normative literature provide recommendations for determining the mechanical properties for saline soils with easy and moderately soluble salts, but the amount of difficult-to-dissolve salts is not taken into account.

Studies suggest that in order to ensure the safe operation of buildings and structures built on saline soils, it is necessary to study the process of leaching of insoluble salts, especially when the mechanical properties of the soil are exposed to long-standing water. An experimental study of the laws of change of mechanical properties of water from saline soils over a long period of time. This is because the issues of assessing the change in the mechanical properties of saline soils in the long-term exposure to water to insoluble salts have not been fully studied.

The saline loamy and loamy soils in the territory of Uzbekistan, in particular in Pakhtakor district of Jizzakh region, where capital, industrial and civil construction is currently booming, are taken as the object of research and its mechanical characteristics in the article.

The purpose of this dissertation is to develop a methodology for studying the mechanical properties of saline and sedimentary soils when used with water and solutions and long-term leakage, in order to use the parameters of soils in the calculation of the foundation of structures.

The main feature of saline soils is the change in their mechanical properties during the washing of salts, there are two main types of washing of salts:

- filter washing, in which the washing of the salt in the soil is carried out by the filtration flow of the liquid under the pressure gradient and is of practical importance for soils with high permeability;
- diffusion washing, in which the washing of the salt in the soil occurs as a result of the movement of ions due to the difference in the concentration of salts in solution. This is typical for low absorbent soils.

The laws of changing in salinity level and mechanical characteristics when saline soils are exposed to water for a long time under laboratory conditions were studied and expressions were proposed to predict them [1].

[a] https://orcid.org/0000-0001-8935-7513
[b] https://orcid.org/0009-0006-0226-6349

Literature review. Existing guidelines and normative literature provide recommendations for determining the mechanical properties for saline soils with easy and moderately soluble salts, but the amount of difficult-to-dissolve salts is not taken into account. Studies suggest that in order to ensure the safe operation of buildings and structures built on saline soils, it is necessary to study the process of leaching of insoluble salts, especially when the mechanical properties of the soil are exposed to long-standing water. An experimental study of the laws of change of mechanical properties of water from saline soils over a long period of time. This is because the issues of assessing the change in the mechanical properties of saline soils in the long-term exposure to water to insoluble salts have not been fully studied. Many scientists have worked on engineering-geological research and their use. Including, M.D. Braja, G.P. David, W. Kuhn, B.G. Neal, A.R. Harutyunyan, I.L. Bartholomey, V.M. Bezruk, P.B. Babakhanov, A.A. Glaz, A.I. Grot, R.S.Ziangirov, N.P.Zatenatskaya, M.F.Уerusalimskaya, M.O.Karpushko, A.K.Kiyalbaнev, A.A.Kirillov, N.A.Klapatovskaya, Уu.V.Kuznetsov, A.D. Kayumov, T.Kh. Qalandarov, S.S. Mordovich and many scientists. The following scientists also studied the deformation and strength parameters of soils containing ocon and moderately soluble salts: Bezruk B.I., Glaz A.A., Dolmatov B.I., Lomize L.N., Povilonckiy V.M., Petrukhin V.P., Rozhdectvenckiy E.D., Ukhov C.B., Chokhonelidze G.N., Shulginoy V.P. and others. In 1983, V. M. Bezruk [12] developed classifications of saline soils for the construction of buildings and structures. The specificity of this classification is as follows: the amount of salts in the ground is taken into account starting from 0.3%, in which salinity is divided into two types: 1) chlorinated and chlorinated-chlorinated; 2) saturated, chloride-saturated and coda salinity. V.P. Petrukhin [12] developed a classification in which the minimum amount of water-soluble salts depends on the density of soils in accordance with the design goals of civil and commercial buildings and constructions.

2. Research methodology

Based on the task set and the results of previous research, the methodological part of the experiment was based on the following laws:

- In the process of interaction of ground distilled water with water, its structure changes as the amount of soluble salts in the water decreases.
- Changes in soil structure during alkali washing lead to a decrease in strength and an increase in deformation (additional suffocation subsidence).

Changes in the composition and volume of salts in the soil can affect the water-physical properties of soils, in particular, the composition of the microaggregate, plasticity parameters, viscosity, etc. After the initial grunt was thoroughly examined, the diffuser or filter lye was rinsed.

3. Results and Discussion

Changes in the composition, structure, and mechanical properties of (C, φ) solutions were evaluated due to the fact that solutions leave a certain amount of salts from the solution in a diffuse manner after prolonged exposure to distilled water (alkaline washing rate-β). Filtration of salts in the soil is carried out according to the lifting current scheme in the FIM device. A pre-tested sample of the natural structure was placed on the device according to the same scheme. B on the side surfaces of the sample for loss of filtration on стенке.P.It it was processed in accordance with the methodology proposed by Petrukhin [1]. The sample was scraped off with a diameter smaller than the ring of the F-IM tool (D=50 cm^2), plastic glue on its side surfaces is rubbed into the groove, and wax is poured into the gap between the ring and the sample. This treatment allows us to calculate that the liquid moves only through the volume of the soil.

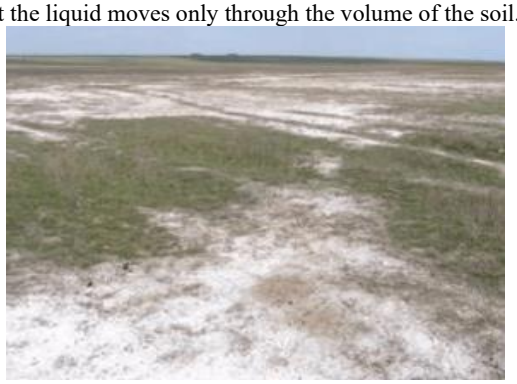

Fig. 1. View of the saline areas in the saline area of our country

Filtration washing with alkaline was carried out under pressure, often without squeezing the soil, that is, the soil was in conditions of constant volume during the experiment. Water filtration was carried out under the influence of high pressure gradients (up to J = 100), which formed a column of water. The limit value was determined by a jump (J=10, 30, 60, 100), slowly, not in one piece. During the experiment, the filtrate was selected to determine the amount of washed salts, its volume and minerals were recorded. To determine the consistency characteristics of the studied grinds, instruments developed by the "Gidroproekt" system are used, registering a uniformly cut surface [2]. Depending on the physical condition of the soil, methods of rapid cutting of samples are used.

Grinding machines, the structure and humidity of which are a natural method of rapid cutting, are tested without prior condensation. The amount of moderate pressure at which cutting is performed is selected taking into account the thickness of the soil and the weight of the structure. After a moderate load is set, experimental work is carried out no later than 5 minutes after the start of the pulse load generator.

Locker rooms were given with splashes. Their volume was determined by the value of moderate pressure and was 5% of its volume. Each stage was carried out until the deformation was conditionally stabilized (0.01 mm/min). After the filtration process was completed, the amount of salt was determined in the "Solemer" device of the PNIIIS design [5].

4. Conclusion

A study conducted to study their salinity characteristics and the degree of salinity associated with the amount of initial plaster and the degree of salt leaching during prolonged exposure to water based on salt gratings of buildings and structures allows us to draw the following conclusion. Salts of complex soil, in particular, when water enters the mush with which the plaster is salted for a long time, give them a description of the consistency and amount of salt in them, that is, the degree of salinity decreases, which

in turn leads to a decrease in the stagnation of the foundation of buildings and structures and additional deposition. Before designing buildings and structures, it is necessary to determine the initial salinity and solubility of salt – the degree of alkalinity and, accordingly, the salinity characteristics, as well as the degree of salt leaching - the initial salinity of the salty soil of the area in depth.

References

[1] Zafarov O., G'ulomov D., Murodov Z. "Conducting engineering-geological researches on bridges located in our country and diagnosing their super structures, methods of eliminating identified defects," AIP Conference Proceedings. - AIP Publishing, № 1, 2023, pp. 1 - 7.

[2] Bobojonov R., Zafarov O., Yusupov J. "Soil composition in the construction of engineering structures, their classification, assessment of the impact of mechanical properties of soils on the structure," AIP Conference Proceedings. - AIP Publishing, № 1, 2023, pp. 1 - 8.

[3] Maxkamov Z. et al. "Conducting engineering and geological research on the design and construction of buildings and structures in saline areas," AIP Conference Proceedings. - AIP Publishing, № 1, 2023, pp. 1 - 6.

[4] Kayumov A., Zafarov O., Kayumov D. "Changes of mechanical properties in humidification saline soil based in builds and constructions," AIP Conference Proceedings. - AIP Publishing, № 1, 2023, pp. 1 - 5.

[5] Hudaykulov R. et al. Filter leaching of salt soils of automobile roads //E3S Web of Conferences. - EDP Sciences, 2021. - T. 264. - C. 02032.

[6] Maslov N. N. Fundamentals of engineering geology and soil mechanics. Textbook for high schools. - M.: Higher School, 1982.- 511 p.

[7] Dmitriyev V.V., Yarg L.A. Methods and quality of laboratory study of soils: textbook / V.V. Dmitriyev, L.A. Yarg. - M.: KDU, 2008. - 502 p.

[8] Trofimov V. T., Koroleva V. A. Laboratory work on soil science. –M.: KDU, University book, 2017. - 654 p.

[9] Trofimov V. T. et al. Ground science. - M., Publishing House of Moscow State University, 2005. - 1024 p.

[10] Muzaffarov A. A., Fanarev P. A. Engineering and geological support for the construction of highways, airfields and special structures. Tutorial. M.: MADI, 2016. -180 p.

[11] V. P. Petrukhin, Construction of structures on saline soils. - M.: Stroyizdat, 1989. - 264 p.

[12] Kayumov Abdubaki Djalilovic A. D., Zafarov O. Z., Saidbaxromova N. D. Basic parameters of physical properties of the saline soils in roadside of highways //Central Asian Problems of Modern Science and Education. - 2019. - T. 4. - №. 2. - C. 30-35.

[13] Irisqulova K. N., Zafarov O. Z. Construction of highways in saline soils //Academy. - 2021. - №. 8 (71). - C. 27-29.

[14] Zafarov O. Z., Irisqulova K. N. Q. Modern technologies of road construction //Science and Education. - 2022. - T. 3. - №. 2. - C. 312-319.

[15] Maxkamov Z. et al. Conducting engineering and geological research on the design and construction of buildings and structures in saline areas //AIP Conference Proceedings. - AIP Publishing, 2023. - T. 2789. - №. 1.

Information about the author

Shaumarov Said Sanatovich	Tashkent State Transport University "Building and industry facilities Construction Department professor (DSc), E-mail: shaumarovss@mail.ru Tel.: +998712990026 https://orcid.org/0000-0001-8935-7513
Zafarov Olmos	Tashkent State Transport University, Independent researcher, PhD, docent, E-mail: olmos.zafarov@mail.ru Tel.: +998952651000 https://orcid.org/0009-0006-0226-6349

CONTEXT / MUNDARIJA

CONTEXT / MUNDARIJA